

A STUDY OF THE TRANSPORT OF SOLIDS IN HOSPITAL  
ABOVE GROUND DRAINAGE SYSTEMS

ROBIN HARRY MAURICE WAKELIN, BSC.

A THESIS SUBMITTED FOR THE DEGREE OF DOCTOR OF PHILOSOPHY  
IN BUILDING TECHNOLOGY OF BRUNEL UNIVERSITY, UXBRIDGE

DEPARTMENT OF BUILDING TECHNOLOGY  
BRUNEL UNIVERSITY  
UXBRIDGE

JANUARY 1978

# A STUDY OF THE TRANSPORT OF SOLIDS IN HOSPITAL ABOVE GROUND DRAINAGE SYSTEMS.

R H M WAKELIN BSc

## SUMMARY

The transport of solids in "horizontal" above ground drainage pipes was the subject of an investigation aimed at establishing a method for the design of deposit free drainage systems. Tests were based on the measurement of solid velocity in a discharge pipe of variable gradient, the solid being a maternity pad either with or without three paper towels.

A test rig capable of supporting discharge pipes of various materials, enabling the incorporation of bends and junctions, was employed and an instrumentation method for measuring solid velocity, depth of flow and rate of flow was developed.

Results showed that solid velocity in straight discharge pipes can be characterized by three separate zones of flow, the second zone being the most fundamental, with solid velocity defined by an equation of the form  $V = C_1 - C_2\sqrt{L/G}$ , where  $C_1$  and  $C_2$  are empirical coefficients,  $L$  is the distance travelled from the w.c. discharge and  $G$  is the pipe gradient. The limits of the flow zones can be defined by values of  $\sqrt{L/G}$ , the larger limit defining the maximum length of deposit free discharge pipe at any gradient.

The effect of pipe fittings on the velocity of the solid can be represented by a sharp velocity reduction followed by a gradual velocity regain and may be ignored as long as the pipe fitting is positioned approximately 5 metres before the end of the second flow zone conditions, as defined by a value of  $\sqrt{L/G}$ , thus allowing sufficient length for the velocity to regain its straight pipe characteristic value.

A design method is presented, based on the experimental data collected, which in its present form can be applied to check for the possible deposition of solids within the "horizontal" discharge pipe system, either due to traversing excessive lengths of horizontal pipework or as a result of bend or junction positioning.

#### ACKNOWLEDGMENTS

The work reported was supported by DHSS Commission Number H70/R/E/74Y(230) and was carried out at Brunel University.

Loans of equipment from Marley, Armitage Shanks, Glynwed and Schott Kem are gratefully acknowledged.

The author wishes to record his thanks to Dr J A Swaffield, Senior Lecturer in Building Technology, for his advice, expertise, dedicated assistance and encouragement throughout the research. Professor Urry is to be thanked for making available the facilities of the Department of Building Technology, Brunel University. Mr C Langshaw, who acted as the main liaison between Brunel and DHSS, together with various members of DHSS Study Group 9, are to be thanked for their help and advice.

Finally the author would like to thank Mrs Conway for so expertly and patiently typing the manuscript.

CONTENTS	Page No.
Summary	(ii)
Acknowledgments	(iii)
Contents	(iv)
List of Figures and Tables	(vii)
Notation and Terminology	(xvi)
1. INTRODUCTION	1
2. HISTORICAL BACKGROUND	4
2.1 Origins of drainage	4
2.2 Events leading up to modern sanitary law	5
2.3 Brunel's Contribution	7
2.4 Methods of drainage design	9
2.4.1 Drainage design at the start of the century	10
2.4.2 The necessity for greater freedom of design	11
2.4.3 Definition of modern design requirements	11
2.4.4 Two-pipe system	11
2.4.5 One-pipe system	12
2.4.6 Single stack system	12
2.4.7 Separation of soil and surface water	14
2.4.8 CP 304: 1968	14
2.5 Pilot study - implications and theories	15
2.6 In conclusion	15
3. THEORY	16
3.1 Parameters affecting drainage performance	16
3.2 Theoretical analysis of straight pipe solid deceleration	18
3.3 Theoretical analysis of drainage pipe fittings	21
4. APPARATUS AND INSTRUMENTATION	22
4.1 General apparatus	22
4.1.1 Large support rig	22
4.1.2 Small support rig	23
4.1.3 Discharge pipe and support system	23
4.1.4 Ladder support method and gradient adjustment	24
4.1.5 W.C. inlet and vertical stack outlet	25
4.1.6 Second support rig	27
4.1.7 Third support rig	27
4.1.8 Flushing mechanism	28
4.1.9 Discharge collection tank	28
4.2 Instrumentation	30
4.2.1 Original method of velocity measurement	31
4.2.2 Timer counter velocity measurement	32
4.2.3 Photocell method for depth of flow measurement	34
4.2.4 Float/LVDT depth measurement	36
4.2.5 Volume flow rate measurement	37
5. EXPERIMENTAL METHOD	38
5.1 Waste materials	38
5.1.1 Maternity pad	38
5.1.2 Kleenex paper towels	38
5.1.3 Bowater Scott paper towels	38
5.1.4 Choice of waste materials	39
5.1.5 Placing of waste materials in w.c. pan	40

5.1.6	Previous research involving the transport of waste solids in drainage systems	41
5.2	Orifice sizing for depth measurement	43
5.2.1	Analysis of orifice effects	43
5.2.2	Program testing	46
5.2.3	Theoretical response of the depth measuring instrumentation	46
5.2.4	Comparison of response rate with orifice area	46
5.2.5	Initial tests	48
5.3	Depth of flow calibration	50
5.4	Collection tank LVDT calibration	50
5.5	Velocity calibration	51
5.6	W.C. discharge characteristics test rig	51
5.7	Straight plastic pipe test rig	53
5.8	Straight cast iron pipe test rig	54
5.9	Plastic bends test rig	59
5.10	Plastic junctions test rig	59
5.11	Cast iron bend and junction test rig	61
5.12	Straight glass pipe test rig	62
6.	DATA HANDLING AND PRESENTATION OF RESULTS	63
6.1	Data input	63
6.2	Presentation of results	64
7.	DISCUSSION OF RESULTS	67
7.1	W.C. discharge characteristics	67
7.1.1	Kleenex and Bowater Scott Paper Towels	69
7.1.2	High level cistern flush pipe restrictors	72
7.1.3	Effects of venting the w.c. discharge	75
7.1.4	Variation between P-trap and S-trap w.c's	75
7.1.5	Depth of flow	76
7.1.6	Conclusions on w.c. discharge characteristics	76
7.2	Straight pipe deceleration characteristics	77
7.2.1	Flow observations	78
7.2.2	Straight plastic pipe	81
7.2.3	Straight plastic pipe - effect of w.c. venting	84
7.2.4	Straight plastic pipe - variation between materials	84
7.2.5	Straight plastic pipe - variation between w.c's	85
7.2.6	Straight plastic pipe - optimum minimum gradient	86
7.2.7	Straight plastic pipe - stack venting effect	87
7.2.8	Variation between maternity pads and sanitary towels	87
7.2.9	Straight plastic pipe - zone limits	88
7.2.10	Straight plastic pipe - depth of flow	89
7.2.11	Straight cast iron pipe	91
7.2.12	Straight cast iron pipe compared to straight plastic pipe	93
7.2.13	Straight cast iron pipe - effect of w.c. venting	93
7.2.14	Straight cast iron pipe - variation between materials	94
7.2.15	Straight cast iron pipe - variation between w.c's	94
7.2.16	Straight cast iron pipe - zone limits	94
7.2.17	Straight glass pipe	95
7.2.18	Straight glass pipe - flow observation	95
7.2.19	Straight glass pipe compared to plastic and cast iron.	96
7.2.20	Straight glass pipe - variation between materials	97
7.2.21	Straight glass pipe - zone limits	98
7.2.22	Conclusions on straight pipe deceleration characteristics.	98

7.3	Effects of bends and junctions	100
7.3.1	Effects of bends and junctions - flow observation	101
7.3.2	Analysis of the effects of bends and junctions	104
7.3.3	Effect of a 135° plastic bend	107
7.3.4	Effect of 2 x 135° plastic bends, one metre apart	108
7.3.5	Effect of a 92½° plastic bend	108
7.3.6	Effect of a 135° plastic junction with varying angles of branch entry	109
7.3.7	Effect of venting the upstream end of the main drain for the junction tests	111
7.3.8	Effect of angle of branch entry on the straight pipe flow through a 135° plastic junction	111
7.3.9	Effect of a 92½° horizontal entry plastic junction	112
7.3.10	Effect of a 92½° cast iron bend and a 92½° horizontal entry cast iron junction	113
7.3.11	Design limits for bend and junction positions	114
7.3.12	Conclusions on effects of bends and junctions	116
7.4	The design method for above ground horizontal drainage systems	118
8.	LIMITATIONS OF THE RESEARCH	121
8.1	Selection of waste materials	121
8.2	Venting of the w.c. discharge	122
8.3	Vertical stack outlet	123
8.4	Junction testing	123
8.5	Pipe condition and deterioration	124
8.6	Effects of installation and use	125
8.7	Larger installations	125
8.8	Limitations of the design method	126
9.	CONCLUSIONS AND FURTHER WORK	128
	Summary of design method	131
10.	REFERENCES	133
11.	FIGURES AND TABLES	136 - 268
12.	APPENDICES	269
12.1	Appendix I. Prediction of depth measuring system response. Computer programs FLOT and SLOT	270
12.2	Appendix II. Data presentation program WCHAR	283
12.3	Appendix III. Least squares analysis program LSQ1	291

## LIST OF FIGURES AND TABLES

Figure No.		Page No.
1	Photograph of the complete test rig as originally developed and used during the initial tests.	136
2	Photograph of the complete straight glass pipe test rig	137
3	Photograph of the large support rig used to support the w.c. and other appliances	138
4	Photograph of the vertical column support method	139
5	Schematic layout of test rig instrumentation and control systems, as originally developed	140
6	Photograph of the original discharge collection tank and small support rig	141
7	Schematic section through discharge collection tank, illustrating depth control and measurement systems	142
8	Photograph of a single maternity pad travelling along the straight glass pipe	143
9	Photograph of the depth of flow measurement U-tube and float chamber and photocells/light source rings	144
10	Photograph of the original instrumentation table	145
11	Photograph of the instrumentation table as finally developed	146
12	Pen recorder traces from both photocells and depth measuring LVDT for a water only flush at 1/100	147
13	Pen recorder traces from both photocells and depth measuring LVDT for a 1 MP flush at 1/100	148
14	Photograph of the waste materials and plastic bends as used during the research project and during the pilot study	149
15	Schematic layout of float chamber and U-tube connection to waste pipe used to record depth variations	150
16	Layout of circular and slot orifices in pipe wall investigated	151

Figure No		Page No
17	Theoretical float response to a ramp water depth input profile for 1,4 and 12 x 3.67 mm diameter orifices	152
18	Theoretical float response to a ramp water depth profile for 1 and 3 wall slots	153
19	Float response to a water only flush, as recorded by the LVDT and pen recorder, for a range of wall orifice areas	154
20	Response rate of float for a range of wall orifice areas	155
21	Layout of photocells along pipe for initial tests, and also orientations of light source and photocell	156
22	Effect of 10 slot orifices on local water and solid velocities as shown by velocity profiles	157
23	Schematic layout of rig for w.c. discharge characteristic tests	158
24	Schematic elevation of straight plastic pipe test rig	159
25	Schematic elevation of straight cast iron pipe test rig	160
26	Schematic plan view of test rig for testing a plastic 135° knuckle bend at 3.88 metres from w.c.	161
27	Schematic plan view of test rig for testing a plastic 135° knuckle bend at 5.90 metres from w.c.	162
28	Schematic plan view of test rig for testing a plastic 135° knuckle bend at 7.937 metres from w.c.	163
29	Schematic plan view of test rig for testing a plastic 92½° radiused bend at 3.93 metres from w.c.	164
30	Schematic plan view of test rig for testing a plastic 92½° radiused bend at 5.975 metres from w.c.	165
31	Schematic plan view of test rig for testing a plastic 92½° radiused bend at 8.017 metres from w.c.	166
32	Schematic plan view of test rig for testing 2 plastic 135° knuckle bends at 5.927 and 7.010 metres from w.c.	167
33	Schematic layout of a 135° junction with horizontal entry	168

Figure No.		Page No.
34	Schematic plan view of test rig for testing a plastic 135° junction with horizontal branch entry	169
35	Schematic layout of a 135° junction with 45° entry via a 148° adjustable bend	170
36	Schematic plan view of test rig for testing a plastic 135° junction with 45° branch entry	171
37	Schematic layout of a 135° junction with vertical entry via a 135° knuckle bend	172
38	Schematic elevation of test rig for testing a plastic 135° junction with vertical branch entry	173
39	Schematic layout of 92½° junction with horizontal branch entry	174
40	Schematic plan view of test rig for testing a plastic 92½° junction with horizontal branch entry	175
41	Schematic layout of a 135° junction for tests on straight pipe flow through junction with branch entry at varying angles	176
42	Schematic plan view of test rig for testing straight pipe flow through a plastic 135° junction with branch entry at varying angles	177
43	Schematic plan view of test rig for testing a cast iron 92½° radiused bend at 6.323 metres from w.c.	178
44	Schematic plan view of test rig for testing a cast iron 92½° junction with horizontal branch entry	179
45	Schematic elevation of straight glass pipe test rig	180
46	W.C. discharge characteristic test results	181
47	W.C. discharge characteristic retest results on (ASL)	182
48	Pen recorder traces showing photocell and LVDT output for (APLV1) and (ASLV1) during w.c. discharge characteristic tests	183

Figure No.		Page No.
49	Pen recorder traces showing photocell and LVDT output for (TPLV1) and (TSLV1) during w.c. discharge characteristic tests	184
50	Pen recorder traces showing photocell and LVDT output for (APHV1) and (ASHV1) during w.c. discharge characteristic tests	185
51	Pen recorder traces showing photocell and LDVT output for (TPHV1) and (TSHV1) during w.c. discharge characteristic tests	186
52	Schematic illustration of flow zones along waste pipe and forces acting on solid	187
53	(APLU1) straight plastic pipe tests, V plotted against L	188
54	(APLU1) straight plastic pipe tests, V plotted against $\sqrt{L}$	189
55	(APLU1) straight plastic pipe tests, V plotted against $\sqrt{L/G}$	190
56	Straight plastic pipe tests, single maternity pad unvented, V plotted against $\sqrt{L/G}$ , for all low level w.c's.	191
57	Straight plastic pipe tests, single maternity pad vented, V plotted against $\sqrt{L/G}$ , for all low level w.c's.	192
58	Straight plastic pipe tests, maternity pad plus three Kleenex paper towels, unvented, V plotted against $\sqrt{L/G}$ , for all low level w.c's	193
59	Straight plastic pipe tests, maternity pad plus three Kleenex paper towels, vented, V plotted against $\sqrt{L/G}$ , for all low level w.c's.	194
60	Straight plastic pipe tests, maternity pad plus three Bowater Scott paper towels, unvented, V plotted against $\sqrt{L/G}$ , for all low level w.c's	195
61	Straight plastic pipe tests, maternity pad plus three Bowater Scott paper towels, vented, V plotted against $\sqrt{L/G}$ , for all low level w.c's	196
62	(APL1) straight plastic pipe, velocity profiles showing stack venting effect	197

Figure No.		Page No.
63	(ASL) straight plastic pipe, velocity profiles showing variation between a maternity pad and a sanitary towel	198
64	(APLV1) straight plastic pipe, depth profiles at 1/40	199
65	(APLV1) straight plastic pipe, depth profiles at 1/60	200
66	(APLV1) straight plastic pipe, depth profiles at 1/80	201
67	(APLV1) straight plastic pipe, depth profiles at 1/100	202
68	(APLV1) straight plastic pipe, depth profiles at 1/150	203
69	(APLU3) straight plastic pipe, depth profiles at 1/40, solids together	204
70	(APLU3) straight plastic pipe, depth profiles at 1/40, solids separate	205
71	(ASLV1) straight plastic pipe, depth profiles at 1/100	206
72	(TPLV1) straight plastic pipe, depth profiles at 1/100	207
73	(TSLV1) straight plastic pipe, depth profiles at 1/100	208
74	(APLV) straight plastic pipe, depth profiles at 1/100, water only	209
75	(ASLV) straight plastic pipe, depth profiles at 1/100, water only	210
76	(TPLV) straight plastic pipe, depth profiles at 1/100, water only	211
77	(TSLV) straight plastic pipe, depth profiles at 1/100, water only	212
78	(APLU1) straight cast iron pipe, V plotted against $\sqrt{L/G}$	213
79	(APLV1) straight cast iron pipe, v plotted against $\sqrt{L/G}$	214

Figure No.		Page No.
80	(APLU2) straight cast iron pipe, V plotted against $\sqrt{L/G}$	215
81	(APLV2) straight cast iron pipe, V plotted against $\sqrt{L/G}$	216
82	(TSLU1) straight cast iron pipe, V plotted against $\sqrt{L/G}$	217
83	(APLV1) straight glass pipe, V plotted against $\sqrt{L/G}$	218
84	(APLV2) straight glass pipe, V plotted against $\sqrt{L/G}$	219
85	Diagrammatic explanation of effects of a bend or junction and definition of relative areas of interest	220
86	(APLU1) 135° plastic bend at 3.88 m from w.c., V plotted against $\sqrt{L/G}$	221
87	(APLV1) 135° plastic bend at 3.88 m from w.c., V plotted against $\sqrt{L/G}$	222
88	(APLV2) 135° plastic bend at 3.88 m from w.c., V plotted against $\sqrt{L/G}$	223
89	(APLU1) 135° plastic bend at 5.90 m from w.c., V plotted against $\sqrt{L/G}$	224
90	(APLV1) 135° plastic bend at 5.90 m from w.c., V plotted against $\sqrt{L/G}$	225
91	(APLV2) 135° plastic bend at 5.90 m from w.c., V plotted against $\sqrt{L/G}$	226
92	(APLU1) 135° plastic bend at 7.937 m from w.c., V plotted against $\sqrt{L/G}$	227
93	(APLV1) 135° plastic bend at 7.937 m from w.c., V plotted against $\sqrt{L/G}$	228
94	(APLV2) 135° plastic bend at 7.937 m from w.c., V plotted against $\sqrt{L/G}$	229
95	(APLV1) 2 x 135° plastic bends at 5.927 m and 7.010 m from w.c., V plotted against $\sqrt{L/G}$	230
96	(APLU1) 92½° plastic bend at 3.93 m from w.c., V plotted against $\sqrt{L/G}$	231

Figure No.		Page No.
97	(APLV1) 92½° plastic bend at 3.93 m from w.c., V plotted against $\sqrt{L/G}$	232
98	(APLV1) 92½° plastic bend at 5.975 m from w.c., V plotted against $\sqrt{L/G}$	233
99	(APLV1) 92½° plastic bend at 8.017 m from w.c., V plotted against $\sqrt{L/G}$	234
100	Photograph of start of blockage build up for vertical junction entry	235
101	Photograph of total blockage for vertical junction entry	236
102	Photograph of total blockage for vertical junction entry, showing paper towel having backflowed up the main drain	237
103	Photograph of full test rig for vertical junction entry tests	238
104	(APLU1) 135° plastic junction with horizontal entry, V plotted against $\sqrt{L/G}$	239
105	(APLV1) 135° plastic junction with horizontal entry, V plotted against $\sqrt{L/G}$	240
106	(APLV2) 135° plastic junction with horizontal entry, V plotted against $\sqrt{L/G}$	241
107	(APLV3) 135° plastic junction with horizontal entry, V plotted against $\sqrt{L/G}$	242
108	(APLU1) 135° plastic junction with 45° entry, V plotted against $\sqrt{L/G}$	243
109	(APLV1) 135° plastic junction with 45° entry, V plotted against $\sqrt{L/G}$	244
110	(APLV2) 135° plastic junction with 45° entry, V plotted against $\sqrt{L/G}$	245
111	(APLV3) 135° plastic junction with 45° entry, V plotted against $\sqrt{L/G}$	246
112	(APLU1) 135° plastic junction with vertical entry, V plotted against $\sqrt{L/G}$ , including effect of venting the non-live main drain	247
113	(APLV1) 135° plastic junction with vertical entry, V plotted against $\sqrt{L/G}$	248

Figure No.		Page No.
114	(APLV2) 135° plastic junction with vertical entry, V plotted against $\sqrt{L/G}$	249
115	(APLV3) 135° plastic junction with vertical entry, V plotted against $\sqrt{L/G}$	250
116	(APLV1) 135° plastic junction with straight pipe flow through junction with varying angle of branch entry, V plotted against $\sqrt{L/G}$ including variation between maternity pads	251
117	(APLV2) 135° plastic junction with straight pipe flow through junction with varying angle of branch entry, V plotted against $\sqrt{L/G}$	252
118	(APLV1) 92½° plastic junction with horizontal entry, V plotted against $\sqrt{L/G}$	253
119	(APLV2) 92½° plastic junction with horizontal entry, V plotted against $\sqrt{L/G}$	254
120	(APLV1) 92½° cast iron bend at 6.323 m from w.c., V plotted against $\sqrt{L/G}$	255
121	(APLV1) 92½° cast iron junction with horizontal entry, V plotted against $\sqrt{L/G}$	256
122	Schematic representation of the design method	257

Table No.		Page No.
1	Summary of w.c. discharge characteristics test results	258
2	Summary of w.c. discharge characteristics retest results on (ASL)	259
3	Tabulation of w.c. failure rates and coefficients for straight plastic pipe	260
4	Percentage flush ahead of solid for straight plastic pipe tests	261
5	Percentage flush ahead of solid for straight cast iron pipe tests	262
6	Tabulation of w.c. failure rates and coefficients for straight cast iron pipe	262
7	Percentage flush ahead of solid for straight glass pipe tests	263
8	Tabulation of w.c. failure rates and coefficients for straight glass pipe	263
9	Summary of results for plastic bend tests	264
10	Summary of results for plastic junction tests	266
11	Summary of results for cast iron bend and junction tests	268

## NOTATION

A, a	Cross sectional area
C	Coefficient
$C_D$	Orifice discharge coefficient
$C_a, C_b, C_e, C_f$	Empirical constants
$C_s$	Head loss coefficient due to venting arrangement at the stack
$C_v$	Head loss coefficient due to effect of venting the w.c. discharge
$C_1$	Empirical coefficient representing the theoretical solid velocity at entry to the discharge pipe, assuming zone 1 does not exist
$C_2$	Empirical coefficient defining the solid deceleration
$C_3$	Defined as $C_1/C_2$ which gives the mean $\sqrt{L/G}$ value at zero solid velocity
$C_4$	The percentage difference between the $C_3$ value for plastic and $C_3$ value of either cast iron or glass pipe
D, d	Pipe diameter
dH	Differential of head difference
ds	Solid thickness
do	Diameter of orifice
F	Variance ratio
$F_1$	W.C. failure rate, defined as a percentage of the number of times the solids do not leave the w.c. pan divided by the total number of successful flushes.
$F_2$	Partial w.c. failure rate, defined as a percentage of the number of towels left in the w.c. trap divided by the total number of towels used, ignoring total w.c. failures.
f	Friction factor
$f_{1-7}$	A function of, each subscript indicating a different function
G	Pipe gradient defined as h/L

$g$	Acceleration due to gravity
$H$	Instantaneous head difference
$h$	Change in pipe elevation
$K, k$	Pipe material defined by its roughness size
$k_L$	Orifice loss coefficient
$L$	Distance along pipe in metres, measured from the w.c. inlet centre line
$L_B$	Distance of a bend from the w.c., in metres
$L_P$	Length of pipe section
$l_s$	Length of solid
$m$	Hydraulic mean depth defined as the ratio of the cross sectional area of flow to the perimeter in contact with the fluid
$N_B$	Number of bends per unit length of pipe
$N_J$	Number of junctions per unit length of pipe
$n$	Sample size (suffix defines the sample applicable)
$Q$	Rate of flow
$Q_F$	Volume of flush
$Q_b$	Volume of flush following solid out of the trap
$Re$	Reynolds number
$S$	Standard deviation (suffix defines the sample applicable)
$S^2$	Sample variance (suffix defines the sample applicable)
$T_f$	Duration of flush
$T_O$	Solid saturation time
$T_s$	Material soaking time
$t$	Student's $t$ (statistics)
$tw$	Pipe wall thickness

$V$	Solid velocity
Vol	Volume discharged
$V_o$	Solid velocity at pipe entry
$V_s$	Velocity of solid as it leaves the w.c. trap
$V_w$	Water velocity
$W$	Solid weight saturated
$W_o$	Solid weight dry
$W_s$	Width of solid
$\Delta t$	Time increment
$\epsilon$	Pipe wall roughness, including pipe joint effects
$\epsilon_s$	Surface roughness of solid
$\eta$	Probability of a stoppage occurring
$\mu$	Fluid viscosity
$\rho$	Fluid density
$\rho_s$	Solid density
$\sigma^2$	Population variance (suffix defines the sample applicable)
$\hat{\sigma}^2$	Best estimate of the population variance (suffix defines the sample applicable)
$\phi$	A function of

## TEST IDENTIFICATION CODING

A	Armitage Shanks
T	Twyfords
P	P-trap
S	S-trap
L	Low level cistern
H	High level cistern
U	Unvented w.c. discharge
V	Vented w.c. discharge
1	Single maternity pad
2	Maternity pad plus three Kleenex paper towels
3	Maternity pad plus three Bowater Scott paper towels
4	Either single maternity pad with no flush pipe restrictor fitted, only used during the w.c. discharge characteristics testing or Single sanitary towel, only used during the straight plastic pipe testing.
5	Single maternity pad, 30.2 mm diameter flush pipe restrictor fitted
6	Maternity pad plus three Kleenex paper towels, 30.2 mm diameter flush pipe restrictor fitted.

Note: Normal flush pipe restrictors fitted for high level cisterns unless indicated to the contrary. Armitage Shanks 28.2 mm diameter restrictor in 30.8 mm bore flush pipe. Twyfords 23.8 mm diameter restrictor in 30.8 mm bore flush pipe.

## ABBREVIATIONS AND DEFINITIONS

DVM	Digital volt meter
I.D.	Internal diameter
LVDT	Linear voltage displacement transducer
Plastic	Refers to UPVC
PTFE	Polytetrafluorethylene
O.D.	Outside diameter
R-C	Resistor-capacitor network
UPVC	Unplasticized polyvinyl chloride
% FAS	Percentage flush ahead of the solid at entry to the discharge collection tank
Vented and Unvented	Unless stated to the contrary this refers to either vented or unvented w.c. discharge
$\sqrt{L/G}$	A term defined as the square root of (distance along the discharge pipe divided by the pipe gradient) and which is a function of solid deceleration and has the units (metres) <sup>1/2</sup> .

## 1. INTRODUCTION

A modern hospital requires an ever increasing range and complexity of building services, which can now account for half the capital cost of a new hospital project (1). One of these building services, drainage, which in terms of capital cost is by no means the most expensive of services, accounting for some 6% of the total cost of the engineering installations (1), is probably one of the most essential and fundamental of all. Until recently, the design of the drainage system has been based on previous experience with few constraints imposed by space requirements, which place limits on such features as pipe gradients, positions of discharge stacks and pipe positions. The modern trend towards high rise hospital buildings with limited inter-floor and duct space, with the resultant installation problems created by the interaction with other services, coupled with the need for economy, and the recent requirement for totally internal drainage systems by both building regulations, which have been subsequently relaxed, and aesthetic considerations, created the necessity for both a better understanding of the mode of transport of solids in horizontal discharge pipes and its application to the design and provision of efficient drainage systems. Hospitals are almost unique in their drainage requirements due to the generally heavier discharge loads imposed on the system, and the requirement for a minimum of ingress of bacteria into the hospital environment. Obviously, frequent blockages necessitate frequent clearing, which increases the risk of bacteriological release, affects the efficiency of the hospital and involves expensive maintenance.

It was for these reasons that the Department of Health and Social Security (DHSS), through their Study Group 9, approached the Department of Building Technology at Brunel University for advice. The Department of Building Technology carried out an intensive pilot study in the summer of 1974 aimed at investigating and identifying the parameters influencing the efficiency of above ground hospital drainage systems, and to comment on the feasibility of an integrated design technique for these systems. The success of the pilot study, reported by Swaffield (2), resulted in the three year research programme which is presented in this thesis.

Due to the lack of other work in this area that dealt specifically with the characteristics of solid transport, the research programme was based initially on Swaffield's work. The programme involved monitoring the mode of waste solid transport along UPVC, cast iron and glass 100 mm diameter discharge pipes, with various bends and junctions being included during the later phases of the testing. All eight DHSS approved w.c. pans, all operating on a 9.1 litre flush, were tested, including the effect of venting the w.c. discharge. Waste materials consisting of a maternity pad or a maternity pad plus two types of three paper towels were adopted as a representative hospital w.c. discharge load. The testing involved the measurement of solid velocity and depth of flow along the discharge pipe, together with various other parameters considered important. The results obtained from these tests, together with full

descriptions of the apparatus, specialized instrumentation developed, test procedures and the various computer programs used to analyse the test data are presented in this thesis.

## 2. HISTORICAL BACKGROUND

### 2.1 Origins of Drainage.

According to reference (3), the earliest recognisable attempts at sanitation can be traced back to neolithic man, who excavated pits for the disposal of refuse and excrement. It is likely that the motivation to provide even this crude form of sanitation was based, either directly or indirectly, on a wish to improve either health standards, or living conditions. With the passage of time and man's increasing drift towards community dwelling, the necessity for sanitation obviously increased.

The earliest identifiable use of foul drainage was found at Knossos in Crete and has been dated at 3000 B.C. Generally streams and water courses were used to convey waste material away from the occupation site, but where these were at some distance, ditches and drainage channels were constructed to serve as open sewers. Remains of these have been discovered at Khorsabad, Assyria (800 B.C), constructed of brick and arched over with a brick vault. Many of the larger Greek and Roman houses were provided with their own drainage systems which were, in the principal centres, connected to municipal sewers conveying both foul and storm water, to discharge either into natural water courses or, in the case of a coastal town, into the harbour.

It is perhaps relevant to mention the Roman writer Vitruvius, who stated that aqueducts should have a minimum gradient of  $1/5000$ , indicating the extremely high standards of construction of the Roman

aqueducts. Vitruvius also discussed the dangers inherent in the use of lead pipes for drinking water, and advised the use of earthenware pipes, a piece of advice which was unfortunately unheeded for over 2000 years.

## 2.2 Events leading up to Modern Sanitary Law

In medieval times monasteries often had the best water supply and drainage systems. At Christ Church, Canterbury, waste water and storm water was carried under the "necessarium" or latrine to flush the drain. At St. Albans, a stone cistern was provided to store rain water used to flush the latrine. Most medieval drainage systems discharged directly into a convenient water course close at hand, or in the case of castles and manor houses, the moat was utilized.

In towns and cities, sewage disposal was generally provided for each house via a cesspit. In hot weather these pits became offensive and water supplies were often contaminated when the pits overflowed.

The accumulation of filth and waste matter caused by lack of proper sanitation and congestion, led to repeated outbreaks of serious epidemics. The Black Death, an outbreak of bubonic plague, which spread from the East and was contracted from infected rats, is estimated to have caused the death of one-third of the population of England in 1348 and 1349. Plague recurred on several occasions over the next three hundred years as conditions tended to deteriorate rather than improve. By the end of the 16th century conditions were so bad, and the overcrowding of houses and tenements had created such pockets

of congestion, that the Crown took action in 1592 with an Act which sought to restrict the building of further dwellings within the City of London and its environs. However the sanitary conditions in London continued to be highly unsatisfactory and in 1765 35% of the London death rate was accounted for by children under two years of age. In that same year the Commissioners of Sewers and Pavements presented a report highlighting the problems, such as rubbish accumulation and inadequate drainage.

Finally, during the early 19th century, public conscience was stirred, resulting in a growing awareness of the appalling insanitary conditions in towns and cities. Sewage treatment, as used today, did not exist, and a drainage system was merely a pipe taking foul water by the shortest route to the nearest watercourse. It was not until the 1850's that proposals were made to intercept, by artificial channels and sewers, the daily flow of London's sewage and carry it to outfalls, well downstream of the city. The Metropolitan Board of Works was created in 1855 to assume responsibility for London's sewers. A network of sewers was laid and the watercarriage system of disposal introduced, which led to a much improved standard of public health.

In the meantime, in 1848, the Public Health Act was passed and modern sanitary law came into being, prompted by the recurrent outbreak of cholera and typhoid. The Public Health Act of 1875 provided for the appointment of persons qualified to act as surveyors of paving, drainage etc. Subsequent Acts of Parliament have continued to extend

and modernise legislation to deal with matters connected with the public health aspects of building in urban and rural communities.

### 2.3 Brunel's Contribution

It is perhaps ironical that the great engineer, Isambard Kingdom Brunel, should have been one of the original advocates of efficient drainage for hospitals (4) and that the University bearing his name should now be involved in an area of research aimed specifically at realising this ideology. It is therefore perhaps relevant to consider Brunel's achievements in designing one of the first purpose built hospitals.

Due to the appalling health conditions prevailing at Scutari hospital during the Crimean war and the dedication of Florence Nightingale, who highlighted the problems, the people in Britain were so profoundly shocked as to censure the Government of Lord Aberdeen, who was succeeded by Lord Palmerston. In February 1855 a Sanitary Commission was sent to Scutari by Lord Panmore. As a result, I.K. Brunel was asked if he would design a hospital which could be quickly built in England and then shipped out for assembly on some predetermined site. Brunel then proceeded to design a 1000 bed hospital based on a standard unit of two wards each for 24 patients, each unit being self contained with its own nurses rooms, water closets, outhouses etc. There were fixed wash basins and invalid baths of Brunel's own design and each unit was sent out with its own wooden trunk drainage

system with the specific instructions:

"do not let anything induce you to alter the general system and arrangement that I have laid down."

Doctor Parkes was appointed Chief Medical Superintendent of the new hospital and was described by Brunel as

"an enthusiastic, clever, agreeable man, devoted to the object, understanding the plans and works and quite disposed to attach as much importance to the perfection of the building and all those parts I deem most important as to mere doctoring."

Brunel's foresight is also epitomised by the ventilation system designed to force air into the wards and not to extract it as that might draw smells from the closets into the wards. Brunel himself said

"if I have a monomania it is a belief in the efficiency of sweet air for invalids."

Brunel's passionate concern for detail is exemplified by a passage from a letter to Dr. Parkes:

"You will be amazed to find certain boxes of paper for the water closets - I find that at a cost of a few shillings per day an ample supply could be furnished and the mechanical success of the w.c's will be much influenced by this. I hope you will succeed in getting it used and not abused. In order to assist in this important object I send out some printed notices or handbills to be stuck up, if you see no objection, in the closet room opposite each closet exhorting the men to use the apparatus properly and telling them how to do so."

The erection of Brunel's hospital began on May 21st and was ready to admit 300 patients by July 12th and was fully equipped, with its full quota of 1000 beds, by December 4th. From the first suggestion to final completion took under 10 months, an incredible achievement,

especially by modern standards. In the short time it was operating before peace was declared, fifteen hundred sick and wounded men passed through its wards, of whom only 50 died. Brunel's view of the success of his hospital is summed up by the following extract from one of his letters:

"Everybody here expresses themselves highly satisfied with everybody there and what we have done. I should wish to show that it was no spirit but just a sober exercise of common sense."

#### 2.4 Methods of Drainage Design

Reference (5) defines the essential requirements of a drainage system which can be summarized as the need to carry away the foul water from a building quickly and quietly, avoiding blockages, with freedom from nuisance or risk of injury to health. It is not until the methods by which these requirements are achieved, that the complexity of drainage system design becomes apparent. Drainage pipes must be adequately sized and provided with sufficient falls to ensure the efficient passage of both water and solids. Foul air is prevented from entering the building, from the drainage pipes, by the provision of traps at each sanitary appliance designed to retain an adequate water seal at all times. Due to pressure fluctuations created within the drainage system special precautions are necessary to prevent the destruction of the trap seals.

#### 2.4.1 Drainage Design at the Start of the Century

A design method, based on a set of rules evolved by trial and error during the latter part of the nineteenth century, provided drainage systems which worked satisfactorily but with questionable economy. By-laws consolidated these rules into an inflexible design system with a definition of responsibility typified by the following extract from the Public Health Act of 1891:

"If a watercloset or drain is so constructed or repaired as to be a nuisance or injurious or dangerous to health, the person who undertook or executed such construction or repair shall, unless he shows that such construction or repair was not due to any wilful act, neglect, or default, be liable to a fine not exceeding twenty pounds."

The regulations required that the trap of every sanitary appliance should be vented, and also stipulated the method by which this should be achieved. A general rule, quoted in reference (6), termed Maguire's Rule, stipulated that the gradient of a drainage pipe should be "unit drop in ten times the pipe diameter measured in inches" or in S.I. units, unit vertical drop in a horizontal distance defined by the pipe diameter measured in millimetres divided by 2.54. The rule is based on minimum self cleansing velocities (0.75 m/s) and is generally applicable to below ground drainage gradients. However the rule appears to form the basis of the old rule of thumb saying 4" drains 1 in 40, 6" drains 1/60 etc. This would indicate that larger drains can be laid at flatter gradients, which is obviously a misconception since, for a given fall, the smaller the pipe the greater the depth of flow and the higher

the velocity, assuming maximum 3/4 bore depth of flow.

#### 2.4.2 The Necessity for Greater Freedom of Design

The more recent trend towards larger and better buildings with totally internal drainage systems, with the added necessity for economy, has resulted in the development of new methods of design. Accordingly, legislation has been changed to the extent that standards of performance are now required rather than the compliance to a set of rules. This obviously imposes greater responsibility upon the designer, who is now provided with a number of solutions, the final choice generally being dictated by economy.

#### 2.4.3 Definition of Modern Design Requirements

The requirements of a drainage installation can be listed as follows:-

- a) the installation should be watertight
- b) pipes should be smooth bored, correctly aligned, laid to sufficient gradients as to ensure the non-deposition of solids and be economically sized to accommodate all probable flow conditions.
- c) the installation should be economically designed so as to prevent excessive pressure fluctuations within the system, and hence prevent trap seal loss.

#### 2.4.4 Two-pipe System

The two-pipe system, as defined in reference (7) and so called because the "soil" and "waste" were piped separately, was the traditional but now outdated system of sanitation. The two discharge pipes were ultimately combined into one common drain below ground, and

each was provided with its own independent ventilating or anti-siphonage pipework. This system therefore involved a total of four vertical stacks.

#### 2.4.5 One-pipe System

In the one-pipe system, "soil" and "waste" are conveyed together into one common pipe with all branch ventilating or anti-siphonage pipes connected to one main ventilating pipe. This system therefore involved a total of two vertical stacks, with obvious economic advantages.

#### 2.4.6 Single-stack System

This system, suitable for use in both low-rise and high-rise buildings but subject to certain limitations, has a single stack as the name implies, without ventilating pipes. As long as careful consideration is given to both avoiding excessive pressure fluctuations within the drainage system and preventing self siphonage, this system is obviously the most economic of all, enabling savings of up to between 30% and 40% as suggested by references (1) and (8). The modified single stack system is used where only partial ventilation of the system is required.

A considerable amount of research and analysis work has been carried out by the Building Research Establishment (BRE) in this country and also by the National Bureau of Standards in America, in order to identify the feasibility of this drainage system in various applications. In Great Britain, the most notable contributions to

this general area are references (9) and (10) in which the effects of self siphonage were investigated, (11) in which the effects of induced siphonage were investigated, and (8) in which a method for the sizing of drainage and vent stacks in multi-storey buildings is presented. More recently, reference (12) reviewed the current knowledge on the fluid mechanics of drainage systems and reference (1) analysed the economic advantage of the single-stack system. Investigations of a more specific nature are presented in references (13), (14) and (15) and reference (16) advises changes to the present scales of provision of sanitary appliances based on an analysis of usage patterns and probability theory. The references mentioned above give a brief outline of the more fundamental topics of research in this area, as carried out by the BRE in this country.

As mentioned, the National Bureau of Standards in Washington DC has also carried out a considerable amount of work in this area with two of the most fundamental contributions being presented in references (17) and (18).

It is interesting to note that of all the mentioned references which involved w.c. discharges, only references (9), (11) and (18) included tests involving solids in the w.c. discharges, and that these were only included to investigate their effect on pressure variations within the system. The work reported in this thesis is therefore intended to be complementary to this previous work by providing information on a previously uninvestigated area namely the mechanism of solid transport in discharge pipes.

#### 2.4.7 Separation of Soil and Surface Water

The Public Health Act of 1936 requires that:

"no pipe for conveying rain water from a roof shall be used for the purpose of conveying the soil or drainage from any sanitary convenience."

However the Act does not extend to Scotland, Northern Ireland or London, and in these areas it is permitted to connect roof rain water outlets directly to the soil or drainage discharge pipes, and although this can provide certain advantages, the practice is perhaps inadvisable due to the possibility of unpredictably excessive flow rates and the risk of entry of foreign matter.

#### 2.4.8 CP 304: 1968

In order that the foregoing considerations may be put into practice, the present legislations on above ground drainage designs are summarized in the current British Standard Code of Practice 304. This document (19), which is currently being revised, deals with the design, installation, testing and maintenance of discharge and ventilating pipes for buildings. The method of sizing both vertical stacks and horizontal branches is based on a system of discharge unit values, defined in the code. The maximum length, size and range of gradients applicable to single branches serving waste appliances without the provision of ventilating pipework, is based on previous experience, test data, and the prevention of trap seal loss and self-siphonage. Where provision of ventilating pipework is required, the code provides details of sizing and the degree of ventilation required.

## 2.5 The Possibility of Drainage Design Based on Solid Transport Characteristics

The initial research in this area, reported by Swaffield (2), was a new approach to the design of horizontal drainage systems. Whilst CP304 is adequate for general design, it is based to a large extent on tests carried out with water only. The aim of the work reported in (2) was the provision of a better understanding and appreciation of the way in which solids are conveyed along above ground horizontal drainage pipes, and to investigate the feasibility of a design method based on the prevention of solid deposition. Whilst some of the theories presented in (2) have subsequently been disproved by this more detailed investigation, the feasibility of the postulated design method has been demonstrated.

## 2.6 In Conclusion

This brief summary of drainage evolution, design and legislation can obviously only outline the progress made. However it is possibly worth noting that the motivation for good drainage design has remained largely unchanged - the prevention of disease and infection. To this continuing aim has now to be added the results of the immense changes in both the social and health provision expectation of the population over the short period covered by the U.K. legislation, tempered only by the economic restraints inherent in our developing society.

### 3. THEORY

#### 3.1 Parameters Affecting Drainage Performance

Swaffield (2) suggested that the probability of a stoppage occurring could be defined as:

$$\eta = \phi \left( \frac{L}{D}, G, \frac{K}{D}, C_s, N_J, N_B, \frac{T_s}{T_o}, \frac{T_f}{T_s}, \frac{W_o}{W}, C_v, \frac{Q_F}{Q_b}, \frac{l_s}{ds}, \frac{W_s}{ds}, \frac{V_s^2}{Dg} \right) \quad (3 - 1)$$

the notation being defined in the following three categories:

##### i) Pipe characteristics

L - pipe length

D - pipe diameter

G - pipe gradient

K - pipe material defined by its roughness size

$C_s$  - head loss coefficient due to venting arrangement at the stack

$N_J$  - number of junctions per unit length of pipe

$N_B$  - number of bends per unit length of pipe

##### ii) Input device characteristics

$T_f$  - duration of flush

$T_s$  - material soaking time

$Q_F$  - volume of flush

$Q_b$  - volume of flush following solid out of trap

$V_s$  - velocity of solid as it leaves the w.c. trap

$C_v$  - head loss coefficient due to effect of venting the w.c. discharge

## iii) Material properties

ls - solid length	}	representing a shape parameter
Ws - solid width		
ds - solid thickness		
To - solid saturation time		
Wo - solid weight dry		
W - solid weight saturated		

Whilst (3 - 1) attempts to define the parameters involved, the phenomena involved in the passage of water and solids along a drainage pipe are in fact considerably more complex. From the tests carried out by Swaffield, it is possible to appreciate some of the undefined parameters involved. The definition of material properties covers only a single waste solid such as a maternity pad, but does not define the parameters involved in the travel of a maternity pad with paper towels, which are considerably more complex due to the random discharge of each of the paper towels, and the probable interaction of the various solids. The effect of junctions and bends in a drainage pipe is definitely more complex than shown in equation (3 - 1) since individual bends and junctions require definition of angle, radius of curvature and velocity reducing effect. The definition of the input device characteristics of a w.c. is also probably inadequate due to the complexity of the flow rate profiles as indicated in reference (14). The effect of pipe material, as characterised by its roughness size K, requires greater definition due to the effects of pipe jointing.

Therefore, whilst equation (3 - 1) gives an insight into the complexity of some of the parameters involved in drainage flow, it should be appreciated that it does not adequately define all the parameters.

### 3.2 Theoretical Analysis of Straight Pipe Solid Deceleration

The previous section detailed the complexity of the parameters involved in an overall analysis of the flow characteristics in a drainage system. However, by considering the simpler case of solid deceleration in a straight pipe, it is possible to carry out a theoretical analysis.

The velocity of the solid and the adjacent fluid may be analyzed by means of the techniques of dimensional analysis. Assume that the solid velocity  $V$  is described by the following function:

$$v = f_i(\rho, \mu, \varepsilon, m, l_s, d_s, w_s, \rho_s, \varepsilon_s, L, h, g, V_o, V_w) \quad (3-2-1)$$

- where
- $\rho$  - fluid density
  - $\mu$  - fluid viscosity
  - $\varepsilon$  - pipe wall roughness, including pipe joint effects
  - $m$  - hydraulic mean depth of flow
  - $l_s, d_s, w_s$  - length, depth and width of solid
  - $\varepsilon_s$  - surface roughness of solid
  - $\rho_s$  - solid density
  - $L$  - distance along pipe
  - $h$  - change in pipe elevation
  - $g$  - acceleration due to gravity
  - $V_o$  - solid velocity at pipe entry
  - $V_w$  - water velocity

Thus 15 variables describe the flow in three dimensions

(mass, length and time), yielding 12 dimensionless groups:

$$\frac{V}{\sqrt{Lg}} = f_2 \left( \frac{V_0}{V_w}, \frac{V_w}{\sqrt{mg}}, \frac{\rho V_w m}{\mu}, \frac{\epsilon}{m}, \frac{d_s}{m}, \frac{l_s}{d_s}, \frac{w_s}{d_s}, \frac{\epsilon_s}{\epsilon}, \frac{L}{m}, \frac{e_s}{e}, \frac{h}{L} \right) \quad (3-2-2)$$

$\frac{V}{\sqrt{Lg}}$  is a form of Froude Number based on the solid velocity

$\frac{V_0}{V_w}$  defines the solid velocity at pipe entry

$\frac{V_w}{\sqrt{mg}}$  is a true Froude Number for the water ahead of the solid

$\frac{\rho V_w m}{\mu}$  is the flow Reynolds Number based on hydraulic mean depth

$\frac{\epsilon}{m}$  is the pipe relative roughness

$\left. \begin{array}{l} \frac{d_s}{m} \\ \frac{l_s}{d_s} \\ \frac{w_s}{d_s} \end{array} \right\}$  describe the solid's geometry and its pipe blockage effect

$\frac{\epsilon_s}{\epsilon}$  defines the relative roughness of the solid and the pipe, hence determining solid friction

$\frac{L}{m}$  defines the change in hydraulic mean depth due to water leakage past the solid as it travels along the discharge pipe

$\frac{e_s}{e}$  is the mass ratio term

$\frac{h}{L}$  is the pipe gradient G

From Swaffield's results obtained during the pilot study it would appear that the value of Reynolds Number for a water only flush is greater than 10,000 and hence the dependence of flow resistance on Reynolds Number is minimal and the  $\frac{\rho V_w m}{\mu}$  term may be dropped from the expression.

For tests on one waste material and one type of discharge pipe, the expression becomes:

$$\frac{V}{\sqrt{Lg}} = f_3 \left( \frac{V_0}{V_w}, \frac{V_w}{\sqrt{mg}}, \frac{L}{m}, \frac{h}{L} \right) \quad (3-2-3)$$

During the initial tests a limited amount of flow observation, together with Swaffield's findings (2), allow certain simplifying assumptions to be made. It was observed that  $m$ , i.e. as indicated by water depth in a constant cross section pipe, remains relatively constant for most of the solid travel, except immediately on entry to the discharge pipe. Therefore  $\frac{L}{m}$  can be ignored. In the case of observations on clear UPVC pipe, the velocity of the water ahead of the solid is not significantly greater than the solid velocity, and hence, as a first approximation, any effects dependent on a velocity difference between solid and water based on the term  $\frac{V_w}{\sqrt{mg}}$  can be ignored. Hence expression (3-2-3) becomes:

$$\frac{V}{\sqrt{Lg}} = f_4 \left( \frac{V_o}{V_w}, \frac{h}{L} \right) \quad (3-2-4)$$

or substituting  $G$  for  $\frac{h}{L}$

$$\frac{V}{\sqrt{Lg}} = f_5 \left( \frac{V_o}{V_w}, G \right) \quad (3-2-5)$$

Open channel flow theory indicates that the square root of gradient is the determining factor and since flatter gradients will logically cause greater deceleration it is suggested that  $1/\sqrt{G}$  might be the determining gradient term, giving:

$$\frac{V}{\sqrt{Lg}} = f_6 \left( \frac{V_o}{V_w}, \frac{1}{\sqrt{G}} \right) \quad (3-2-6)$$

If the analysis is further restricted to one type of w.c., which is assumed to exhibit reasonably repeatable water discharge velocity, then  $V_w$  will be constant at entry to the discharge pipe. Also assuming

g to be constant, the essential parameters involved in predicting solid velocity along the discharge pipe can be stated as:

$$V = f_v(V_0, \sqrt{L}, \frac{1}{\sqrt{G}}) \quad (3-2-7)$$

Therefore for one type of waste solid, one type of discharge pipe and one type of w.c. the solid velocity is dependant on initial entry velocity, the square root of distance along the pipe and the square root of the inverse of gradient, which can be verified by plotting velocity readings against both  $\sqrt{L}$  and  $\sqrt{1/G}$ .

Obviously several simplifying assumptions have been made in arriving at equation (3-2-7). Since the maternity pads, and paper towels where applicable, leave the w.c. trap in a fairly random fashion, and the effective shape varies, the terms  $\frac{ds}{m}$ ,  $\frac{ls}{ds}$  and  $\frac{Ws}{ds}$  do not strictly remain constant for a particular set of test conditions, and therefore some scatter is to be expected about any graphical plots based on equation (3-2-7).

### 3.3 Theoretical Analysis of Drainage Pipe Fittings

It is not worthwhile attempting a theoretical analysis of the effects of pipe fittings, such as bends or junctions, due to the extra parameters involved, and the complex interaction of all these parameters. However, assuming that a solution of the straight pipe solid deceleration characteristics is possible, as outlined in the previous section, then it should be possible to account for the effects of bends or junctions by reference to this straight pipe datum.

#### 4. APPARATUS AND INSTRUMENTATION

##### 4.1 General Apparatus

Figure 1 is a photograph of the test rig developed at the start of the research project while Figure 2 is a photograph of the test rig in use at the end of the project. The original test rig and the various modifications made to this rig during the course of the project are described in detail below.

##### 4.1.1 Large Support Rig

Figures 1 and 3 show the rig provided to act as a support for any sanitary appliance which discharges into a hospital drainage system. The support rig, constructed from dexion angle, consisted basically of a platform on which could be mounted a w.c. and a variable height flushing cistern as well as other sanitary appliances such as a disposable bed pan macerater unit, as is the case in Figures 1 and 3. It should be noted that the w.c. unit shown in Figures 1 and 3 is the original unit used during the pilot study and is not a standard unit, since the cistern height is at the old medium level which has since been superseded. The rig was designed to be capable of safely supporting loads of 1000 kg. The rig also supports the inlet end of the discharge pipe as can be seen in Figure 3. The large support rig was used in this form throughout the research project, with the only variation being that, for the heavier cast iron and glass drainage pipe systems, the inlet end of the discharge pipe was supported independently of the rig.

#### 4.1.2 Small Support Rig

Figure 1 shows the rig, constructed from dexion angle, which was provided as a support for the vertical stack and outlet end of the discharge pipe. A linear scale attached to the rig provided the necessary discharge pipe slope measurement. This support rig was only used during the initial instrumentation development stage and during the w.c. discharge characteristic testing, after which the pipe support system was adapted to accommodate longer pipe lengths, as detailed in Section 4.1.4.

#### 4.1.3 Discharge Pipe and Support System

Three different types of discharge pipe were tested during the research project, namely

- (1) Marley 102 mm (4") I.D. transparent UPVC pipe
- (2) Glynwed Timesaver 102 mm (4") I.D. spun cast-iron pipe
- (3) Schott-Kem 102 mm (4") I.D. glass pipe

The Marley transparent UPVC pipe was specially made for research purposes and met the same specifications and tolerances as the normal Marley UPVC drainage pipe. During the initial stages of the project, clear acrylic pipe couplers were used, as shown in Figure 1, but, due to the brittleness of this material, several couplers split, and consequently, normal opaque UPVC couplers were used for the straight plastic pipe testing and for the remainder of the research project. Pipe lengths of a standard 2 m were used throughout for all three drainage pipe systems. To ensure rigidity and linearity of the discharge pipe, heavy duty aluminium ladders of either 6.1 m (20')

or 7.3 m (24') lengths were used, each ladder being supported at each end. By hanging the ladders vertically, as shown in Figure 1, it was possible to achieve a high modulus of rigidity with minimum weight. The discharge pipe was supported beneath the ladder with pipe clamps fixed to 5/16" whitworth studding which passed through the hollow rungs of the ladder and was tightened at the top and bottom with nuts and washers. In order to counteract the deflection of the ladder under both its own weight, and the applied load, it was necessary to vary the gap between the ladder and the pipe to achieve linearity of the discharge pipe.

After attaching the discharge pipe under the ladder support, and having adjusted the ladder to be approximately horizontal, the centre line of the inlet end to the discharge pipe was adjusted to a standard 300 mm below the platform level of the large support rig. The discharge pipework was then levelled horizontally using a Vickers Cooke S33 Surveyor's level set up with the height of collimation at the same level as the top external surface of the inlet end of the discharge pipe, thus enabling single handed level adjustment without the need of a levelling staff. The discharge pipe was then levelled by adjusting the studding supports to an accuracy of  $\pm 0.2$  mm.

#### 4.1.4 Ladder Support Method and Gradient Adjustment

For plastic pipe testing, the inlet end of the ladder was supported on the large support rig by two eye bolts clamped to the top of the ladder as shown in Figure 3. This fixing method provided a swivel support capable of height adjustment. For the short pipe length testing,

namely the w.c. discharge characteristic testing, a single 6.1 m ladder was used, supported at the discharge end on steel studding attached to the small support rig. Linear vertical scales attached to the two support rigs and of a known separation enabled control, with the aid of a spirit level, of the height of the discharge pipe, and hence gradient control, by adjusting the steel studding and the eye bolts.

For all other straight pipe testing, independent supports were made up which utilised the steel roof trusses, spaced at 3.05 m (10') down the length of the laboratory. For each support, two vertical lengths of dexion angle were supported on the floor and clamped to a roof truss with a separation between the two vertical columns of 230 mm, thus allowing the ladder support and suspended pipe to pass between them, as shown in Figure 4. The ladder was supported between the vertical columns by turn buckles which provided a simple method of height adjustment. Vertical linear scales, attached to each of the vertical support columns provided the pipe gradient control.

#### 4.1.5. W.C. Inlet and Vertical Stack Outlet

The w.c. inlet into the "horizontal" discharge pipe varied depending on whether the w.c. was a P-trap or an S-trap. The P-trap w.c. connection was achieved with a Plastic Terrain adaptor No.125.4.5. fitted with a Terrain No 9124 rubber w.c. connector. This was close coupled to a 104° Key Terrain junction using a short length of 110 mm O.D. clear UPVC Marley pipe. A short vertical length of the same Marley pipe was then fitted to the bottom of the junction and a 92½°

Key Terrain bend joined in turn to the bottom of this pipe and then fitted to the horizontal pipe. The length of this vertical pipe was cut to provide the standard 300 mm from the platform level of the large support rig to the centre line of the horizontal discharge pipe. The top of the 104° junction was fitted with a 100 mm x 50 mm reducer which could be sealed with a threaded plug for the unvented w.c. discharge tests or left open for the vented tests.

The S-trap w.c. connection was achieved with a Terrain plastic and rubber w.c. connector, the plastic part of the connector being provided with a 50 mm O-ring seal boss. For vented w.c. discharge tests, a long right-angled 50 mm diameter vent pipe was fitted to this boss. For unvented tests this vent pipe was removed and a 50 mm plug used to seal the boss. A short length of 110 mm O.D. clear UPVC pipe was fitted to the plastic w.c. connector and a 92½° Key Terrain bend fitted to the lower end of this pipe, and the bend then joined in turn to the horizontal discharge pipe. The length of the vertical pipe was again cut to provide the standard 300 mm from the platform level to the centre line of the horizontal discharge pipe. Figure 23 shows the method by which either a P-trap, or an S-trap, w.c. with either vented, or unvented, discharge, was accommodated into the test rig.

In the case of the cast iron pipe, similar cast iron pipe fittings were used, except that a multikwik size No.1 self-sealing w.c. connector was used and in the case of the S-trap w.c. pans, no provision could be made for venting the w.c. discharge.

In the case of the glass pipe, only a P-trap w.c. was tested. Unfortunately, the glass pipe fittings required to connect the w.c. pan to the horizontal glass discharge pipe were not available for the glass pipe testing. The UPVC P-trap system, outlined above, was used instead by connecting the horizontal glass pipe to the 92½° Key Terrain UPVC bend.

In all pipe material types, the outlet end of the discharge pipe was fitted with a 92½° junction, with short lengths of pipe fitted above and below the junction, to simulate a vertical stack connection.

#### 4.1.6 Second Support Rig

In order to accommodate bends into the straight pipe rig described in Section 4.1.4, two free standing A-frame support rigs were constructed from dexion angle, and a 6.1 metre single span heavy duty aluminium ladder was hung between these supports, the discharge pipe being supported under the ladder with steel studding. By using the straight pipe rig with the second support rig, it was possible to accommodate any bend into the rig by manoeuvring the second support rig into the required position.

#### 4.1.7 Third Support Rig

In order to accommodate junctions into the straight pipe rig, an extra rig was required to support the non-live discharge pipe upstream of the junction. Due to limitations of laboratory size, it was impossible to use the ladder system of pipe support and

therefore the third support rig was a single free standing support rig constructed from dexion angle, which in turn supported a dexion angle U-beam, to provide the actual pipe support. The length of upstream pipe supported on this rig was 3.8 metres. By using the straight pipe rig, with the second and third support rigs, it was possible to accommodate any junction into the rig by manoeuvring the two movable support rigs either side of the straight pipe rig.

#### 4.1.8 Flushing Mechanism

In order to overcome the variable human element involved in flushing the w.c. an automated method of flushing was devised. A two-way compressed-air ram was attached to the cistern flushing arm by wire, with an electrically operated 5 port solenoid valve connected to the ram, and also to a button switch positioned on the instrumentation table, as shown in Figure 5. It was therefore possible, by pressing the solenoid valve switch, to apply a standard and repeatable force on the flush handle of the cistern. This did not, however, ensure a repeatable w.c. flush due to the other variables involved.

#### 4.1.9 Discharge Collection Tank

Figures 6 and 7 show the original discharge collection tank, and its ancillary equipment. The tank consisted of a 227 litre drum into which the waste stack discharged. In order to monitor the discharge entering the tank, it was necessary to prevent the drum emptying until required. The drum was fitted with a short upstand pipe connected to an S.M.C. Commodore 130 central heating pump which discharged into a laboratory floor drain via a flexible hose. To prevent self siphonage of the drum, the end of the hose was raised above the maximum level in

the drum. It was therefore impossible for the drum to drain, unless the pump was switched on.

In order to lower the water level in the tank to a standard level before each w.c. flush, a Waverley liquid level control unit was fitted to the tank. Two probes were attached inside the tank, one at the required minimum level, the other near the top of the tank. The level control unit was connected to a push button switch, positioned on the instrumentation table, as shown in Figure 5, and also connected to the pump. Having completed a test, the pump was started by pressing the switch, the pump continuing to run until the level in the tank dropped to the level of the lower depth sensor, at which point the pump automatically stopped. The upper depth sensor served as an emergency overflow, switching on the pump automatically if the water rose to this level. A small mesh fisherman's net placed in the tank below the vertical stack separated the waste solids from the flush water. This collection tank was used for all the testing up to and including the testing of the straight cast iron pipe.

At this stage, due to the national water shortage which occurred in 1976, and the fact that testing required up to 2,300 litres of water per day, a recirculating water supply system was incorporated into the test rig. Instead of discharging the collection tank into the laboratory drainage system, the discharge was collected in a 227 litre fibreglass storage tank. A Beresford PV100 centrifugal pump was then used to recirculate the water from the storage tank to the w.c. cistern via 25 mm diameter reinforced PVC hose. A combined suction strainer and non-return valve was fitted to the storage tank on the suction side

of the pump. The discharge side of the pump was fitted with a valve controlled by-pass pipe back into the storage tank, as well as the valve controlled supply to the w.c. cistern. By varying the two control valves, the flow rate to the cistern was adjusted to be identical to the original laboratory water supply flow rate used previously, giving a cistern filling time of 75 seconds. In order to minimise the accumulation of waste material in the water, a fine gauze filter bag was used to isolate the solids in the collection tank. Problems were experienced with discolouration of the recirculating water due to rust formation and the cause of this was traced to the 227 litre steel drum used as the collection tank. The problem was overcome by changing the drum for a 227 litre parallel sided fibreglass water butt incorporating all the features of the original drum shown in Figure 7. Due to the gradual build-up of fine waste material in the recirculating water, it was found necessary to change the water after approximately 1,000 tests, but this still provided a saving of 8,865 litres of water per 1,000 tests.

#### 4.2 Instrumentation

At the start of the research project it was decided to monitor the following parameters:

- a) water velocity
- b) solid velocity
- c) depth of flow
- c) rate of flow

The instrumentation system capable of accurately monitoring these variables, and the various modifications carried out during the project, is described in detail below.

#### 4.2.1 Original Method of Velocity Measurement

The original method of velocity measurement developed by Swaffield is described in reference (2). The method was based on the use of photo-electric cells and an H327-5 five channel pen recorder, with paper speeds of 1 to 250 mm/s.

Five photo-electric cells and light sources were mounted at 3.71 m intervals along the 110 mm O.D. transparent Marley discharge pipe and were linked to the pen recorder via a control box. As the leading edge of the water component of the flush passed each light source, so the output from the corresponding photo cell, mounted diametrically above the light source, was decreased, this change in output being displayed on the pen recorder by a change in pen deflection. As the leading edge of the solid passed each light source so the photo cell voltage output dropped to almost zero, giving a more pronounced and readily identifiable pen deflection. By analysing the traces on the pen recorder, knowing both the pen recorder paper speed and the separation of the photocell sensors along the pipe, it was possible to calculate mean water and solid velocities. The method of mounting the photocells and light sources used adapted Marley pipe clamps as shown in Figures 8 and 9.

Whilst this velocity measuring system was ideal for the first stage of the investigation, the method had several shortcomings in the context of the continuing three year investigation. It was considered essential to measure "point velocities" using a sensor separation as small as 0.1 m, as opposed to mean velocities over 3.71 m as used by Swaffield.

The limitations of this method are best analysed by considering the accuracy of the measurements, taking a water or solid velocity of 2 m/s and linear paper measurement accuracy of  $\pm 1.0$  mm and a pipe length of 14 m.

Sensor Separation mm	Paper Speed mm/s	Velocity Measurement Accuracy %	Estimated No. of tests per 50 m roll of paper
3710	50	$\pm 1.1$	36
3710	250	$\pm 0.2$	7
100	250	$\pm 8.0$	7

It was considered that a velocity measurement accuracy of  $\pm 8\%$  was unacceptable and also it was envisaged that testing would involve at least 10,000 w.c. flushes, requiring approximately 1,500 rolls of pen recorder paper. In order to obtain accurate and reliable data it was essential to provide a more sophisticated velocity measurement method, as described below.

#### 4.2.2 Timer Counter Velocity Measurement

Initially five OMB Electronics type 745 timer counters were purchased, capable of timing from  $10\mu\text{s}$  to 1s in 6 decades. The principle of this velocity measurement method was to start a timer by the change of voltage from a photocell and to similarly stop the timer with another photocell a known distance along the discharge pipe. In order to provide the necessary ancillary instrumentation, the Brunel University

"Electronics Construction Division" was approached to design and construct, a 6 channel timer control console incorporating the following facilities:

- a) A control to enable variation of the sensitivity so that the timers could be triggered by various depths of water and various types of solids.
- b) Null indicators to enable simple selection of correct output level.
- c) A system of latching to prevent any timer being retriggered by either water, or solids, following the initial triggering material.
- d) A push button facility to reset the latching facility described in (c), prior to the next flush.
- e) A push button facility to reset all the timers to zero.
- f) A patchwork system of leads and sockets to enable any timer to be started or stopped by any photocell.

Initially the original 6 channel black control box used to control the voltage output from the photocells was used. Figures 5 and 10 show the resultant timer control console and ancillary equipment. The velocity measurement system described was used for the instrumentation development and the w.c. discharge characteristic testing, but required modification for the subsequent tests.

The velocity measurement system described above used 6 photocells and 5 timers, which limited its application since four of the six photocells were required to both stop one timer and start another, thus preventing independent positioning of point velocity measuring stations. A sixth timer counter was purchased and the "Electronics Construction Division" made up a second 6 channel timer control console similar to the one described, and which was cross linked to

the original console via the patchwork leads. The original 6 channel black box was changed for a single 12 channel photocell control console incorporating the following facilities:-

- a) Potentiometer control of voltage output from the photocells as previously.
- b) Push button facility to read the voltage output from individual photocells on a digital volt meter (DVM).
- c) Switching facility for either damped or undamped photocell output. The damped output was provided via a resistor-capacitor network to remove the high frequency oscillations in voltage output, caused by the water "turbulence" close to the w.c. discharge.
- d) Push buttons to extinguish individual light sources to check base voltage output from the photocells and to aid adjustment of the triggering sensitivity.
- e) As well as the photocell/light source leads, and the leads linked to the timer control consoles, an extra set of leads was provided to enable the photocell voltage variations to be displayed on a pen-recorder.

Figure 11 shows all the control consoles and ancillary equipment used for the straight plastic pipe testing and for the remainder of the research project.

#### 4.2.3 Photocell Method for Depth of Flow Measurement

Figures 12 and 13 show the variation of voltage output from the photocells as water and solids travel down the pipe. The voltage output is obviously affected by the depth of flow in the pipe although there are obviously other parameters causing the sharp variations recorded, such as the presence of surface waves. By damping the output voltage from the photocells it was hoped to develop a depth measuring system that could be calibrated to provide linear measurement of flow depth. However, damping the output voltage sufficiently to prevent

the unwanted fluctuations also resulted in virtually zeroing the voltage change caused by a certain depth of water flow in the pipe. An attempt was therefore made to eliminate the external light sources which appeared to be causing reflection problems on the surface of the water flow.

Initially the external light was prevented from entering the pipe by wrapping black card round the outside of the pipe. No significant improvement in damping the voltage fluctuations from the photocells was achieved. It was then appreciated that the light sources themselves might be causing reflection on the internal bore of the pipe and to test this theory the black card was attached to the internal bore of the pipe. Again, no significant improvement in damping the voltage fluctuations from the photocells was achieved. It was, therefore, apparent that it was not reflection of light causing the voltage fluctuations but refraction, due to the rippled surface of flow.

By dyeing the water in the pipe it was anticipated that a more significant voltage drop from the photocells, due to depth of water, would be achieved. By adding increasing quantities of ink to each water flush it became apparent that no decrease in voltage fluctuations was being achieved and that there was no simple method of monitoring depth of flow using photocells.

#### 4.2.4 Float/LVDT Depth Measurement

The method finally adopted consisted of monitoring the vertical movement of a float attached to the core of a Linear Voltage Displacement Transducer (LVDT), supported in a U-tube connected into the discharge pipe. This method was adopted as it appeared to be the simplest and most practical solution to the problem of monitoring depth of flow in the discharge pipe. A 92½° Osma strap boss with a 51 mm boss socket was strapped to the discharge pipe, with an orifice cut in the pipe wall. The first type of U-tube was made up of a 51 mm x 38 mm reducer attached to the boss socket and then further reduced down to 19 mm. The U-tube itself, shown in Figure 9, was made up of Osma 19 mm pipe and elbows, terminating with a 140 mm length of 25 mm diameter perspex tube. This U-tube system was used successfully for the instrumentation development and w.c. discharge characteristic testing, but after these tests it was found that the joint between the Osma 19 mm UPVC tube and the 25 mm perspex tube was leaking due to the incompatibility of the two materials. The U-tube was therefore redesigned by reducing the 51 mm strap boss to 32 mm and making up the U-tube itself from Osma 32 mm pipe and elbows, also using this pipe for the vertical open end of the U-tube.

Providing that a sufficiently large orifice was made in the drainage pipe, the level of water in the U-tube would vary as the depth of flow in the pipe varied. A float was then used to support the core of a 6 volt linear voltage displacement transducer which was connected

directly to a quick response pen recorder. A detailed study of the optimum orifice requirement was carried out and is described in section 5.2.

#### 4.2.5 Volume Flow Rate Measurement

As well as monitoring water and solid velocities and depth of flow in the pipe it was also important to record the rate of flow. This was achieved by mounting a  $\pm 0.2$  m linear voltage displacement transducer in the 227 litre discharge collection tank described in section 4.1.8. A large float supported the core of the transducer, and the whole LVDT was surrounded by a 200 mm diameter pipe with cut outs at the base to serve as a stilling pot, as shown schematically in Figure 7. The 18 volt LVDT was connected directly to the quick response pen recorder. Since both types of collection tank used were vertical sided, and hence of constant cross sectional area, it was possible to calibrate the pen recorder trace in terms of volume. Figures 12 and 13 show the collection tank depth-time profiles for both a water only flush and for a single maternity pad flush. Comparing the traces in Figures 12 and 13 it is possible to distinguish the point (point D, Figure 13) at which a solid enters the collection tank. Having established the point at which the solid enters the collection tank it is possible to read off the volumes of water preceding and following the solid.

## 5. EXPERIMENTAL METHODS

### 5.1 Waste Materials

The waste materials used during the research project involved maternity pads, Kleenex paper towels and Bowater Scott paper towels.

#### 5.1.1 Maternity Pad

The maternity pads, used throughout the research project, were Dr. Whites C2 grade. When dry a maternity pad is approximately 280 mm long by 70 mm wide by 18 mm thick, weighing approximately 20 gms when dry and 250 gms when saturated. Soaking time required to become fully saturated was between 30 and 60 seconds. Figure 14 shows the range of waste materials used including a maternity pad.

#### 5.1.2 Kleenex Paper Towels

These towels, used in threes for the tests with a maternity pad, are white paper tissue hand towels and are supplied in rolls. Three Kleenex paper towels weigh approximately 15 gms when dry and 140 gms when saturated. Soaking time required to become fully saturated is 60 seconds. Figure 14 shows a roll of Kleenex paper towel.

#### 5.1.3 Bowater Scott Paper Towels

These towels, used in threes for the tests with a maternity pad, are green paper hand towels and are supplied individually folded. Three

Bowater Scott paper towels of type 20, weigh approximately 10 gms when dry and 80 gms when saturated, indicating that they are approximately half as absorbent as Kleenex paper towels. Soaking time required to become fully saturated is between 30 and 60 seconds. Figure 14 shows a pack of Bowater Scott paper towels of the type used throughout the project.

#### 5.1.4 Choice of Waste Materials

The choice of the waste materials used in this project was dictated partly by suggestions from DHSS and also by the findings of Swaffield's pilot study (2). As well as the waste materials already described, Swaffield used rolled, tied maternity pads and also simulated faeces made up from horse serum and baby milk powder used with a maternity pad plus 3 Bowater Scott paper towels. From a user survey carried out by Mrs Jean Swaffield, no evidence was found to show that patients rolled and tied their sanitary towels or maternity pads and consequently it was decided not to use this form of waste material for testing. From the tests carried out during the pilot study it was concluded that simulated faeces caused little significant difference to waste solid velocities and due to the extra expense and testing problems involved, the inclusion of this waste material was not justified for future testing.

The final choice of waste materials consisted of:-

- i) Single maternity pad
- ii) One maternity pad plus three Kleenex paper towels
- iii) One maternity pad plus three Bowater Scott paper towels.

A maternity pad was chosen as the main waste solid since it was obviously necessary to have a representative drainage load that was either the same as or worse than the normal drainage load. Previous experience indicated that maternity pads caused particular problems in hospital drainage systems and that therefore, if the drainage system were designed to dispose of these successfully then there would be an incorporated safety factor when considering normal drainage loads. Another benefit of designing the drainage system to dispose of maternity pads is that it was hoped that this method of maternity pad disposal would be adopted in the future, assuming that the local authority did not object.

The inclusion of paper towels with a maternity pad was based on the fact that these towels are often disposed of via the drainage system and also it was essential to investigate the travel of multiple waste materials as well as single waste materials.

#### 5.1.5 Placing of Waste Materials in W.C. Pan

A standard procedure of placing the waste materials in the w.c. pan was adopted throughout the research project in order to reduce the variability involved. For the single maternity pad tests the pad was folded in half and placed in the w.c. pan with the folded end of the pad towards the back of the pan. As the pad became fully saturated it tended to sink and open out since the lower folded section became saturated first.

For the maternity pad plus towel tests the maternity pad was placed in the pan first as described above. One paper towel was then screwed up, dunked under the water and then placed on top of the maternity pad. The remaining two paper towels were then used to dry the hands and were placed in the pan in a generally screwed up condition. At least 60 seconds was then allowed to elapse before flushing the w.c. to ensure full saturation of the waste material which as stated required 30 to 60 seconds.

#### 5.1.6 Previous Research Involving the Transport of Waste Solids in Drainage Systems

Previous research work involving the use of waste solids for testing drainage systems is very limited. References (9) and (11) contain details of tests, carried out at the Building Research Station, involving w.c. discharges with either six pieces of newspaper, each measuring 203 mm x 152 mm, or six pieces of newspaper, each measuring 152 mm x 102 mm, or six pieces of toilet paper. Reference (18) contains details of some more recent testing carried out under the control of the American National Bureau of Standards. Some of these tests involved w.c. loads of either a large size diaper, or a large size sanitary napkin with three loosely-wadded balls of 4 double thickness squares of toilet tissue. The work described in references (9), (11) and (18) was specifically aimed at investigating pressure fluctuations within drainage systems in order to limit trap seal losses. All the solids caused various amounts of increased trap seal losses when compared to otherwise identical water only flushes. Whilst the aims of these investigations were very different to the

aims of this research programme, it is interesting to note that the NBS sanitary napkin plus toilet tissue test material represents a very similar w.c. load to the maternity pad plus paper towels tests adopted as representative for the purposes of this research programme.

Another topic of research, carried out at BRE in 1963, to investigate the possibility of blockages occurring in drains carrying intermittent flow, involved the use of either cubes or prisms made of either pulverised fuel ash, siporex or fire brick, and also of 305 mm x 229 mm pieces of newspaper. Unfortunately, the results were not published, but the tests were specifically aimed at investigating the transport of these waste materials in below ground drainage pipes laid with varying standards of badly made joints. The results are not of direct relevance to this research programme, but they indicated that for drains up to at least 12 metres long, blockages were more likely to be caused by badly made joints than by too shallow gradients.

Work involving the investigation of the travel of solids in drainage systems has also been carried out recently in Japan, although the research was published (20) after the start of this research programme. The main relevant conclusions of this research were that simulated excreta of lower specific gravity travels faster and further in a "horizontal" discharge pipe, and that smaller bore discharge pipes are more efficient. It was also shown that the velocity of the solids was greater for steeper pipe gradients. The results reported in (20) will be very relevant to the future phases of the drainage research programme at Brunel University.

## 5.2 Orifice Sizing for Depth Measurement

The depth measuring device, shown in Figure 9 and mentioned in Section 4.2.4, depends for its operation on the monitoring of the voltage output of a linear voltage displacement transducer coupled directly to a float which responds to changes in fluid depth in the discharge pipe. The float was contained in a U-tube supplied with fluid from the waste pipe via a mesh of holes or a series of slots in the bottom of the pipe. Obviously the response of this instrumentation system, as a whole, was dependant on the damping caused by these orifices, and the optimum choice of orifice number and size was the subject of the theoretical analysis below, and a series of practical tests carried out employing water only flushes, as described in section 5.2.4.

### 5.2.1 Analysis of Orifice Effects

Under quasi-steady flow conditions the discharge  $Q$  from the waste pipe through the u-tube is given by:

$$H = Q^2 \left( \frac{\sum f L_p}{3d^5} + \frac{\sum k_L}{2gA^2} \right) \quad (5-2-1)$$

where  $H$  is the instantaneous head difference between the level in the waste pipe and the U-tube float chamber,  $f$  is the friction factor applicable for each pipe section of length  $L_p$ , diameter  $d$  and area  $A$ ,  $k_L$  is the orifice loss coefficient, expressed in terms of local flow kinetic head, for each fitting in the U-tube and the entry orifices. Equation (5-2-1) may be simplified to:

$$H = Q^2 C \quad (5-2-2)$$

Thus if  $H_1$  is the average head difference over a short time  $\Delta t$  then the average flow out of the drain over time  $\Delta t$  is:

$$Q_1 = \sqrt{\frac{H_1}{C}} \quad (5-2-3)$$

and the volume discharged in this time is:

$$\text{Vol} = Q_1 \Delta t \quad (5-2-4)$$

and the consequent rise in the fluid level, and hence the float, in the float chamber of cross sectional area  $A$  is:

$$dH = \text{Vol}/A = Q_1 \Delta t/A \quad (5-2-5)$$

In order to carry out these calculations, values of  $f$  and  $k$  for each individual pipe and pipe fitting in the U-tube must first be determined.

Values of friction factor  $f$  for the U-tube pipes are readily calculated from the smooth pipe relationship:

$$f = 16/Re \quad 0 < Re < 2300$$

$$\text{or } f = 0.079/Re^{1/4} \quad 2300 < Re$$

where  $Re$  is the local flow Reynolds Number.

Values of loss coefficients are similarly available (21) for the various pipe fittings employed and total 2.95 for the configuration used, as shown in Figure 15.

The orifice loss coefficient applicable to the orifices in the waste pipe wall are somewhat more difficult to determine, as little published work exists on such orifices, as shown in Figure 16, where the wall thickness to orifice diameter ( $tw/d_o$ ) ratio is appreciable.

Reference (22) does contain measured values of  $k_L$  for  $tw/d_o$  ratios of 0.25 to 1.5 and from this work it is possible to estimate an orifice loss coefficient for the particular case considered here. Assuming an orifice diameter of 3.7 mm, a wall thickness of 2.38 mm, yields a  $tw/d_o$  ratio of 0.64 and an orifice discharge coefficient  $C_D$  of 0.58 where

$$Q_o = C_D a \sqrt{2gH} \quad (5-2-6)$$

where  $Q_o$  is the flow through the orifice and  $H$  is the instantaneous head difference across the hole of area  $a$ .

The loss coefficient for the orifice in terms of flow kinetic head may be expressed as:

$$k_L = 2gH/V^2 \quad (5-2-7)$$

where  $V$  = mean velocity of flow through the orifice. From equations (5-2-6) and (5-2-7) and using the continuity equation:

$$k_L = \frac{1}{C_D^2} \approx 3 \quad (5-2-8)$$

Given these values, a simple program FLOT was written in Fortran and run on the Brunel University ICL 1903 computer to determine the theoretical response rate for each orifice geometry considered. A full print out of FLOT, together with flow diagram, notation and typical output is contained in Appendix 1 of this report. This program was modified, as SLOT, to predict performance of slot orifices in the pipe wall, and is also presented in Appendix 1.

### 5.2.2 Program Testing

In order to determine the likely response of the instrumentation, a realistic input drain pipe depth vs time profile was devised. By reference to (14) it may be seen that, for an S-trap, high level w.c. system, the maximum depth achieved in a water only flush is of the order of 25 mm in a 1/100 drain (also confirmed by Swaffield's earlier work) and this depth is likely to be achieved in 1 second. The theoretical profile shown in Figure 17 was thus devised, giving an overall duration of 6 seconds and a 1 second reduction in depth, which, although not representative of the much slower reducing depth change observed in practice, was included as a worst case for the program.

### 5.2.3 Theoretical Response of the Depth Measuring Instrumentation

Figure 17 illustrates the dept-time profiles for the waste pipe and the float chamber for a range of circular orifice configurations. Figure 18 illustrates the similar results for a range of slot orifice configurations.

### 5.2.4 Comparison of Response Rate with Orifice Area

A series of tests were carried out to investigate the float response rate with various orifice areas. Initially one 3.67 mm diameter hole was drilled in the pipe wall and several flushes carried out, recording the float response on the pen recorder. The number of holes was then increased to 4 and then 8, 12, 18 and 24 respectively. The pen

recorder traces for these tests are shown in Figure 19. Various other orifice sizes and numbers were also investigated, ending up with a 50 mm diameter orifice, the trace of which is also shown in Figure 19. All the results of the tests were finally plotted on a graph of float response rate against orifice area, shown in Figure 20. This graph indicates that the optimum response rate is achieved with a minimum orifice diameter of 19 mm, which was to be expected since the size of the U-tube was also 19 mm. It was therefore proved that a perfect float response could be achieved with a total orifice area of 284 mm<sup>2</sup>.

Since the purpose of using a large number of small diameter orifices was to prevent either waste material entering the U-tube or the orifice retarding the solid, it was decided to investigate the use of a number of 2 mm wide slots which would still prevent waste material entering the U-tube but would give a greater total orifice area and improved float response rate as shown by Figures 17 and 18. It was found that by providing 10 x 2 mm wide slots, giving a total orifice area of 740 mm<sup>2</sup>, as shown in Figure 16, that not only was a perfect float response rate achieved, but it was possible to identify the passage of a solid over the orifice, which is important since the estimation of the volumes of water preceding and following a solid are important. Figures 12 and 13 show the difference in float response for a water only flush and a single maternity pad flush.

Whilst the slot orifices were used successfully for the w.c. discharge characteristic testing, problems were encountered with the straight pipe testing. The total horizontal pipe length used for

the w.c. discharge characteristic testing was 1.192 m with the depth measurement orifice slots being 350 mm from the w.c. discharge. It was therefore possible to smooth the internal bore of the pipe after cutting the slots to remove any unnecessary obstruction to flow. The remainder of the plastic pipe testing entailed providing orifices at the mid-points of 2 metre pipe lengths which caused difficulties in smoothing the internal bore of the waste pipe. The slot orifices were therefore replaced by a grid of 40 x 3 mm diameter holes which were drilled from the inside of the pipe through a 50 mm diameter hole in the top of the pipe which was sealed afterwards, thus preventing the formation of burrs inside the pipe. It was found that these circular orifices worked as efficiently as the original slots.

#### 5.2.5 Initial Tests

A series of four initial tests were carried out to investigate whether the orifice slots cut in the pipe wall for depth of flow measurements caused any interference to the flow of water or solids in the pipe. These tests were carried out with the six photocell sensors spaced out evenly over a 500 mm length of pipe, grouped around the orifice slots, using a 100 mm photocell separation. Figure 9 shows a photograph of the layout of the photocell rings and depth measuring U-tube with LVDT and float. Figure 21 shows a schematic layout of the photocells along the pipe. Note the orientation of the photocell/light source ring used in these tests and shown in Figures 9 and 21. This angled arrangement was used throughout the research project, although it was later found better

to reverse the photocell and light source so that the photocell was on top. The advantage of this arrangement was that any residual water flowing down the invert of the pipe would not disrupt the light falling on the photocell and would therefore not cause voltage variations from the photocells. Figure 22 shows a graphical plot of the velocity data obtained from tests 1 - 4. It would appear from Figure 22 that the orifice slots do have a slight effect on the flow velocity, particularly in the case of the water only tests. After resmoothing the bore of the pipe in case of burrs remaining after cutting the slots, the tests were rerun. At this stage it was appreciated that the velocity of the leading edge of the water fluctuates constantly due to the presence of waves travelling along the discharge surface and that therefore the results for the water only tests shown in Figure 22 are not highly significant. The solid velocity results indicate that the slots cause a slight reduction in solid velocity, but that the variation in fact rapidly diminishes and is insignificant 250 mm after the slots. It was therefore established that the orifice slots caused insignificant velocity disruption.

Tests 1 - 4 also showed the benefit of being able to monitor point velocities rather than mean velocities over 3.71 metres as in the pilot study. Obviously it would have been impossible to monitor the effect of the orifice slots in such detail. If the individual solid times are added together and divided by 0.5 m thus representing a mean velocity over 0.5 m, the overall means give 0.76 m/sec with orifices and 0.75 m/sec without orifices leading to the conclusion

that the slots in fact cause the solid to speed up. However, Figure 22 shows that the slots do cause the solid to slow down but that a velocity regain then occurs returning the solid velocity back to normal soon after.

### 5.3. Depth of Flow Calibration

The waste pipe flow depth recording system was calibrated by marking and displacing each float upwards a distance of 10,20,30,40 mm and adjusting the pen recorder gain and zero to align the pen displacement to 10, 20, 30, 40 mm deflection respectively, allowing an unscaled depth measurement to be achieved. At the same time the height of the LVDT tube was adjusted so that the null position corresponded to the 20 mm displacement mark, thus ensuring that the  $\pm 2$  cm LVDT's were operating within their linear range.

### 5.4 Collection Tank LVDT Calibration

The rate of flow monitoring, carried out by the LVDT in the collection tank, was calibrated by adjusting the pen recorder gain and zero so that the standard 9.1 litres w.c. discharge entering the collection tank resulted in a full 40 mm pen deflection. Prior to this calibration the ball valve of the w.c. cistern was always adjusted to give a 9.1 litre (2 gallons) w.c. discharge.

It was noted that the cistern level marks were consistently above the level necessary to give a 9.1 litre flush, the error being of the order

1 to 2 litres. It is appreciated that the level is dependant on supply pressure, 210 kN/m<sup>2</sup> in this case, however in water conservation terms the excess volume is appreciable.

#### 5.5 Velocity Calibration

The timer counters were checked for accuracy by comparing the indicated time taken by a single maternity pad to travel the known distance between each pair of photocells to the pen recorder output from the relevant photocells. During these calibration runs the pen recorder was run at 250 mm/sec allowing the maximum time increment measurement accuracy to be achieved. Any adjustments necessary were carried out by fine control of the triggering sensitivity level. In order to retain repeatable triggering levels, the voltage output of each photocell was checked prior to each test, the chosen operating level being 100 - 300 millivolts.

The calibration procedures above were carried out prior to each set of tests and checks made at regular intervals throughout the testing.

#### 5.6 W.C. Discharge Characteristics Test Rig

Figure 23 illustrates the test rig employed for the w.c. discharge characteristic tests. Solid velocity was recorded over 622 mm of discharge pipe, 0.476 metres downstream of the w.c. discharge. Problems arising due to the use of the velocity measuring instrumentation in

the highly "turbulent" flow regime close to the waste pipe entry were overcome by introducing an R-C filter network into the photocell output circuit.

Flow depth was continuously recorded at a point 350 mm from the w.c. discharge and the volume of water ahead of the solid monitored by means of the linear displacement transducer in the discharge collection tank.

Eight different w.c.'s were tested during this phase of the research project, each w.c. being tested with the correct cistern as supplied and advised by the relevant manufacturer. The eight w.c. types were Armitage Shanks and Twyfords, P and S-trap, high and low level cistern. These eight w.c. units make up the full range of DHSS approved units. The high level cistern w.c.'s are designed to operate with flush pipe restrictors in order to reduce splashing from the pan during flushing. The effect of these flush pipe restrictors was also investigated by carrying out the full tests with the flush pipe restrictors fitted and carrying out limited tests with the flush pipe restrictor removed. The Twyfords high level S-trap w.c. was also tested with a larger than normal flush pipe restrictor, since the manufacturer supplied the incorrect size, the tests being rerun after this error had been corrected.

As can be seen in Figure 23, it was possible to accommodate any one of the eight different w.c.'s and cisterns on the large support rig, this being done in such a way as to avoid altering the discharge pipe, and hence ensuring standard discharge pipe conditions. All the w.c.

discharge characteristic tests were carried out with the discharge pipe horizontal. Three waste solid materials were tested namely, single maternity pad, maternity pad plus three Kleenex paper towels, and maternity pad plus three Bowater Scott paper towels, although the latter waste material type was abandoned after consultation with DHSS.

#### 5.7 Straight Plastic Pipe Test Rig

Following the w.c. discharge characteristic tests, which involved a shortened test pipe, the discharge pipe was extended by the introduction of a second 6.1 m ladder and mid span support point, the two ladders being spliced together with dexion angle. The measurement of solid velocity was carried out with six pairs of photocells spaced along the discharge pipe as shown in Figure 24.

Flow depth was continuously recorded at four points along the discharge pipe as shown in Figure 24. As mentioned earlier, the slots in the pipe wall for feeding the depth measuring U-tubes were replaced by 40 x 3 mm diameter holes, to reduce the possibility of interfering with the passage of the solids. As in all the testing, total volume flow against time was monitored by means of the protected float-linear voltage displacement transducer mounted in the collection tank, and from which it was possible to determine the volume of water ahead of the solid at entry into the collection tank. Pipe gradients of 1/40, 1/60, 1/80, 1/100 and 1/150 were tested.

The three waste material types were tested throughout this phase of the research project. Limited tests were also carried out using Dr Whites size 2 sanitary towels in order to obtain a comparison between this waste material type and the normal maternity pad used throughout the research project. Tests were also carried out to investigate the effect of stack venting.

From the results of the w.c. discharge characteristic tests, which indicated the relative inefficiency of the high level w.c. units, it was agreed with DHSS to only use low level w.c. units for all the remaining testing. Therefore only the four low level w.c.'s were tested during this phase of the research project.

Unfortunately the Twyford's S-trap low level w.c. was dropped and broken prior to the solid deceleration tests, and therefore the results from this phase of the research project and all subsequent tests relative to this pan were obtained using an apparently identical replacement pan.

#### 5.8 Straight Cast Iron Pipe Test Rig

Certain modifications were required to the test rig in order to accommodate the Glynwed 102 mm internal diameter spun cast iron discharge pipe. Due to the extra weight involved, five support points were used instead of the two used in the straight plastic pipe test rig. The cast iron pipe was run parallel to the plastic pipe with the w.c. positioned on the other side of the large support rig. Two 7.3 m heavy duty aluminium ladders were used to

support the pipe, the ladders being rigidly spliced together with dexion angle. The total length of the cast iron pipe was 14.421 metres from the centre line of the vertical w.c. discharge pipe entry to the centre line of the vertical stack. Two different low level w.c. units were tested namely the Armitage Shanks P-trap and the Twyford's S-trap. Five different pipe gradients at 1/40, 1/60, 1/80, 1/100 and 1/150 were tested under both vented and unvented w.c. discharge conditions. Due to the problems experienced with the Bowater Scott paper towels this waste material was not tested. These problems were due to the fact that these towels had a tendency to discharge before the maternity pad with the risk of obtaining non-representative velocity data since the opaque pipe prevented this occurrence being observed. Therefore only single maternity pads and maternity pads with three Kleenex paper towels were tested. The only other changes made to the rig involved the fitting of the "photocell and light source" rings to the opaque cast iron pipe.

The original 8 x 2 m lengths of cast iron pipe supplied by Glynwed appeared to have been excessively coated with bitumen and, due to subsequent vertical stacking of the pipes, drips of bitumen had formed on the internal bore of the pipe. The manufacturer agreed that the pipes were not representative of their spun cast iron pipe and therefore replaced all the 2 m lengths of pipe originally provided.

In order to accommodate the light sources and photocells two pairs of diametrically opposite 4.8 mm (3/16") diameter holes 20 cm apart were drilled in the centre of 6 of the 2 m pipe lengths. It was then

necessary to devise a method of sealing the holes in the pipe wall to enable light to pass through them without water leakage.

40 cm lengths of UPVC pipe with a single cut were pushed onto the cast iron pipe and silicon lubricant was used to seal round each hole. However, due to the tight fit of the UPVC sleeves, it was necessary to push them into position which resulted in the silicon lubricant being forced into the holes, thus drastically reducing the amount of light passing through them.

In order to prevent the lubricant being squeezed into the holes, 40 cm lengths of UPVC pipe were cut diametrically, enabling each half to be placed over the holes and sealed with silicon lubricant. However, when the pipe clamps holding the photocells and light sources were tightened round the UPVC sleeves, the lubricant was again squeezed into the holes.

In an attempt to prevent the lubricant squeezing into the holes, a more dense sealing medium of seelastik was used, but again this squeezed into the holes when the pipe clamps were tightened.

In order to keep the sealant away from the holes an O-ring was placed round each hole, with the sealant applied outside the O-ring. This prevented the sealant entering the holes but when water was flushed down the pipe a water lens was created in the annular gap between the cast iron pipe and the plastic sleeve which resulted in light dispersion and low voltage output from the photocells preventing sufficient distinction between water and solids passing over the light source.

In order to increase the light intensity on the photocells the relatively opaque UPVC sleeves were replaced with small sections of Acrylic pipe, using silicon lubricant on the O-ring. However, water tended to seep past the O-rings, which was obviously unsatisfactory.

In order to provide a better seal, seelastik was used instead of the silicon lubricant, which satisfactorily prevented water seepage, but the water lens effect still prevented sufficient light intensity on the photocell.

In order to prevent the formation of the water lens, it was necessary to remove the annular gap, but without allowing sealant to be squeezed into the holes. Acrylic sections of pipe were bonded to the cast iron pipe by heating the bitumen coating on the cast iron pipe until it was soft and then pushing the Acrylic section on to the pipe. However water leakage occurred due to the roughness of the cast iron pipe.

In order to seal the Acrylic pipe onto the cast iron pipe more efficiently, thick bitumen paint was applied to the cast iron pipe and the Acrylic section pushed onto this, whilst still soft. However water leakage still occurred.

A different approach was then investigated, involving the use of 1" diameter thin acetate sheet stuck over a  $\frac{1}{2}$ " diameter hole punched in a 2" wide length of glazing tape stuck to the cast iron pipe to provide a window over both the upper and lower holes. This method produced reasonable voltage outputs from the photocells. However it was found that a rust layer formed on the internal surface of the lower acetate

window. The reason why the rust layer was concentrated on the acetate window, but not on the internal bore of the pipe, is not fully appreciated, but would appear to be due to an electrostatic field being created by the water passing over the acetate and attracting rust particles by magnetic force.

In order to reduce the amount of rust, the holes in the cast iron pipe wall were coated with bitumen paint, and the glazing tape reapplied to the pipe. An overnight film of rust still formed on the lower acetate window, although much reduced. However it was obvious that it would be necessary to clean the windows before each day's testing.

To gain access to clean the lower window, the upper hole was enlarged to  $\frac{1}{4}$ " diameter and it was then possible to push the photocell into this hole using PTFE tape round the photocell body to seal the hole. Therefore, before each day's testing, the photocells were removed and the lower window cleaned with a piece of cotton wool, soaked in white spirit, attached to the end of a piece of welding rod.

This method finally resulted in an output from the photocells of 100-400 millivolts which was in excess of the requirements for triggering the timers and it was therefore possible to continue testing as normal. Figure 25 shows the relevant positioning of the velocity points.

### 5.9 Plastic Bends Test Rig

In order to accommodate bends into the straight pipe rig, the second support rig was constructed as described in section 4.1.5. Two different bends were tested, namely a Key Terrain 135° knuckle bend (Type No.101) and a Key Terrain 92½° radiused bend (Type No. 101.4.92). Figures 26, 27 and 28 show the various 135° bend positions tested with the relevant positioning of the velocity measuring points. Figures 29, 30 and 31 show the various 92½° bend positions tested again with the relevant positioning of the velocity measuring points. A combination of two 135° bends was also tested and Figure 32 shows the relevant dimensions involved in this test rig.

Two different waste material types were tested, namely a single maternity pad and maternity pad plus three Kleenex paper towels, with the w.c. discharge under both vented and unvented conditions, although the majority of the tests were carried out under vented w.c. discharge conditions. Discharge pipe gradients of 1/40, 1/50, 1/60, 1/70, 1/80, 1/90, 1/100 and 1/150 were tested where relevant, the criterion for gradient limits being established by the requirement for zone 2 flow conditions at the various bend positions.

### 5.10 Plastic Junctions Test Rig

Junctions were accommodated into the straight pipe rig by the use of the second and third support rigs, described in sections 4.1.6 and 4.1.7 respectively. Two types of junction were tested, namely a Key Terrain

135° sharp angle junction and a Key Terrain 92½° swept angle junction, with a junction position of approximately 6 metres from the w.c. All tests in this phase were carried out with an Armitage Shanks P-trap low level w.c. unit. Testing of the 135° junction involved the following waste material types: single maternity pad with both vented and unvented w.c. discharge, a maternity pad plus three Kleenex paper towels and a maternity pad plus three Bowater Scott paper towels, both the latter two with vented w.c. discharge. The 92½° junction was tested with vented w.c. discharge with a single maternity pad and a maternity pad plus three Kleenex paper towels.

The 135° junction was tested with three different angles of entry of the branch drain into the main drain, namely: horizontal entry, 45° entry via a 148° adjustable bend and vertical entry via a 135° knuckle bend. Figures 33 and 34 show the junction orientation and the relative positioning of velocity and depth measuring points for the horizontal junction entry. Figures 35 and 36 show the same for the 45° junction entry and Figures 37 and 38 show the same for the vertical junction entry.

The 92½° junction was tested with horizontal branch entry as shown in Figure 39 and Figure 40 shows the relative positioning of the velocity measuring points.

In order to investigate the effect of angle of branch entry on the straight main drain flow through the junction, the 135° junction was

tested with angles of entry of  $0^{\circ}$  (horizontal),  $15^{\circ}$  and  $30^{\circ}$ , using both a single maternity pad and a maternity pad plus three Kleenex paper towels, both with vented w.c. discharge. Figures 41 and 42 show the junction orientations and the relative positioning of the velocity measuring points.

#### 5.11 Cast Iron Bend and Junction Test Rig

In order to identify whether or not the effects of cast iron bends and junctions were similar to those of UPVC pipe fittings, tests were carried out on a  $92\frac{1}{2}^{\circ}$  cast iron bend and a  $92\frac{1}{2}^{\circ}$  cast iron junction, installed with the Glynwed 102 mm I.D. spun cast iron pipe tested previously. All tests were carried out with vented w.c. discharge, using a single maternity pad. Figure 43 shows a schematic view of the  $92\frac{1}{2}^{\circ}$  bend test rig showing the relative positions of the velocity measuring points, while Figure 44 illustrates the  $92\frac{1}{2}^{\circ}$  horizontal entry junction.

The only variation in the method of incorporating the velocity measuring photocell system to that described in section 5.8 involved the sealing of the bottom windows in the pipe wall. The original glazing tape had deteriorated causing the adhesive to become smeared over the acetate windows. To prevent a recurrence of this, the glazing tape was changed for waterproof scotch tape fitted as before with thin acetate sheet windows. This method worked perfectly with the added benefit that it was unnecessary to clean the inside surface of the acetate windows at the start of each day's testing, as was found necessary in the previous cast iron pipe testing.

Pipe gradients of 1/40, 1/60, 1/70, 1/80 and 1/100 were tested where appropriate, depending on whether the solid would clear the pipe fitting.

#### 5.12 Straight Glass Pipe Test Rig

The Glass pipe was supported on the same rig as the cast iron pipe except that only three ladder support points were used instead of five. The total length of the glass pipe was 14.373 metres from the centre line of the vertical w.c. discharge pipe entry to the centre line of the vertical stack. Only the Armitage Shanks P-trap low level w.c. unit was tested, with vented w.c. discharge. Five pipe gradients at 1/40, 1/60, 1/80, 1/100 and 1/150 were tested with single maternity pad, and a maternity pad plus three Kleenex paper towels.

The fitting and use of the photocell/light source rings presented no problems and a high photocell voltage output was obtained. Figure 45 shows a schematic view of the straight glass pipe test rig with the relevant positioning of the velocity measuring points.

## 6. DATA HANDLING AND PRESENTATION OF RESULTS

### 6.1 Data Input

During testing the data was punched onto paper tape using a Teletype (type 2742A) punch. As well as recording the data on the paper tape, the input data was simultaneously typed onto paper, therefore facilitating the checking of the punched data with the recorded data and hence reducing human errors to a minimum. Paper tape was chosen as the data input medium since paper tape does not deteriorate with time whereas computer cards do have this tendency.

A label system of data identification was adopted, referred to as LABL 1,2,3,4, or 5. At the start of each test, details of the test were punched under LABL 1 to identify each line of alphanumeric input. Details included: w.c. type and venting condition, test number, test series to which test related, details defining discharge pipe type and gradient, details of bends or junctions where relevant, date, details of waste material type and any other relevant data.

Under LABL 2 the following data was punched: full scale deflection of the pen recorder for a standard 9.1 litre flush as monitored by the discharge tank LVDT, the number of velocity measuring points, the positions in metres from the w.c. of the velocity measuring points and the separation of each pair of photocells.

The main test data was input under LABL 3, and involved: the run number, pen recorder deflection for the point at which the solid entered the

discharge collection tank, the position of a stoppage measured in metres from the w.c., if there being no stoppage, then position recorded as -1.0, and the times to travel between each pair of photocells as recorded by the timer counters, read as integer values. The velocities recorded by a solid which, after stopping, was cleared by a water only flush, were also recorded in the hope that this data, whilst not of direct relevance, might prove useful at a later stage. In the case of the cast iron pipe, obviously it was impossible to identify the exact position of stoppages. If a stoppage occurred between a pair of photocells making up a velocity measuring point, the stoppage position was recorded as the position of this velocity measuring point. Where a stoppage occurred between velocity measuring positions, the stoppage position was recorded as being mid-way between the two relevant velocity measuring positions. When a w.c. failure occurred, this was identified by recording a full scale discharge tank LVDT pen recorder deflection. Where the solid stopped between the photocells of a velocity measuring point, the time was input as zero, whilst a timer failure was identified by -1.

LABL 4 and LABL 5 were used to identify, respectively, either the continuation of the data for another set of test results or the end of the data on the paper tape.

## 6.2 Presentation of Results

The above input data was processed by computer program WCHAR, or an identical program COPY, used because on some occasions two separate paper tapes were processed together, and the computer does not allow two programs,

of the same name, to be processed at the same time. This program was written in Fortran, and was run on the Brunel University ICL 1903 computer. The program identified the type of data input according to the LABL number.

For each test the program reproduced all the test details exactly as input under LABL 1. All the data input under LABL 2 and LABL 3 was then processed, the end of a set of results being identified by a pen recorder deflection for the LVDT in the collection tank greater than the maximum deflection. The program then printed out the total number of w.c. flushes and the number of w.c. failures, followed by the positions of the velocity measuring points and the photocell separations. After printing the necessary headings the following results were output: the run number, % FAS, the calculated volume of water entering the collection tank ahead of the solid, stoppage position where relevant and the solid velocities, calculated from the solid travel times and photocell separations. A w.c. failure was ignored and no results printed out, but the number of w.c. failures was summed and printed out as stated above.

All the data for each test was also processed through subroutine STATIS which identified the maximum and minimum values of each parameter and calculated the mean and standard deviation, these values then being printed out. All velocities after a stoppage were taken as zero for the statistical analysis. Finally the program carried out a distribution analysis of the velocity data and printed out the number of velocities lying within predetermined velocity band widths.

A full print out of WCHAR together with a simple flow diagram and representative output is contained in Appendix II.

Another parameter, which was recorded and calculated manually, was the partial w.c. failure rate ( $F_2\%$ ) as opposed to the total w.c. failure rate ( $F_1\%$ ).  $F_1$  was calculated as the number of w.c. failures divided by the number of successful w.c. flushes, expressed as a percentage.  $F_2$  was calculated as the total number of towels left in the w.c. pan after a flush divided by the total number of towels successfully discharged from the pan, expressed as a percentage. W.c. failures were ignored in calculating  $F_2$ , since they had already been taken into account in calculating  $F_1$ .

Various other computer programs were written during the research project but these are described in the discussion of results section since their relevance can only be appreciated after some initial discussion of the results.

## 7. DISCUSSION OF RESULTS

The work carried out during this research project divided itself logically into the following eight stages:-

- i) Test rig and instrumentation development
- ii) W.c. discharge characteristics testing
- iii) Straight plastic pipe testing
- iv) Straight cast iron pipe testing
- v) Effects of plastic bends
- vi) Effects of plastic junctions
- vii) Effects of cast iron bends and junctions
- viii) Straight glass pipe testing

The test rig and instrumentation development work has been fully described in the preceding sections, with details of the initial tests. To avoid repetition, this section is divided into the following three categories, in order to present together related tests, not necessarily in the chronological sequence in which they were undertaken:-

- 7.1 W.c discharge characteristics
- 7.2 Straight pipe deceleration characteristics
- 7.3 Effects of bends and junctions

### 7.1 W.c Discharge Characteristics

Figure 23 shows a schematic layout of the test rig used for the w.c. discharge characteristic testing. Table 1 summarises the results of the tests carried out and Figure 46 is a graphical presentation of the solid discharge velocity results. The following parameters were monitored during the w.c. discharge characteristic tests:-

- i) W.c. failure rate (the percentage failure of the w.c. to discharge the maternity pad, and in the case of the towel tests, at least one paper towel as well)
- ii) Partial w.c. failure rate (the percentage of towels left in the w.c. pan ignoring total w.c. failures)
- iii) Solid velocity as mentioned previously
- iv) Percentage flush entering the discharge collection tank ahead of the solid (% FAS)
- v) Depth of flow in the discharge pipe.

It was anticipated that better w.c. performance could be defined by those having lower values for (i), (ii) and (iv) and higher values for (iii) and (v), the higher value of (v) only applying to the depth of water behind the solid. It was appreciated that a compromise would probably be needed since the relationships between (i) - (v) would not be well defined. It is likely that friction would be a predominant parameter with regards solid deceleration and since friction force is proportional to velocity squared, a doubling of entry velocity does not imply a doubling of deposit free pipe length. Therefore it was expected that (iv) would be the major criteria in defining the efficiency of w.c. performance and should obviously be as low as possible.

Prior to discussing the results from this phase of the research project, it is important to note that the results obtained for the Armitage Shanks S-trap low level w.c. unit appeared to be very much worse than those for all the other low level w.c. units. This was shown by the high w.c. failure rate of 18% overall, partial w.c. failure rate, and the marked scatter in the velocity results. This particular w.c. pan had been used throughout the pilot study and rig development work with long periods without use during this work, and it was concluded that hard water scale formation was the cause of these detrimental results.

A new, identical, pan was therefore retested and these results are presented in Table 2 and Figure 47. The retest results confirm that the original pan was below standard in its performance and therefore the discussion below is based on the retest results.

#### 7.1.1 Kleenex and Bowater Scott Paper Towels

Following the tests on the Armitage Shanks low level S and P-trap w.c. units a statistical analysis, based on references (23) and (24), was carried out to establish whether or not it was necessary to continue testing with both towel combinations, and also both vented and unvented w.c. discharges. This analysis was carried out using Fisher's F-test and the student's t-test as explained below.

The F-test is used to test the significance of the difference between sample variances by the Variance Ratio test, referred to as either Snedecor's F-test or more generally Fisher's F-test since the test depends mathematically on Fisher's Z distribution, F being defined as:-

$$F = \frac{\text{greater estimate of the variance of the population}}{\text{lesser estimate of the variance of the population}}$$

To take account of the bias in small samples, Bessel's correction is applied to obtain the best estimate of the population variance.

$$\text{Therefore } F = \frac{\hat{\sigma}_1^2}{\hat{\sigma}_2^2}$$

$$\text{where } \hat{\sigma}_1^2 = \frac{n_1 s_1^2}{(n_1 - 1)}$$

$$\text{and } \hat{\sigma}_2^2 = \frac{n_2 s_2^2}{(n_2 - 1)}$$

If the calculated value of F is less than the tabulated value of F, from reference (23), for a chosen level of significance, then the null

hypothesis of  $\sigma_1^2 = \sigma_2^2$  is accepted, otherwise the alternative hypothesis of  $\sigma_1^2 \neq \sigma_2^2$  is proven.

The student's t-test is used to compare the means of two samples and define whether the difference between them is significant at a chosen level of significance. This test assumes that the two samples are independent estimates of the same population variance, which should first be established using the F-test. The student's t is defined as

$$t = \frac{\text{Error in Means}}{\text{Standard error of mean}}$$

If the calculated value of t is less than the tabulated value of t, from reference (23), for a chosen level of significance, then the null hypothesis of the difference in the means equals zero, is accepted.

To assist in the calculations of F and t, a very simple computer program was written, to calculate these values, from which it was possible to establish the following conclusions:-

- i) the discharge velocities of the two types of paper towels tested generally had the same population variance at the 0.10 level of significance and that the difference between their means was not significant at the 0.20 level of significance. It was therefore pointless testing both paper towel combinations, although this does not preclude there being a significant difference between the deceleration characteristics of the two types of towel further along the discharge pipe.

- ii) the variation in discharge velocities due to venting the w.c. discharge was proved to be insignificant for the Armitage Shanks low level S-trap w.c. but significant for the similar P-trap w.c. It was therefore necessary to test both unvented and vented w.c. discharges in the remaining w.c. discharge characteristic testing.
  
  - iii) The variation in discharge velocities between the P-trap and S-trap w.c.'s was highly significant as was expected.
  
  - iv) An analysis of all the discharge velocity results indicated that thirty w.c. flushes were sufficient to give a good approximation to the standard normal distribution (23) and this philosophy was adopted for the remainder of the research project.
- Some interesting points that emerged during the statistical analysis work described, were related to the velocity frequency distribution histograms. As described in section 6.2, the computer program WCHAR carried out a distribution analysis of the velocity and printed out the number of velocities lying within predetermined velocity band widths. When the data, for the single maternity pad tests, were plotted in the form of frequency histograms, a symmetrical normal distribution curve was evident with a velocity range of approximately 0.8 to 1.9 m/s. It was concluded that the lower velocity limit was dictated by the mode of w.c. operation, since a solid either remained in the pan, resulting in a w.c. failure, or was discharged at

a velocity of 0.8 m/s or higher. When the velocity distribution data for the maternity pad plus paper towels tests were plotted in the form of frequency histograms, a bimodal distribution curve was evident, with a velocity range of approximately 0.8 to 2.4 m/s. The first peak of this bimodal distribution approximately corresponded to the unimodal normal velocity distribution of the single maternity pad, and a second peak occurred within a higher velocity range. This bimodal distribution confirmed observations made during the testing, that the solids were discharged either separately, resulting in a similar velocity distribution to the single maternity pad distribution, or as a single combined solid, at a higher velocity, resulting in a second velocity distribution peak.

#### 7.1.2 High Level Cistern Flush Pipe Restrictors

The DHSS approved high level cistern w.c. units tested, were similar in design to their respective low level cistern counterparts, the only obvious variation being that high level w.c.'s have top entry flush pipes, whereas low level w.c.'s have rear entry flush pipes. Since the high level pans are of the same design as the low level pans it is generally necessary to fit a flush pipe restrictor into the high level flush pipes to prevent water splashing onto the seat and/or the floor. Obviously this will reduce the hydraulic advantage gained by the high level cistern.

All four high level pans were tested with the flush pipe restrictor, as supplied by the manufacturers, fitted; Armitage Shanks using a 28.2 mm diameter restrictor and Twyfords using a 23.8 mm diameter restrictor.

The Twyfords S-trap w.c. was also tested with a 30.2 mm diameter restrictor

in error. This error was caused by the fact that this was the original size of restrictor supplied, the error only becoming apparent when the Twyfords P-trap w.c. was tested, when considerable splashing of the w.c. seat and the floor occurred. After checking with Twyfords, the correct size restrictor, namely 23.8 mm diameter, was supplied and the tests rerun. All the pans, except the Twyfords P-trap, were also tested without flush pipe restrictors.

The results summarised in Table 1 and shown graphically in Figures 46 and 47 indicated several interesting points. The Armitage Shanks high level pans gave a higher discharge velocity than the comparable Armitage Shanks low level pans, the mean increase in velocity being 0.21 m/s for P-trap and 0.19 m/s for S-trap w.c. pans. However, although this appears logical, each Armitage Shanks high level w.c. unit was tested without the 28.2 mm diameter flush pipe restrictor and in both cases the discharge velocity was reduced by approximately 0.04 m/s, giving the opposite effect to that expected. This velocity reduction was not sufficiently significant to draw any firm conclusions, but did indicate that the Armitage Shanks flush pipe restrictor served no useful purpose, possibly due to the fact that the restrictor is made of a fibrous material which becomes soft when saturated, therefore reducing its effectiveness. The sharp change of flow direction on entry to the top of the pan therefore appears to cause sufficient velocity reduction as to prevent the splashing of water over the rim of the pan.

The high level pans also had a higher mean percentage flush ahead of the solid than the respective low level pans. However, without the flush pipe restrictor the high level pans had comparable figures for % FAS

compared to the respective low level pans. In every case the flush pipe restrictors caused the solids to leave the pan later in the flush when compared to the tests without flush pipe restrictors.

When considering the Twyfords high level w.c. units it is interesting to note that in general the 23.8 mm diameter flush pipe restrictor gave discharge velocities slower than the equivalent low level pan, but the 30.2 mm diameter restrictor gave higher discharge velocities than the comparable low level pan, thus indicating that the Twyfords high level w.c. pans tend to be over restricted, destroying the benefit of the increased cistern height. The Twyfords P-trap high level w.c. unit was not tested without the 23.8 mm diameter flush pipe restrictor as even with the 30.2 mm diameter restrictor, water tended to spill over the front of the pan indicating that a restrictor is essential for this pan but not as small as 23.8 mm diameter.

The high level cistern units gave high w.c. failure rates, particularly in the case of the over-restricted Twyfords S-trap which had an average of 10%. However the low level cistern units tended to have a higher partial w.c. failure rate compared to the respective high level cistern units.

Due to variations between the water inlet passages of w.c. pans nominally of the same design, it is obviously not possible to stipulate one restrictor size and it was recommended to DHSS that consideration be given to supplying a range of restrictors to be trial fitted during each w.c. installation. However DHSS felt that this would be impracticable, and since no benefit was gained by the use of high level

cisterns, DHSS recommended discontinuing the use of high level units wherever practically feasible. Consequently no further tests were carried out on high level w.c's during the remainder of the research project.

#### 7.1.3 Effects of Venting the W.C. Discharge

Approximately 74% of the tests indicated that venting the w.c. discharge resulted in a higher discharge velocity, the overall mean increase being 0.06 m/s or 3%. From the figures for % FAS the effect of venting the w.c. discharge appeared to be random. The results are therefore not sufficiently definite to draw any firm conclusions.

#### 7.1.4 Variation between P-trap and S-trap w.c's

The S-trap w.c's gave a consistently higher discharge velocity than the comparable P-trap w.c., this increase in velocity varying between 0.02 and 0.45 m/s. The figures for %FAS showed that the S-trap w.c's discharged the solids later in the flush since the %FAS was on average 3.3% higher for the S-trap w.c's. At this stage it was not possible to define whether the P-trap or the S-trap w.c's were the more efficient, since the higher discharge velocity was counteracted by the higher % FAS of the S-trap pans and the inter-relationship of these two parameters was not known.

#### 7.1.5 DEPTH OF FLOW

Figures 48, 49, 50 and 51 show tracings of representative depth of flow profiles for each w.c. unit tested. The depth of flow for S-trap w.c. pans was shallower than that of the equivalent P-trap w.c. pans. This observation bears out the earlier observation that S-trap pans gave a higher discharge velocity than P-trap pans. Another worthwhile observation was that in general the depth of flow either side of the solid was approximately the same and was between 10-20 mm. This observation appeared to contradict certain observations noted by Swaffield (2), which indicated that at a point 8 metres from the w.c. the depth of flow ahead and behind the solid was 10 mm and 40 mm respectively. The explanation of this apparent contradiction was due to the fact that the more recent depth of flow observations were made at a point only 350 mm from the w.c. discharge, and it therefore appeared that the preceding water had a higher velocity than the solid and therefore the preceding depth of flow diminished further along the pipe and the water behind the solid tended to dam up behind the decelerating solid. This resultant difference in head propelled the solid along the pipe.

#### 7.1.6 Conclusions on W.C. Discharge Characteristics

From a statistical analysis, it was shown that the difference between Kleenex and Bowater Scott paper towels was insignificant with regards w.c. discharge velocity, with maternity pads, and also that thirty tests were sufficient to give a good approximation to the standard normal distribution. Two modes of discharge of paper towels with a maternity

pad occurred, either with the pad and towels separated or as a single combined solid.

The increased hydraulic advantage of high level cisterns was diminished by the fitting of a flush pipe restrictor, required to prevent water splashing over the rim of the pan. It is suggested that various size flush pipe restrictors should be trial fitted during the installation of a high level w.c. unit in order to prevent splashing, but without over-restricting the flush pipe, and hence retaining some of the hydraulic head advantage.

The slight benefit of venting the w.c. discharge was minimal. It was shown that the S-trap w.c.'s exhibited a higher discharge velocity, and a lower depth of flow, but at the expense of a higher % FAS, than the P-trap w.c.'s, but that the inter-relationship of these parameters was not definable, and therefore no conclusions could be drawn as to the relative performance of the two types of w.c. trap.

## 7.2 Straight Pipe Deceleration Characteristics

Figures 24, 25 and 45 show schematic layouts of the three test rigs used for the straight pipe solid deceleration characteristics testing, conducted on three different discharge pipe materials: Marley UPVC, Glynwed Spun Cast Iron and Schott-Kem Glass respectively. Solid velocity was monitored at six points along the discharge pipe and in the case of the UPVC pipe, the depth of flow was monitored at four points along the pipe. In addition the following parameters were

recorded: w.c. failure rate, partial w.c. failure rate, percentage flush entering the discharge tank ahead of the solid, and stoppage position where relevant.

The bulk of the testing was carried out on the UPVC pipe since it was anticipated that, following the theoretical analysis shown in section (3.2), the relationships indicated by equation (3-2-7) could be established and that the other two discharge pipe materials would exhibit similar characteristics.

#### 7.2.1. Flow Observations

Observation of the mechanism of solid/liquid motion along the straight plastic discharge pipe suggested the presence of a number of distinct zones, or regimes, in the flow, where the type of flow observed was determined by the predominance of one or other of the various forces acting.

Typically, on discharge from the w.c. trap and entry to the discharge pipe, the solid velocity was of the order of 1.5 - 2.5 m/s, Figures 46 and 47, however it was observed that over the first 2 - 3 metres of pipe this velocity was reduced considerably, to almost zero in some cases, due to the random impact of the solid on the sides of the discharge pipe, caused by the "turbulent" nature of the flow in this section adjacent to the w.c. entry. A second contributory factor to this rapid inlet deceleration was the forces applied to the solid as a consequence of traversing the 92½° bend at entry to the discharge

pipe. The centrifugal force here tended to force the solid onto the pipe surface thus increasing frictional resistance. Due to this initial deceleration, the solid travelled considerably slower than the following flush water and, depending on the solid blockage effect, water tended to dam up behind the near stationary solid. This build up of water, observed to be as much as 40 to 50 mm deep, effectively provided an impulse to the solid, accelerating it down the discharge pipe so that, typically, by the 3 to 5 m mark, a velocity of approximately 1m/s had been regained.

This entry zone, where the solid velocity was predominately determined by centrifugal and impact forces rather than by fluid frictional forces, will be referred to as zone 1.

Once the solid was moving it came under the action of a system of forces comprising the frictional resistance to motion, a component of solid weight force, which acted in the flow direction and aided motion, and a pressure force due to the difference in depth across the solid and which remained constant apart from a small loss due to fluid leakage past the solid. Under dynamic equilibrium conditions, the velocity of the solid would be such that these forces were in balance and the frictional resistance, which will be proportional to the square of solid velocity, would be equal to the pressure and weight component forces. However, due to the impact of the water on the near stationary solid towards the end of zone 1, the solid velocity was higher than that which could be expected from the action of the pressure and weight force, so that the frictional resistance was greater than the sum of these forces and the solid decelerated under the action of this

out of balance resultant force. Now as the frictional force is proportional to velocity squared the solid deceleration was not linear with respect to distance travelled along the discharge pipe and appeared to be more likely to be dependant on  $\sqrt{L}$ , where L was the distance travelled. This zone, where the velocity of the solid is reduced by the frictional resultant force, will be referred to as zone 2.

As the velocity was progressively reduced along the zone 2 pipe length, so the out of balance friction force was reduced until a point was reached where the frictional force equalled the sum of the weight and pressure forces. At this stage the amount of water leaking past the solid became critical as this gradually reduced the driving pressure force, causing gradual further deceleration. Since the rate of water leakage past the solid was relatively small compared to the volume of water still retained behind the solid, this final zone could have theoretically continued for a considerable distance. However, any slight disruption to this delicate force balance, caused by an irregularity such as a pipe coupling, would either have caused solid deposition or have delayed the solid whilst allowing further water leakage, thus causing premature solid deposition. This zone, where the deceleration was governed by water migration past the solid will be referred to as zone 3.

Consideration of the forces acting in zone 3 also explained a common observation of a solid deposit resuming motion after a short time. This was caused by sufficient water damming up behind to increase the pressure force, particularly if the water level ahead had fallen, thus increasing the pressure difference across the solid.

Zone 3 was basically unstable as any minor obstruction was sufficient to cause either loss of driving water level difference across the solid, or solid deposition. Due to this it is recommended that pipe design length be limited at any gradient so that zone 3 flow conditions are never reached.

Figure 52 illustrates the three zones mentioned above.

### 7.2.2 Straight Plastic Pipe

Figure 53 presents values of solid velocity  $V$  plotted against position along the discharge pipe  $L$  for a single maternity pad discharged from an Armitage Shanks P-trap unvented low level w.c. unit. The limits of the three zones mentioned in the preceding section are also shown. It can be seen that the points fall onto a series of curves.

As mentioned in the preceding section, flow observation indicated that solid deceleration in zone 2 was dependant on the out of balance frictional resistance which in turn is proportional to velocity squared. It was therefore suggested that solid deceleration might be expected to be dependant on  $\sqrt{L}$  as predicted in equation (3-2-7) from the dimensional analysis. Therefore, the data shown in Figure 53 were replotted against  $\sqrt{L}$  as shown in Figure 54, resulting in a series of straight line relationships for zone 2 flow conditions. From equation (3-2-7) it would be expected that this data would compress onto one line if the data were plotted as  $V$  against  $\sqrt{L/G}$  where  $G$  is the pipe gradient. Figure 55 illustrates this for the

data previously plotted in Figures 53 and 54, proving the dependence of solid velocity on  $\sqrt{L/G}$ . It will be seen that for zone 2 the data yields a relationship of the form

$$V = C_1 - C_2 \sqrt{\frac{L}{G}} \quad (7-2-1)$$

where  $C_1$  represents the theoretical solid velocity at pipe entry assuming zone 1 does not exist, and  $C_2$  is a measure of the solid deceleration, hence the negative sign. It will be seen from Figure 55 that the zone boundaries are also defined by  $\sqrt{L/G}$ .

Figures 56 to 61 illustrate all the velocity data obtained during the straight plastic pipe testing, plotted as  $V$  vs  $\sqrt{L/G}$ , all these plots supporting the form of equation (7-2-1). A degree of scatter is noticeable, as predicted in section 3.2, due to the change of shape of the solids during discharge from the w.c. trap and passage through zone 1. The scatter is more noticeable for the maternity pad plus paper towel tests due to the greater range of solid configurations possible.

Having established equation (7-2-1) it was necessary to obtain values of  $C_1$  and  $C_2$  for all the conditions tested. It is possible to obtain approximate values from Figures 56 to 61, but in order to obtain exact numerical values for  $C_1$  and  $C_2$ , a least squares analysis was carried out on the mean velocity data obtained from computer program WCHAR. A computer program, LSQ1, was written using a subroutine CURFIT based on the "least squares" method set out by McCracken and Dorn (25). The mean velocity data calculated by program WCHAR was read into LSQ1 which then carried out a least squares analysis of the velocities with respect to  $\sqrt{L/G}$  in zone 2, initially for each test carried out

and then for each block of tests containing the data for each w.c. material, and venting condition, and including all the gradients tested. Approximate limits of zone 2 were obtained from Figures 56 to 61 and were also read into programme LSQ1, the program then ignoring the velocity data applicable to zones 1 and 3. Appendix III includes a printout of program LSQ1 together with a representative sample of the output.

Having obtained the values of  $C_1$  and  $C_2$  for each w.c. type, material, and venting condition, it was possible to analyse the variation of  $C_1$  and  $C_2$  to account for variation between materials, w.c. type and venting condition. However, due to the inter-relationship of  $C_1$  and  $C_2$  it was not easy to define the variations mentioned. It can be appreciated from Figure 55 that the most important point on the graph will be the value of  $\sqrt{L/G}$  at zero velocity. It is appreciated that since the start of zone 3 flow conditions occurs at a velocity between 0.1 and 0.2 m/s, this value of  $\sqrt{L/G}$  does not define the maximum limit of zone 2, but for the purposes of comparison provides a useful parameter. The value of  $\sqrt{L/G}$  at  $V = 0$  is defined as  $C_3$  and is established by:-

$$C_3 = C_1 \frac{C_2}{C_2} \quad (7-2-2)$$

The values of  $C_1$ ,  $C_2$  and  $C_3$  are shown in Table 3 together with values of w.c. failure rate ( $F_1$ ) and partial w.c. failure rate ( $F_2$ ). Table 4 shows the values of percentage flush ahead of the solid (% FAS) for all the tests carried out during the straight plastic pipe testing.

### 7.2.3 Straight Plastic Pipe - Effects of W.C. Venting

An analysis of the variation of  $C_3$ , as given in Table 3, with regard to either vented or unvented w.c. discharge indicated that  $C_3$  was slightly higher for the unvented tests, but since the overall difference was only 0.7%, the result was not of sufficient significance to draw any conclusions. An analysis of the variation of %FAS indicated that % FAS was 4.1% lower for the unvented tests, than the vented tests, although only half the unvented tests were lower than the comparable vented tests and therefore no definite conclusions can be drawn.

### 7.2.4 Straight Plastic Pipe - Variation between Materials

An analysis of the variation of  $C_3$ , as given in Table 3, between single maternity pads and maternity pads plus three paper towels indicated that  $C_3$  was always lower for the towel tests, the difference being 17.8% for Kleenex paper towels and 19.5% for Bowater Scott paper towels. The % FAS was higher for paper towels in 80% of the tests. These results were to be expected since the paper towels generally caused the solids to leave the w.c. trap later in the flush and also caused greater friction loss as the solids travelled down the discharge pipe.

There was a slight difference between Kleenex and Bowater Scott paper towels, indicated by the fact that  $C_3$  was on average 2.0% lower for the latter. The % FAS was higher for the Bowater Scott than the Kleenex paper towels in 78% of the tests. The Bowater

Scott towels also caused more w.c. failures and also exhibited a much higher partial w.c. failure rate, the latter being over five times higher for the Bowater Scott compared to the Kleenex paper towels. This was attributed to the very much lower absorption characteristic of Bowater Scott paper towels, as stated in section 5.1.3, and also that even when saturated, they retained some of their stiffness.

#### 7.2.5 Straight Plastic Pipe - Variation Between W.c's

An analysis of the variation of  $C_3$ , as given in Table 3, between P-trap and S-trap w.c's indicated that  $C_3$  was 7.2% higher for the Armitage Shanks S-trap and 9.2% higher for the Twyfords S-trap with the % FAS being 10% higher for the P-traps than the S-traps. The figures for % FAS tended to contradict those from the w.c. discharge characteristic testing, the only explanation for this being that there was more water leakage past the solid during its transport along the discharge pipe from the P-trap w.c. due to the shape of the solid on discharge from the w.c.

An analysis of the variation of  $C_3$ , as given in Table 3, between Armitage Shanks and Twyfords w.c's indicated that  $C_3$  was 6.0% higher for the Armitage Shanks P-trap and 4.0% higher for the Armitage Shanks S-trap. The % FAS was 50% higher overall for the Twyfords pans than the Armitage Shanks pans. The reason for these results appeared to be that the surface area of the water in the pan was greater for the Twyfords designs, thus allowing more water past the solids before the discharge from the pan, resulting in a loss of efficiency as the solids travelled along the discharge pipe.

### 7.2.6 Straight Plastic Pipe - Optimum Minimum Gradient

Prior to the 1/150 pipe gradient tests an attempt was made to determine the optimum minimum pipe gradient. The term "optimum", in this case, defines the requirement for one hundred per cent stoppage probability with sufficient travel down the discharge pipe to provide enough velocity data from the velocity measuring points to enable analysis of the data. Pipe gradients of 1/500, 1/200 and 1/150 were tested which gave stoppage positions of approximately 4.5 m, 6.5 m and 9.0 m respectively. It is interesting to consider these results in retrospect and taking the  $\sqrt{L/G}$  value for the start of zone 3 as 35, the predicted values of length become 2.5 m, 6.1 m and 8.2 m respectively. The latter two values agree well with the measured values especially when account is taken of the increased travel distance due to zone 3 flow conditions. The reason for the much greater measured stoppage position than that predicted for the first value is of fundamental importance. If the values of  $\sqrt{L/G} = 15$  and  $\sqrt{L/G} = 35$ , representing the maximum extent of zones 1 and 2 respectively, are plotted on a graph of  $1/G$  against  $L$ , as shown in Figure 122, it will be seen that as the value of  $1/G$  increases, the boundaries representing the zone limits converge. However, it has already been demonstrated by the w.c. discharge characteristic tests with a value of  $G = 0$ , that the solid travelled a finite distance, and therefore the stated  $\sqrt{L/G}$  zone limits do not apply as  $G \rightarrow 0$  and similarly as  $G \rightarrow \infty$ , and have, in fact, only been shown to be valid in the range of  $1/40 \geq G \geq 1/150$ . This effectively suggests that there is a minimum stoppage position which depends on the depletion of the energy imparted to the solid by virtue of achieving the necessary "escape" velocity to leave the w.c.

### 7.2.7 Straight Plastic Pipe - Stack Venting Effect

The outlet end of the plastic discharge pipe used during all the tests up to this stage had been fitted with a 92½° junction with short vertical pipes to simulate a vertical stack entry. It was decided to investigate whether this was realistic in comparison to a much longer vertical stack system, since air travel in a conventional stack would be reduced due to friction losses in the stack. In order to investigate this effect, a series of seven tests were carried out with either the upward stack sealed off or the downward stack closed by a certain depth of water seal, or both. The results of these tests are shown as velocity profiles in Figure 62. The Armitage Shanks P-trap low level w.c. with a pipe gradient of 1/100 was used for these tests, with w.c. discharge being tested under both vented and unvented conditions. Figure 62 indicates that stack venting effect had a basically random effect except in the case of the totally unvented test during which air was either expelled from or drawn into the pipe via the 60 mm downward stack water seal. An attempt was also made to test under totally unvented conditions with a 270 mm downward stack water seal but this resulted in a hundred per cent w.c. failure rate apparently due to the pressure build up in the discharge pipe.

### 7.2.8 Variation Between Maternity Pads and Sanitary Towels

In addition to the main tests carried out to investigate the deceleration of the various types of "adopted" solids in the pipe, two further tests were carried out with single sanitary towels,

unvented and vented, with the Armitage Shanks S-trap low level w.c. and a pipe gradient of 1/60. Figure 63 shows the velocity profiles of these tests compared with the equivalent single maternity pad results. Over the first 6 metres of travel, the variation between maternity pads and sanitary towels appeared to be random, but over the remaining pipe length there was a definite divergence of the velocities of the two types of solid with sanitary towels having a 21% lower velocity in the unvented case and 17% lower in the vented case, at a point 11 metres from the w.c. Obviously the limited number of tests with sanitary towels prevents any definite numerical conclusion being established, but the results do show a marked trend, apparently due to the smaller blockage factor of the sanitary towel allowing more water leakage. This is verified by the % FAS for the sanitary towels (35%) being twice that of the % FAS for the maternity pads (17.3%).

#### 7.2.9 Straight Plastic Pipe - Zone Limits

It was stated in section 7.2.2 that the zone limits could be defined by values of  $\sqrt{L/G}$ . This is not strictly true since as explained in Section 7.2.6, in the case of a truly horizontal discharge pipe the calculated length limits of zones 1 and 2 will be zero which has already been disproved by the w.c. discharge characteristic tests with a horizontal discharge pipe. Therefore the definition of zone limits by values of  $\sqrt{L/G}$  is an approximation, only applicable to the range of pipe gradients tested. As can be seen from Figures 56-61 the defined limit of zone 1 by a  $\sqrt{L/G}$  value is a fairly crude approximation whereas the limit of zone 2 is a much more reasonable approximation. However, since the limit of zone 2 is the more important value in terms of drainage design, the crudeness of the approximation to the zone 1 limit

is almost irrelevant. From Figures 56 - 61 a value of  $\sqrt{L/G} = 15$  gives a definition of the limit of zone 1 for all the various tests. From these same figures and also from the values of  $C_s$  in Table 3, a value of  $\sqrt{L/G} = 35$  gives a good definition of the limit of zone 2 for the single maternity pad tests and a value of  $\sqrt{L/G} = 30$  gives a reasonable definition of the limit of zone 2 for the towel tests. In the case of the Twyford's P-trap w.c. a safer definition of the zone 2 limit would be  $\sqrt{L/G} = 27$  for the towel tests, due to the fact that this pan exhibited a significantly worse performance than the other w.c. pans, particularly for the towel tests.

#### 7.2.10 Straight Plastic Pipe - Depth of Flow

Depth of flow was monitored at four points along the straight plastic pipe at the positions shown in Figure 24. Figures 64 - 77 show samples of these depth profiles under various test conditions. With the exception of Figure 68, the top four profiles, shown full scale, are the depth of flow profiles for monitoring positions at 1.14 m, 5.20 m, 9.53 m and 11.14 m respectively down the page. The bottom profile is the depth of water in the collection tank with a full scale deflection representing two gallons and it can be seen that the point of solid entry into the tank is readily identifiable. At the bottom of each figure is a one second timer scale giving time scales of either 5 mm/s or 2 mm/s. In the case of Figure 68, space did not permit the inclusion of either the collection tank profile or the one second timer scale.

Generally the maximum depth of water ahead of the solid at 1.14 metres was 15-20 mm with a mean of 17 mm, this depth increasing so that at 5.20 metres the max. depth was 18-24 mm with a mean of 20 mm. From observation, the maximum depth actually occurred at the limit of zone 1 and was therefore likely to be slightly greater than that shown at the second depth monitoring position, which was generally within zone 2 flow conditions. From the start of zone 2 onwards, the depth of water ahead of the solid diminished so that at 11.14 metres it could be as low as 7 mm. The depth of water immediately behind the solid at 1.14 metres was 15 - 18 mm with a mean of 17 mm, and this depth gradually increased as the solid travelled down the pipe so that at 11.14 metres it could be as high as 32 mm. The effect of the preceding water depth diminishing, and the following water depth increasing, was to increase the head difference across the solid by 5 - 16 mm, therefore increasing the pressure force behind the solid, but also increasing the water leakage past the solid.

A comparison between Figures 64 - 68 enables the effect of pipe gradient to be analysed. At 1.14 metres the depth of water immediately in front of and behind the solid was approximately the same at 17 mm. At 5.2 metres the depth in front of the solid was reasonably constant at 19-20 mm and the depth immediately behind increasing with flatter pipe gradients, giving 20 mm for 1/40 and 26 mm for 1/100. The depth in front then diminished further down the pipe with shallower depths for flatter gradients giving 15 mm for 1/40 and 7 mm for 1/150 at 11.14 metres from the w.c. The depth immediately behind increased further down the pipe with greater flow depth for flatter pipe gradients giving 21 mm for 1/40 and 31 mm for 1/100 at 11.14 metres from the w.c. Figure 68 differs from the other depth profiles due to

the occurrence of a stoppage at 8.30 metres from the w.c., between the second and third depth monitoring points. The profiles indicated that the rate of water leakage past the stoppage was fairly low since the depth dropped only 1.5 mm during the two minute time interval between the first and second flush. Calculation gave a figure for the rate of leakage of 0.16 litres/min. Figures 69 and 70 are included to show the difference in flow depth profiles between a maternity pad and three Bowater Scott paper towels travelling either together or separated respectively.

Figures 67, 71, 72 and 73 show depth of flow profiles for the four different low level w.c. pans under identical test conditions. There was no readily identifiable difference between the pans from these depth profiles.

Figures 74, 75 76 and 77 show water only depth of flow profiles for each of the four low level w.c. pans. These profiles indicated that at 1.14 metres the depth was 16 - 22 mm with a mean of 18 mm, and that the depth increased so that at 5.2 metres the depth was 18 -24 mm with a mean of 22 mm. The depth then decreased so that at 11.14 metres it was 14 - 18 mm with a mean of 16 mm. The only readily identifiable difference between the w.c.'s was that the maximum depth of flow all the way along the pipe was 1 to 3 mm lower for the P-trap than the S-trap w.c.'s.

#### 7.2.11 Straight Cast Iron Pipe

All the velocity data obtained during the straight cast iron pipe testing were plotted against  $\sqrt{L/G}$  as shown in Figures 78 to 82.

Whilst there was a greater scatter than in the case of the straight plastic pipe data, the correlation to the form of equation (7-2-1) was still good. Table 5 presents the values of % FAS and Table 6 gives the definitions and values of  $C_1$ ,  $C_2$ ,  $C_3$ ,  $C_4$  and  $F_1$  and  $F_2$ . The figures for w.c. failure rate ( $F_1$ ) and partial w.c. failure rate ( $F_2$ ) were reasonably comparable to those for plastic pipe, as expected, since the discharge pipe material would not affect them.

It was intended to test the cast iron pipe using all three waste material types, but unfortunately the Bowater Scott paper towels presented certain problems, and therefore this material type was abandoned. These problems were due to the fact that one or more of the Bowater Scott paper towels occasionally left the w.c. pan ahead of the maternity pad, and then proceeded to trigger some but not all of the timers, resulting in non-representative velocity data. In all the testing with paper towels the velocity was based on that of the maternity pad and although the triggering of some of the timers by a preceding paper towel occurred with the other pipe materials, it was possible to observe the occurrence and reset the timer before the maternity pad reached the velocity monitoring position. Obviously this was impossible in the case of the opaque cast iron pipe.

### 7.2.12 Comparison of the Straight Cast Iron Pipe Data to those for the Straight Plastic Pipe

The values of  $C_3$  (i.e. the values of  $\sqrt{L/G}$  for which  $V = 0$ ) were lower in all cases for the cast iron pipe compared to the plastic pipe. To enable easier comparison between the pipe materials a fourth parameter  $C_4$  has been devised, such that:

$$C_4 = \frac{C_3 \text{ (UPVC)} - C_3 \text{ (CI)}}{C_3 \text{ (UPVC)}} \times 100 \% \quad (7-2-3)$$

The values of  $C_4$  are shown in Table 6. It can be seen from the values of  $C_4$ , and using  $C_3$  as the basis of comparison, that cast iron was 14 to 18% less efficient than plastic with a mean of 15.5% in the case of the Armitage Shanks P-trap w.c. and 4% less efficient in the case of the Twyford's S-trap w.c. The reason for the difference between the two types of pan is impossible to explain in view of the limited amount of testing carried out on the Twyford's S-trap pan. The values of % FAS were 3% higher overall for cast iron compared to plastic, although it was only higher in 55% of the tests and was therefore not very significant.

### 7.2.13 Straight Cast Iron Pipe - Effect of W.C. Venting

The values of  $C_3$  were slightly higher for unvented than vented w.c. discharge, but only by 1.5% which was not very significant. The values of % FAS were higher for unvented than vented w.c. discharge by 2.4%, but only in 56% of the tests and therefore the difference was of little significance.

#### 7.2.14 Straight Cast Iron Pipe - Variation between Materials

The values of  $C_3$  were higher in all cases for the single maternity pad compared to the maternity pad plus three Kleenex paper towels, by 19% overall. The values of % FAS were lower in all cases for a single maternity pad compared to a maternity pad plus three Kleenex paper towels, by 24% overall. These differences between waste materials agreed well with those for the straight plastic pipe.

#### 7.2.15 Straight Cast Iron Pipe - Variation between W.C'S

Obviously there is insufficient data to enable any quantitative conclusion to be drawn between the Armitage Shanks P-trap and Twyfords S-trap w.c's. However, the variation between the pans agreed with the conclusions based on the straight plastic pipe testing, since  $C_3$  was higher for the Twyfords S-trap w.c.

#### 7.2.16 Straight Cast Iron Pipe - Zone Limits

From Figures 78 to 82 a value of  $\sqrt{L/G} = 15$  gives a reasonable definition of the limit of zone 1 for cast iron pipe. From these same figures and from the values of  $C_3$  in Table 6, a value of  $\sqrt{L/G} = 29$  gives a good definition of the limit of zone 2 for the single maternity pad tests and a value of  $\sqrt{L/G} = 25$  for the maternity pad plus three Kleenex paper towel tests.

### 7.2.17 Straight Glass Pipe

A few tests were carried out on glass pipe in order to compare this pipe material with plastic and cast iron. The aim of this testing was not to obtain sufficient data to enable a complete analysis of the deceleration characteristics of glass pipe but rather to define variations in the solid deceleration behaviour in glass pipe and to obtain the general deceleration characteristics of this pipe material. As with plastic and cast iron, the velocity data were plotted against  $\sqrt{L/G}$  and are shown in Figures 83 and 84. Table 7 presents the values of % FAS and Table 8 gives the values of  $C_1$ ,  $C_2$ ,  $C_3$ ,  $C_4$  and  $F_1$  and  $F_2$ . The values of w.c. failure rate ( $F_1$ ) and partial w.c. failure rate ( $F_2$ ) in the case of the towel tests were approximately twice those for the comparable plastic and cast iron tests, although the single maternity pad tests were comparable. The reason for the worse w.c. failure rates for the paper towel tests appeared to be due to variations in the size of the maternity pads, the larger pads not being discharged from the w.c., and were therefore not attributable to the glass pipe.

### 7.2.18 Straight Glass Pipe - Flow Observation

Observation of the passage of the water and solids in the glass discharge pipe indicated some variations compared with the observations made on plastic pipe. Whilst the existence of zone 1 was confirmed, the degree of initial solid deceleration was reduced, although the previously stated limit of zone 1 was observed to be approximately the same. The reason for this variation was attributed to the smoother pipe surface resulting in a lower solid deceleration at pipe entry

although the zone 1 flow conditions were still the same as for plastic pipe.

The zone 2 flow conditions were similar to those for plastic pipe although water leakage past the solid was higher, and the velocity of the leading water was higher as would be expected with a smoother pipe surface. This resulted in a marked peculiarity between glass and plastic. Since the velocity of the water ahead of the solid was significantly higher than the solid velocity, the depth of water ahead of the solid reduced noticeably as the leading edge of water reached the vertical stack, causing the solid deceleration to be slightly reduced. The position of the solid at which this reduced deceleration occurred was obviously a function of the relative velocities involved, as can be seen in Figures 83 and 84.

#### 7.2.19 Straight Glass Pipe Compared to Plastic and Cast Iron

Prior to the glass pipe testing it was presumed that glass pipe would exhibit lower deceleration characteristics than plastic pipe and hence a lower value of  $C_3$  and a higher value of  $C_4$ , where  $C_4$  in this case is defined as:

$$C_4 = \frac{C_3 \text{ (UPVC)} - C_3 \text{ (GLASS)}}{C_3 \text{ (UPVC)}} \times 100 \% \quad (7-2-4)$$

However, this assumption was proved false, since for a single maternity pad  $C_4$  was 7.4% but -0.4% for a maternity pad plus three Kleenex paper towels. The glass pipe was therefore 7.4% less efficient than plastic pipe with regards the velocity of a single maternity pad, but was 7.5% better than cast iron pipe. This was due to the greater water leakage past the solid with glass pipe which outweighed the advantage

of the smoother pipe bore compared to plastic pipe. However, in the case of the towel tests the glass pipe still exhibited the higher water leakage past the leading maternity pad, but the friction between the towels and pipe was lower than in the cast of plastic pipe, resulting in a slightly better performance characteristic for glass than plastic pipe.

The % FAS was higher for glass than UPVC by 8.8% overall and was even higher (as high as 28%) if the less accurately defined values of % FAS for flatter pipe gradients are ignored. The less accurate figures were due to the problem of defining % FAS after a stoppage, especially in the case of glass pipe where the water leakage past the stoppage remained high. As well as the primary effect of the smoother pipe bore causing greater water leakage past the solid there was a secondary effect due to the higher leading water velocity reducing the depth of flow ahead of the solid and hence increasing the head of water across the solid which in turn increased the rate of water leakage.

#### 7.2.20 Straight Glass Pipe - Variation Between Waste Materials

The value of  $C_s$  was 11% lower for the maternity pad plus three Kleenex paper towels than the single maternity pad. This difference was lower than those for plastic pipe (18%) and cast iron pipe (19%). However this was attributed to the lower towel friction outweighing the disadvantage of the higher water leakage past the maternity pad in the case of glass pipe, as mentioned in the previous section.

### 7.2.21 Straight Glass Pipe - Zone Limits

From Figures 83 and 84 a value of  $\sqrt{L/G} = 14$  gives a reasonable definition of the limit of zone 1 for glass pipe. From these same figures and also from the values of  $C_s$  in Table 8, a value of  $\sqrt{L/G} = 34$  gives a good definition of the limit of zone 2 for the single maternity pad tests and a value of  $\sqrt{L/G} = 30$  for the maternity pad plus three Kleenex paper towel tests.

### 7.2.22 Conclusion on Straight Pipe Deceleration Characteristics

The travel of the types of solids investigated in a straight horizontal discharge pipe may be defined by three distinct zones, each being determined by the predominance of one of the various forces acting. Zone 1, which occurred over the first 3 - 5 metres of discharge pipe from the w.c. inlet, was characterised by a rapid solid deceleration, due to impact forces as the solid traversed the entry bend and first 2 - 3 metres of the discharge pipe. The following flush water then dammed up behind the retarded solid and caused it to accelerate up to a velocity in the order of 1 m/s at a distance of 3 - 5 metres from the w.c., which defined the start of zone 2.

Zone 2 was governed by the resolved component of solid and water weight force, the pressure force due to the difference in water depth across the solid, and the frictional resistance to motion which was proportional to  $V^2$  and was higher than the sum of the other two forces due to the high solid velocity. This resulted in a non-linear

solid deceleration as the solid continued to travel along the discharge pipe until equilibrium of the three forces occurred at a point defined by a value of  $\sqrt{L/G} = 25 - 35$  and which defined the end of zone 2. The velocity of the solid in zone 2 was given by the equation  $V = C_1 - C_2 \sqrt{L/G}$ , where  $C_1$  and  $C_2$  are empirical constants being functions of w.c. type, pipe material, waste solid type and w.c. venting condition.

Zone 3, which was characterised by the dynamic equilibrium of the weight, pressure and frictional forces, was governed by the water leakage past the solid, which, although occurring in zone 2, became increasingly significant as dynamic equilibrium was approached.

Zone 3, typified by velocities below 0.15 m/s, could theoretically extend for a considerable distance since water leakage was relatively small. However, any minor obstruction, such as a pipe coupler, caused a disruption of the critical force balance and resulted in premature solid deposition. Due to the risk of solid deposition in Zone 3, it is recommended that drainage systems be designed so as to avoid zone 3 flow conditions as defined by the relevant  $\sqrt{L/G}$  value.

The limit of zone 1 flow conditions was shown to be approximately defined by a value of  $\sqrt{L/G} = 15$ . For the case of a single maternity pad, onset of zone 3 flow conditions was shown to be defined by  $\sqrt{L/G}$  values of 35, 34 and 29 for UPVC, glass and cast iron pipe materials respectively and for the case of a maternity pad with three paper towels by  $\sqrt{L/G}$  values of 30, 30 and 25 respectively.

Using the  $\sqrt{L/G}$  value for zero solid velocity as defined by the equation  $V = C_1 - C_2 \sqrt{L/G}$  as the means of comparison it was shown that:

the effect of venting the w.c. discharge was insignificant;  
 a waste material combination of a maternity pad with three paper towels was 11% - 20% worse than a single maternity pad;  
 P-trap w.c. pans were up to 8% less efficient than S-trap w.c. pans;  
 UPVC pipe was 7% more efficient than glass pipe for conveying a single maternity pad but had the same performance for conveying a maternity pad with three paper towels;  
 UPVC and glass pipe were approximately 15% and 7% respectively more efficient than cast iron pipe.

Tests on the effect of the degree of stack venting indicated that this was insignificant, in terms of solid velocity, for most practical applications.

### 7.3 Effects of Bends and Junctions on Solid Transport

During the last phase of the research a large number of tests were carried out on various bends and junctions in order to identify the effects of these pipe fittings on the velocity of the solids. The tests involved were as follows:

- i)  $135^\circ$  UPVC bend at 3.88, 5.90 and 7.937 metres from the w.c.
- ii) Two  $135^\circ$  UPVC bends approximately one metre apart at 5.927 m and 7.010 m from the w.c.
- iii)  $92\frac{1}{2}^\circ$  UPVC bend at 3.93, 5.975 and 8.017 metres from the w.c.
- iv)  $135^\circ$  UPVC junction tested with three different angles of branch entry, namely horizontal,  $45^\circ$  and vertical entry at 6.332 m, 6.437 m and 6.430 m respectively from the w.c.

- v)  $92\frac{1}{2}^{\circ}$  UPVC junction with horizontal entry angle at 6.288 m from the w.c.
- vi)  $135^{\circ}$  UPVC junction tested with straight main line flow through the junction with branch entry at  $0^{\circ}$ ,  $15^{\circ}$  and  $30^{\circ}$ , at 6.332 m from the w.c.
- vii)  $92\frac{1}{2}^{\circ}$  cast iron bend at 6.323 m from the w.c.
- viii)  $92\frac{1}{2}^{\circ}$  cast iron junction at 6.323 m from the w.c.

Tests were also carried out to investigate the effect of venting the non-live main branch whilst testing the branch flow, but all other junction tests were carried out with the non-live junction pipe closed to atmosphere. This pipe was closed with polythene sheet taped over the open end of the pipe which served as a check for any marked pressure change in the pipe since any positive or negative pressure change would have caused this membrane to deflect, which in fact it did not.

#### 7.3.1 Effects of Bends and Junctions - Flow Observation

Observation of the passage of solids in the plastic discharge pipe suggested that the bend or junction caused a slight back up effect, which would influence the solid velocity at approach to the pipe fitting, and that downstream of the fitting there was a marked solid deceleration, followed by a gradual acceleration due to the increasing depth of water behind the retarded solid.

The essential difference between a bend and junction was due to back flow up the non-live pipe away from the junction, with the depth of water immediately upstream of the junction in the non-live

pipe, being only fractionally lower than that immediately downstream of the junction due to the effect of pipe gradient. This had a beneficial effect in some respects because some of the water ahead of a solid was "shunted" into the non-live pipe to be returned into the flow behind the solid after it had passed through the junction. However a comparison of the values of % FAS from the junction tests, Tables 10 and 11, showed that the benefit was not very significant since the mean % FAS for the straight pipe tests was 25.0%, Tables 4 and 5, whilst the lowest % FAS for the junction tests was 19.5%, the difference being only half a litre of water, whereas the mean % FAS value for the junction tests was 22.9%, which was not very significantly different from the straight pipe value.

However, this "shunting" effect proved to be disadvantageous with regards the towel tests. Since water back flowed up the non-live pipe there was a probability (approximately 1 in 10) that a paper towel would be "shunted" up this pipe with the water, with a tendency for the towel to become stranded in the pipe. Any further flushes only pushed the towel further up the pipe. Obviously if the branch drain was used more frequently than the upstream main drain, or the main drain had intermittent use compared to the branch drain, then several towels could be stranded up this drain, which would probably result in a blockage formation.

Another problem identified for junctions was the tendency for the solid to stop in the main drain immediately opposite the branch inlet, resulting in some of the following water being diverted by the solid up the non-live main drain, the solid only being shifted if sufficient

water was built up behind it to start it moving downstream. This was particularly noticeable with the maternity pad plus paper towel tests since the preceding maternity pad decelerated or sometimes stopped downstream of the junction, causing the towels, in some cases, to be deposited in the junction opposite the branch entry, and to remain there. This phenomenon, whilst present with all the junction tests, was very apparent on the vertical junction entry tests. An example of this occurrence is shown in Figures 100 to 102. Figure 103 shows the rig used for all the vertical 135° junction tests including a continuous flushing test carried out using a maternity pad plus three Kleenex paper towels. This test was carried out purely for observation, the resultant blockage formation being recorded on polaroid photographs as shown in Figures 100 to 102.

The first flush resulted in the maternity pad almost stopping in the junction but finally stopping approximately one metre downstream of the junction and the three paper towels stopping in the junction opposite the vertical branch entry. The towels stopped in this position basically because, when falling from the junction into the main drain, they fell into the static water dammed up behind the stationary maternity pad. The solids from the second flush landed, and stopped, on top of the towels from the preceding flush, only moving them slightly downstream, although the first maternity pad was carried to the stack by the excess flush water which was diverted over the stationary towels. The main drain was now approximately half full of water upstream of the stoppage, as shown in Figure 100. Further flushes resulted in a total full bore blockage consisting of nine maternity pads and thirty paper towels, with the upstream main drain now full of water,

as shown in Figure 101, and with one towel having backflowed up this drain, as shown in Figure 102. It was necessary to rod the blockage out since not even water only flushes could move it.

### 7.3.2 Analysis of the Effects of Bends and Junctions

A considerable amount of time was spent in trying to analyse the results in order to produce a complete analysis of all the phenomena affecting the velocity of the solid, due to a bend or junction. Unfortunately it was not possible to establish a universal equation to account for the behaviour of the solid after either a bend or junction and, unless considerably more solid velocity data after the pipe fitting can be collected, it is unlikely that a sufficiently detailed analysis will be possible. To give some idea of the complexity of the problem, the following empirical equation was developed in an initial attempt to predict solid velocity downstream of a 135° bend at a particular distance from the w.c.:

$$V = \frac{-C_a \sqrt{L - L_B}}{\sqrt{G}} + C_b G^{C_e} + C_f + \dots \quad (7-3-1)$$

where  $L_B$  is the distance of the bend from the w.c.

$C_a$ ,  $C_b$ ,  $C_e$  and  $C_f$  are empirical constants

$V$  is the solid velocity

$L$  is the distance from the w.c.

$G$  is the pipe gradient.

Whilst this equation fitted a little of the data well, the problem was obviously more complex than this equation indicated since more terms would be required to cover all the data collected, thus requiring the

derivation of several more empirical constants. Equation (7-3-1) only applies to a particular bend position since the solid velocity at approach to the bend is predicted by the constant term  $C_f$  whereas in fact this term should be that indicated by equation (7-2-1). However, as already mentioned, the bend caused a slight back up effect which influenced the solid velocity at approach to the pipe fitting and which would therefore require equation (7-2-1) to be modified.

Therefore, although a complete analysis resulting in a universal equation predicting solid velocity after any pipe fitting is not feasible at this stage, it is possible to quantify the effects of bends and junctions by reference to the various zone 2 linearized straight pipe relationships already established. All the velocity data were therefore plotted directly against  $\sqrt{L/G}$  in order to enable direct comparison with the relevant straight line datum developed for straight pipe flow, as shown in Figures 86 to 99 and 104 to 121.

From these figures, and from the observations made, the effects of a bend or junction can be defined as shown diagrammatically in Figure 85. With reference to Figure 85 the effects of a pipe fitting can be defined as:

- i) A slight back up effect which influenced the solid velocity on approach to the pipe fitting.
- ii) A marked solid deceleration after the pipe fitting, shown as region A - B, giving a maximum deviation of the mean velocity from the straight pipe datum at point B.
- iii) A solid velocity regain, shown as region B - C, in which the solid velocity returned to the straight pipe datum, and in some cases attained a higher velocity than that predicted by the straight pipe datum.

For the purposes of the analysis of pipe fitting effects, approximate values for the length of pipe after the fitting over which there was a significant deviation of the velocity from the straight pipe datum, shown as region A-C in Figure 85, were obtained by noting the  $\sqrt{L/G}$  value at which the velocity curve meets the straight pipe datum, extrapolating or interpolating where necessary, calculating the value of length for the particular gradient and subtracting the pipe fitting position thus giving the length of pipe over which the fitting had a significant effect. This value is defined as  $L_p$  and if the pipe fitting is positioned at least  $L_p$  metres from the onset of zone 3 flow conditions then the effect of the pipe fitting can be ignored for design purposes. The value of  $\Delta V$  was obtained directly from the graph by measurement. The values of  $L_p$ ,  $\Delta V$  and % FAS are given in Tables 9, 10 and 11, for plastic bends, plastic junctions and cast iron bends and junctions respectively.

Prior to considering the test results in individual detail, several general conclusions can be drawn from Figures 86 to 99 and 104 to 121 and from Tables 9, 10 and 11. The existence of the three flow regions, namely 1, 2 and 3 was confirmed. In some instances the velocity regain after a pipe fitting was such that it resulted in the solid attaining a velocity higher than that predicted by the straight pipe datum. It could therefore be concluded that the inclusion of a bend or junction can improve the solid velocity at a point sufficiently far from the bend. However, other tests, notably the  $2 \times 135^\circ$  bends tests, indicated that when this occurred the velocity then dropped again, approaching the straight pipe datum.

The results also confirmed the observation that the pipe fitting caused a slight back up effect, reducing the solid velocity at approach to the pipe fitting. It was not feasible to quantify this back up effect since some scatter of the straight pipe velocities about the straight pipe datum was to be expected.

With reference to Figures 86 to 99 and 104 to 121 it can be seen that although it is possible to draw a smooth curve through the data points of the graphs, it is impossible to identify either the maximum deviation of the velocity from the straight pipe datum or the point at which the velocity approaches the straight pipe datum, with complete accuracy. The only way to obtain better definition of these values would entail monitoring solid velocity at many more points along the discharge pipe. However, with the limited velocity data obtained it was possible to obtain approximate values for the maximum deviation ( $\Delta V$ ) and the length of pipe over which the pipe fitting had a significant effect ( $L_p$ ). Therefore the method of deriving the values of  $\Delta V$  and  $L_p$  should be noted when considering the accuracy of these values.

### 7.3.3 Effect of a 135° Plastic Bend

Figures 86 to 94 show the graphs for the tests on a 135° plastic bend positioned at 3.88 m, 5.90 m and 7.937 m from the w.c. as shown in Figures 26, 27 and 28 respectively. The form of each curve is similar to that shown in Figure 85 for the bend case and comparison of the curves indicated little variation with regards bend position, waste material type or venting condition. From Table 9, the maximum value of  $\Delta V$  was 0.19 m/s and of  $L_p$  was 5.3 metres with mean values of 0.11 m/s

and 3.7 metres respectively. The overall mean % FAS was 26.5 which, when compared to that for similar straight pipe tests of 24.8, indicated that 0.15 litres effectively escaped past the solid in traversing the bend. However, since the effect of the bend was to temporarily retard the solid in the discharge pipe, this higher % FAS could have been due to leakage past the solid, which was within the discharge pipe for a longer period of time. Therefore no firm conclusion can be made with regards the comparison between the % FAS for these tests and that for the straight pipe tests.

#### 7.3.4 Effect of 2 x 135° Plastic Bends, One Metre Apart

Figure 95 shows the graph for the very limited tests on two 135° plastic bends positioned at 5.927 and 7.010 metres from the w.c., as shown in Figure 32. The approximate one metre separation was adopted as the worst case as indicated by the 135° single bend tests, where the maximum velocity deviation occurred approximately one metre after the bend. From Table 9, the mean value of  $\Delta V$  was 0.14 m/s and of  $L_p$  was 4.2 metres, the value of  $L_p$  being measured from the second bend. Therefore the inclusion of the second bend did not increase either  $\Delta V$  or  $L_p$  very significantly.

#### 7.3.5 Effect of a 92½° Plastic Bend

Figures 96 to 99 present the results for the tests on a 92½° plastic bend positioned at 3.93 m, 5.975 m and 8.017 m from the w.c., as shown in Figures 29, 30 and 31 respectively. The form of each curve is

generally slightly more exaggerated than that for the  $135^\circ$  plastic bend case. From Table 9 there is evidence that  $\Delta V$  and  $L_p$  increased slightly for the bend positions closer to the w.c. However, the accuracy of these values, as already explained, and the relatively small variations make any conclusion doubtful. The maximum value of  $\Delta V$  was 0.21 m/s and of  $L_p$  was 5.4 metres respectively.

Comparison of these mean figures to those for the single  $135^\circ$  bend, indicated that although  $\Delta V$  was increased by 45%,  $L_p$  was only increased by 24%. Comparison of the  $92\frac{1}{2}^\circ$  bend results to the  $2 \times 135^\circ$  bend results confirmed the generally accepted view in the drainage design field that two  $135^\circ$  bends are better than one  $90^\circ$  bend where a change of direction of  $90^\circ$  is required. However the difference was not very significant.

#### 7.3.6 Effect of a $135^\circ$ Plastic Junction with Varying Angles of Branch Entry

Three angles of branch entry were tested, namely horizontal,  $45^\circ$  and vertical as shown in Figures 33, 35 and 37 respectively, to investigate the effect of a  $135^\circ$  junction on branch flow solid velocity through the junction.

Figures 104 to 107 show the velocity graphs for the horizontal entry tests. The form of each curve is similar to that shown in Figure 85 for the  $135^\circ$  junction case. From Table 10 there was evidence that  $\Delta V$  increased with flatter pipe gradients and that  $\Delta V$  was higher for the towel tests compared to the single maternity

pad tests. For the purposes of comparison with the other branch entry angles the overall range of  $\Delta V$  was 0.13 to 0.33 m/s with a mean value of 0.23 m/s. The values of  $L_p$  showed no significant variation between the different test conditions, the values varying from 3.9 to 5.0 metres with a mean of 4.6 m.

Figures 108 to 111 show the velocity graphs for the  $45^\circ$  entry tests, the angle of entry being achieved via a  $148^\circ$  adjustable bend. The form of each curve is less pronounced than the horizontal entry curves and is generally between the curves for the bend case and the  $135^\circ$  junction case shown in Figure 85. From Table 10 the values of  $\Delta V$  ranged from zero to 0.15 m/s with a mean value of 0.06 m/s.  $L_p$  varied from 2.3 to 4.9 metres with a mean of 4.0 m. Therefore the velocity disruption effect of the  $45^\circ$  branch entry was less than that of the horizontal branch entry.

Figures 112 to 115 show the velocity graphs for the vertical entry tests, the angle of entry being achieved via a  $135^\circ$  bend. The form of each curve is very much more pronounced than either the horizontal or  $45^\circ$  entry curves and is generally between the curves for the  $135^\circ$  junction case and the  $92\frac{1}{2}^\circ$  junction case shown in Figure 85. From Table 10 the values of  $\Delta V$  were higher for the towel tests than for the single maternity pad tests, with an overall range of 0.13 to 0.35 m/s with a mean value of 0.27 m/s.  $L_p$  varied between 5.1 and 8.2 metres with a mean value of 6.6 m. Comparing these results with those for the horizontal and  $45^\circ$  entry results, indicated that vertical junction entry caused considerably greater velocity disruption than the other two entry angles tested.

### 7.3.7 Effect of Venting the Upstream End of the Main Drain for the Junction Tests

Figure 112 also shows the results of some additional tests, carried out at the start of the junction tests, to investigate the effect of venting the upstream end of the non-live main drain. These tests were carried out on the vertical entry 135° junction rig. The results showed that any variation was random, and that all further tests did not need to include the extra parameter of venting the non-live end of the drain. However, it was established that the length of blank non-live drain included should be long enough to prevent any wave reflections from the closed end affecting the solid velocity downstream of the junction.

### 7.3.8 Effect of Angle of Branch Entry on the Straight Pipe Flow through a 135° Plastic Junction

Figures 41 and 42 show the junction orientations tested and a schematic view of the rig used for these tests. Figures 116 and 117 show the velocity profiles plotted directly against  $\sqrt{L/G}$ . Since the effect of a 135° junction with varying angles of entry had been investigated with regards branch flow into the main drain, it was also important to establish whether the branch entry angle caused disruption to the main drain flow. For the single maternity pad tests at 1/40 there was a significant difference which indicated that the horizontal branch entry reduced the solid velocity by approximately 0.07 m/s, but that this reduction dropped to 0.05 m/s further downstream.

During the single maternity pad tests at 1/100 an attempt was made to identify the variation between different batches of maternity pads, the

method adopted being to test with apparently "normal" maternity pads and then to retest choosing "heavier" pads. The results indicated that the variation was between 0.03 and 0.07 m/s with the "heavier" pads giving slower velocities. This result, whilst not highly significant due to the extremes tested, should be noted when choosing waste materials for future testing. Ignoring the results of the "heavier" pad tests, the single maternity pad tests at 1/100 indicated that the horizontal branch entry reduced the solid velocity by approximately 0.05 m/s but that this reduction dropped to 0.02 m/s further downstream, and was therefore not highly significant.

For the maternity pad plus three Kleenex paper towels tests, the effect of branch entry angle was not very significant with the approximate variation being 0.05 m/s which reduced further downstream to almost zero.

#### 7.3.9 Effect of a $92\frac{1}{2}^{\circ}$ Horizontal Entry Plastic Junction

Figures 39 and 40 show schematic views of the junction and test rig as used in these tests and Figures 118 and 119 show the velocity profiles, the shape of each profile being similar to that shown in Figure 85 for the  $92\frac{1}{2}^{\circ}$  junction case. From Table 10 the relevant values of  $\Delta V$  and  $L_p$  for the single maternity pad tests were approximately 0.32 m/s and 4.7 m respectively, and for the towel tests approximately 0.56 m/s and 8.6 m respectively. Therefore there was a significant difference between the two types of waste material for this particular junction.

### 7.3.10 Effect of a $92\frac{1}{2}^{\circ}$ Cast Iron Bend and a $92\frac{1}{2}^{\circ}$ Horizontal Entry Cast Iron Junction

Some limited tests were carried out on two cast iron pipe fittings namely a  $92\frac{1}{2}^{\circ}$  bend and  $92\frac{1}{2}^{\circ}$  junction tested as shown in Figures 43 and 44 respectively. The purpose of these tests was to identify, and approximately quantify any difference between cast iron and plastic pipe fittings. Since no visual observations could be made, it was only possible to identify the difference by comparing the numerical data from the plastic and cast iron tests. The velocity profiles from the  $92\frac{1}{2}^{\circ}$  bend tests are shown in Figure 120, the shape of each profile being between the bend case and the  $135^{\circ}$  junction case in Figure 85. From Table 11, the values of  $\Delta V$  were very similar to the comparable plastic bend values and the values of  $L_p$  were slightly lower than the comparable plastic bend values. Therefore any design criteria developed for the plastic bend could be safely applied to the cast iron bend.

The velocity profiles from the  $92\frac{1}{2}^{\circ}$  cast iron junction tests are shown in Figure 121 which when compared to Figure 118 for similar test conditions on a similar plastic junction indicated that the cast iron junction caused considerably more solid velocity disruption than the plastic junction. From Table 11 the values of  $L_p$  and  $\Delta V$  were significantly higher than the comparable plastic junction values but were in fact very similar to the maternity pad plus three Kleenex paper towels values for the plastic junction. The values of  $\Delta V$  and  $L_p$  for the cast iron  $92\frac{1}{2}^{\circ}$  junction were approximately 0.59 m/s and 8.6 metres respectively. Figure 118 is also an excellent example of the effect of positioning the

junction too close to the onset of zone 3 flow conditions. Taking the onset of zone 3 as  $\sqrt{L/G} = 30$  then for 1/60 and 1/70 the onset of zone 3 was at 15 m and 12.9 m respectively. Taking the value of  $L_p$  as 8.6 m, then the maximum distance for the junction position was 6.4 m and 4.26 m for 1/60 and 1/70 respectively. Since the actual position tested was 6.332 m, the 1/60 case was just within this limit whilst the 1/70 case was well outside the limit with the result that the maternity pad always stopped within approximately one metre either side of the junction. As explained in Section 6.1, it was not possible to identify exact stoppage positions due to the opacity of the cast iron pipe, although it was possible to identify from the instrumentation, that the solid had stopped between a particular pair of velocity measuring positions.

#### 7.3.11 Design Limits for Bend and Junction Positions

As suggested in Section (7.3.2), the effect of a bend or junction can be ignored for design purposes if the pipe fitting is positioned at least  $L_p$  metres from the onset of zone 3 flow conditions. Therefore the value of  $\Delta V$ , whilst being a useful parameter in comparing the performance of different types of pipe fitting, is not a necessary parameter for design purposes. In the case of pipe fittings which exhibit a very high value of  $\Delta V$ , it was observed that although the solid might actually stop soon after the pipe fitting, the flow conditions already described still caused the solid to be accelerated back to the equivalent straight pipe velocity datum.

From the results presented in Tables 9, 10 and 11, an overall value of  $L_p = 5$  metres covers the majority of the cases tested, and it is therefore suggested that this value be adopted as a general design figure. The exceptions to this general figure were the vertical entry  $135^\circ$  plastic junction, for which an  $L_p$  value of 8.2 metres is suggested, and the  $92\frac{1}{2}^\circ$  horizontal entry plastic and cast iron junctions for which an  $L_p$  value of 8.6 metres is suggested. It is also suggested that these particular cases be avoided in a designed drainage system, but where this is not feasible, that the stated values of  $L_p$  be adopted for the design. The results also indicated the advantage of using a  $45^\circ$  branch entry for the  $135^\circ$  junction since this caused the minimum disruption to both the branch flow and the main drain flow.

If a pipe fitting is positioned such that it is within 5 metres of the point at which zone 3 starts, the nature of zone 3 will be affected because the pipe fitting will cause a disruption of the critical force balance normally achieved in this zone. After traversing a pipe fitting the solid decelerated rapidly as shown by A - B in Figure 85, and this was followed by either a less rapid deceleration or an acceleration as shown by B - C. By definition, the slope of the curve between B and C is flatter than the slope of the straight pipe datum. It is therefore impossible for a true zone 3 situation to develop between B and C because there is an additional force acting in the direction of flow due to an increased depth of water behind the temporarily retarded solid. This additional force could possibly be used to advantage by reducing the 5 metre critical length for the positioning of a pipe fitting before the point at which zone 3 normally starts in the equivalent straight pipe situation. However, this

additional force might be better regarded as a slightly increased safety factor in the designed drainage system.

### 7.3.12 Conclusions on Effects of Bends and Junctions

The effect of a bend or junction on the velocity of the type of solids tested, was to cause a rapid solid deceleration for approximately 1-2 metres after the pipe fitting, which was followed by a velocity regain where the solid velocity returned back to the same velocity as that predicted by the equivalent straight pipe velocity datum given by the relationship  $V = C_1 - C_2 \sqrt{L/G}$ ,  $L$  being measured as the pipe length from the w.c. The length of pipe, defined as  $L_p$ , over which the solid velocity deviated significantly from the straight pipe velocity datum was obtained graphically and was generally below 5 metres, with two notable exceptions. These exceptions were the  $92\frac{1}{2}^\circ$  horizontal entry junction and the vertical entry  $135^\circ$  junction, which exhibited an  $L_p$  value of approximately 8.6 m. It is suggested that, for design purposes, a pipe fitting should not be positioned within  $L_p$  metres of the onset of zone 3 flow conditions as defined by the relevant  $\sqrt{L/G}$  value, since the pipe fitting will not then create premature onset of zone 3 flow conditions. It was shown that, in the case of the  $135^\circ$  junction,  $45^\circ$  entry to the main drain was significantly better than horizontal entry which in turn was better than vertical entry, and it is advised that the latter junction orientation should be avoided, if possible, due to the increased risk of solid deposition opposite the vertical branch entry. This advice tends to disagree with a suggestion made in reference (26) which stated that branch soil

and waste pipes should

"Preferably be connected in the top third  
of the pipeline to prevent backing-up"

which, although logical, does not take account of the increased risk of solid deposition. It is also interesting to note that the suggestion quoted from reference (26) disagrees with a recommendation made in reference (27), that wastes from lavatory basins should enter the main drain at an angle of between  $0^{\circ}$  and  $45^{\circ}$  from the horizontal. Since a shallow angle of branch entry is likely to be affected by a back flow from the main drain, it would be more logical to recommend only the  $45^{\circ}$  entry, since this also reduces the risk of disruption of the main drain flow, as demonstrated by some of the tests reported earlier in this thesis.

Other conclusions, outlined below, were based on comparisons between the various tests carried out. The effect of positioning two  $135^{\circ}$  bends with a one metre separation only increased  $L_p$  from 4.0 m to 4.2 m when compared with the single  $135^{\circ}$  bend. For the limited number of tests carried out on cast iron pipe fittings, it was shown that they exhibited similar characteristics to the UPVC pipe fittings. Tests carried out on the influence of angle of branch entry on the straight main drain flow through the junction indicated that horizontal entry reduced the local solid velocity by approximately 0.07 m/s, and that increasing the angle of branch entry to  $30^{\circ}$  reduced the disruption to almost zero.

#### 7.4 The Design Method for Above Ground Horizontal Drainage Systems

The work reported in this thesis has been specifically aimed at solving some of the problems experienced in hospital drainage systems. Whilst this influenced the choice of representative waste materials, the results can be applied to any above ground drainage system involving long "horizontal" drainage runs. It is emphasised that the design method is based on a deposit free system and that therefore a worst case analysis has generally been adopted throughout.

The design method is based on preventing the development of zone 3 flow conditions. The point at which zone 3 flow conditions start, can be defined by the parameter  $\sqrt{L/G}$ , the values being 35, 34 and 29 for plastic, glass and cast iron respectively, for the single maternity pad case or in the case of a maternity pad plus three paper towels the limits are 30, 30 and 25 respectively. These  $\sqrt{L/G}$  values are not dependant on venting of the w.c. The type of waste material chosen for the basis of the design will depend on the type of drainage load to be expected in the designed system. Generally it is felt that the single maternity pad represents a sufficiently heavy drainage load, except in some special hospital situations.

The effect of pipe fittings can be ignored in the designed system as long as they are positioned at least 5 metres from the onset of zone 3 flow conditions, except in the case of certain pipe fittings, or configurations. The exceptions are the vertical entry  $135^{\circ}$  junction and the  $92\frac{1}{2}^{\circ}$  horizontal entry junctions, for which a pipe length of

approximately 8.6 m would be required between the pipe fitting and the onset of zone 3 flow conditions defined by the relevant  $\sqrt{L/G}$  value.

The design method can be presented graphically as shown in Figure 122, which applies to the single maternity pad case for UPVC pipe. The axes of this graph are the reciprocal of pipe gradient ( $1/G$ ) and the pipe length. It is therefore possible to draw two lines which will define the limits of zone 1 ( $\sqrt{L/G} = 15$ ) and zone 2 ( $\sqrt{L/G} = 35$ ). Obviously the zone 2 limit is the more fundamental of the two for design purposes. It can be seen from Figure 122 the way in which the zone limits converge for flatter pipe gradients. A third line is also plotted in Figure 122 which is the limiting position of any pipe fitting and is defined by  $\sqrt{(L + 5)/G} = 35$ . Thus Figure 122 makes the design procedure extremely simple to apply, since for a chosen pipe gradient, the limiting pipe length and limiting pipe fitting position can be read off directly, or conversely for a given pipe length the relevant pipe gradient can be read off. Obviously other graphs can be drawn for the other pipe materials and waste materials according to the value of the zone 2 limits.

The research programme will be continuing for at least three more years, and during this time further laboratory tests will be carried out, but more importantly, tests will be conducted on existing hospital drainage systems. From these tests it will be possible to establish defined levels of probability for the deposit free travel of solids which will also take account of the actual standards of installation of drainage

systems as opposed to the almost perfect standard achieved in the laboratory. Obviously any additionally required safety factor can also be incorporated into the designed drainage system. It is not anticipated that the design method will be changed significantly from that outlined above, other than to establish different zone  $2\sqrt{L/G}$  values based on defined probability levels.

Until this continuing work has been completed, it is not possible to define the necessary probability levels. However, it is suggested that the postulated design method, based on mean solid velocities, could be used as a check on conventionally designed drainage systems and hence identify and rectify any details likely to cause solid deposition problems in the system.

## 8. LIMITATIONS OF THE RESEARCH

There are several inherent limitations in the research carried out during this project, some of which will require further investigation, but all requiring consideration, which is the purpose of this section. The intention of this three year research programme was to investigate general design parameters in horizontal above ground drainage systems, aimed specifically at hospitals. The requirement of a general investigation resulted in avoiding specific problems of limited application such as, for example, certain problems involved with kitchen waste including grease and fat. Whilst these specific problems obviously require solutions, it was considered essential to first of all establish a general design method and to carry out investigations of specific problems at a convenient time in the future, in subsequent research programmes.

A general philosophy adopted for the investigations described in this thesis was to always consider the worst case condition. This obviously influenced several decisions made during the testing programme, such as the testing of a single w.c., discharging into a long "horizontal" discharge pipe. Whilst there would generally be other appliances also discharging into this pipe, the worst case would be the single w.c. flush with no other discharge from the other appliances for a significant time interval.

### 8.1 Selection of Waste Materials

The reasons for the choice of maternity pads as the main waste solid material are mentioned in section 5.1.4, the main reason being that a

maternity pad represents a worse than general drainage load. Paper towels were also included in order to allow investigation of the travel of multiple solids in a discharge pipe. It is anticipated that the continuing research programme will include an investigation of waste material types including simulated human faeces. Whilst the limitations involved in the selection of a maternity pad as the waste solid were obvious, another limitation became apparent during the testing. There is some variation between maternity pads and more significantly between packets of maternity pads. This was exhibited by the fact that some packets tended to cause more w.c. failures than others, and to overcome this tendency it would be sensible to mix up all the maternity pads, from a box of maternity pads, in order to provide a more random distribution of the pads.

The choice of two types of paper hand towels with maternity pads was based on the need to consider multiple solids. However, since a single maternity pad represents a worse than normal drainage load the continued use of paper towels is probably unnecessary. If a discharge load based on simulated human faeces with conventional toilet paper is proved to be practicable, then this material choice is obviously more sensible and will provide the multiple solids case.

## 8.2 Venting of the w.c. Discharge

The method of connecting the w.c. to the horizontal discharge pipe is described in section 4.1.5. and includes details of the method of venting the w.c. discharge. The vent was provided by either a relatively

short 50 mm diameter pipe or a 50 mm diameter orifice. Obviously this represents a perfect pipework ventilation system since in practice, there would be an appreciable resistance to air flow in the ventilation pipework. However, since the tests indicated that the effect on solid velocity of venting the w.c. discharge was negligible, this limitation is considered insignificant.

### 8.3 Vertical Stack Outlet

The outlet end of the discharge pipe was fitted with a  $92\frac{1}{2}^{\circ}$  junction with short lengths of pipe fitted above and below the junction to represent a vertical stack connection as described in section 4.1.5. Obviously the air flow into or out of the discharge pipe was virtually unrestricted, whereas in practice there would be an appreciable resistance to air flow due to the long stack. Whilst this presents a limitation on the work carried out, an investigation of stack venting effects indicated negligible variations in solid velocity with restricted air flow.

### 8.4 Junction Testing

All the tests carried out on junctions were based on branch flow through the junction with a non-live main line. This represents a major limitation of the work on junctions and it is intended that testing of branch flows entering a live main line discharge pipe will be included in the continuing research programme.

## 8.5 Pipe Condition and Deterioration

As stated earlier, all the testing was carried out on virgin pipe, and since the tests were based on uncontaminated waste, no deterioration of, or solid deposit on, the discharge pipes occurred. Although opinion varies as to extent, there is evidence that growth build up occurs on discharge pipes. The effect of this growth is debatable since it will tend to smooth the roughness of cast iron pipe, but could reduce the cross sectional area of flow if growth were to continue unchecked. Whilst it might be possible to install a section of well used pipe into the research rig, it is unlikely that the condition of the growth or deposit will be representative as it would not be replenished. This might be due to any change in the pattern of usage prior to removal, the effect of moving the pipe, and any delay during the move and during the testing of the pipe. To overcome these problems, it is hoped to carry out insitu testing, preferably in an older hospital, as part of the continuing research programme.

If future testing indicates that the efficiency of discharge pipes is reduced with time, then the  $\sqrt{L/G}$  zone 2 limit will need to be reduced to accommodate this deterioration. However if the efficiency increases with usage then the  $\sqrt{L/G}$  zone 2 limit should not be increased since the drainage system must operate satisfactorily during all stages of its use. One pipe material not affected by growth formation is glass pipe, since any growth or deposit can be removed by chemical flushing at regular intervals.

## 8.6 Effects of Installation and Use

The standard of installation of the discharge pipes on the drainage rig is considerably better than that achieved on site. During the testing, pipe alignment and gradient adjustment was carried out to an accuracy of at least  $\pm 0.5$  mm. The effects of installation errors and possibly building settlement will require consideration in establishing the eventual  $\sqrt{L/G}$  zone 2 limits for design purposes.

Although it is possible to design a drainage system with a 100% probability of being free of normal deposits, blockages will still occur due to abuse of the system. Foreign materials have a renowned tendency to find their way into the drainage system and hospitals suffer from this tendency more than others. It is impossible to design the drainage system for this contingency, and provision of rodding points and access will remain as imperative as ever. No attempt has been made during the testing to investigate the effect of rodding points etc. but their effect is not likely to be significant, as long as common sense is applied to their positioning in order to avoid disruption of flow.

## 8.7 Larger Installations

In practice, a drainage system would involve a large number of horizontal discharge pipes, with branches, connected to the vertical discharge stacks. The tests carried out were on a single horizontal discharge pipe with a vertical stack connection at the outlet end. This represents a small element of the much larger matrix of the normal drainage system.

In practice, the discharge travelling down a vertical stack from floors above might influence the velocity of the solids in the horizontal pipes discharging into the stack lower down, and this has not been tested in this research, mainly due to limitations in laboratory size.

The Building Research Establishment have carried out investigations of the influence of stack discharge on horizontal discharge pipes, but only from the point of view of pressure fluctuations within the drainage system, generally considering water only discharges. The effect of pressure fluctuations, within the system, on solid velocities in horizontal discharge pipes, and also the effect, of any water backflow up the horizontal discharge pipes from the stack, might require further investigation. The effect of relatively large solids falling down the central air core of vertical stacks possibly causing significant pressure reductions might also require further investigation. It should be noted that no trap seal loss was observed during any of the tests carried out during the reported research programme.

#### 8.8 Limitations of the Design Method

The tests have been based on a single sample of each of the eight DHSS approved hospital w.c. pans, and it has been assumed that each is representative of its type, or that variation between w.c.'s of a particular type is not significant. Whilst the validity of these assumptions can be questioned, the postulated design method will not be affected other than in the establishment of the  $\sqrt{L/G}$  zone 2 limits.

The  $\sqrt{L/G}$  zone 2 limits presented in section 7.4 are based on mean velocities, as stated. These limits will need to be altered in the light of the continuing research programme and with the establishment of defined safety factors and probability theory. As mentioned in section 7.2.9, the definition of zone limits by values of  $\sqrt{L/G}$  is not valid for very steep or very flat pipe gradients, but are at least applicable over the range of pipe gradients tested from 1/40 to 1/150.

## 9. CONCLUSIONS AND FURTHER WORK

Comparative tests on the eight DHSS approved w.c. units indicated that the hydraulic advantage gained by a high level cistern is reduced by the fitting of a flush pipe restrictor, which is required to prevent water splashing over the edge of the pan. The effect of the flush pipe restrictor was to reduce the performance of the w.c. pan and could even result in a lower standard of performance than the comparable low level w.c. Due to variations between pans of nominally the same design, it is suggested that some of the hydraulic advantage of a high level cistern could be retained if various size flush pipe restrictors were trial fitted at the time of installation of the w.c., but if this proved impractical, the use of high level cisterns appears to provide no significant advantage.

The travel of solids in straight discharge pipes may be characterised by three zones which can be defined by the various forces acting on the solid, where solid refers to a maternity pad, either with or without three paper hand towels. At discharge pipe entry from the w.c., the solid decelerated rapidly due to the impact forces as the solid traversed the entry bend and first 2 - 3 metres of discharge pipe. The following flush water then dammed up behind the retarded solid and caused it to accelerate up to a velocity of approximately 1 m/s at a distance of 3 - 5 metres from the w.c. This entry region, which was governed by impact forces and subsequent solid acceleration is termed zone 1. The limit of zone 1 was shown to be

approximately defined by the parameter  $\sqrt{L/G} = 15$ , where  $L$  is the distance from the w.c. in metres and  $G$  is the pipe gradient. After achieving a velocity of approximately 1 m/s at entry to zone 2, the solid came under the influence of a relatively stable system of forces consisting of the resolved component of the solid and water weight, and the pressure force due to the difference in water depth across the solid, both acting in the direction of travel and the frictional resistance to motion which was proportional to the square of solid velocity. Due to the relatively high solid velocity, the latter force caused a non-linear solid deceleration throughout zone 2 until dynamic equilibrium of the three forces occurred at a point defined by  $\sqrt{L/G} = 25-35$ , and which defined the end of zone 2. Dimensional analysis suggested, and test data confirmed, that the solid velocity ( $V$ ) in zone 2 could be defined by the equation  $V = C_1 - C_2 \sqrt{L/G}$ , where  $C_1$  and  $C_2$  are empirical constants, being functions of w.c. type and venting condition, pipe material, and solid type. Zone 3, which was characterised by velocities below approximately 0.15 m/s, was governed by the rate of water leakage past the solid resulting in a reduced pressure force. Due to the relatively low rate of water leakage, zone 3 flow conditions could theoretically have continued for a considerable pipe length, but any minor obstruction, such as a pipe coupler, caused a disruption of the critical force balance and resulted in premature solid deposition. The length of zone 3 was therefore unpredictable and due to the risk of solid deposition, it is recommended that drainage systems be designed so as to avoid zone 3 flow conditions. The end of zone 3 can be defined by

$\sqrt{L/G}$  values of 35, 34 and 29 for UPVC, glass and cast iron pipe materials respectively, for a single maternity pad, or in the case of a maternity pad plus three paper towels by values of 30, 30 and 25 respectively. The type of waste material chosen for the basis of the design would depend on the type of drainage load to be expected in the designed system.

The effect of pipe fittings can be defined by reference to a datum of the zone 2 straight pipe velocity. Immediately after a pipe fitting there was a rapid solid deceleration for approximately 1 - 2 metres, followed by a velocity regain where the solid velocity returned back to the same velocity as that predicted by the straight pipe velocity datum. The length of pipe over which the solid velocity deviated significantly from the straight pipe velocity datum is defined as  $L_p$  metres. The value of  $L_p$  was generally below 5 metres except in the cases of the  $92\frac{1}{2}^\circ$  junction and the vertical entry  $135^\circ$  junction which exhibited an  $L_p$  value of approximately 8.6 m. If a pipe fitting is positioned at least  $L_p$  metres from the onset of zone 3 flow conditions as predicted by the relevant  $\sqrt{L/G}$  zone 2 value, premature solid deposition is avoided and the effect of the pipe fitting can be ignored, and it is suggested that 5 metres be adopted for design purposes, except for the two cases mentioned which require a pipe length of 8.6 m, but should be avoided if possible. It was also shown that  $45^\circ$  entry to the main drain of the  $135^\circ$  junction was preferable to horizontal entry since this junction orientation caused a lower velocity deviation and also prevented the risk of back flow up the branch drain from the main drain, also resulting in less disruption of the solid velocity in the main drain flow through the junction.

The results presented and discussed can be applied as a design method to be used in conjunction with existing techniques. For the convenience of the designer, this check method is presented below in summarized form.

The design method postulated is readily expressed in a graphical form with axes of pipe length and the reciprocal of pipe gradient with plots of the two zone boundaries given by the relevant  $\sqrt{L/G}$  values with the limiting position of pipe fittings being defined by a third plot representing an  $L_p$  value of 5 metres. The  $\sqrt{L/G}$  and  $L_p$  values presented, are based on mean velocities. These values will require minor alteration based on levels of probability of solid deposition to be established during the continuing research programme after the investigation of various other factors. The design method presented therefore requires further refinement, but it is suggested that it could be used as a check on conventionally designed drainage systems in order to identify and rectify any design details likely to cause solid deposition.

To apply this check, which is relevant to any discharge pipe length of more than 2 metres, either the graphical method can be used, or the relevant numerical  $\sqrt{L/G}$  method. The value of  $\sqrt{L/G}$  determining the maximum deposit free pipe length at any gradient should be 35, 34 or 29 for plastic, glass and cast iron pipe materials respectively, or for exceptionally heavy expected discharge loads, values of 30, 30 or 25 respectively should be used. Initially the maximum "horizontal" pipe length from any w.c. to the vertical stack should be calculated ( $L$ ), together with the designed discharge pipe gradient ( $G$ ), and the value of  $\sqrt{L/G}$  established. If this value is less than the appropriate figure of 25, 29, 30, 34 or 35, depending on the expected discharge load and pipe material, then the possibility of zone 3 flow conditions occurring is negated, together with the attendant deposition probability.

If there is no pipe fitting within 5 metres of the vertical stack, no further calculations are needed, but if this is not the case, then the following check should be made. To ensure that any pipe fitting does not produce premature onset of zone 3 flow conditions, the maximum length of pipe between a w.c. and any pipe fitting should be calculated ( $L$ ) and this value must be less than the value of  $L$  calculated from  $\sqrt{(L+5)/G} = 25, 29, 30, 34$  or 35, depending on the expected discharge load and pipe material. If the onset of zone 3 flow conditions is indicated by either of the calculations, it will be necessary to increase the discharge pipe gradient to ensure that zone 3 will not occur in the designed system.

In addition, the experimental data indicated that it is inadvisable to use vertical junction entry (i.e. branch entry to the crown of the discharge pipe), or branch entry via a  $92\frac{1}{2}^\circ$  junction.

As well as the design method outlined, several other fundamental conclusions can be drawn. The efficiency of w.c. discharge could be considerably improved by reducing the volume of water discharged ahead of the solids. The mean percentage flush ahead of the solids for each test, as measured at the stack outlet, varied between 15.5% and 57.8% with an overall mean value of 26.5% which represents 2.4 litres of water. The effect of venting the w.c. discharge did not have any significant effect on the solid velocity and therefore the requirement for the provision of ventilation pipework is not affected by this research. The P-trap w.c. pans tested were approximately 8% less efficient than the comparable S-trap w.c. pans, as defined by the onset of zone 3 flow conditions. UPVC pipe was 7% more efficient than glass pipe for conveying single maternity pads, but had the same performance for conveying a maternity pad with paper towels. UPVC pipe was approximately 15% more efficient than cast iron pipe.

Due to the lack of previous research into the mechanics of flow in drainage systems, considerable further work is required to provide an adequate understanding for the design of efficient drainage systems. However, confining the consideration of further work to that indicated by the research reported, the following topics appear relevant: an investigation of different types of waste material, including simulated human faeces; further investigations of different pipe fittings, including branch flow through a junction with simultaneous main drain flow; investigations of existing drainage installations in order to account for pipe installation errors and pipe condition, preferably with insitu testing; and finally the establishment of stated levels of probability of deposit free drainage systems.

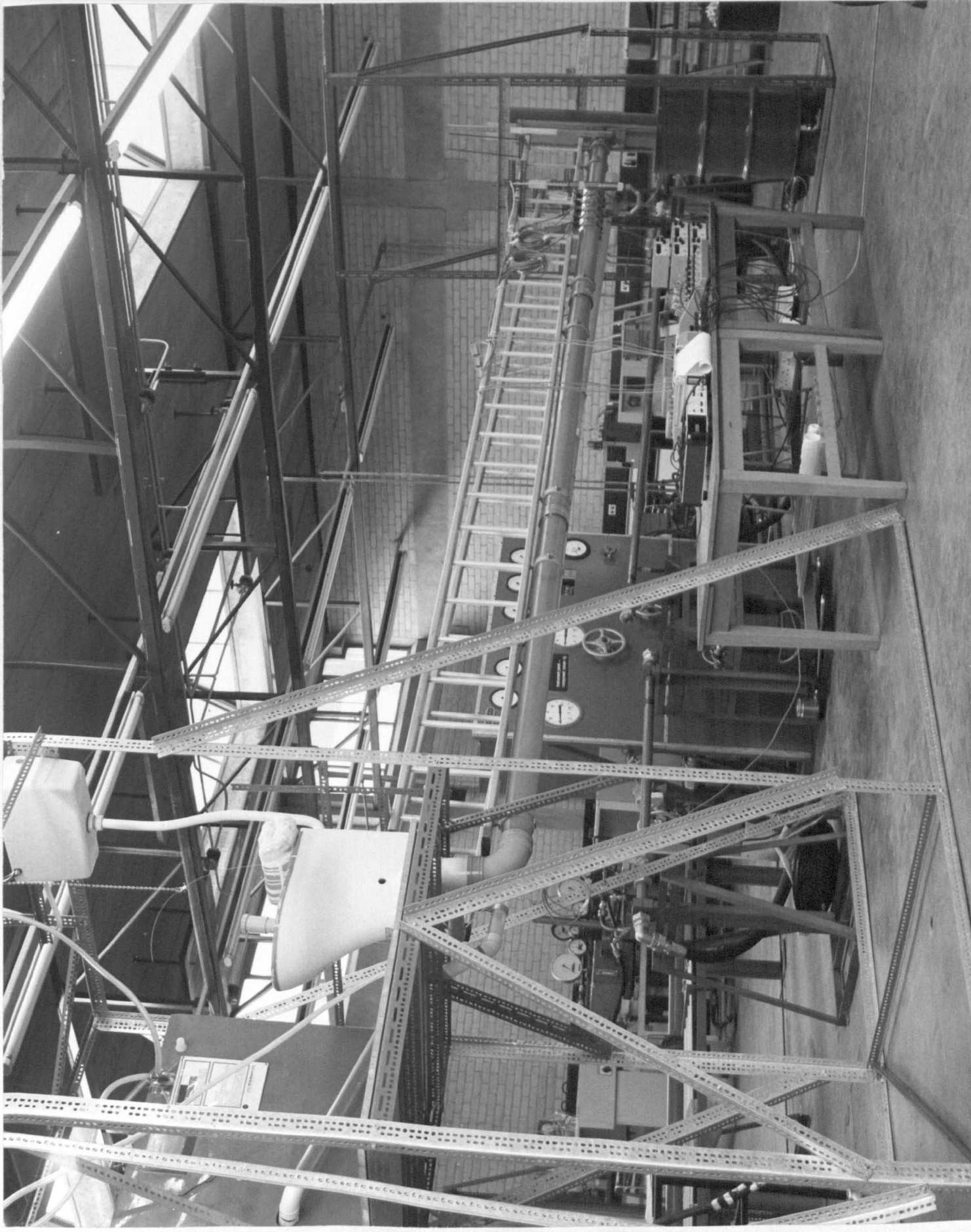
## 10. REFERENCES

- (1) Wise, A. F. E. "Research for better sanitary services"  
BRE paper 9/73, March 1973.
- (2) Swaffield, J. A. "A study of the transport of waste solids in above ground sanitary drainage systems"  
The Public Health Engineer, No 17, September 1975.
- (3) Bowyer, J. "History of building"  
Crosby Lockwood Staples, 1973.
- (4) Rolt, L. T. C. "Isambard Kingdom Brunel"  
Longman Group Ltd., 1972.
- (5) Burberry, P. "Environment and services"  
a volume in the series  
"Mitchell's building construction"  
B. T. Batsford Ltd., 1970.
- (6) Woolley, E. L. "Drainage details in S.I. metric"  
Northwood Publications Ltd., 1971
- (7) Thompson, T. A. "A guide to sanitary engineering services"  
Macdonald and Evans Ltd., 1972.
- (8) Lillywhite, M. S. T.  
and  
Wise, A. F. E. "Towards a general method for the design of drainage systems in large buildings"  
BRE paper 27/69, August 1969.
- (9) Wise, A. F. E. "One-pipe plumbing:- some recent experimental hydraulics at the Building Research Station"  
Journal of the Institution of Public Health Engineers, Vol 51, 1952.
- (10) Wise, A. F. E. "Self-siphonage in building drainage systems"  
Proceedings Institution of Civil Engineers, Part 3, Vol 3, No 3., 1954.
- (11) Wise, A. F. E.  
and  
Croft, J. "Investigation of single-stack drainage for multi-storey flats"  
Journal Royal Sanitary Institute, Vol 74, No 9, 1954.

- (12) Wise, A. F. E. "Drainage services in buildings - a review of some fluid mechanics aspects of the subject"  
BRE paper 35/73, December 1973.
- (13) Pink, B. J. "A study of water flow in vertical drainage stacks by means of a probe"  
BRE paper 36/73, December 1973.
- (14) Pink, B. J. "Laboratory investigation of the discharge characteristics of sanitary appliances"  
BRE paper 37/73, December 1973.
- (15) Pink, B. J. "The effect of stack length on the air flow in drainage stacks"  
BRE paper 38/73, December 1973.
- (16) Davidson, P. J.  
and  
Courtney, R. G. "Revised scales for sanitary accommodation in offices"  
BRE paper 35/76, April 1976.
- (17) Wyly, R. S. "Investigation of the hydraulics of horizontal drains in plumbing systems"  
National Bureau of Standards,  
Monograph 86, December 1964.
- (18) Wyly, R. S.  
and  
Sherlin, G. C. "Performance of a single-stack DWV system utilizing low-angle stack-branch confluence and bottom shunt venting"  
National Bureau of Standards,  
Building Science Series 41,  
April 1972.
- (19) British Standards  
Institution "Sanitary pipework above ground"  
British Standard Code of Practice  
CP 304: 1968
- (20) Tsukagoshi, N.  
and  
Matsuo, Y. "Performance tests for the carriage of excreta in the drainage system connected to water saving type closets" A preliminary report.  
CIB W62 Symposium "Drainage and water supply for buildings",  
September 1975.
- (21) Miller, D. S. "Internal flow, a guide to losses in pipe and duct systems"  
B.H.R.A. 1971.
- (22) Charlton, J. A. "Pneumatic breakwater, the two dimensional water flow induced by air rising from a submerged source"  
B.H.R.A. report RR 864, 1961.

- (23) Stoodley, K. D. C. "Basic statistical techniques"  
Bradford University Press in  
association with Crosby Lockwood  
Staples, 1974.
- (24) Moroney, M. J. "Facts from figures"  
Penguin Books Ltd., 1969.
- (25) McCracken, D. D.  
and  
Dorn, W.S. "Numerical methods and FORTRAN  
programming "J. Wiley, 1964.
- (26) Barrett, R. T. "Hospital drainage"  
Hospital Service Engineering No 16,  
March 1971.
- (27) Payne, R. "Hospital drainage systems"  
Hospital Service Engineering No 13,  
March 1970.

Figure 1. Photograph of the complete test rig as used during the initial tests.  
Note: the large and small support rigs, the ladder support method for the pipe and the instrumentation table.



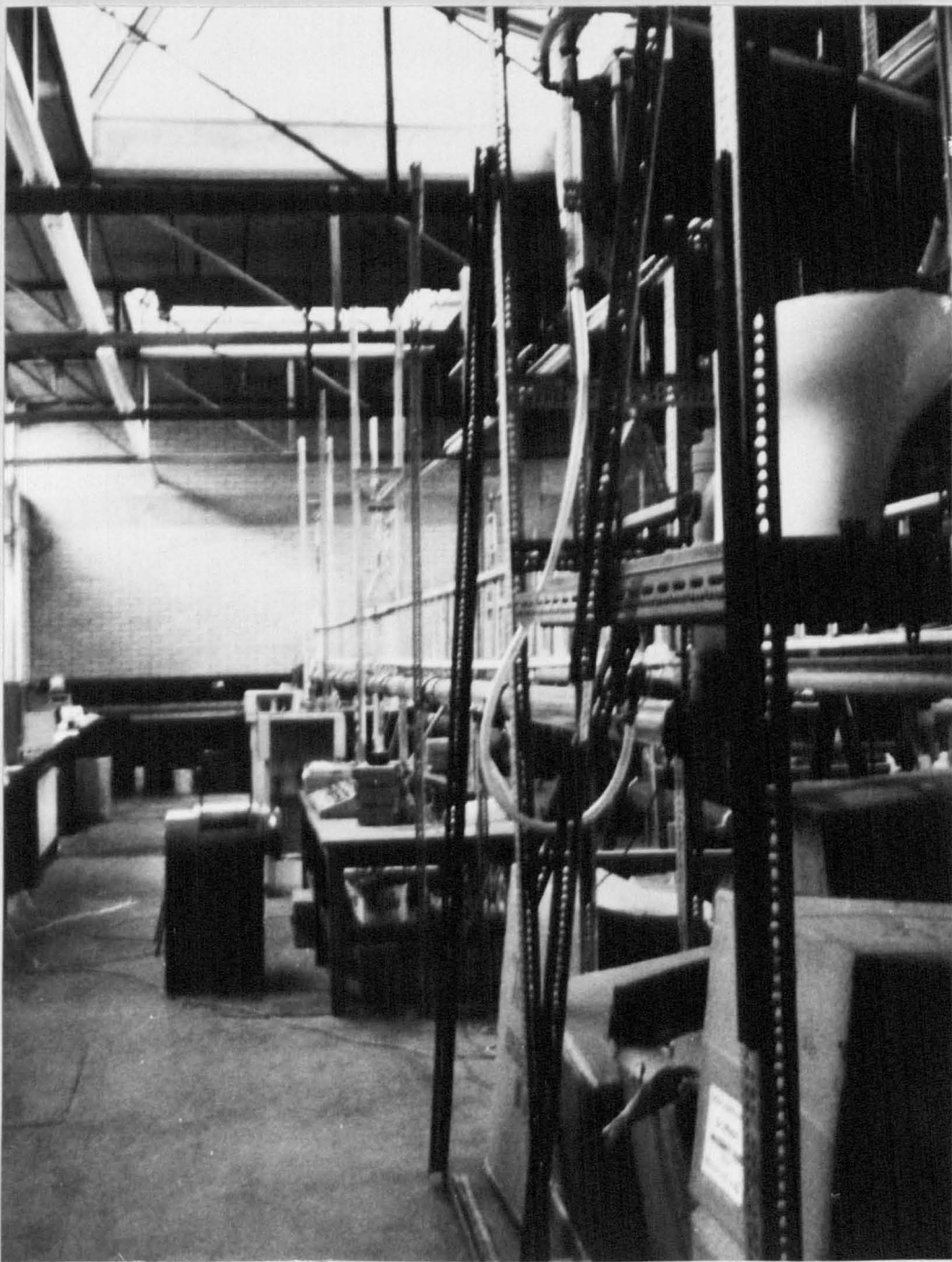


FIGURE 2. General view of the straight glass pipe test rig.  
Note: the large support rig and the vertical column supports.



FIGURE 3. Photograph of the large support rig.  
Note: inlet end of waste pipe support,  
bedpan disposal unit in background and  
an s-trap low level w.c. fitted with a  
medium level cistern.

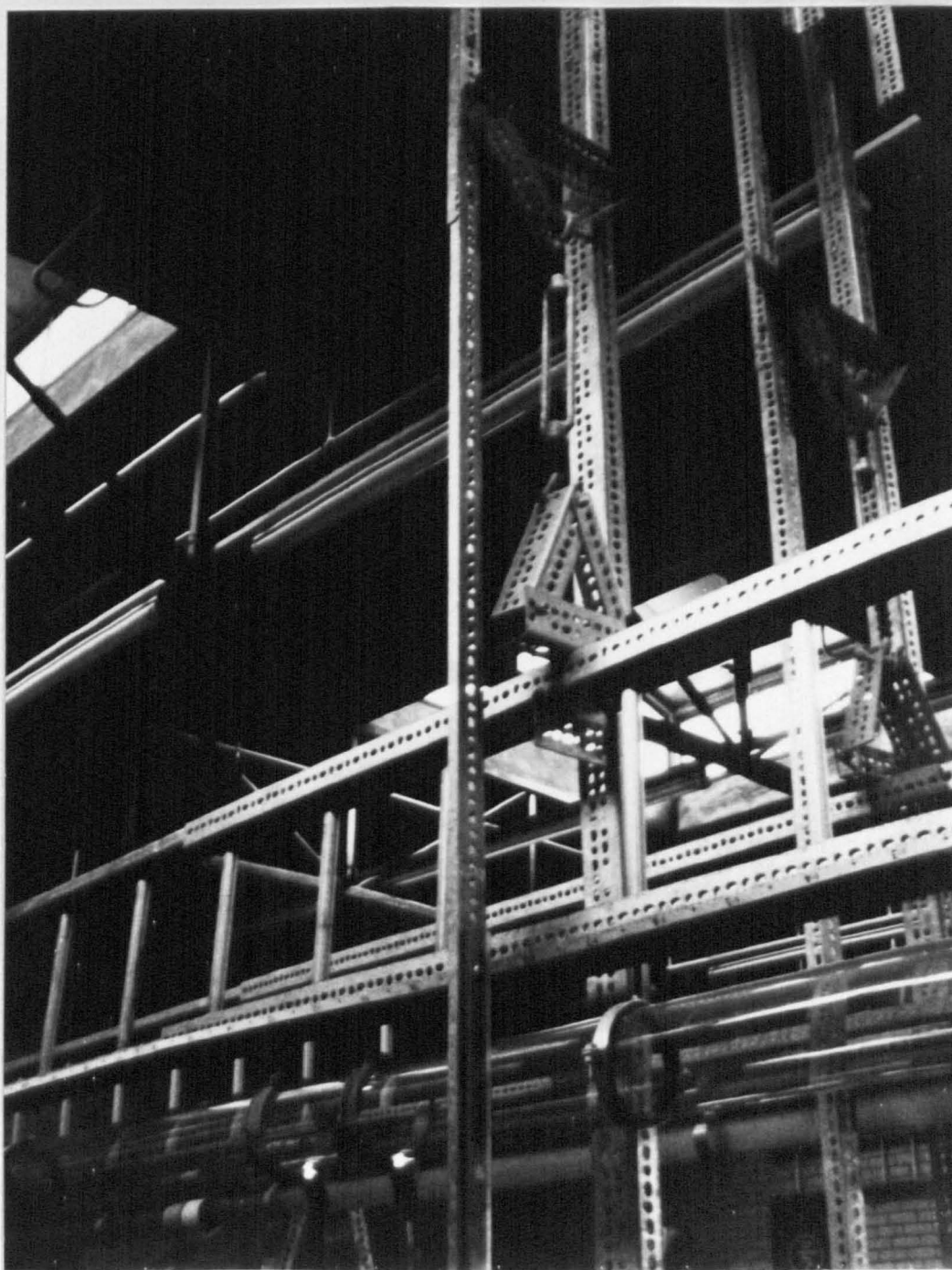


FIGURE 4. View of a vertical column support for the ladder support system. Note: the ladders spliced together with dexion angle, the two dexion columns with a vertical linear scale attached to the nearer column and the turnbuckle support to facilitate rapid discharge pipe gradient adjustment.

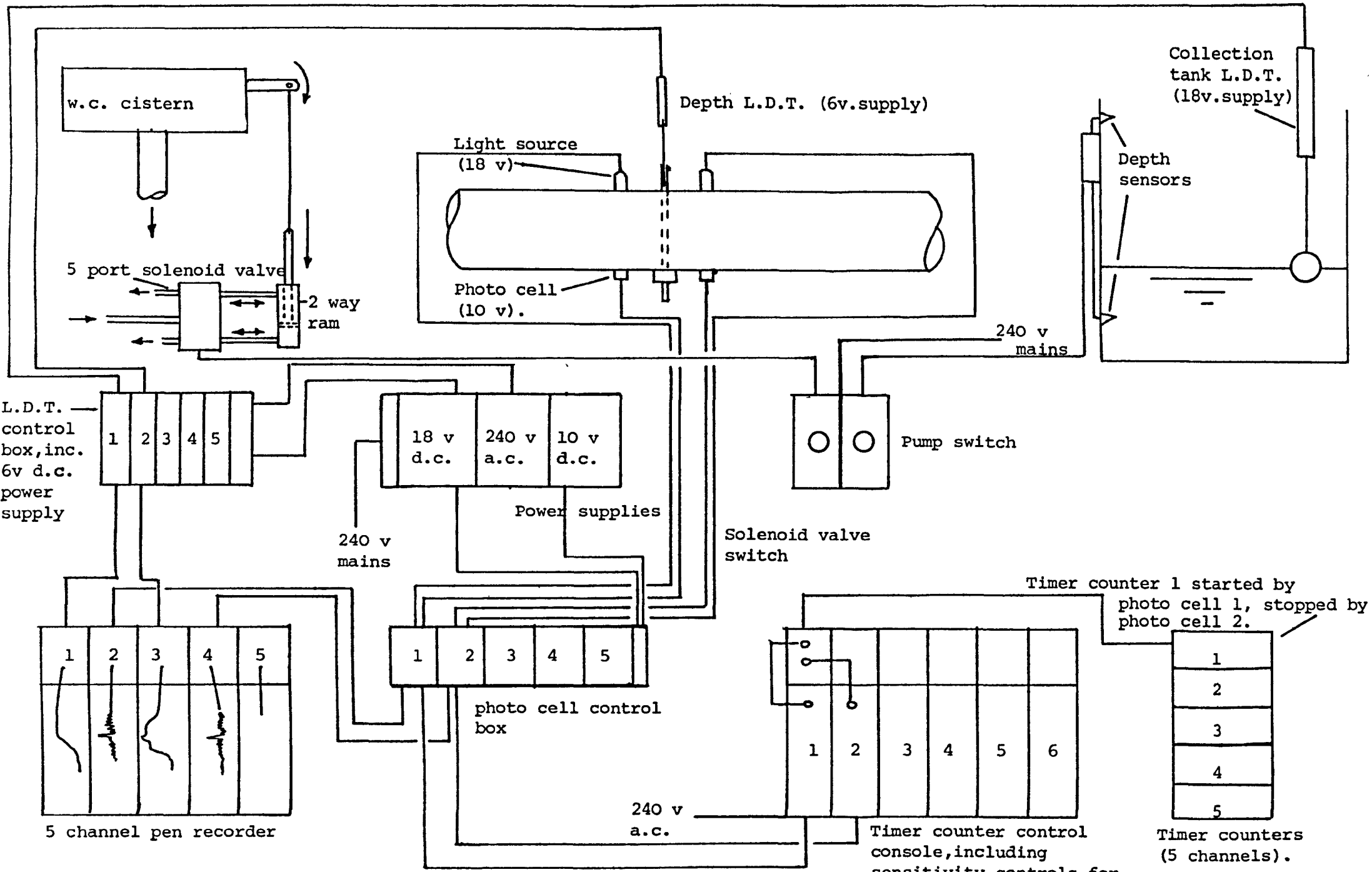


FIGURE 5. Schematic layout of test rig instrumentation and control systems, as originally developed.

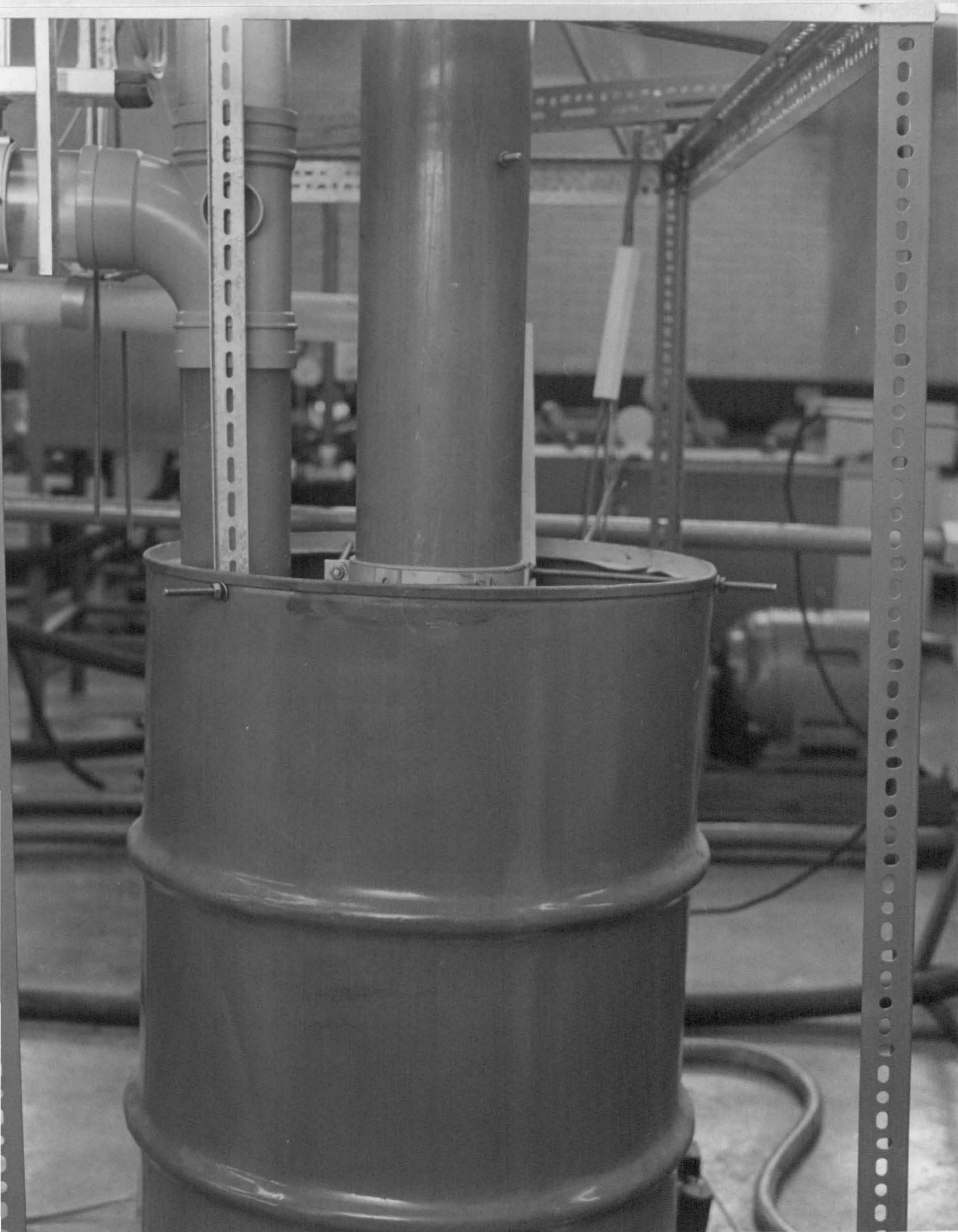


FIGURE 6. Photograph of the small support rig and original collection tank. Note: vertical discharge stack and depth measurement stilling pot.

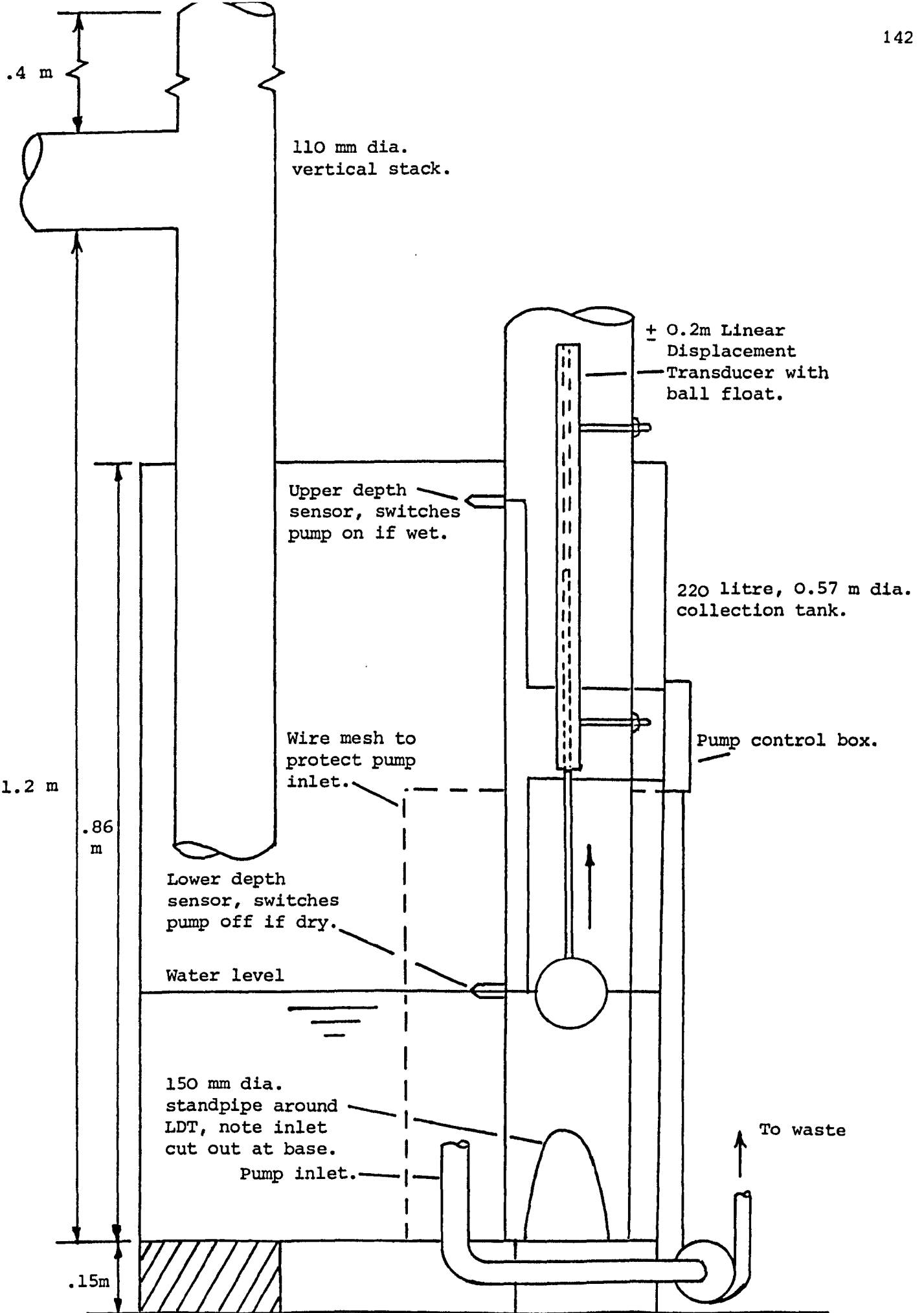


Figure 7. Schematic section through discharge collection tank, illustrating depth control and measurement systems.

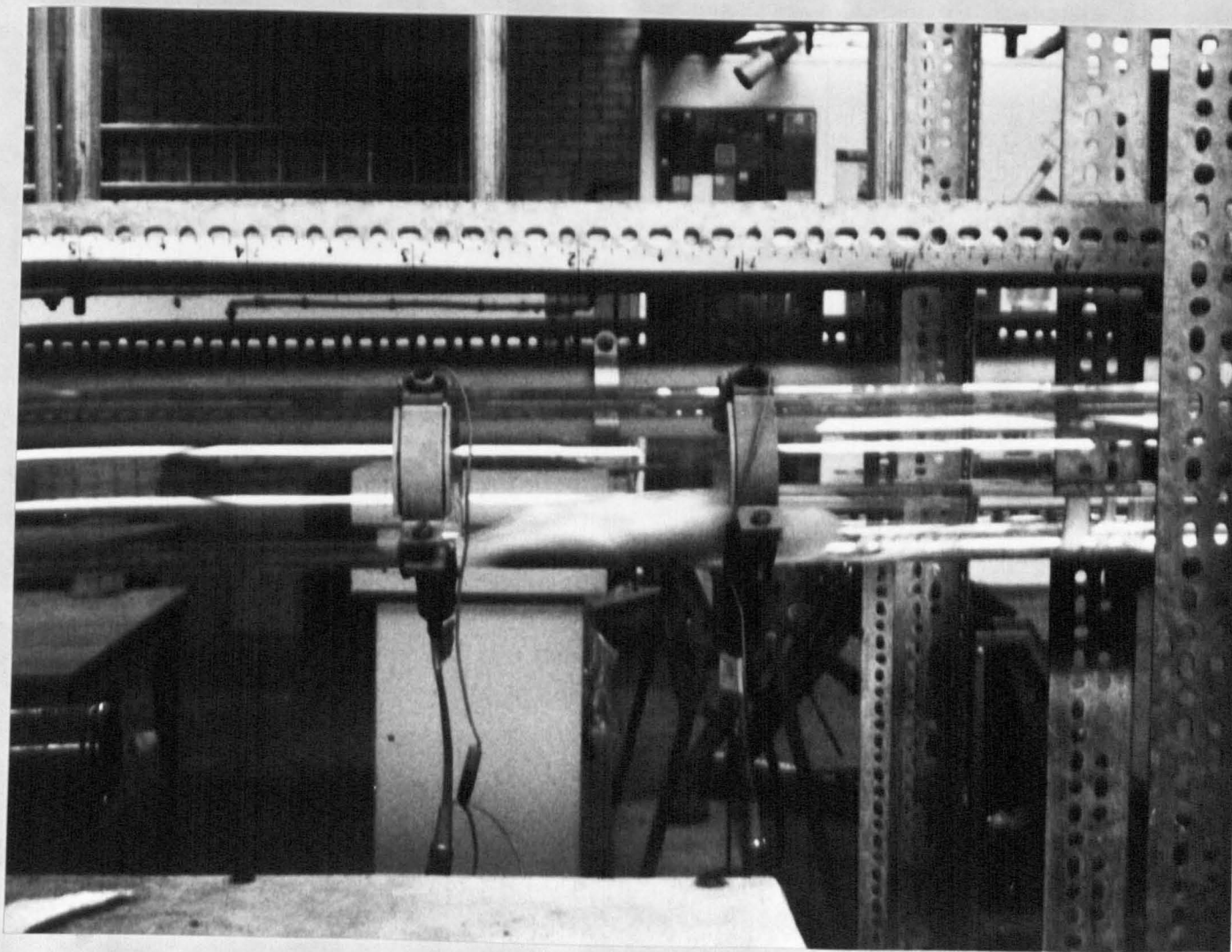
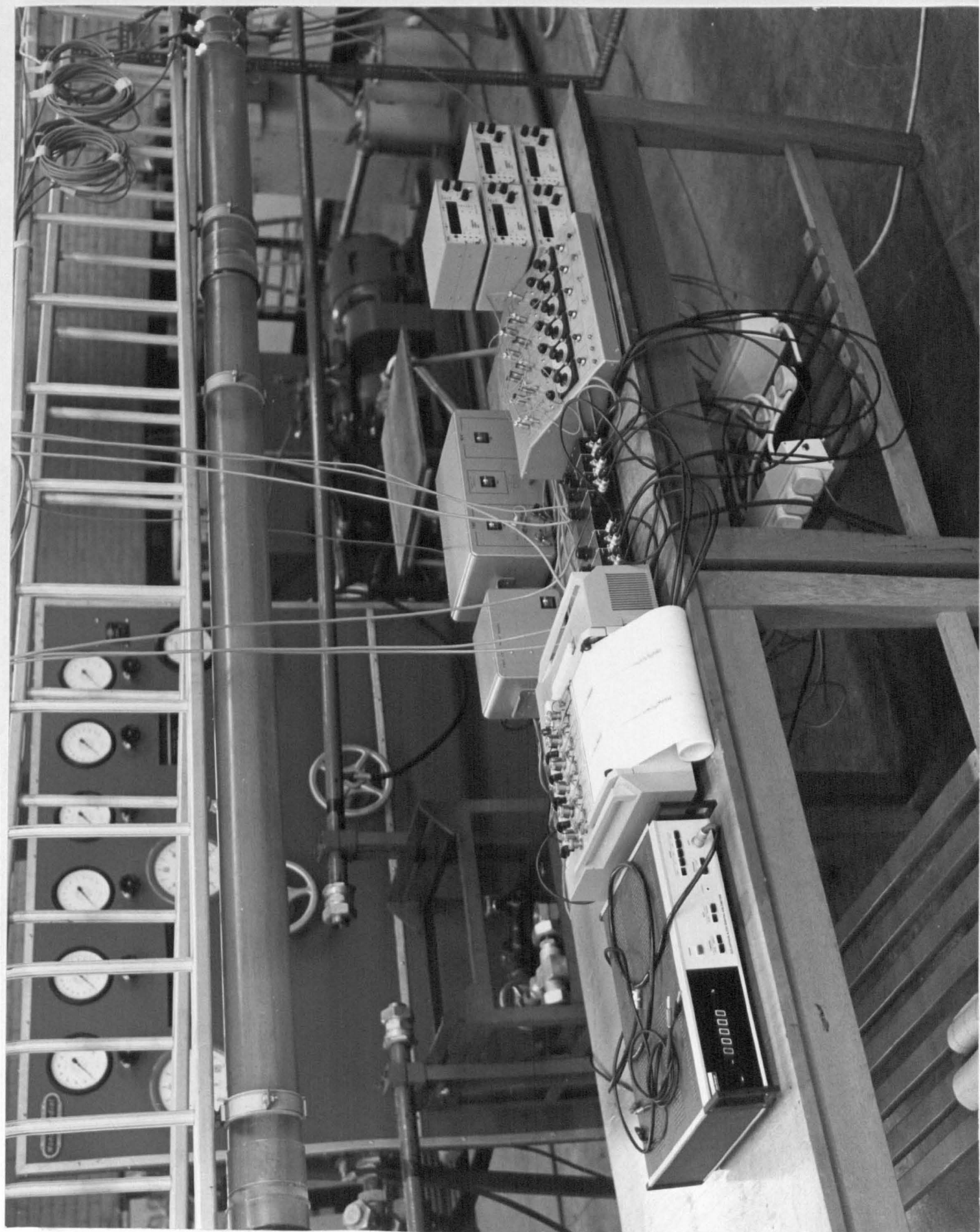


FIGURE 8. Photograph of a single maternity pad travelling along the straight glass pipe. Note: the characteristic shape of the solid and the water before and after, the photocell/light source rings and the linear scale attached to the ladder measuring distance from the w.c.



FIGURE 9. Layout of depth measurement u-tube and float chamber.  
Note: photocell layout as used in the initial tests.

FIGURE 10. Layout of the original instrumentation table.  
From left to right, back row:  
LVDT control box including 6v d.c. power  
supply, and power supplies including 18v d.c. for  
light sources, 240v a.c. for control console and  
10v d.c. for photocells.  
Front row: digital voltmeter, 5 channel pen recorder,  
photocell control box, timer counter control  
console, 5 timer counters.



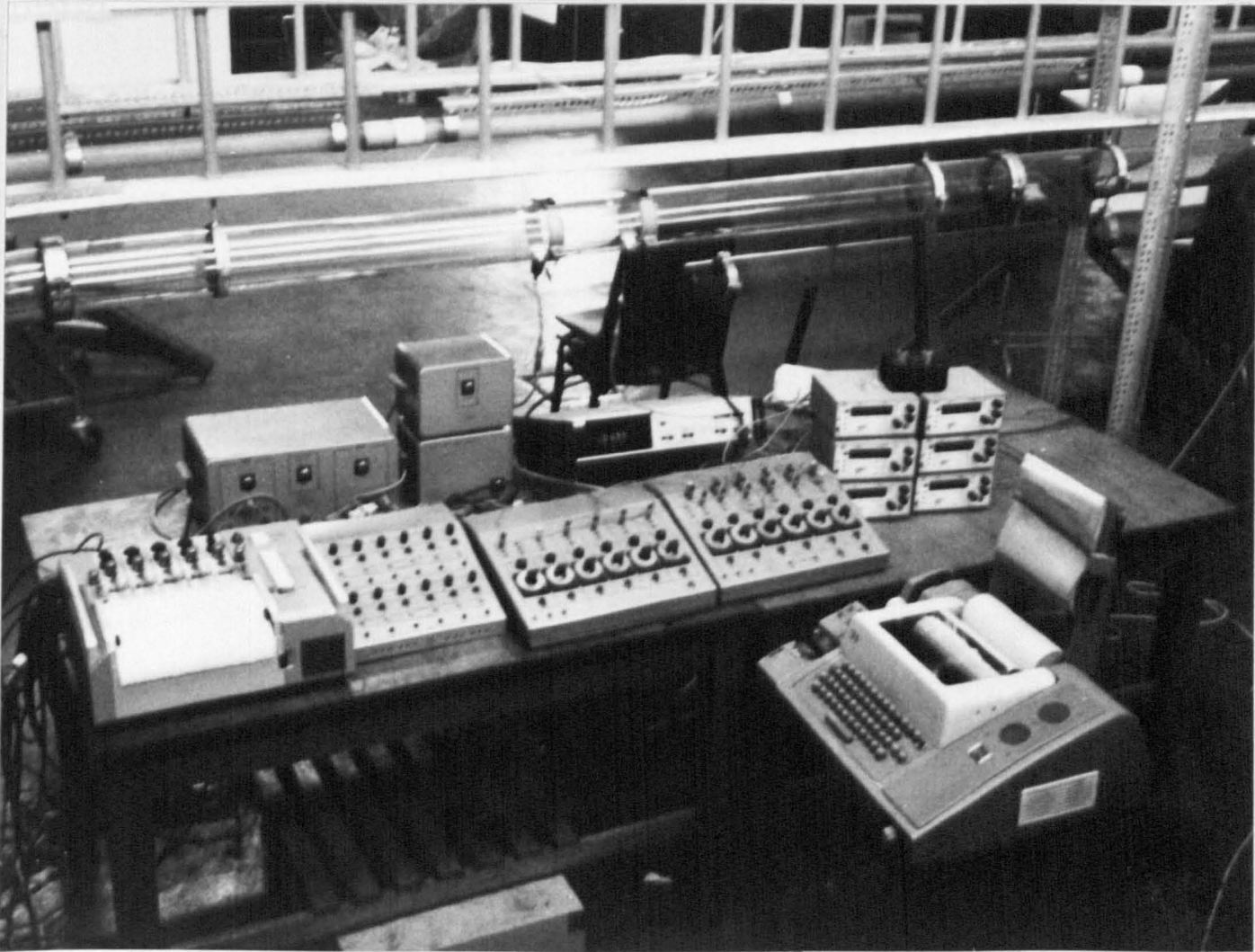


FIGURE 11. View of the improved instrumentation table. From left to right, back row: Power supplies including 18v d.c., 240v a.c. and 10v d.c., upper power supply to second timer counter control console, lower 6v d.c. LVDT power supply and digital voltmeter.

Front row: 5 channel pen recorder, improved photocell control console, second timer counter control console, original timer counter control console, six timer counters and automatic flush and discharge tank pump down control box.

Foreground: Teletype paper tape punch.

Figure 11 shows the photocell and depth measuring  
linear displacement transducers for a water only  
flow rate of 1/100 gradient.

Note change of pen recorder speed after 14 seconds.

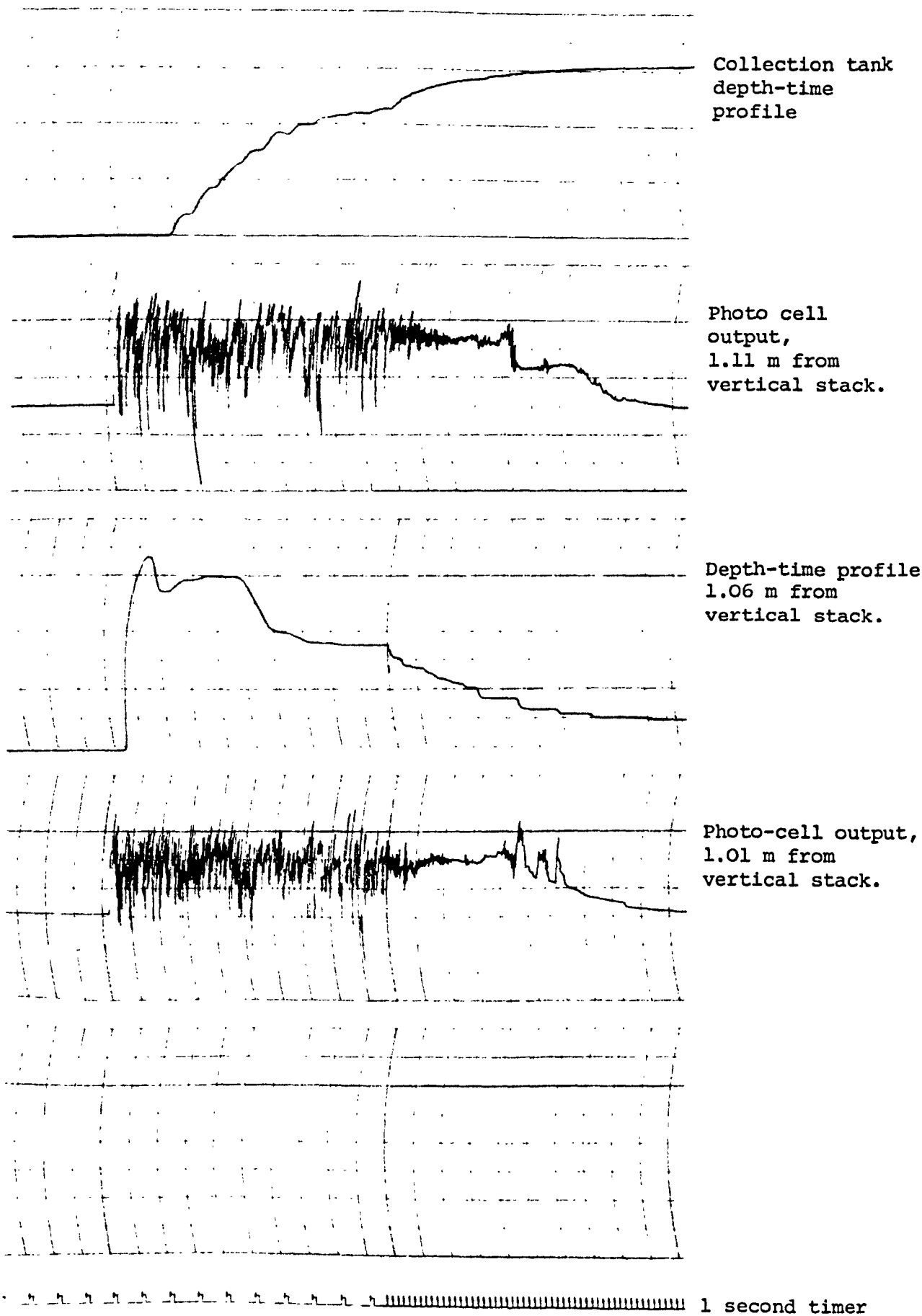


Figure 12. Records from both photo cell and depth measuring linear displacement transducers for a water only flush at a 1/100 gradient.

Note change of pen recorder speed after 14 seconds.

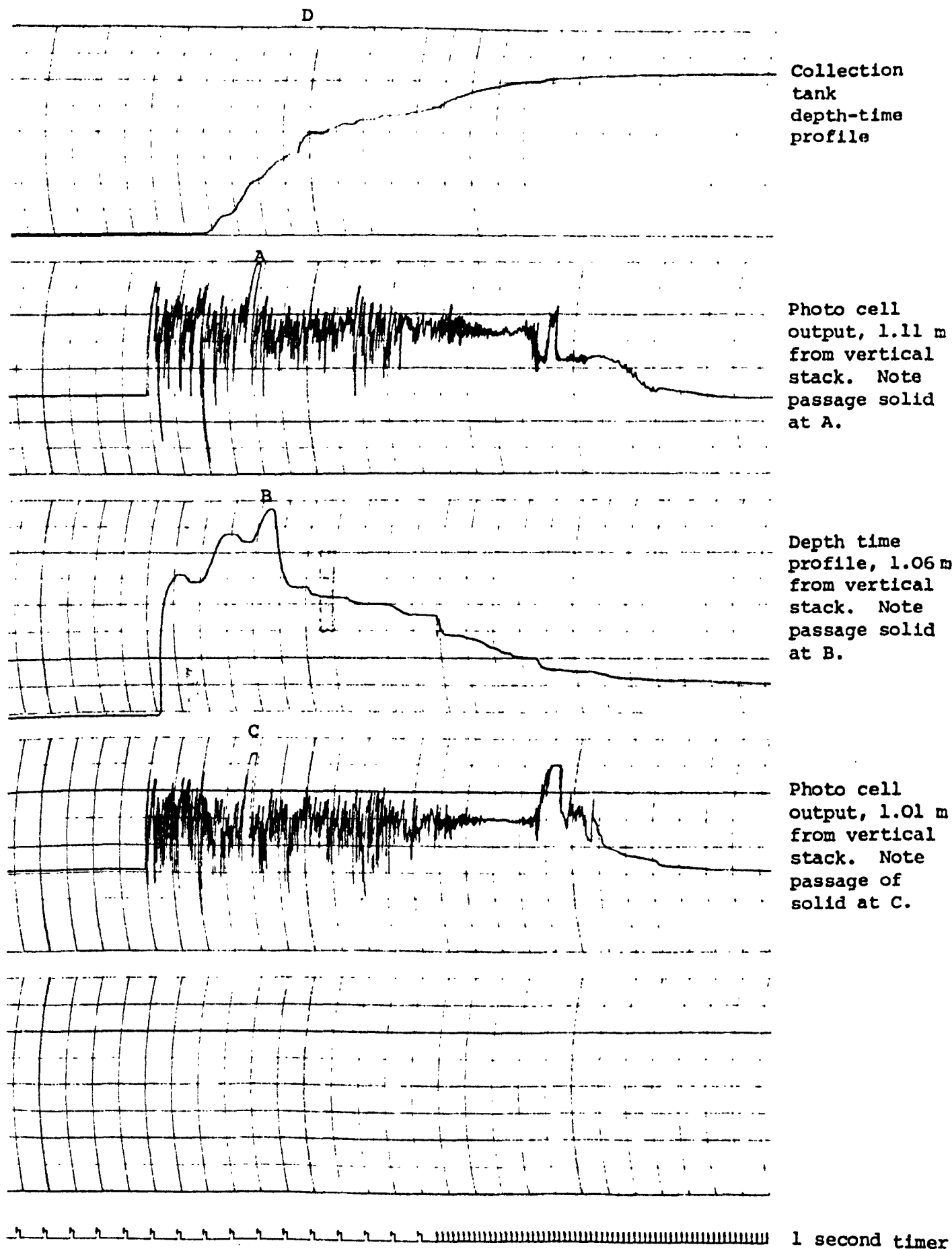


Figure 13. Records from both photo cell and depth measuring linear displacement transducers for a single m.p. flush at a 1/100 gradient. Note passage of solid recorded on photocell outputs (points A and C) and also on LDT outputs (points B and D).



FIGURE 14. Photograph of the waste materials used during the research and during the pilot study. Back row, left to right: Kleenex paper towel roll, Bowater Scott 20 paper towel pack, 135° plastic knuckle bend and 92½° plastic radiused bend. Front row, left to right: Dr White C<sub>2</sub> pack of maternity pads and flat and rolled examples of these and a clear acrylic pipe coupler. Front centre: Simulated faeces kit made up of horse serum and baby milk powder.

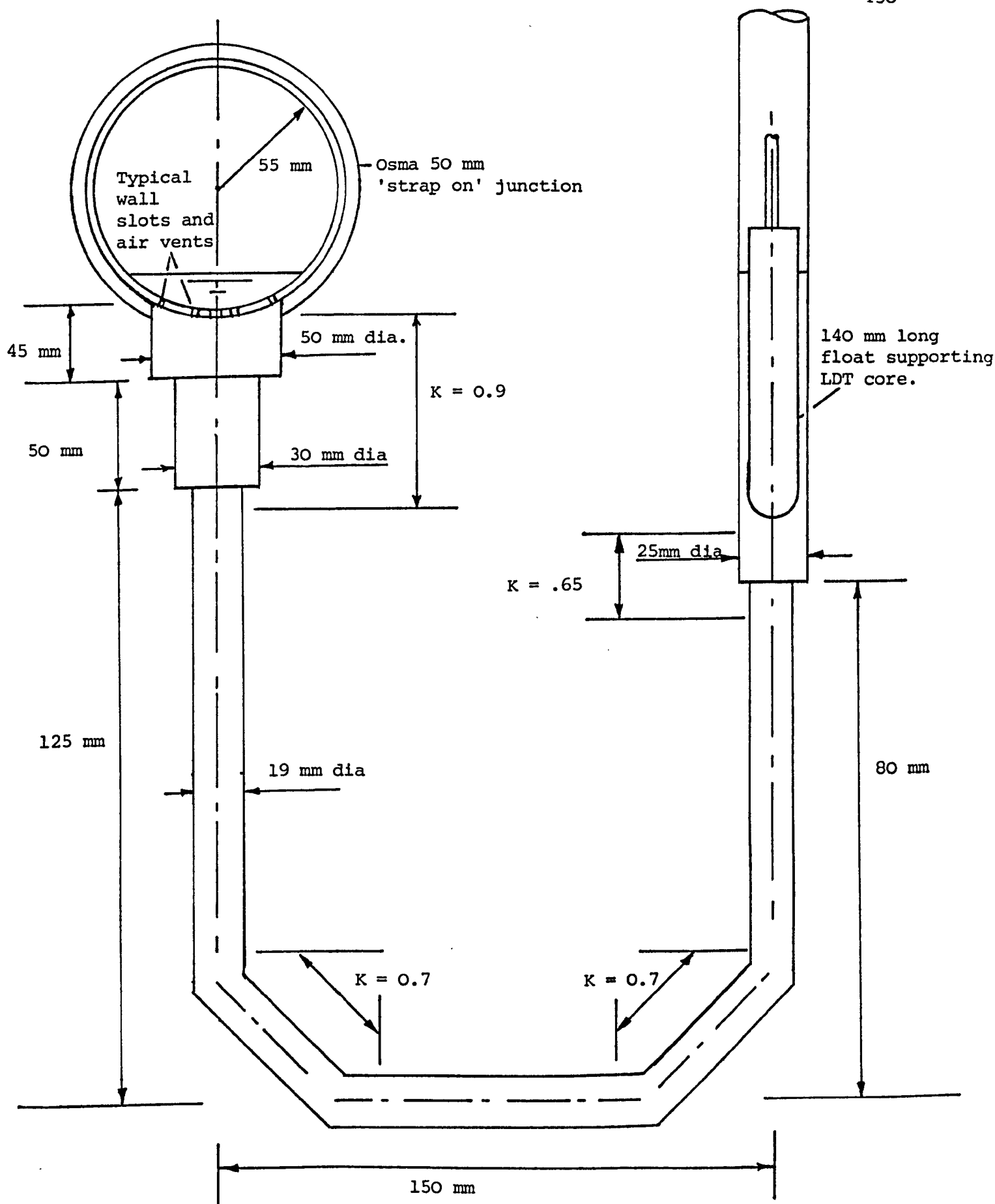


Figure 15. Schematic layout of float chamber and U-tube connection to waste pipe used to record depth variations. Note values of fitting loss coefficients  $K$ .

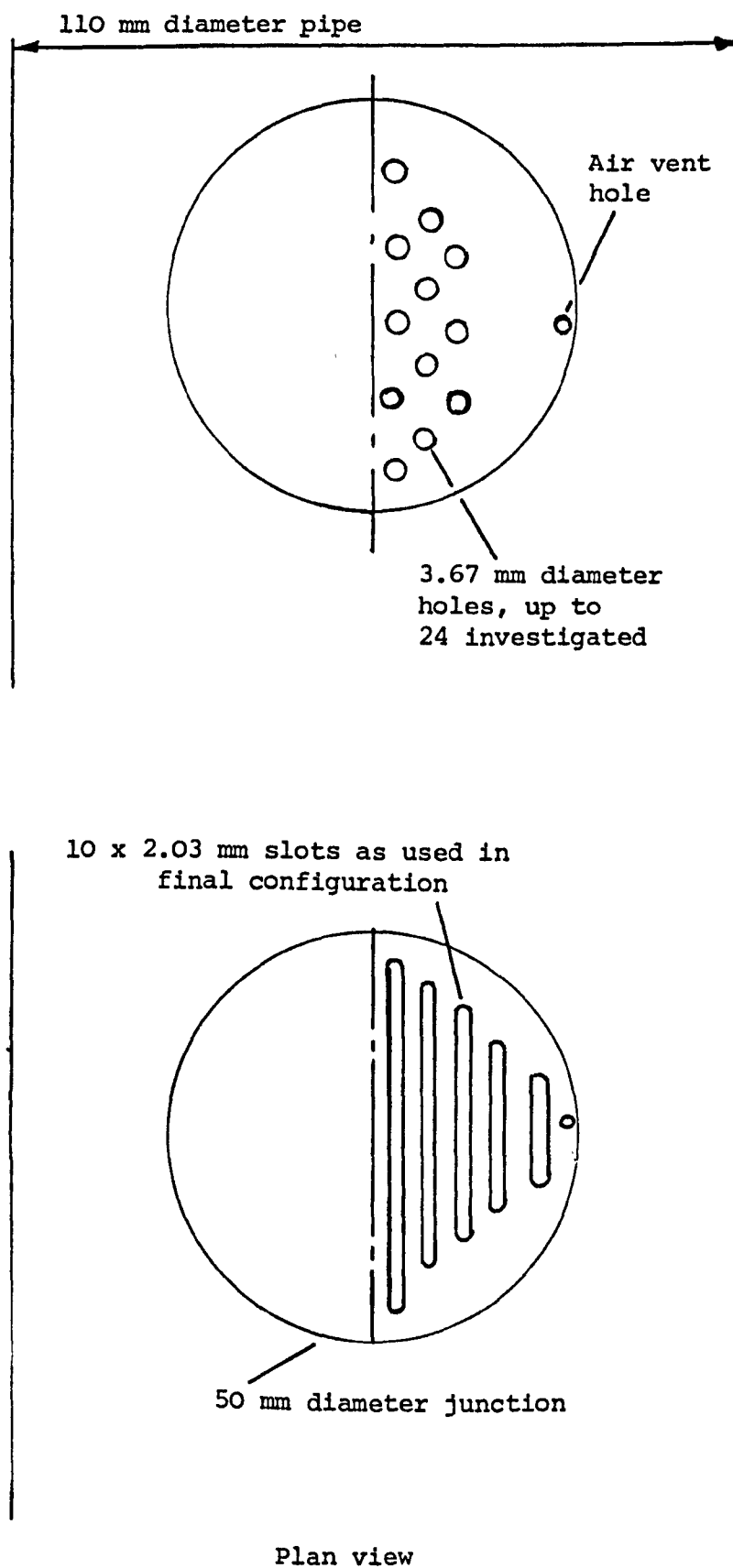


Figure 16. Layout of circular and slot orifices in pipe wall investigated. Note presence of air vent holes.

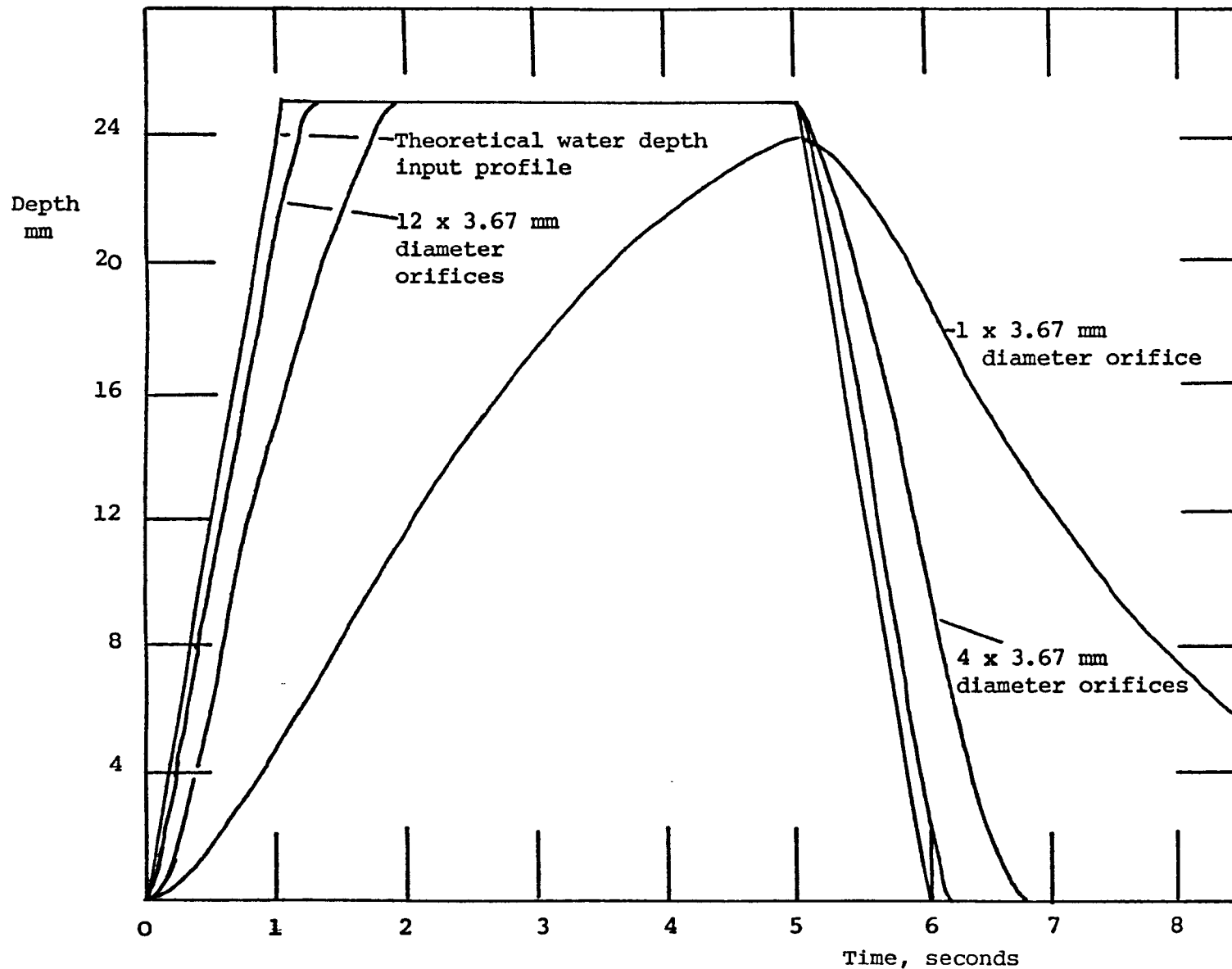


Figure 17. Theoretical float response to a ramp water depth input profile for 1, 4 and 12 x 3.67 mm diameter orifices. Results for 14 - 24 x 3.67 mm diameter orifices too close to input profile to plot.

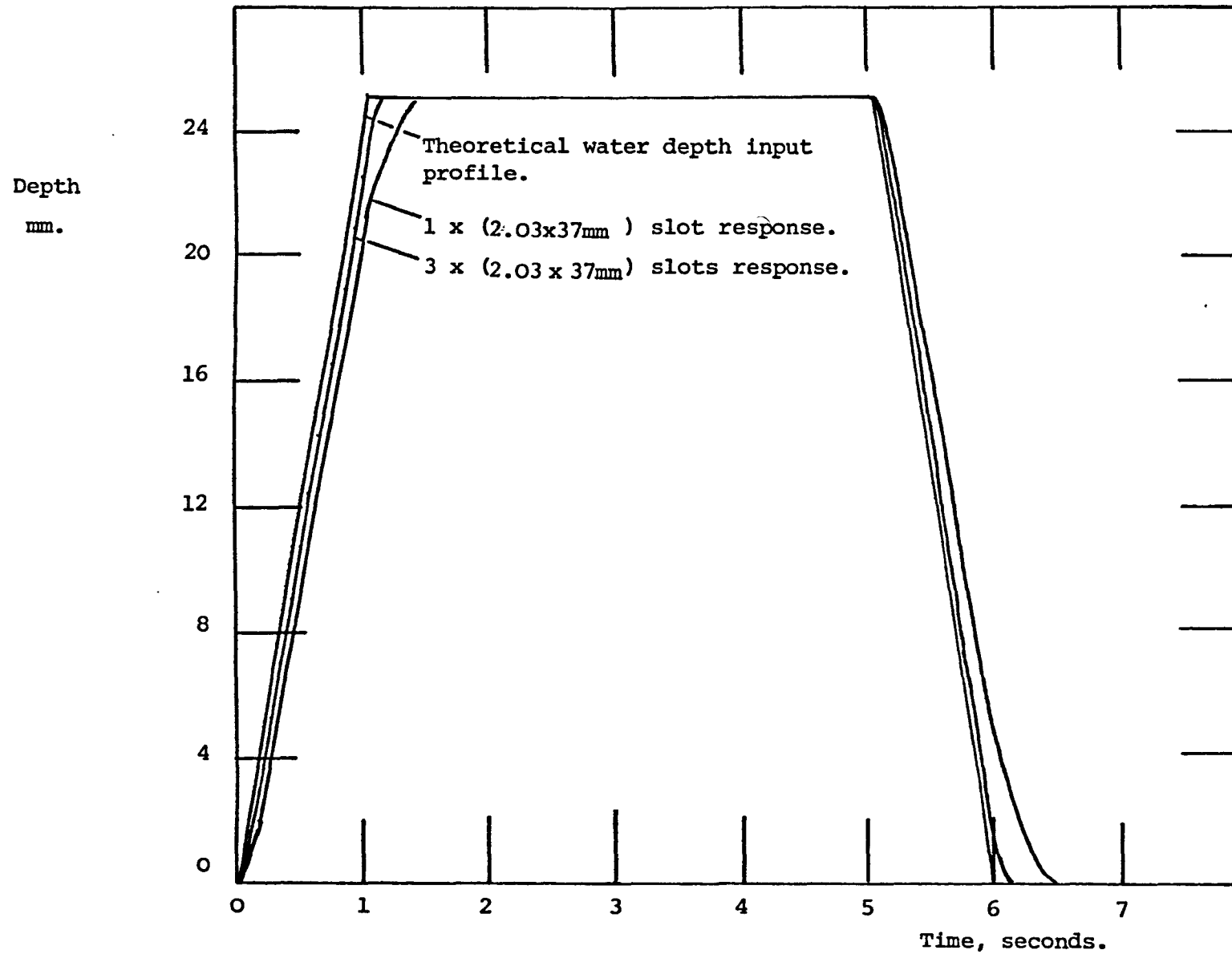


Figure 18. Theoretical float response to a ramp water depth profile for 1 and 3 wall slots. Results for 4 - 10 slots too close to input profile to plot.

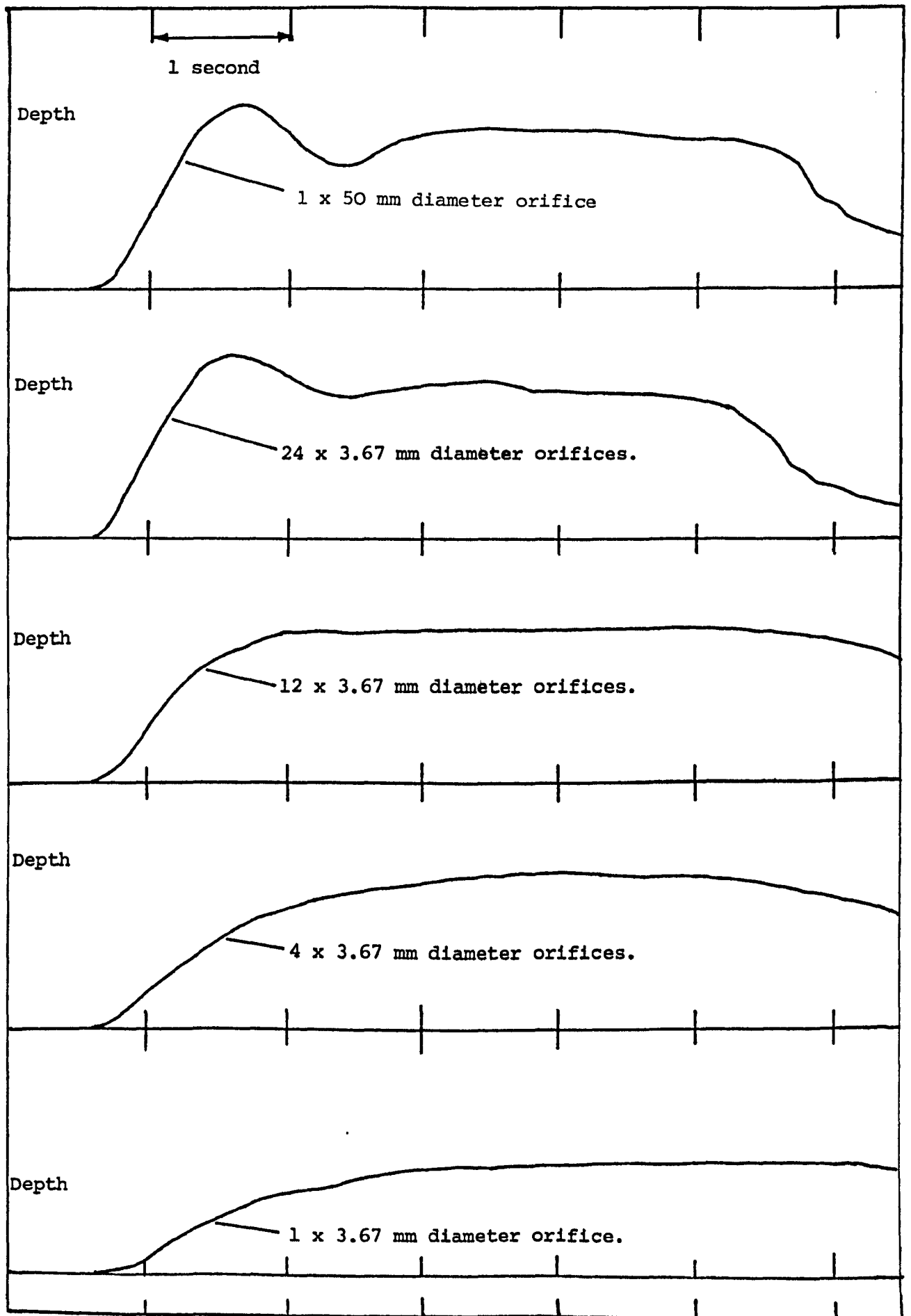


Figure 19. Float response to a water only flush, as recorded by the Linear Displacement Transducer and pen recorder, for a range of wall orifice areas. Pipe gradient 1/100.

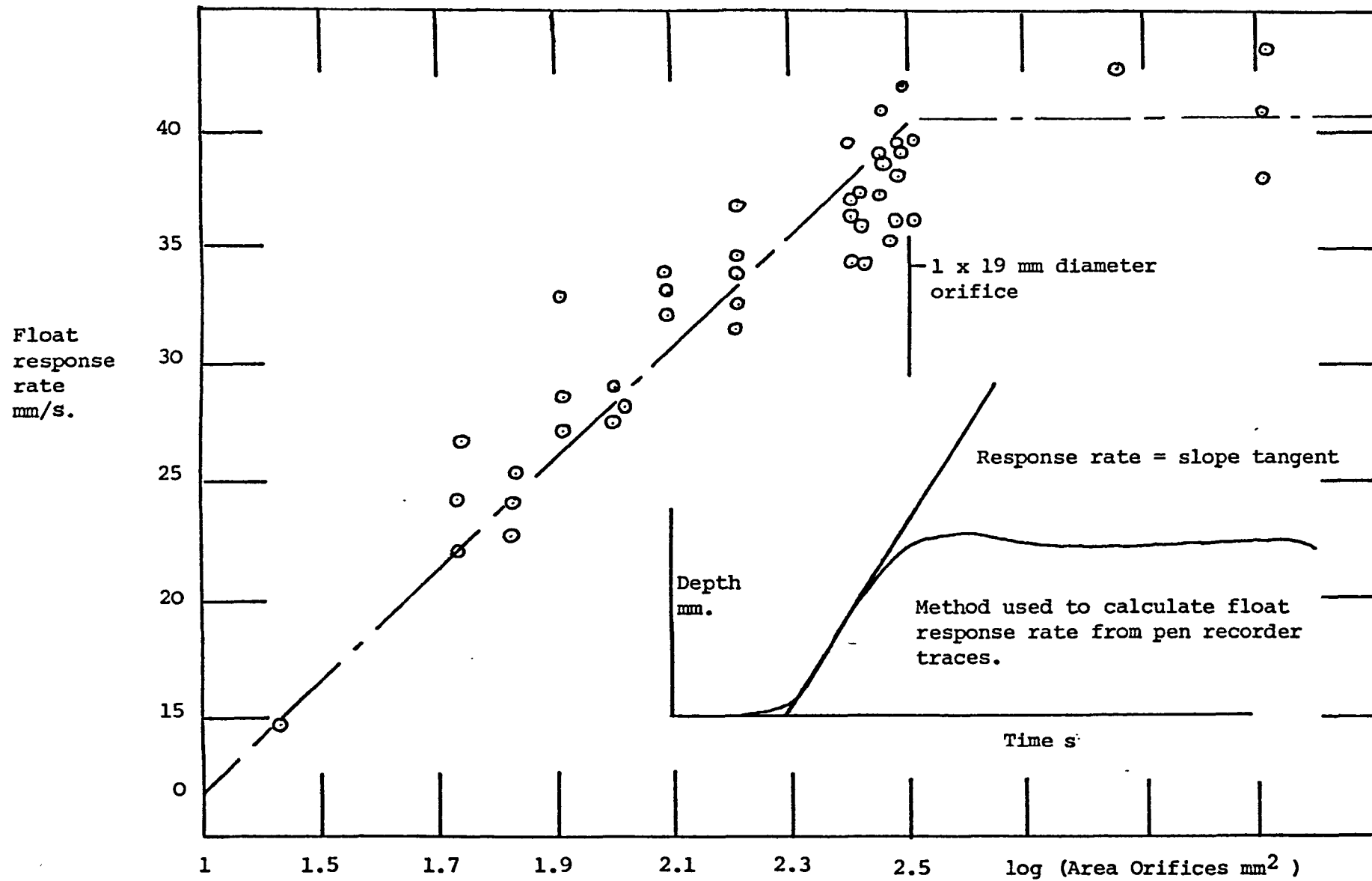


Figure 20. Response rate of float for a range of wall orifice areas.

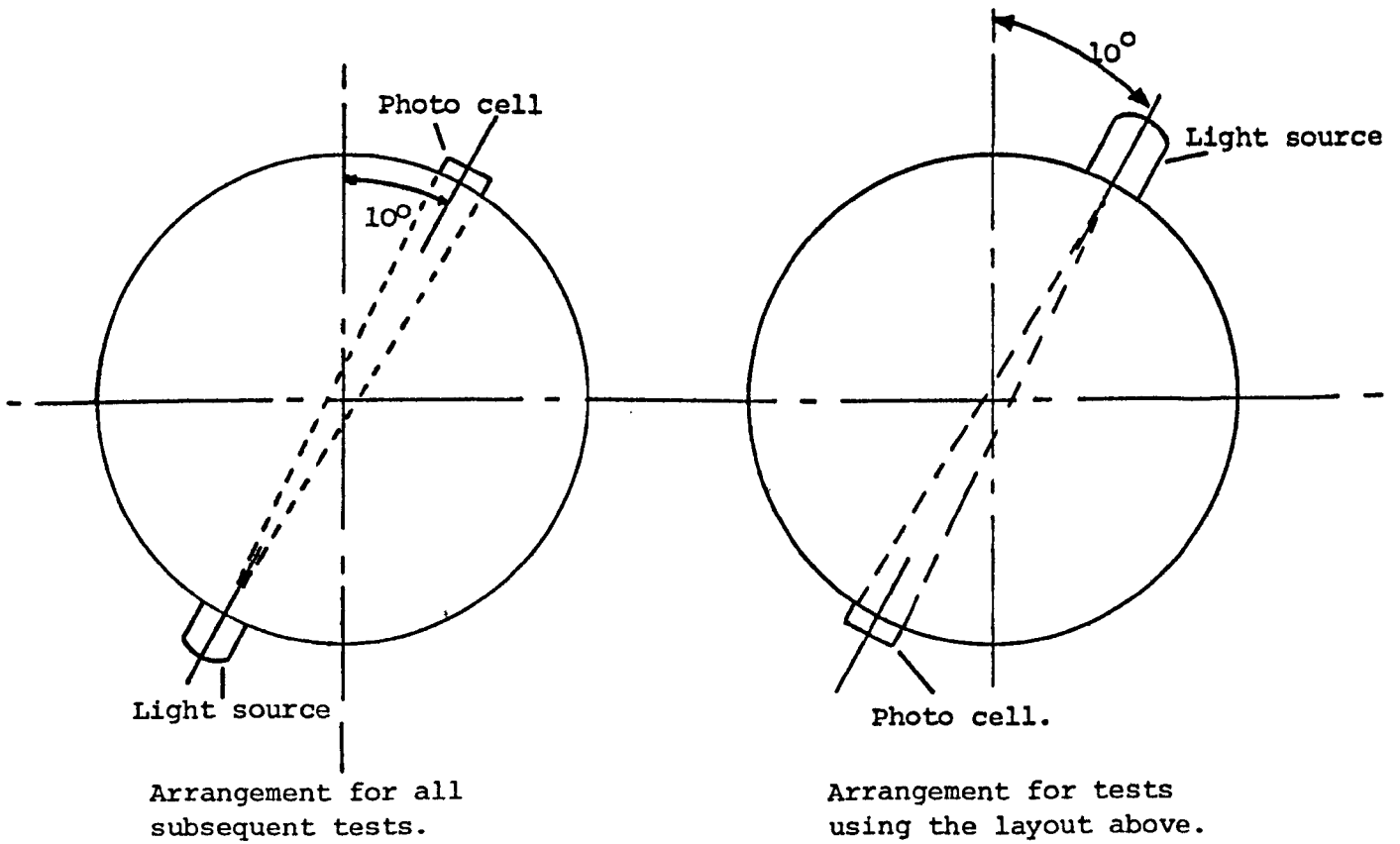
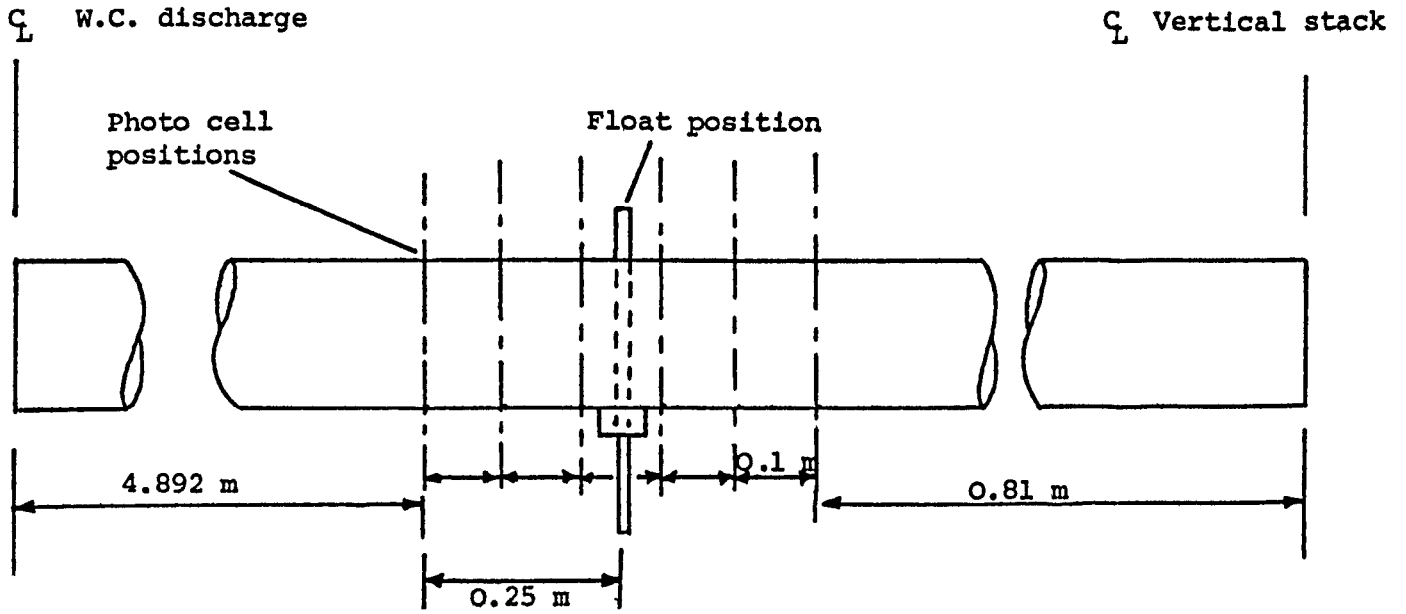


FIGURE 21. Layout of photocells along the pipe for initial tests. Note the angled arrangement of the light source and photocell.

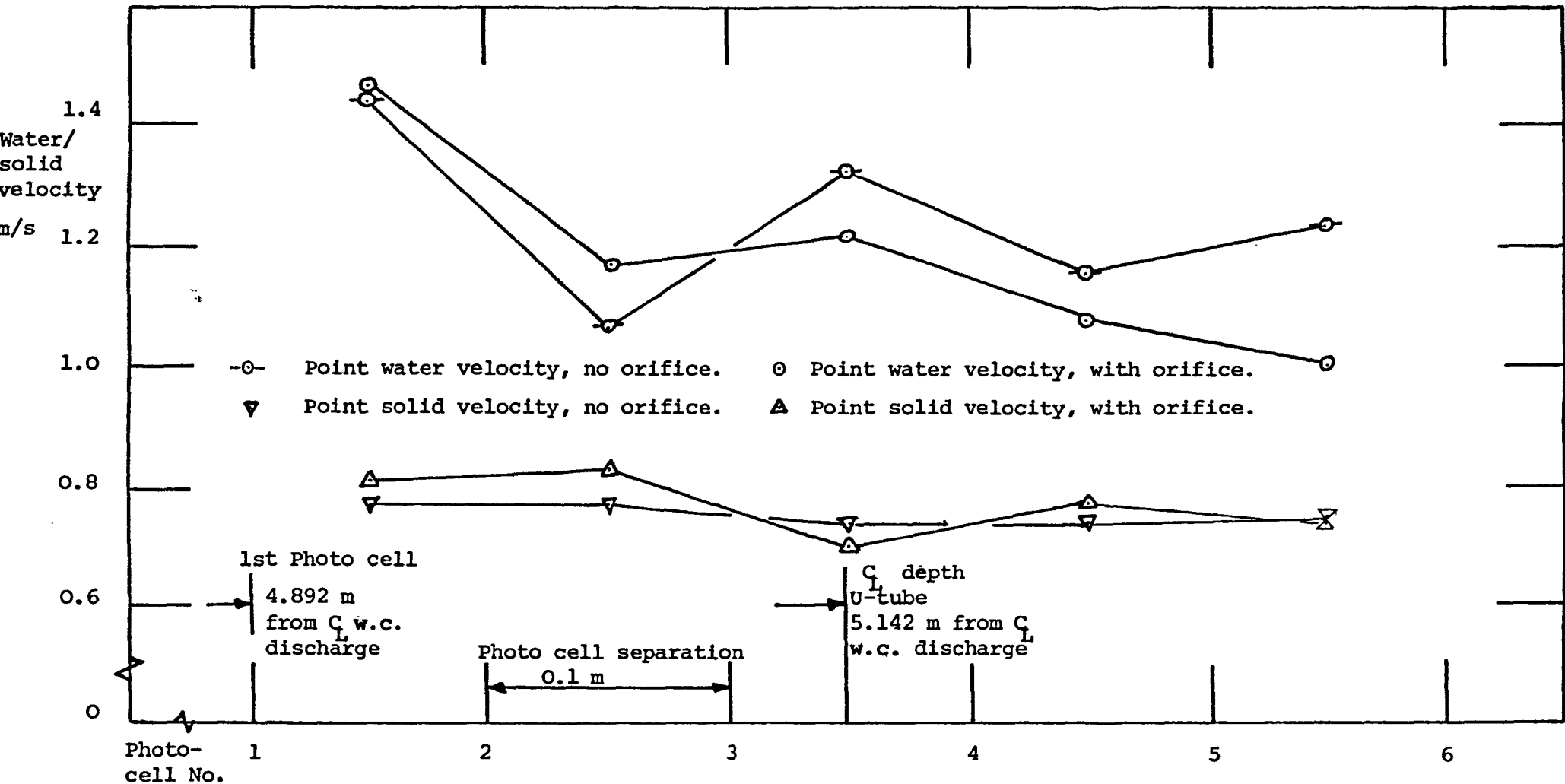


Figure 22. Effect of 10 slot orifices feeding depth recording U-tube on local water and solid velocities, as measured by photocells and timer counter instrumentation. Pipe gradient 1/100, single MP flush used for solid velocity measurement.

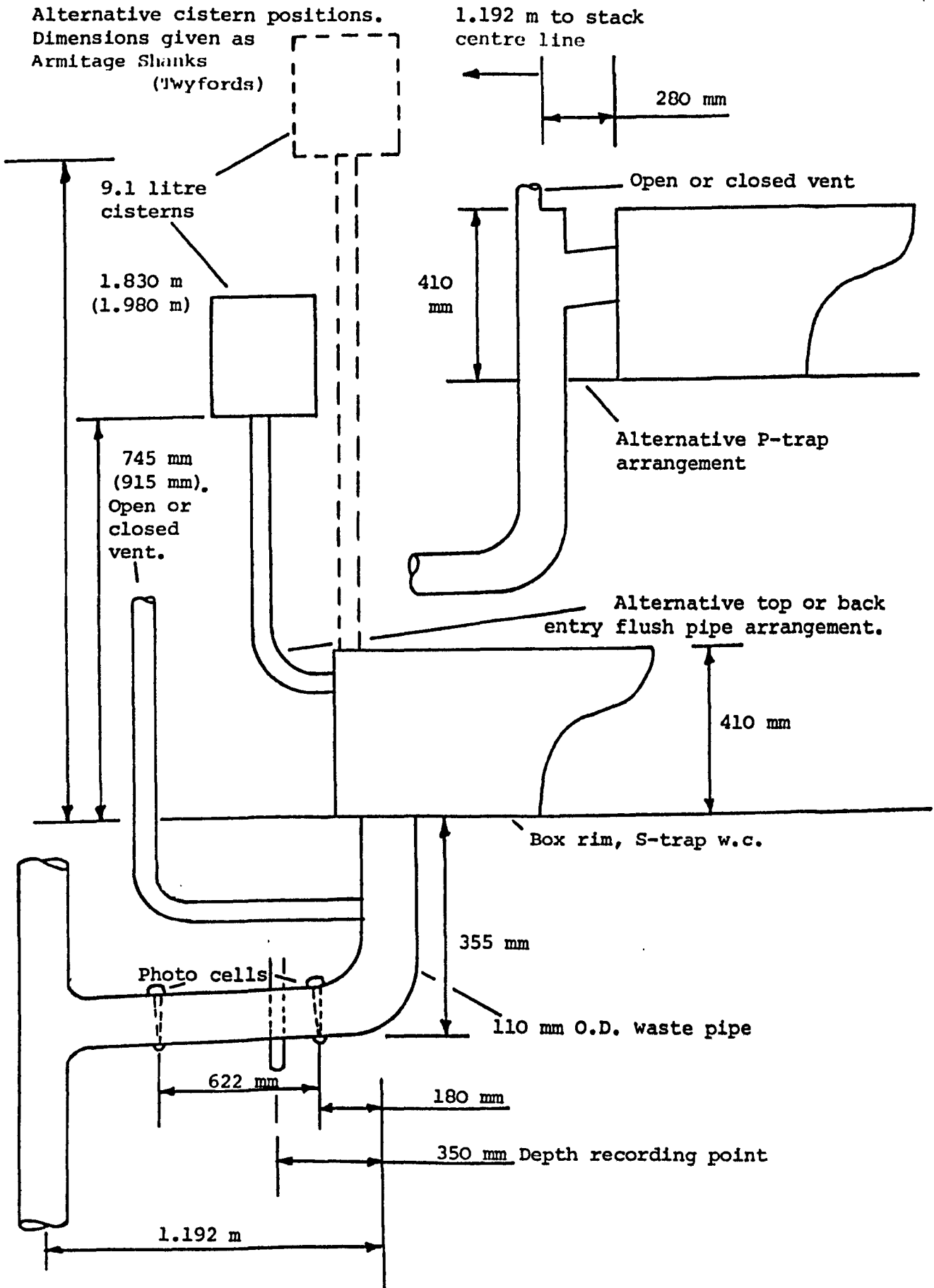


FIGURE 23. SCHEMATIC LAYOUT OF RIG FOR W.C. DISCHARGE CHARACTERISTIC TESTS.

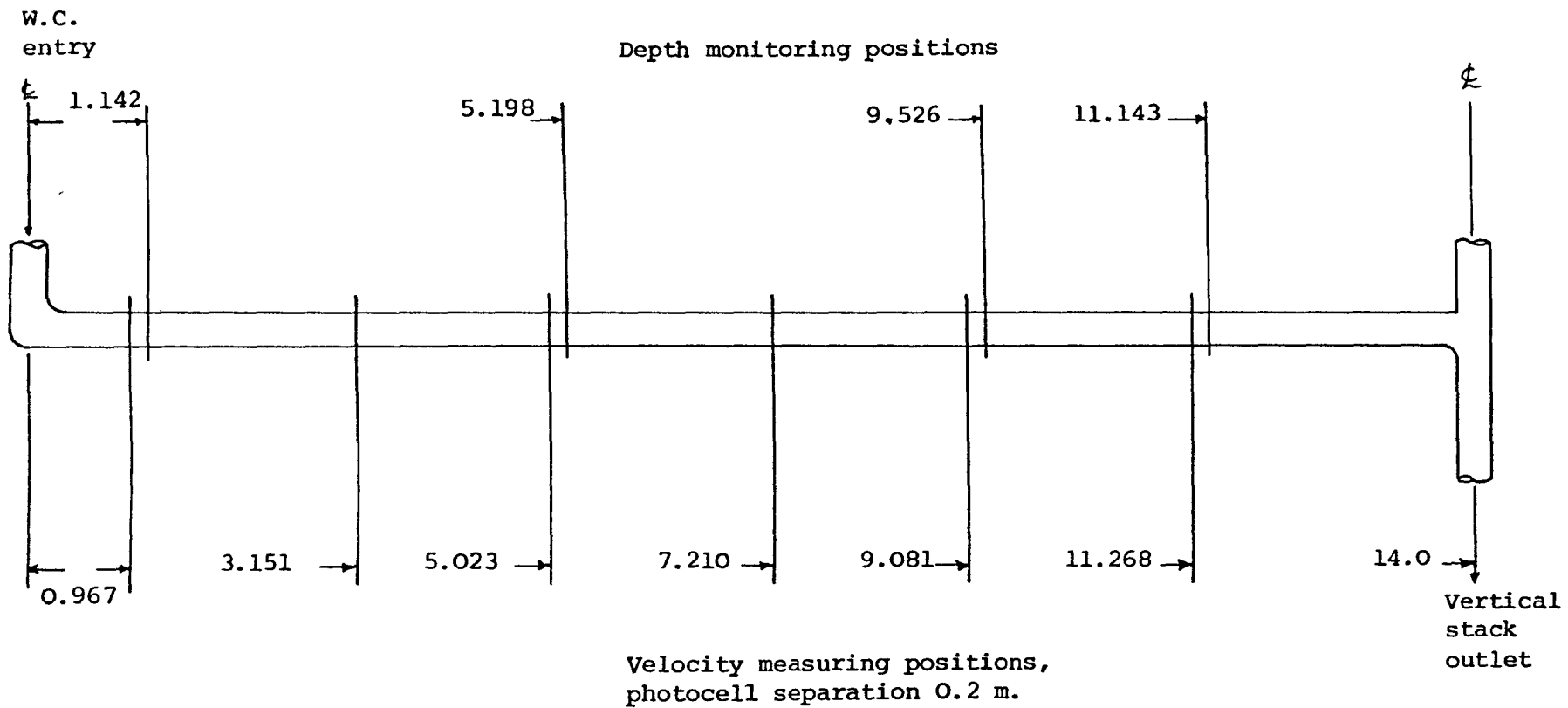


FIGURE 24. Schematic elevation (NTS) of straight plastic pipe test rig.  
 Note: all measurements in metres.

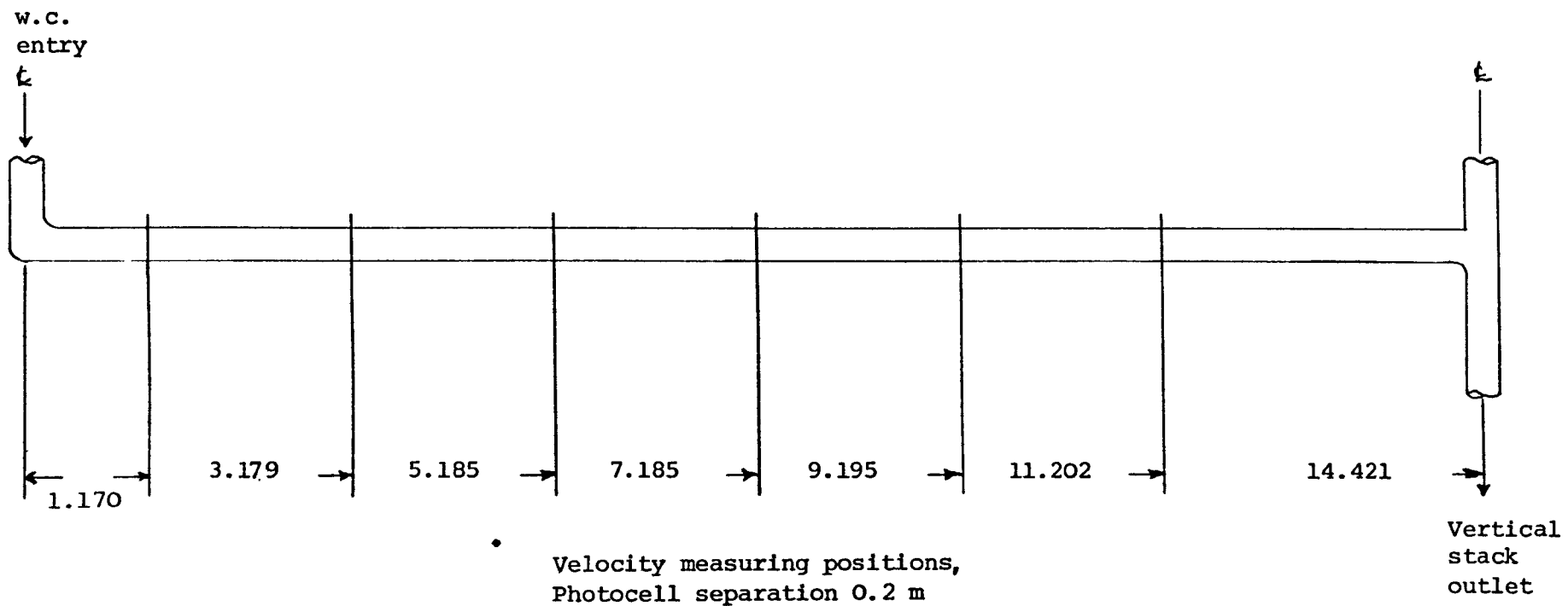


FIGURE 25. Schematic elevation (NTS) of straight cast iron pipe test rig.  
Note: All measurements in metres.

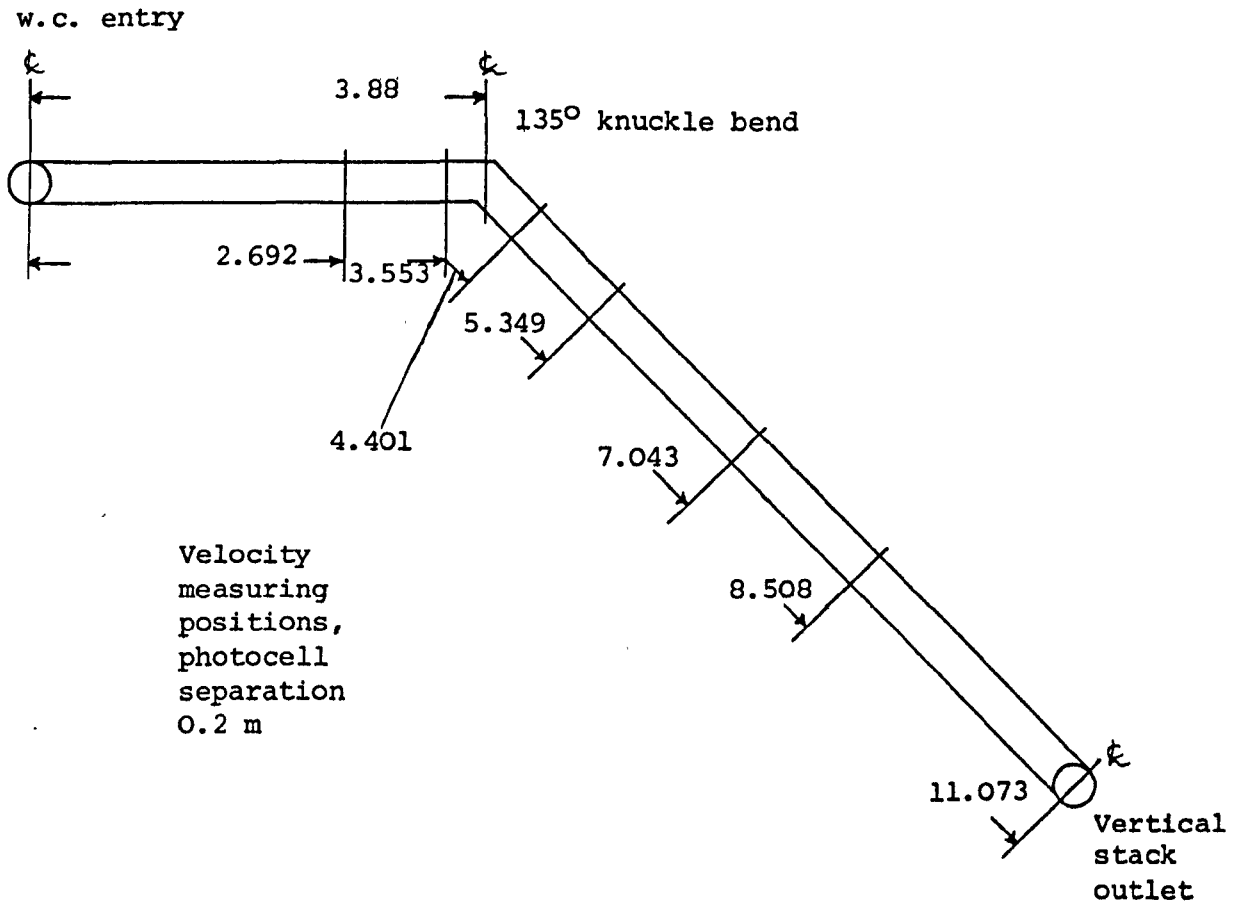


FIGURE 26. Schematic plan view (NTS) of test rig for testing a plastic 135° knuckle bend at 3.88 metres from w.c. Note: All measurements in metres.

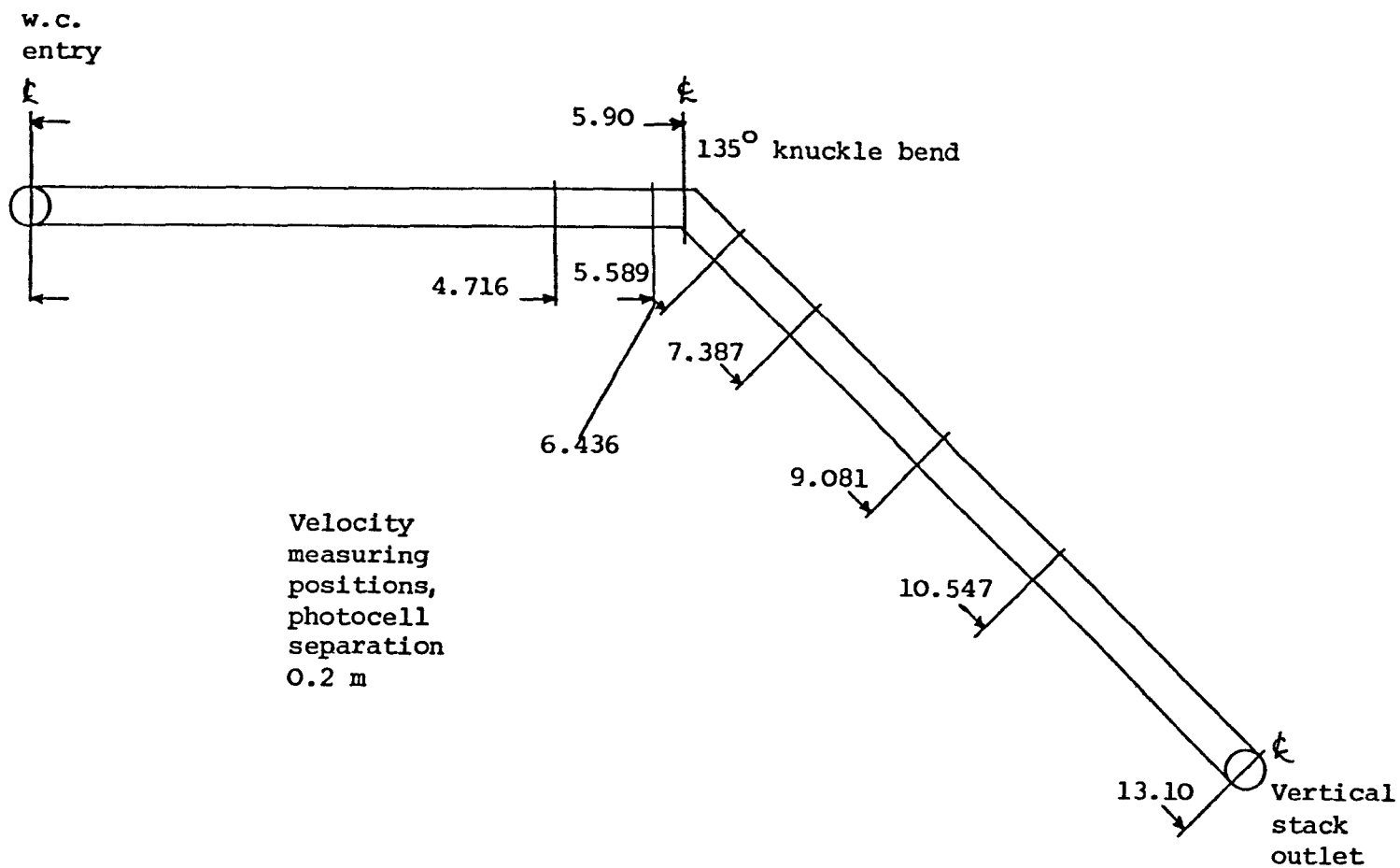


FIGURE 27. Schematic plan view (NTS) of test rig for testing a plastic 135° knuckle bend at 5.90 metres from w.c.  
 Note: All measurements in metres.

w.c.  
entry

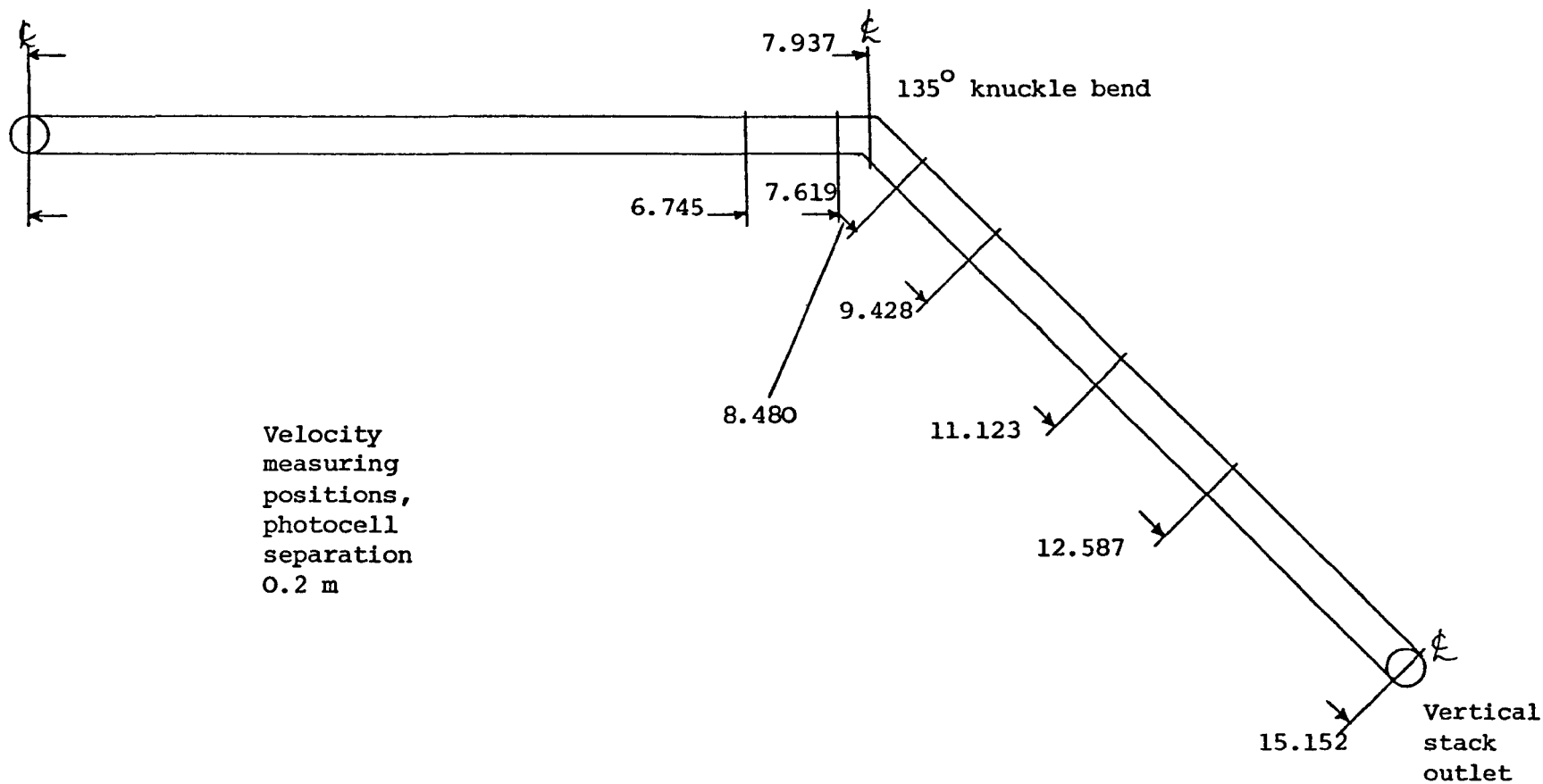


FIGURE 28. Schematic plan view (NTS) of test rig for testing a plastic 135° knuckle bend at 7.937 metres from w.c.  
Note: All measurements in metres.

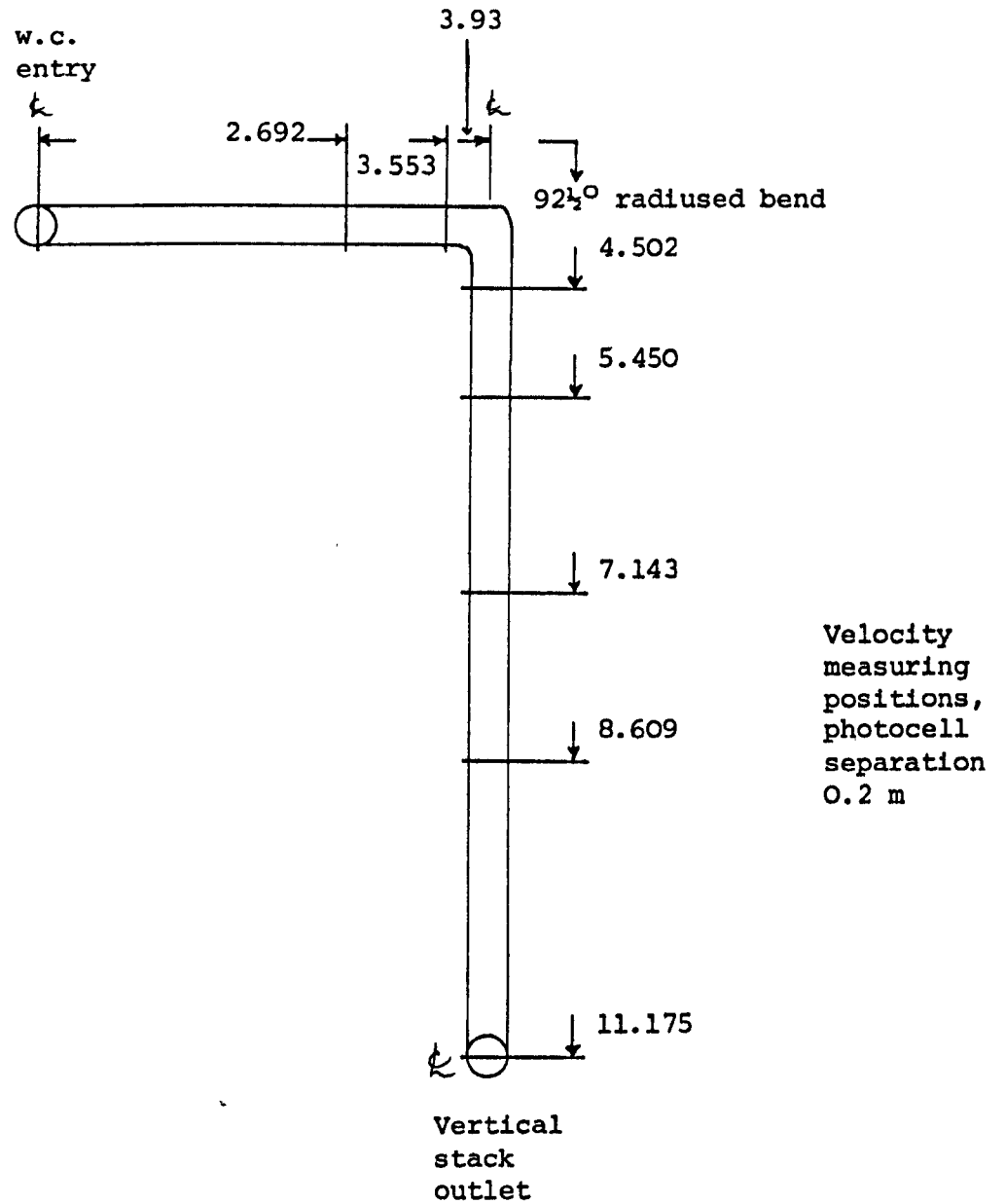


FIGURE 29. Schematic plan view (NTS) of test rig for testing a plastic 92 $\frac{1}{2}$  $^{\circ}$  radiused bend at 3.93 metres from w.c.  
Note: All measurements in metres.

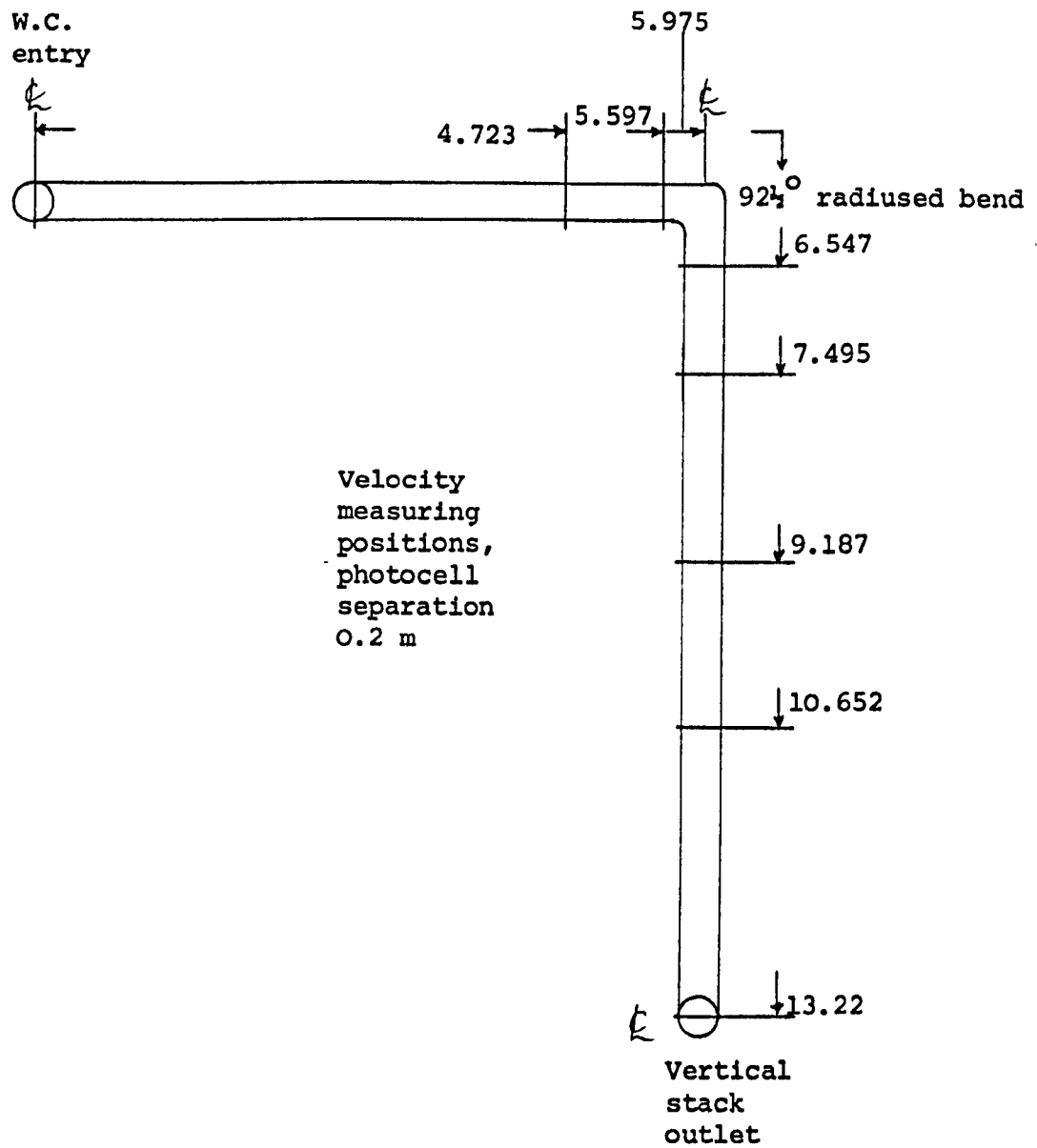


FIGURE 30. Schematic plan view (NTS) of test rig for testing a plastic 92 $\frac{1}{2}$  $^{\circ}$  radiused bend at 5.975 metres from W.C.  
 Note: all measurements in metres.

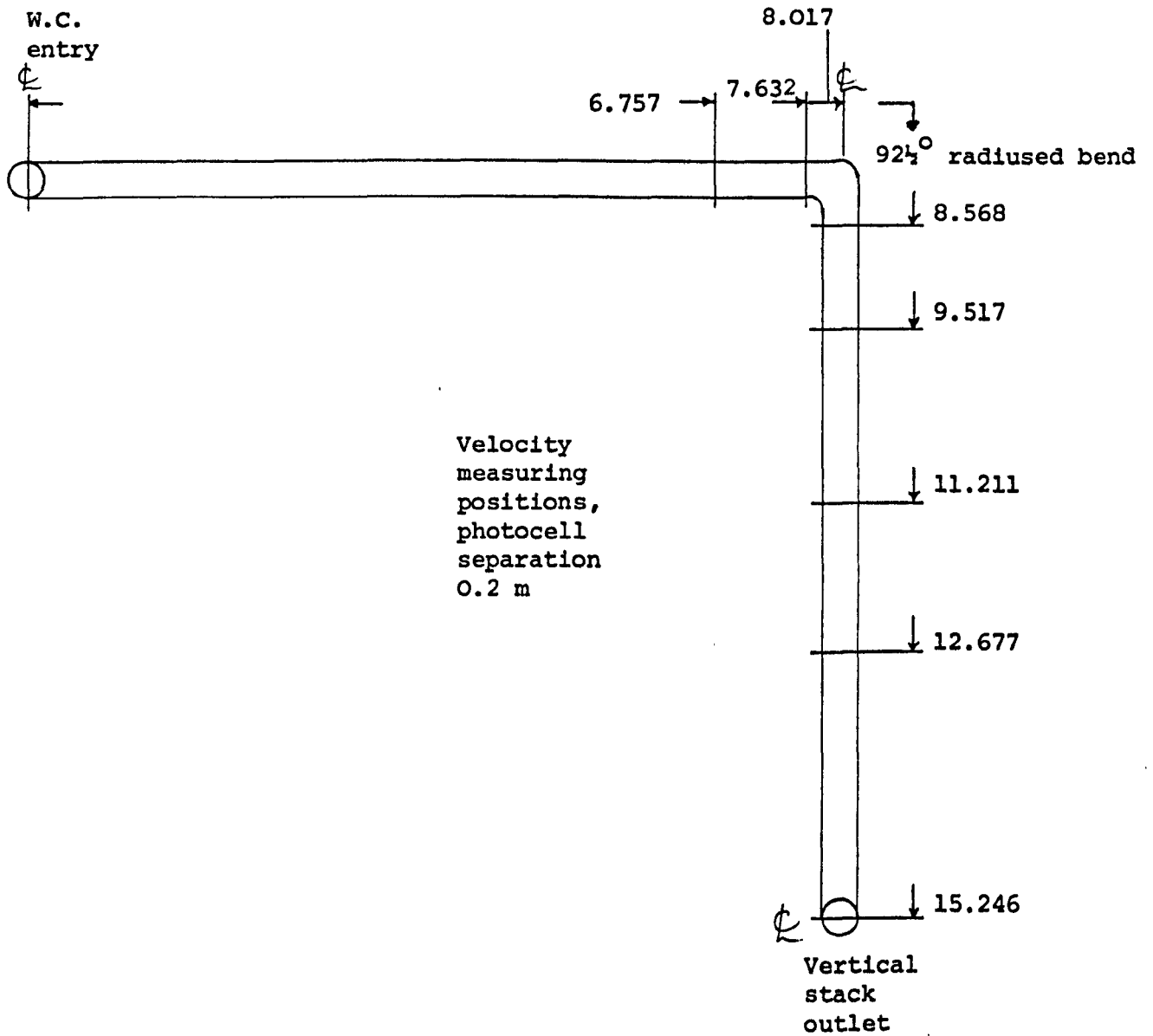


FIGURE 31. Schematic plan view (NTS) of test rig for testing a plastic 92 $\frac{1}{2}$  $^{\circ}$  radiused bend at 8.017 metres from W.C.  
Note: all measurements in metres

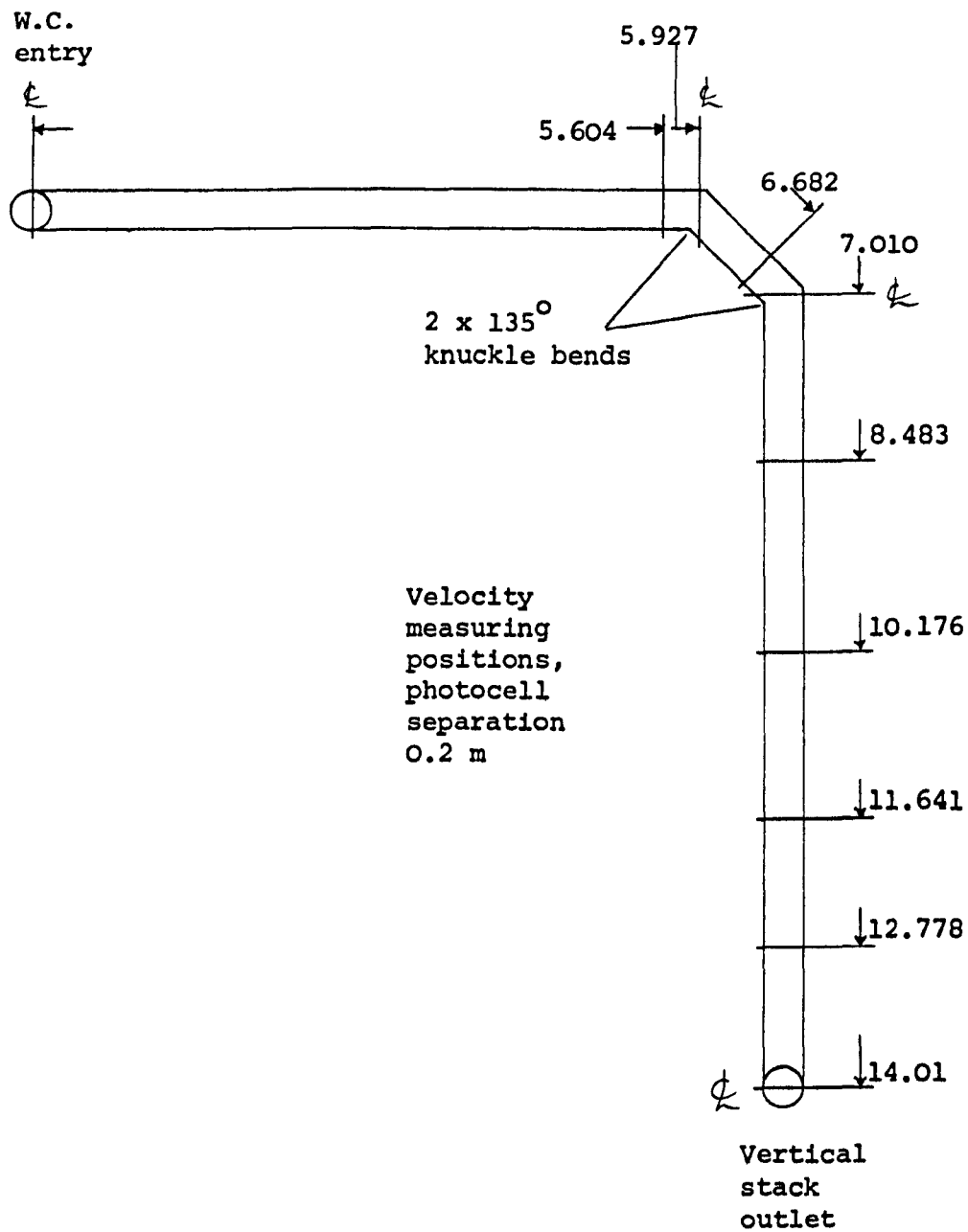


FIGURE 32. Schematic plan view (NTS) of test rig for testing 2 plastic 135° knuckle bends at 5.927 and 7.010 metres from W.C.  
Note: measurements in metres

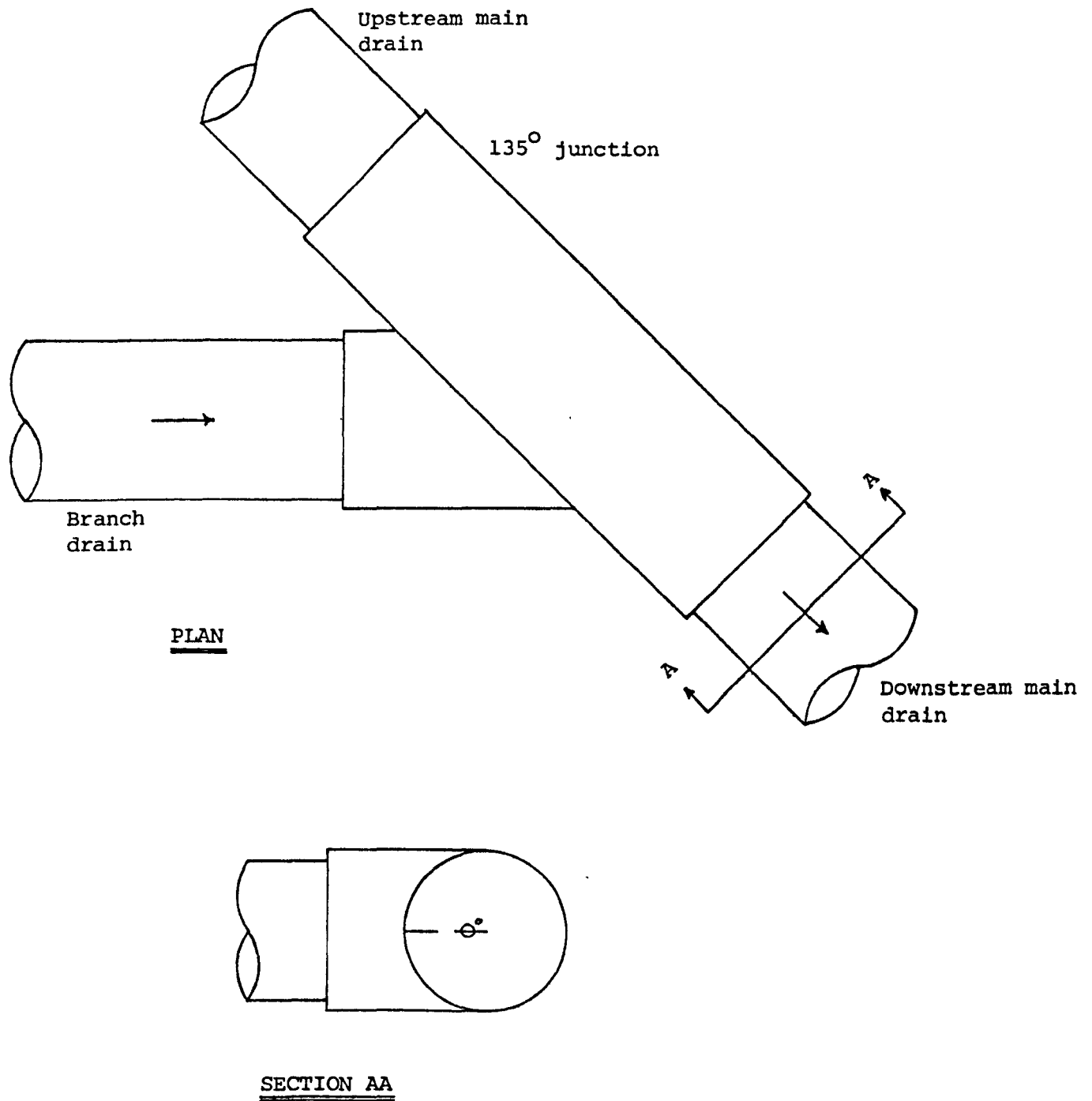


FIGURE 33. Schematic layout (NTS) for tests on entry to main line flow via a 135° junction with horizontal entry.

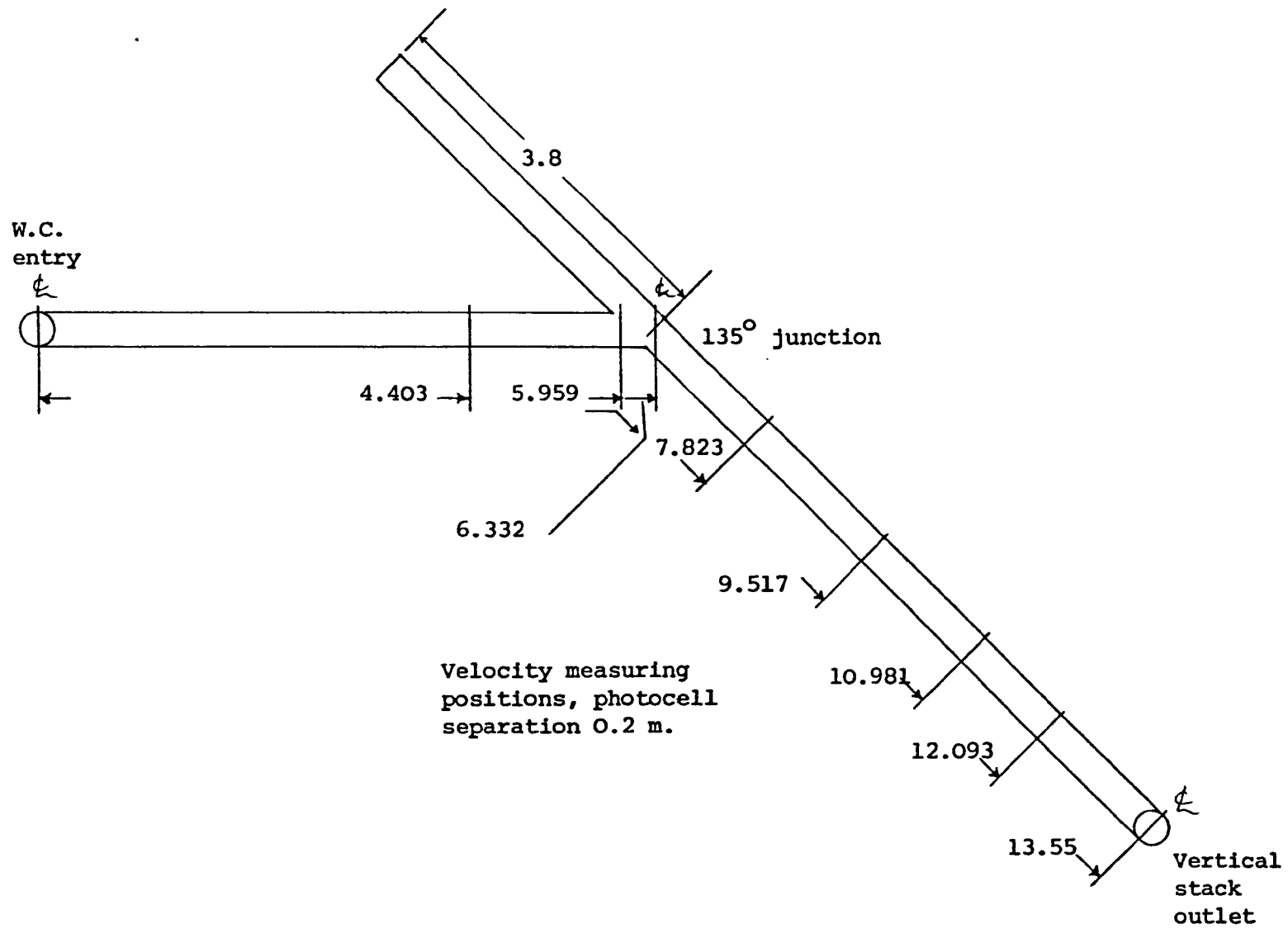


FIGURE 34. Schematic plan view (NTS) of test rig for testing a plastic 135° junction with horizontal branch entry at 6.332 m from W.C.  
 Note: all measurements in metres.

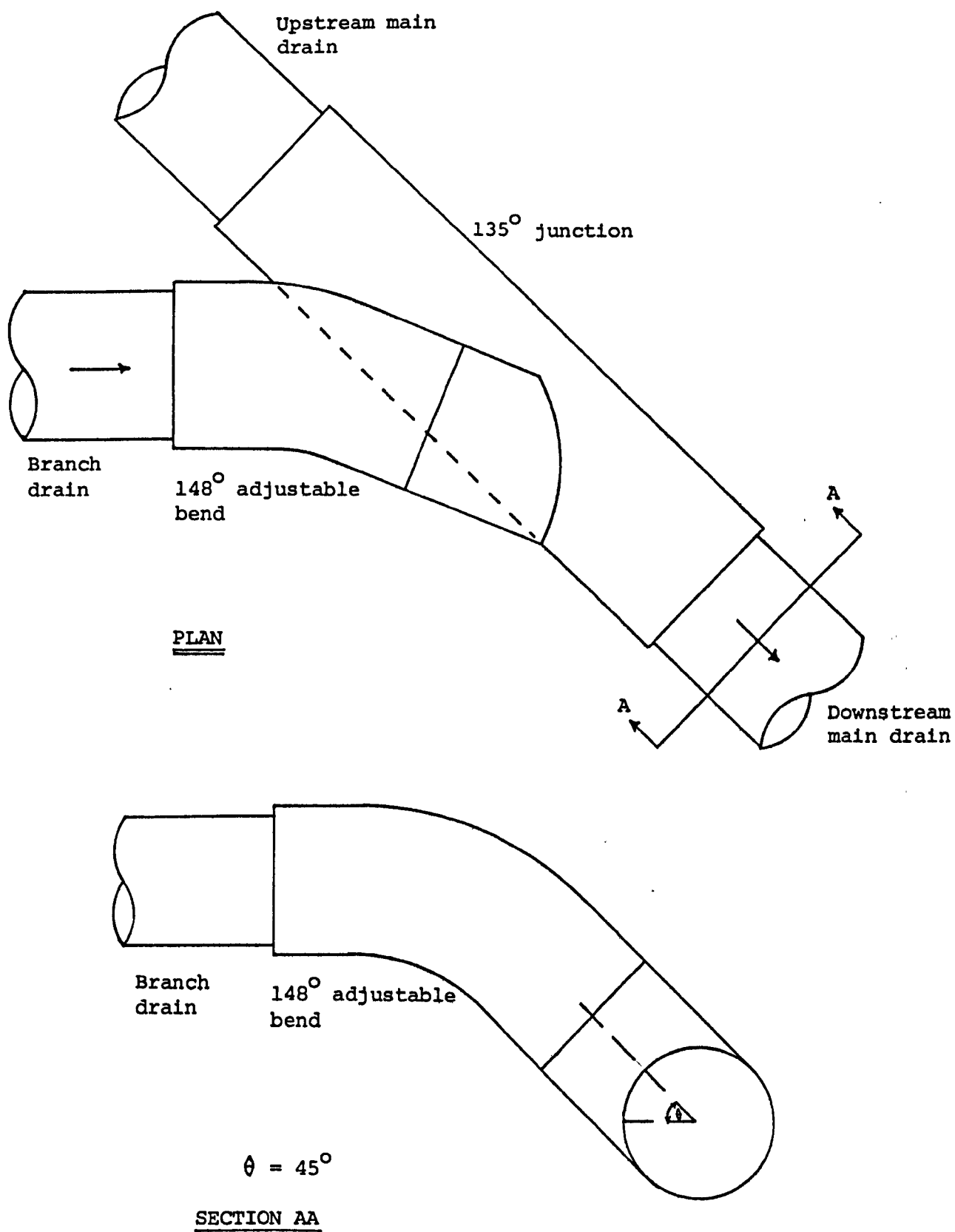


FIGURE 35.

Schematic layout (NTS) for tests on entry to main line flow via a 148° adjustable bend and 135° junction with 45° entry.

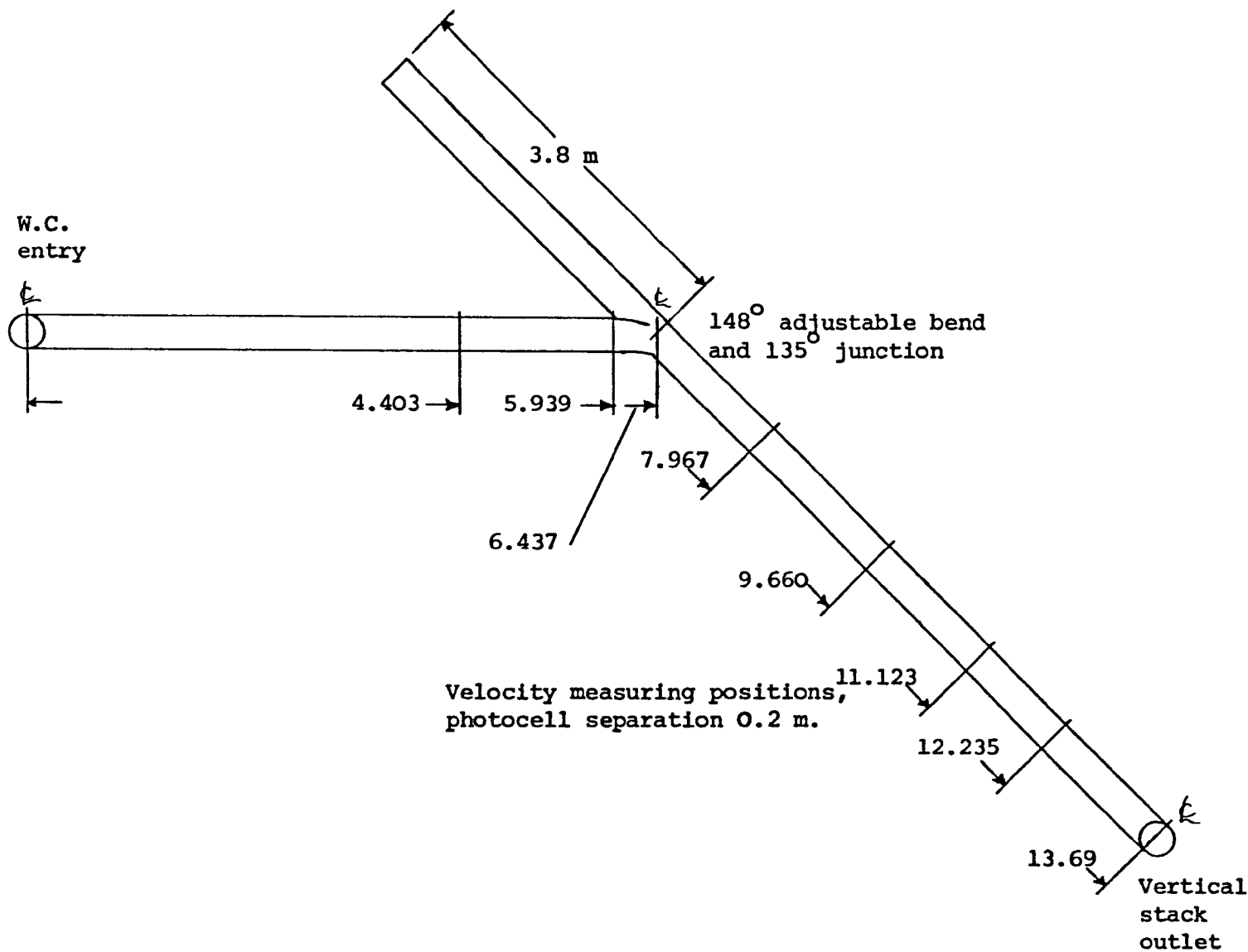


FIGURE 36. Schematic plan view (NTS) of test rig for testing a plastic 135° junction, with 45° branch entry via a 148° adjustable bend, at 6.437 metres from W.C. Note: all measurements in metres.

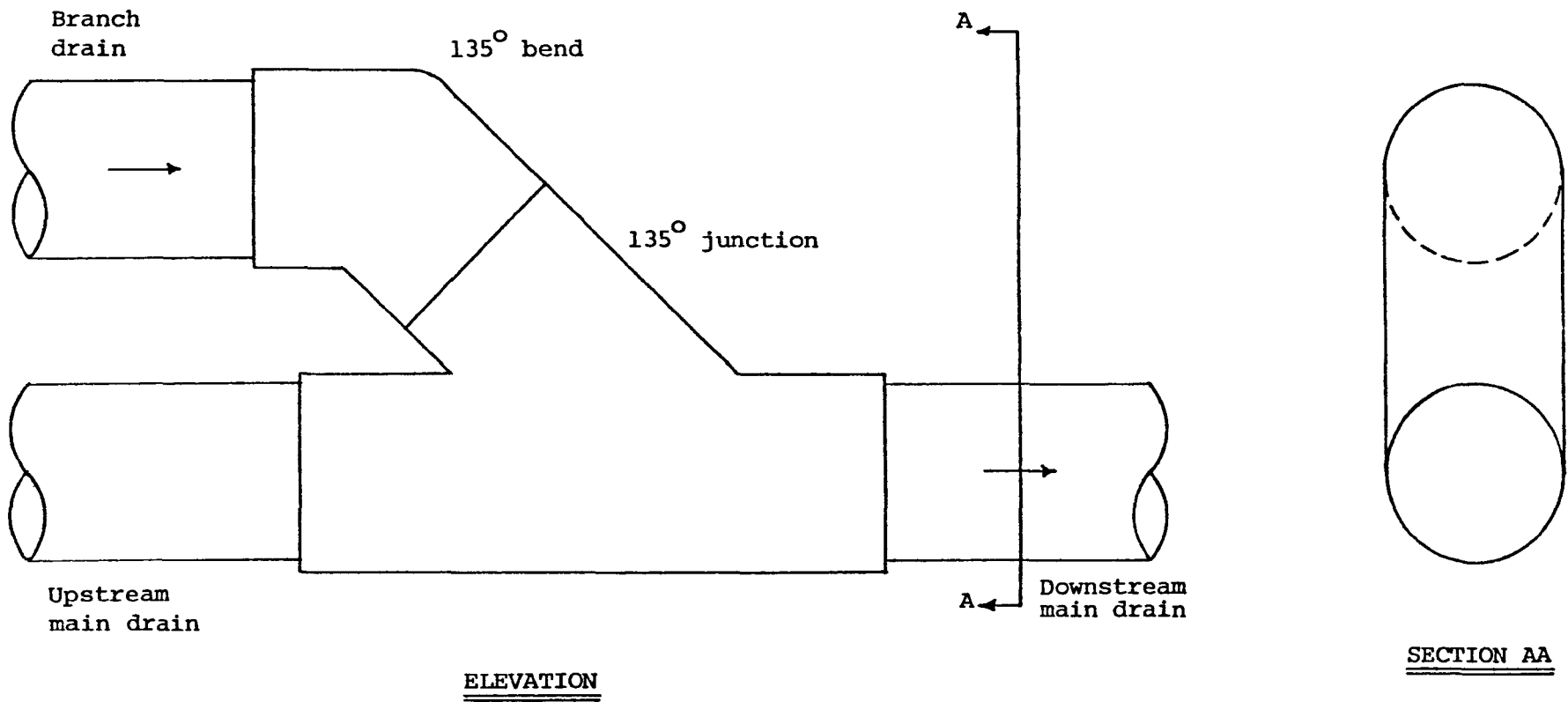


FIGURE 37. Schematic layout (NTS) for tests on entry to main line flow via 135° bend and a 135° junction with vertical junction entry.

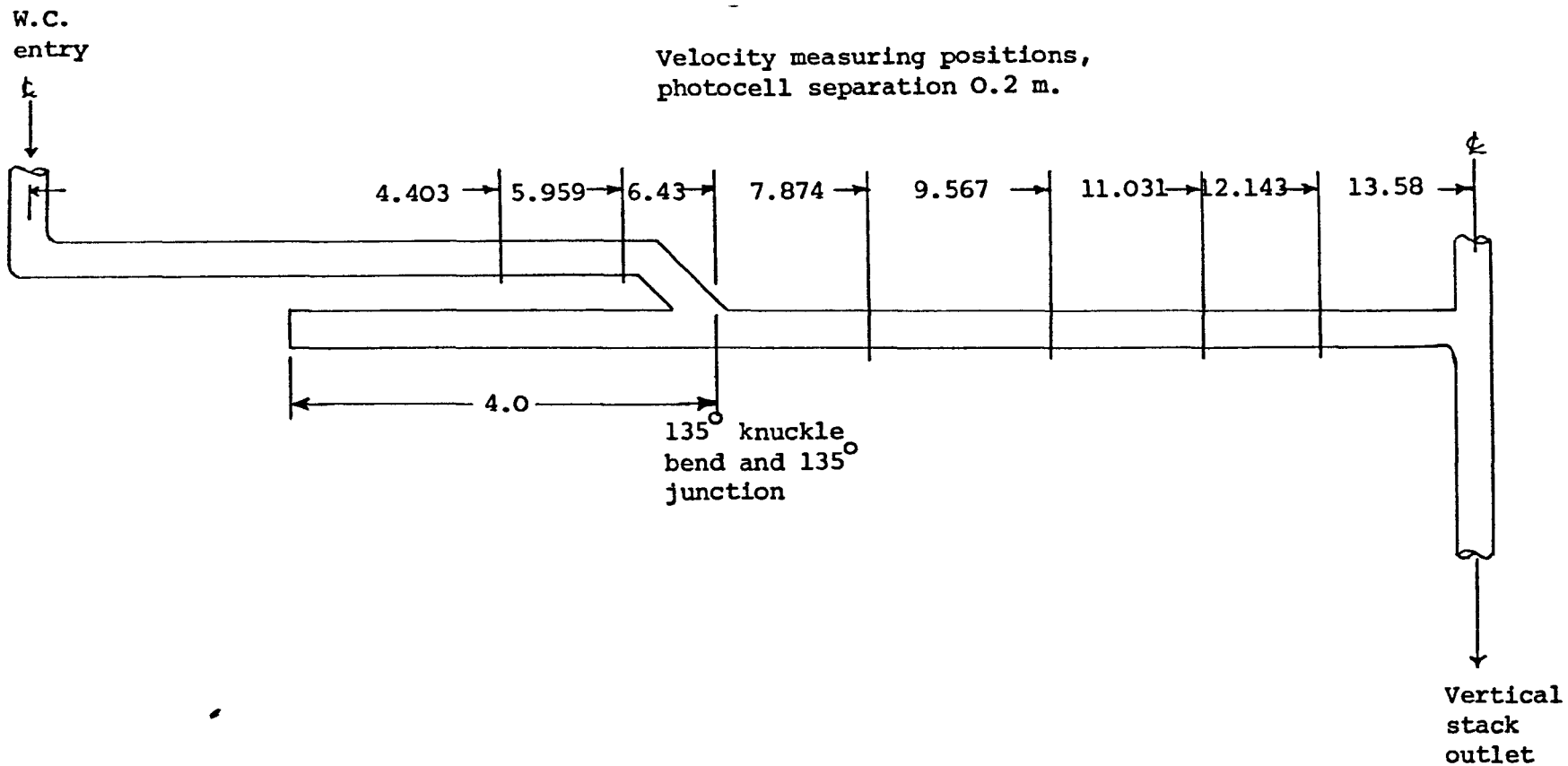


FIGURE 38. Schematic elevation (NTS) of test rig for testing a plastic 135° junction, with vertical branch entry via a 135° knuckle bend, at 6.430 metres from W.C.  
 Note: all measurements in metres.

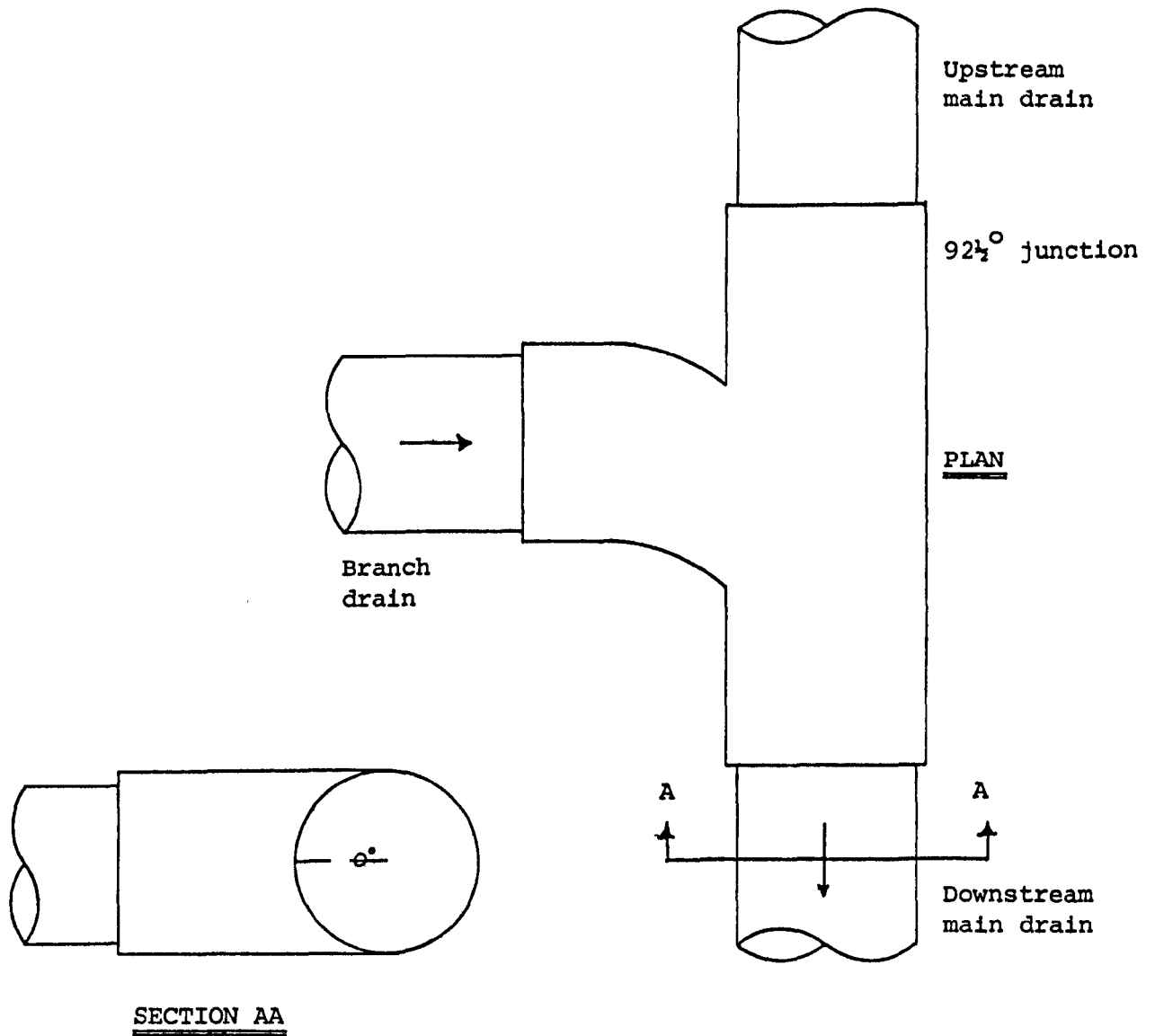


FIGURE 39.

Schematic layout (NTS) for tests on entry to main line flow via a 92 $\frac{1}{2}$  $^{\circ}$  junction with horizontal entry.

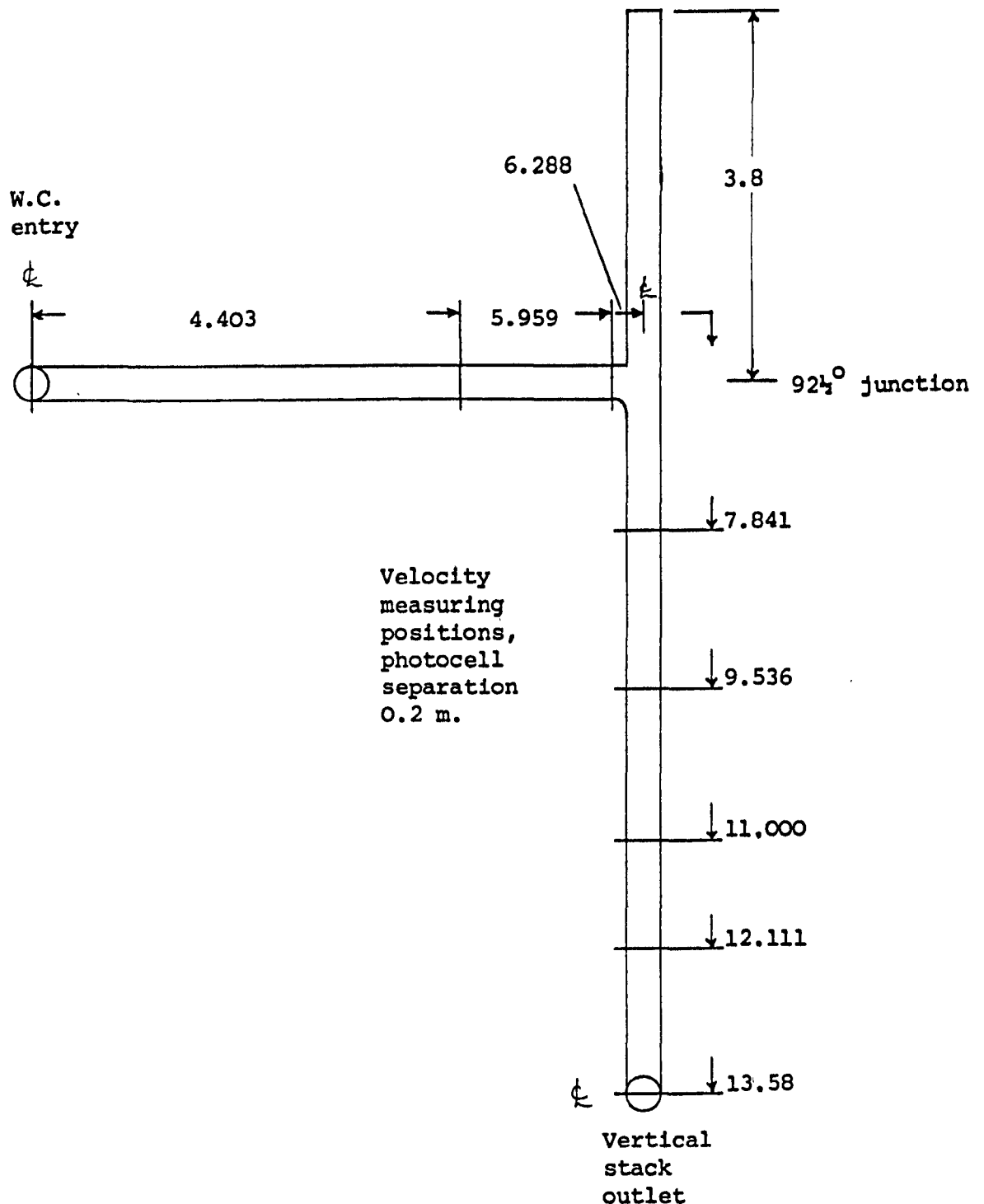


FIGURE 40. Schematic plan view (NTS) of test rig for testing a plastic 92 $\frac{1}{2}$  $^{\circ}$  junction with horizontal branch entry at 6.288 metres from W.C.  
 Note: all measurements in metres.

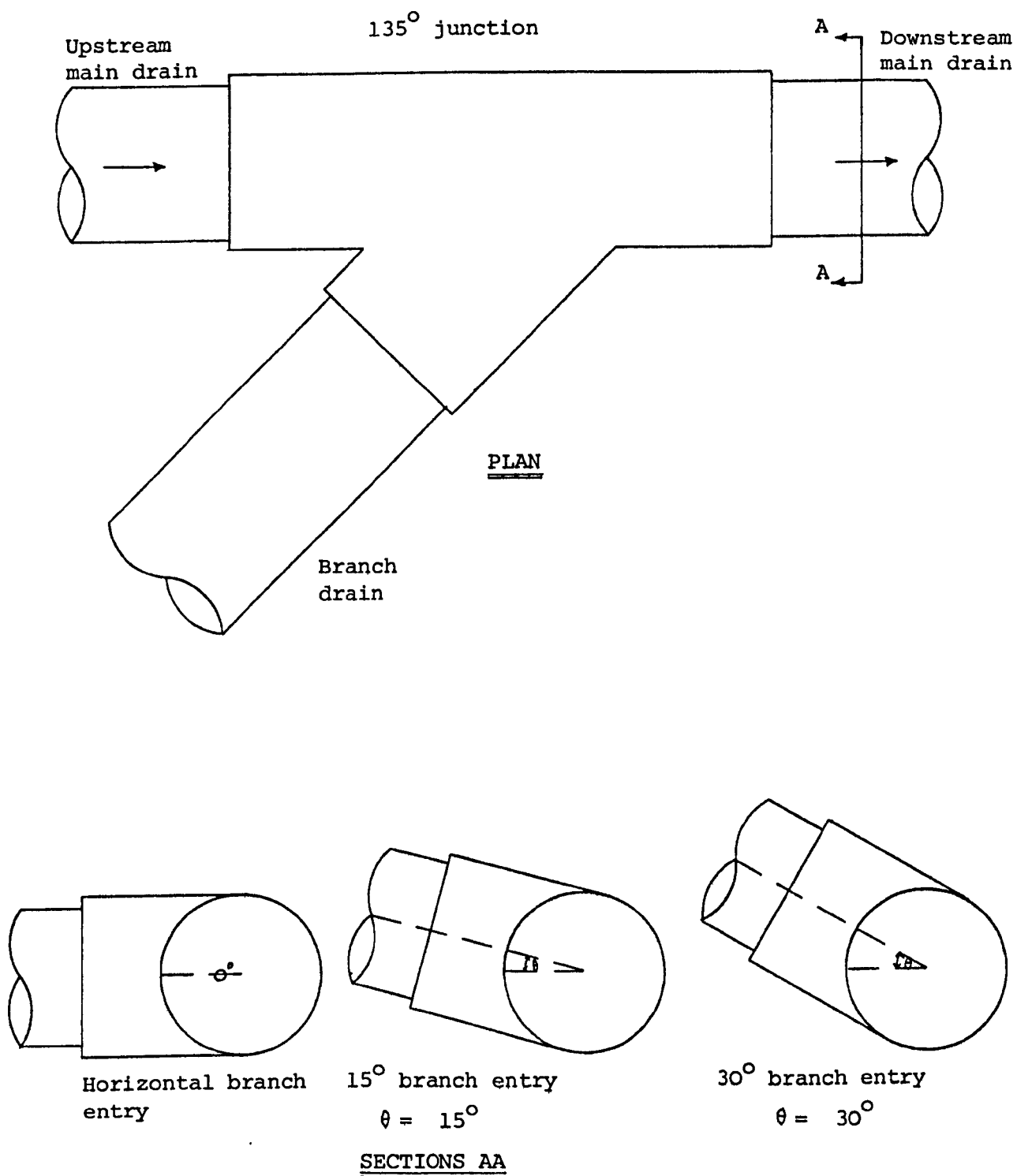


FIGURE 41.

Schematic layout (NTS) for tests on straight pipe flow through 135° junction with junction entry at varying angles.

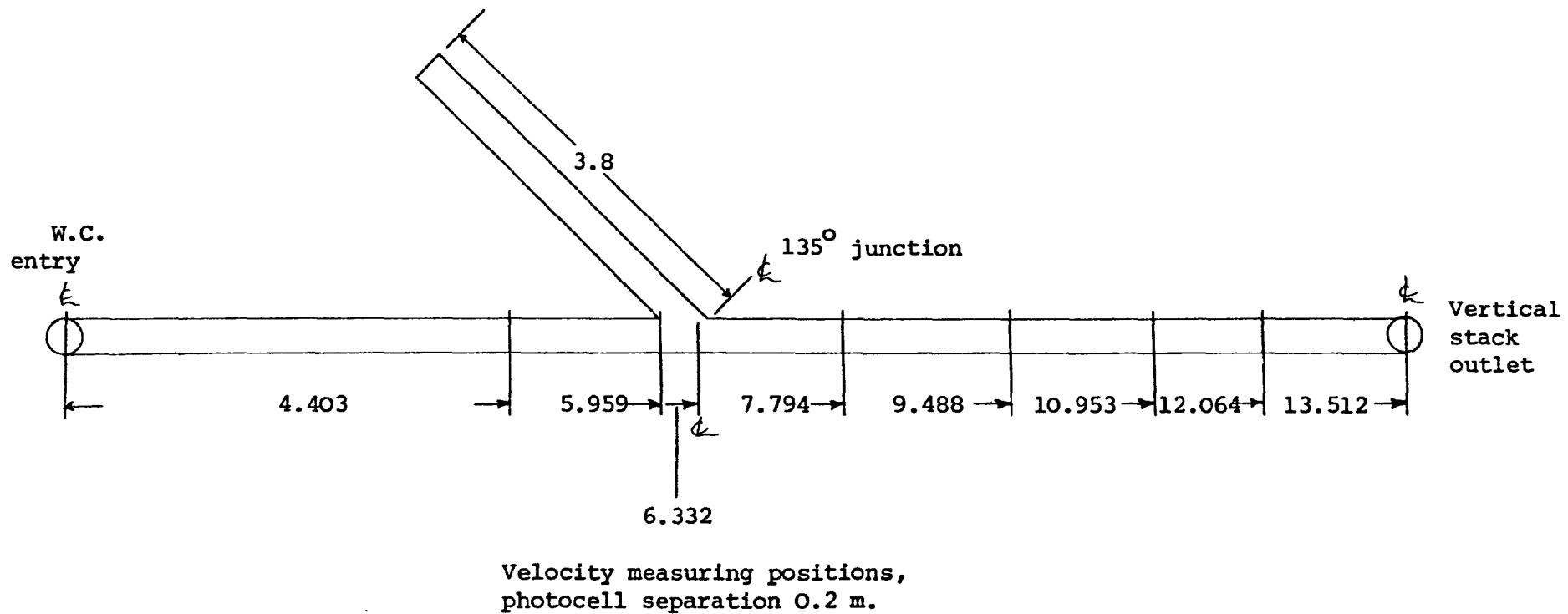


FIGURE 42. Schematic plan view (NTS) of test rig for testing a plastic 135° junction with straight pipe flow through the junction with branch entry at varying angles.  
Note: all measurements in metres.

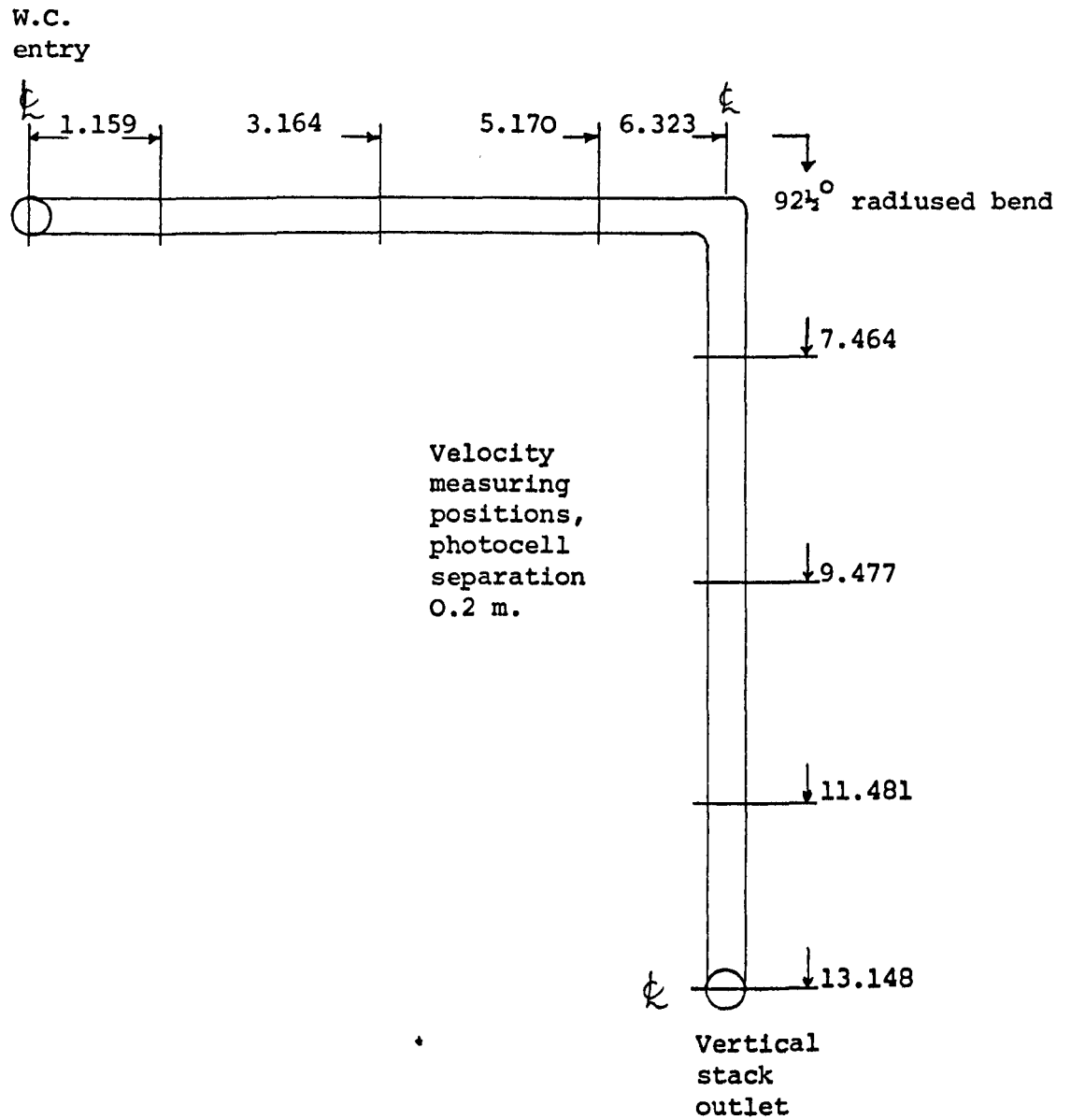


FIGURE 43. Schematic plan view (NTS) of test rig for testing a cast iron 92 $\frac{1}{2}$ <sup>o</sup> radiused bend at 6.323 metres from W.C. Note: all measurements in metres.

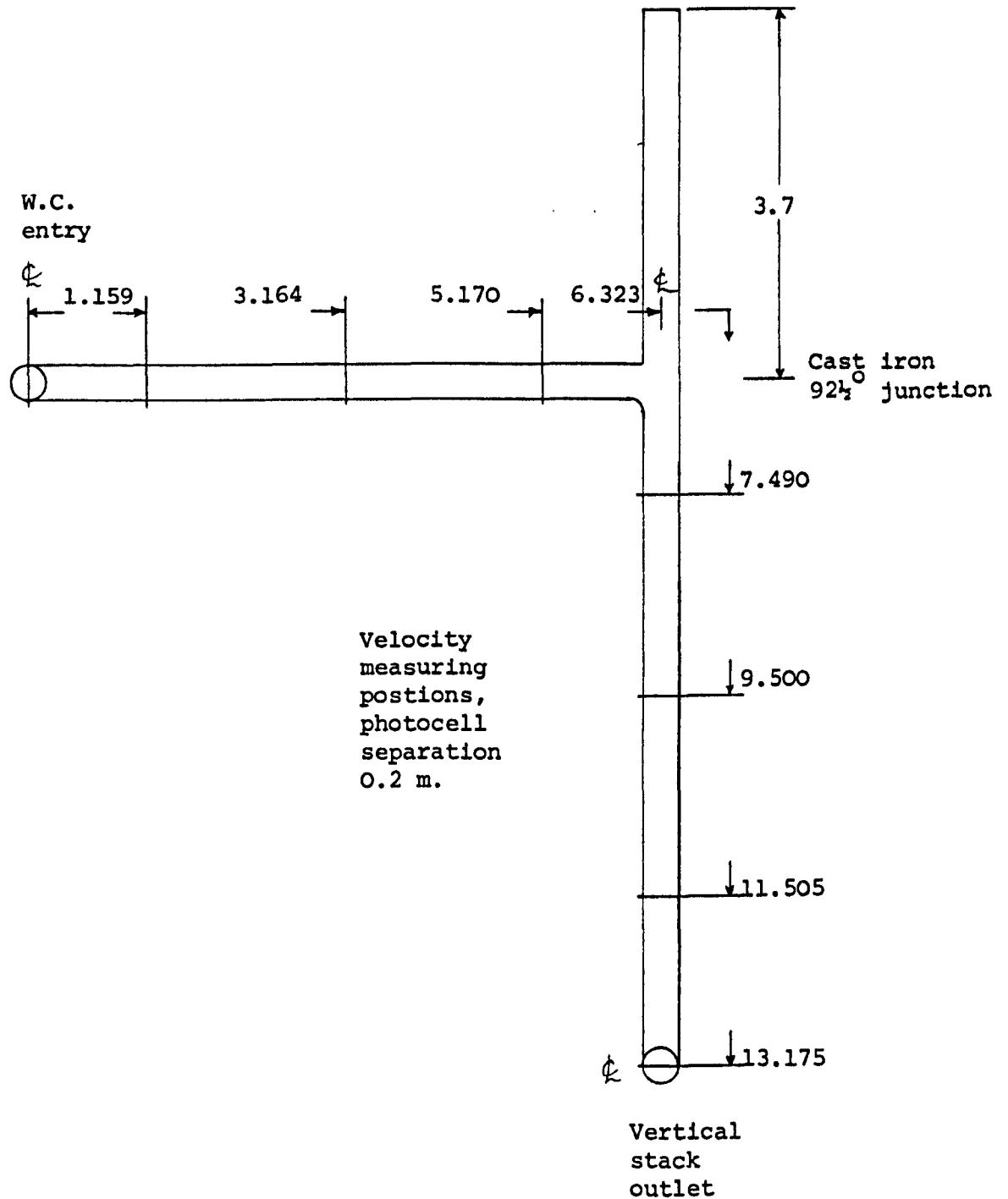


FIGURE 44. Schematic plan view (NTS) of test rig for testing a cast iron 92 $\frac{1}{2}$ ° junction with horizontal entry at 6.323 metres from W.C.  
 Note: all measurements in metres.

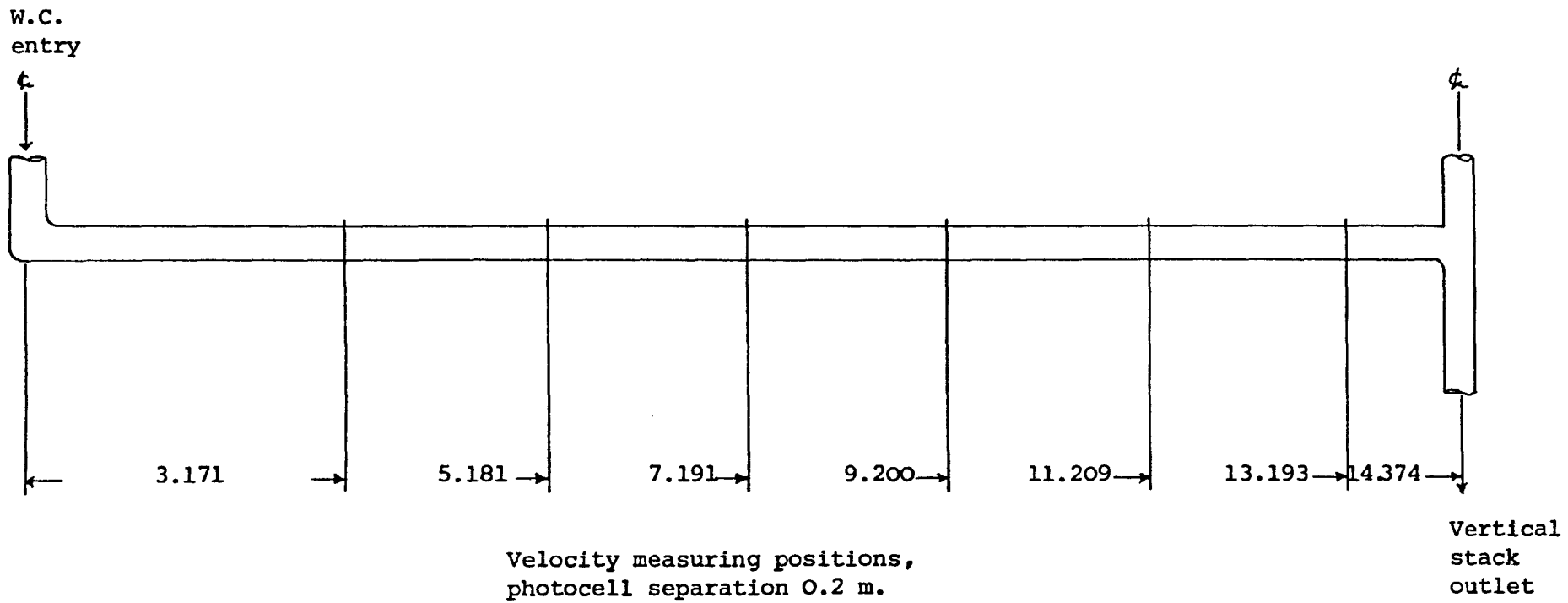


FIGURE 45. Schematic elevation (NTS) of straight glass pipe test rig.  
Note: all measurements in metres.

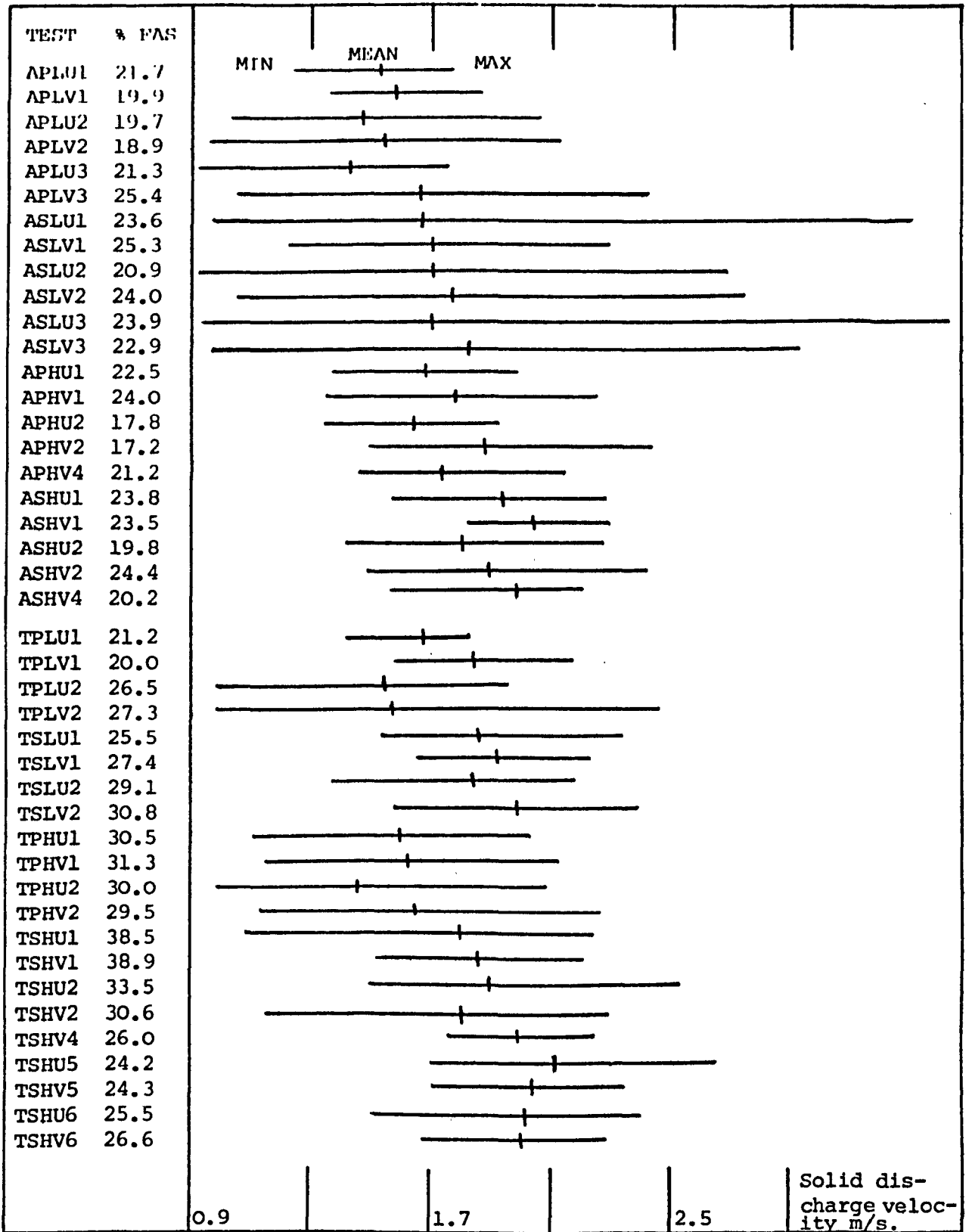


FIGURE 46. W.C. discharge characteristics test results. Summary of solid discharge velocity results for all the w.c. and waste solid combinations, together with the corresponding mean % flush discharged ahead of the solid (%FAS). 9.1 litre flush standard.

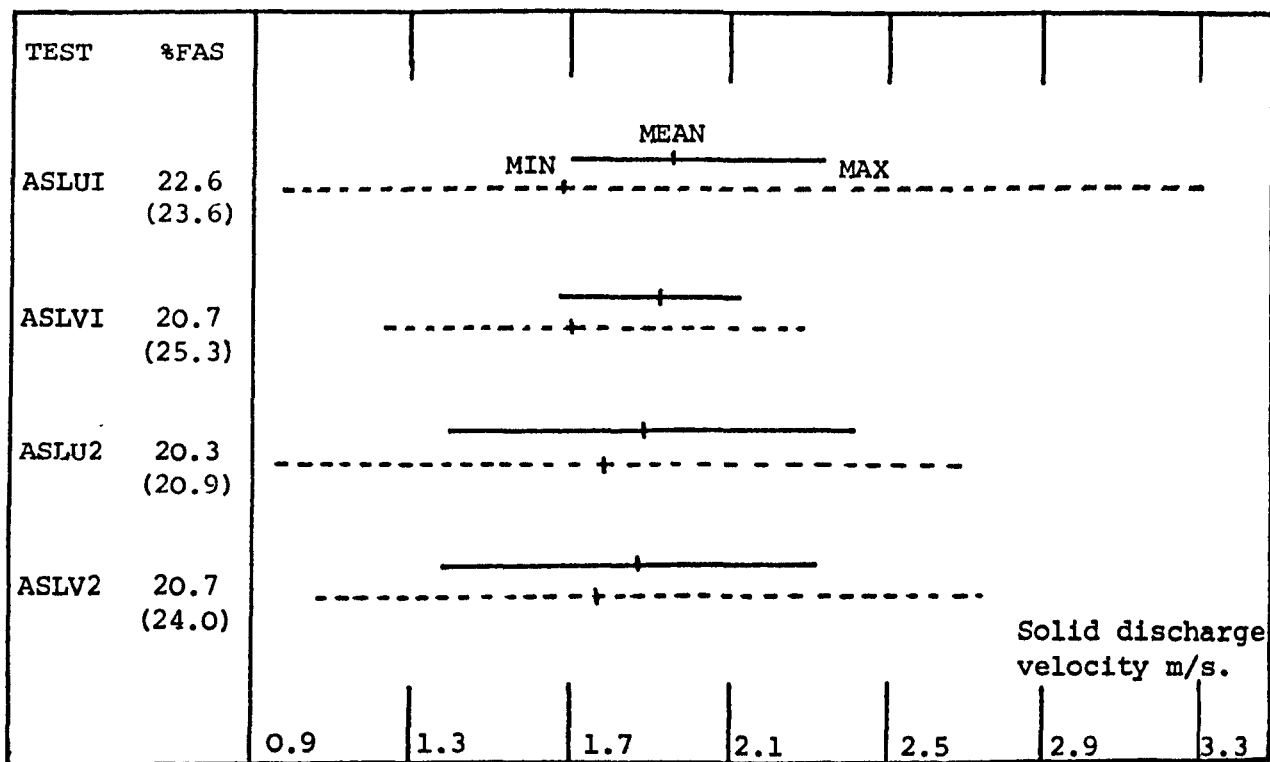


FIGURE 47. W.C. discharge characteristics retest results. Summary of solid discharge velocity results for both the original Armitage Shanks S-trap, low-level cistern W.C. and the replacement unit. Note the decrease in scatter and the higher mean velocity achieved with the new, unused W.C. unit. Figures in parenthesis and ----- lines refer to the original W.C.

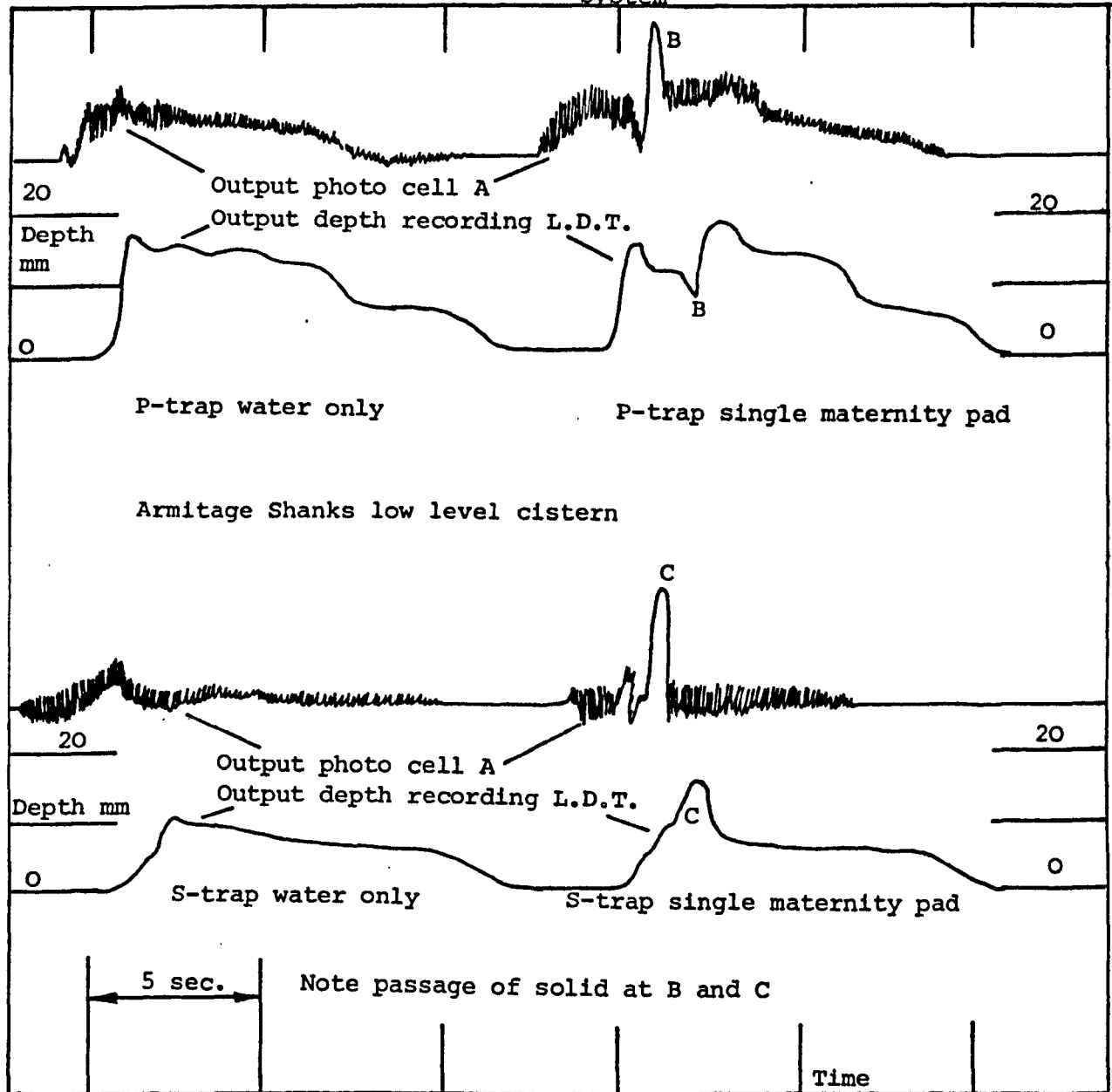
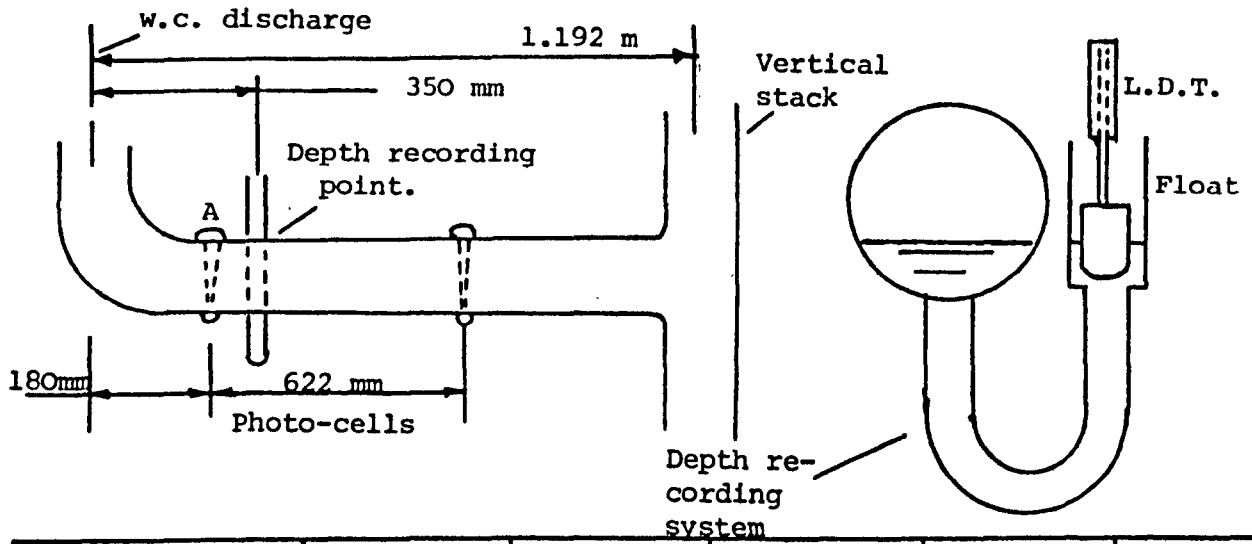


FIGURE 48 PEN RECORDER TRACES REPRESENTING PHOTOCELL AND DEPTH LDT OUTPUT FOR BOTH P AND S-TRAP W.C.'S FOR WATER ONLY AND SINGLE MATERNITY PAD TESTS. BOTH W.C.'S VENTED. W.C. discharge characteristics tests.

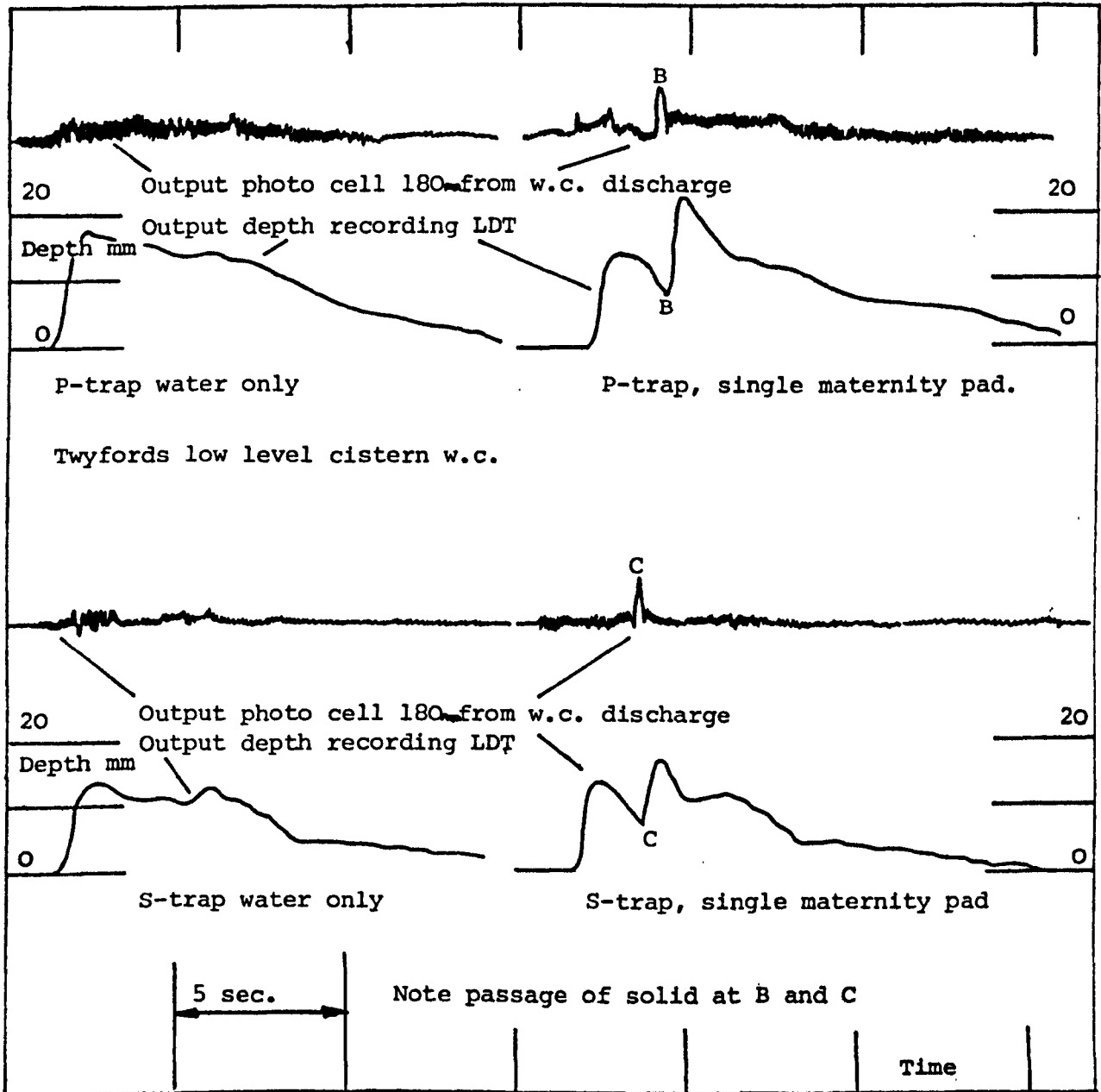


FIGURE 49. PEN RECORDER TRACES REPRESENTING PHOTO CELL AND DEPTH LDT OUTPUT FOR BOTH P AND S-TRAP W.C.'S FOR WATER ONLY AND SINGLE MATERNITY PAD TESTS. BOTH W.C.'S VENTED. W.C. discharge characteristics tests.

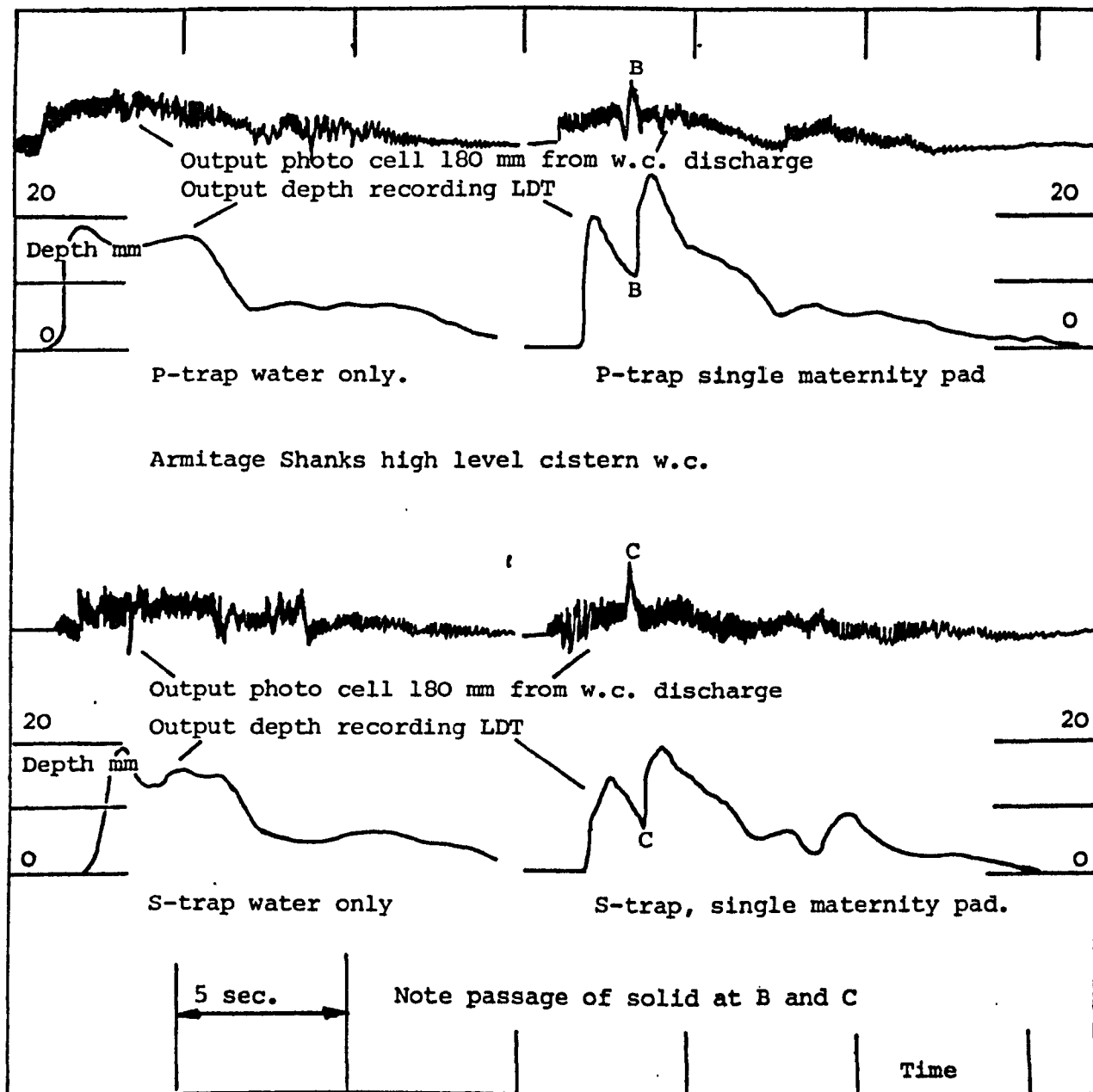


FIGURE 50. PEN RECORDER TRACES REPRESENTING PHOTO CELL AND DEPTH LDT OUTPUT FOR BOTH P AND S-TRAP W.C.'S FOR WATER ONLY AND SINGLE MATERNITY PAD TESTS. BOTH W.C.'S VENTED. W.C. discharge characteristics tests.

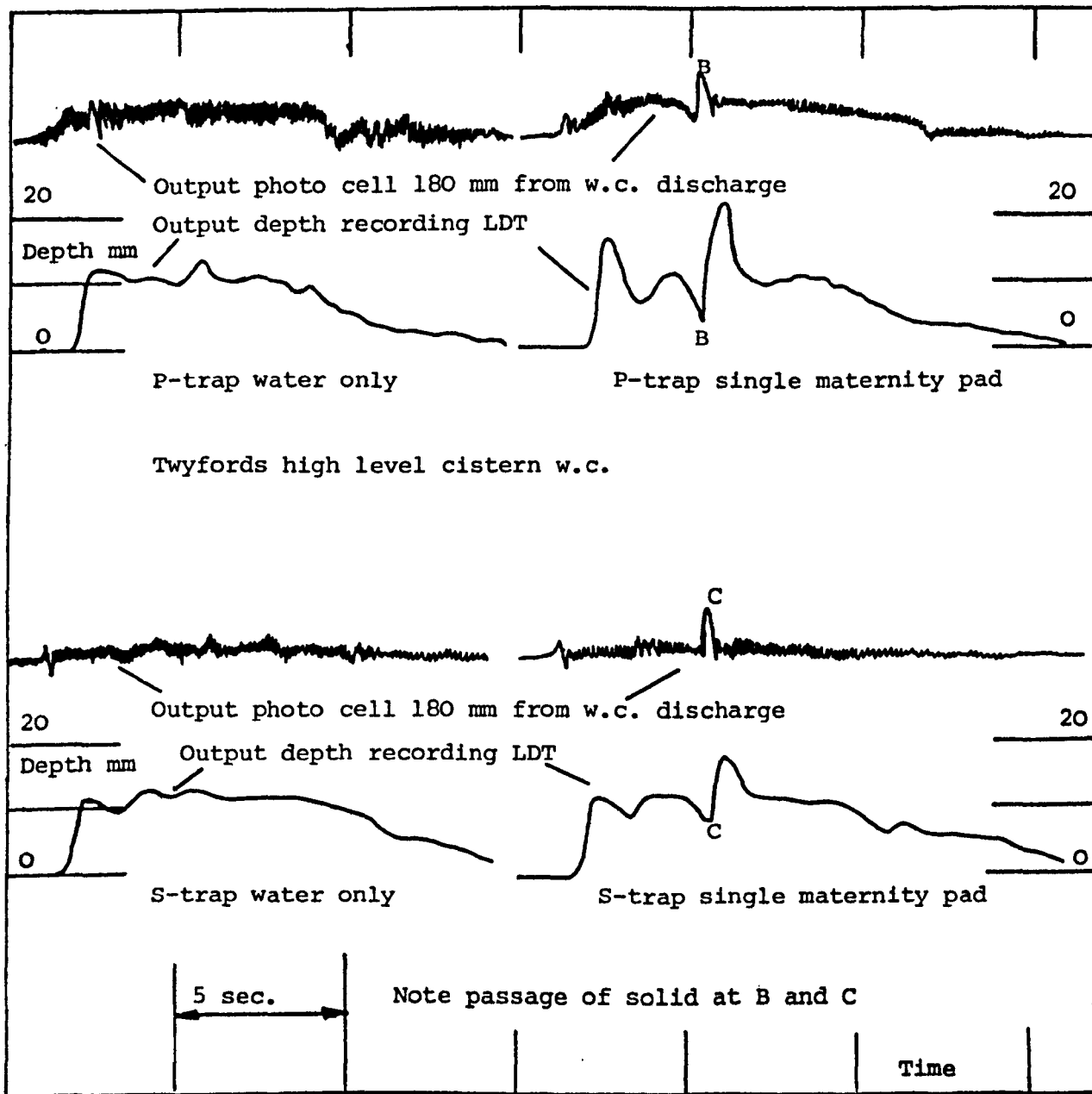


FIGURE 51. PEN RECORDER TRACES REPRESENTING PHOTO CELL AND DEPTH LDT OUTPUT FOR BOTH P AND S-TRAP W.C.'S FOR WATER ONLY AND SINGLE MATERNITY PAD TESTS. BOTH W.C.'S VENTED. W.C. discharge characteristics tests.

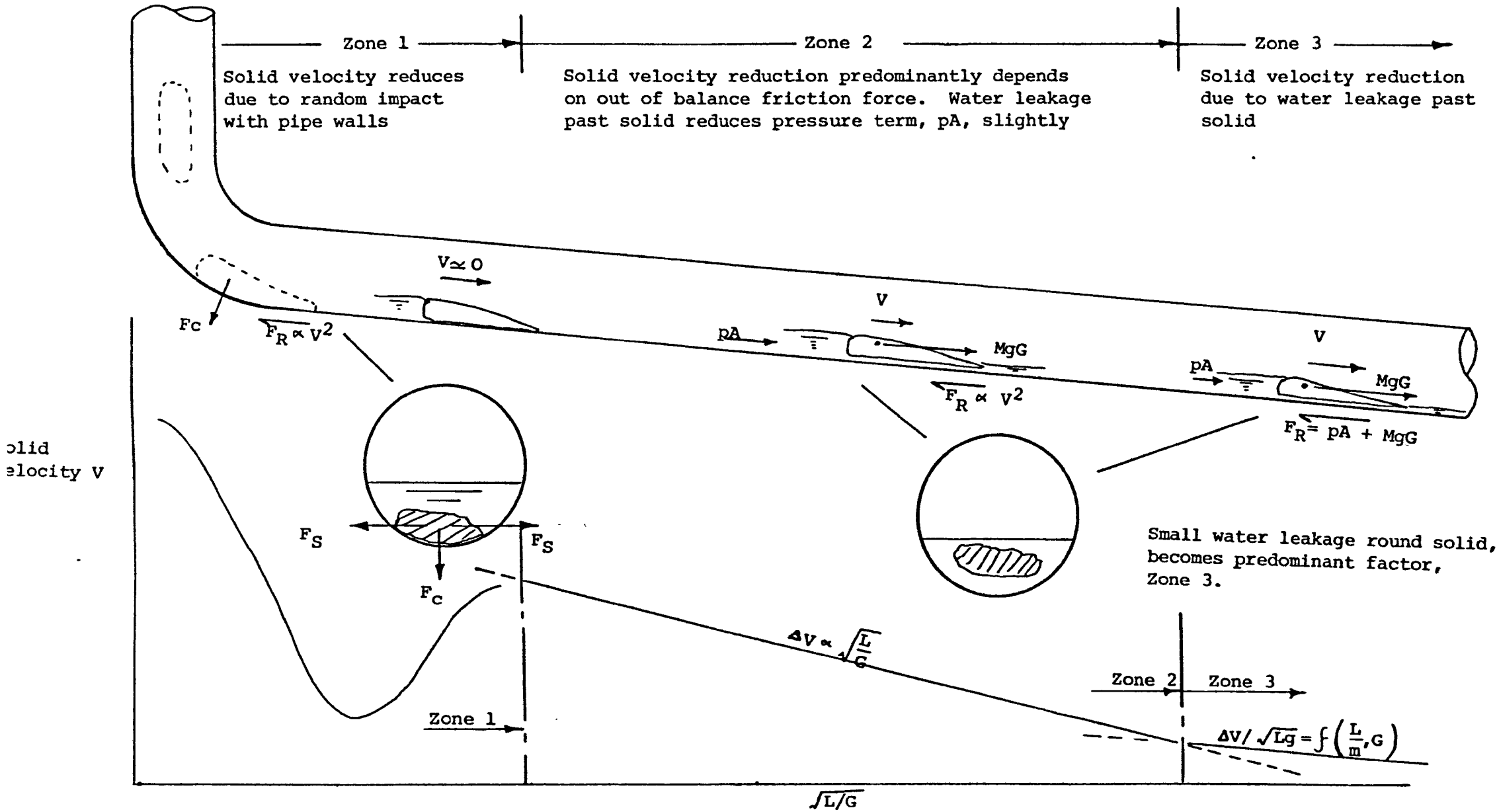


Figure 52. Schematic illustration of flow zones along waste pipe and forces acting on solid.

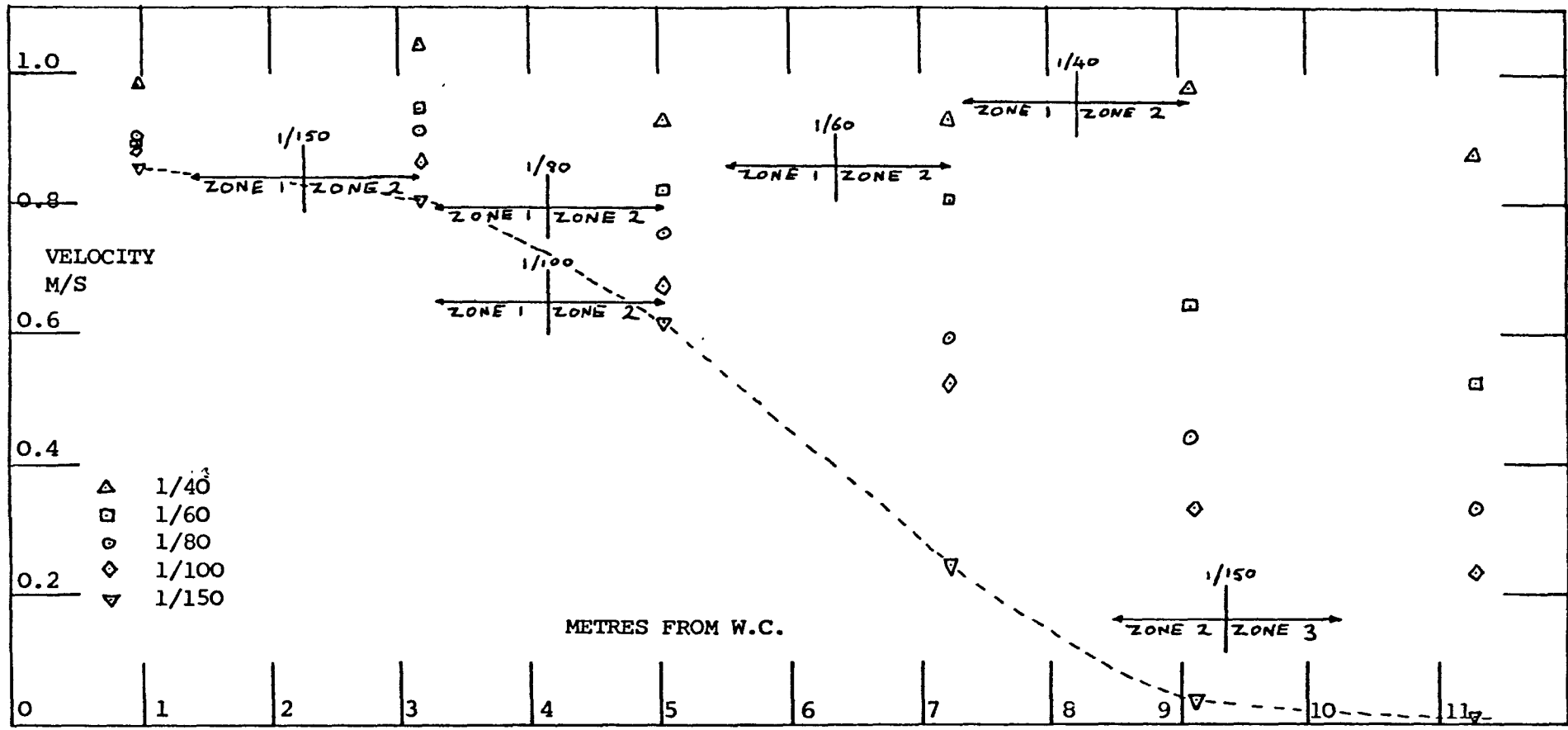


FIGURE 53. (APL1) VELOCITY PROFILES ALONG PIPE FOR ARMITAGE SHANKS P-TRAP LOW LEVEL W.C. SINGLE MATERNITY PAD, UNVENTED, SHOWING VARIATION DUE TO PIPE GRADIENT. ARROWS INDICATE APPROXIMATE LIMITS OF ZONES. STRAIGHT PLASTIC PIPE TESTS

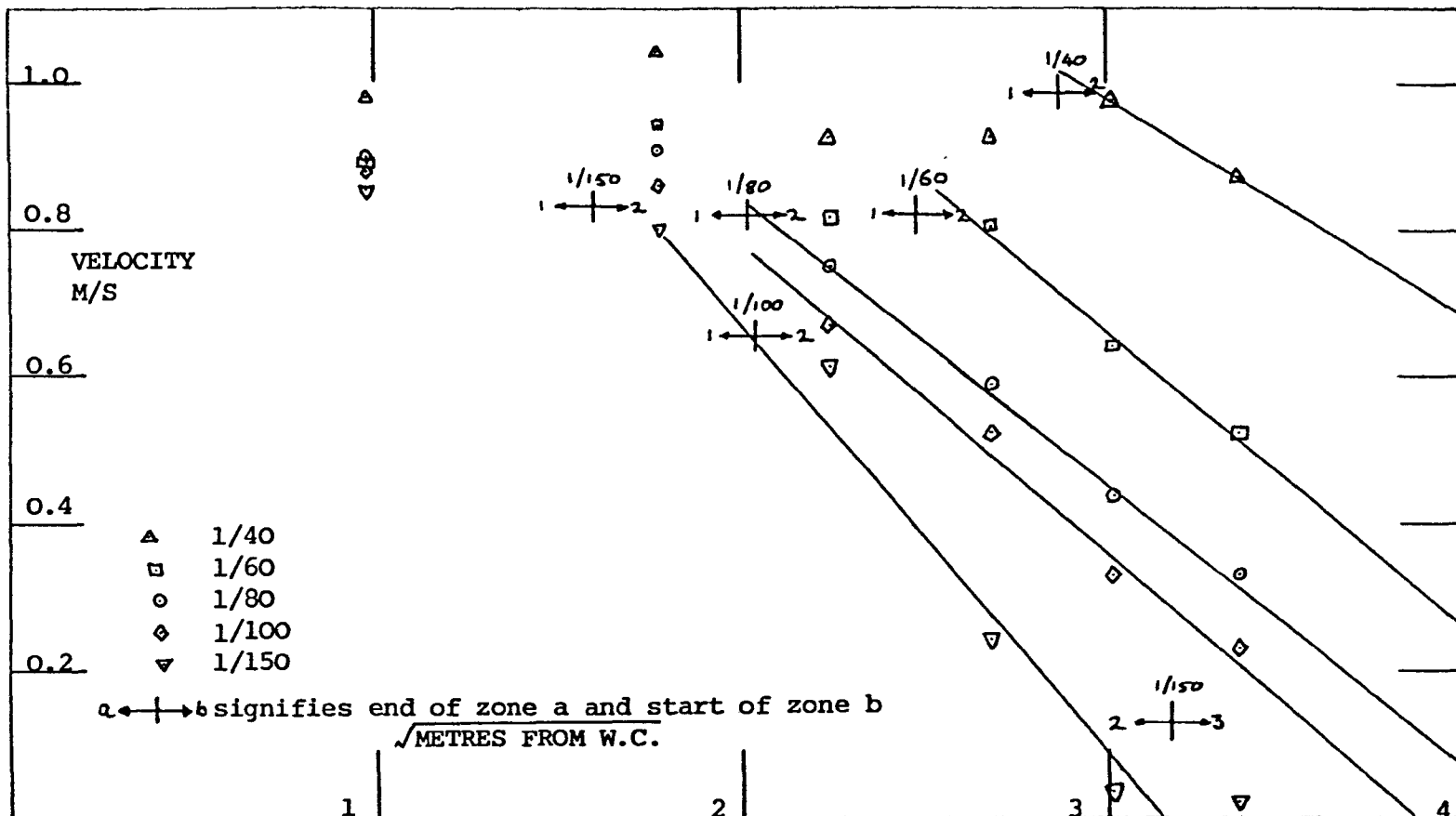


FIGURE 54. (APL1) VELOCITY PROFILES PLOTTED AGAINST SQUARE ROOT OF DISTANCE ALONG PIPE FOR ARMITAGE SHANKS P-TRAP LOW LEVEL W.C. SINGLE MATERNITY PAD, UNVENTED, SHOWING LINEAR RELATIONSHIP BETWEEN VELOCITY AND DISTANCE FROM W.C. IN ZONE 2. ARROWS INDICATE APPROXIMATE LIMITS OF ZONES. STRAIGHT PLASTIC PIPE TESTS

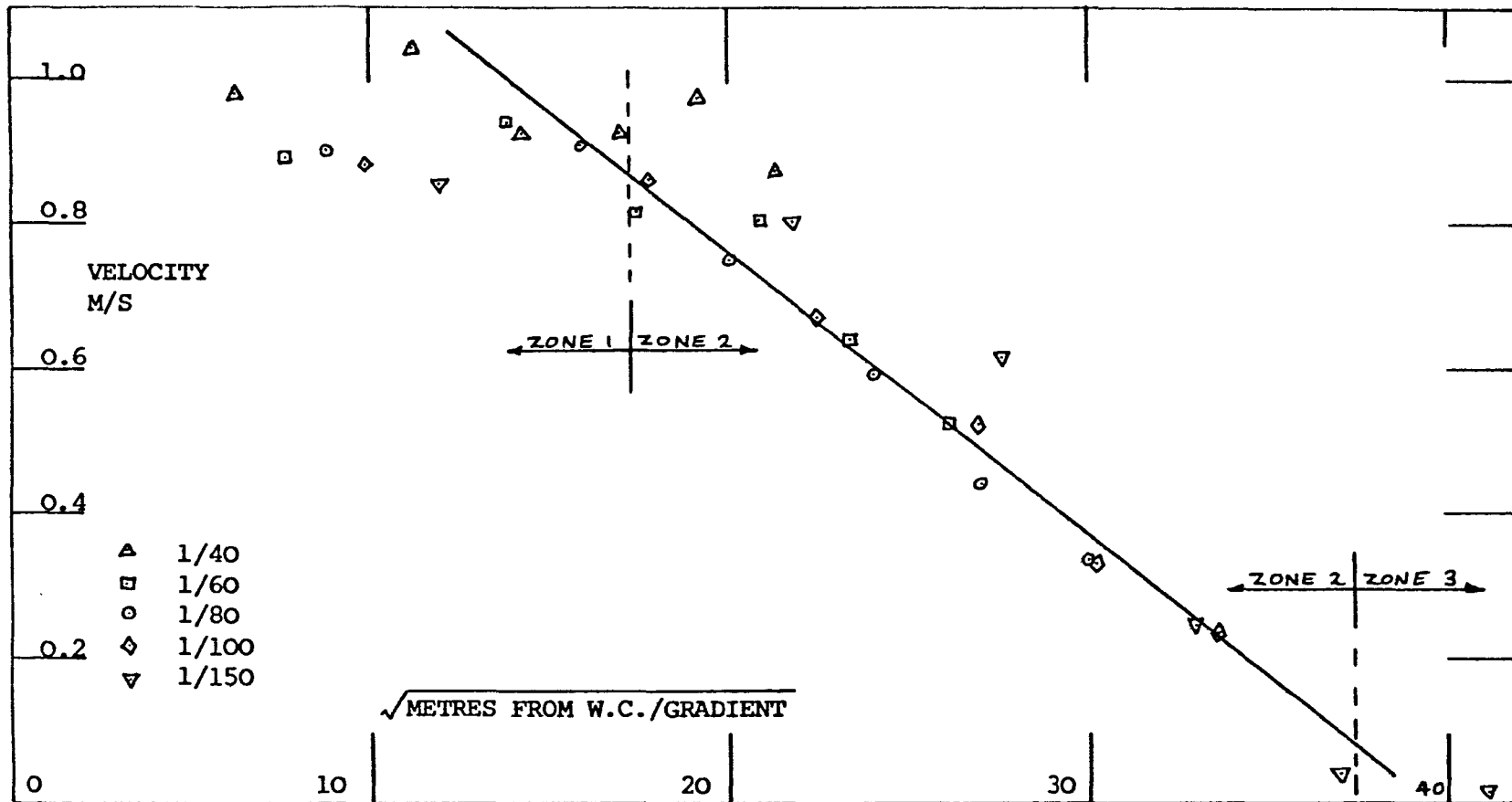


FIGURE 55. (APL1) VELOCITY PROFILES PLOTTED AGAINST SQUARE ROOT OF (DISTANCE ALONG PIPE/GRADIENT) FOR ARMITAGE SHANKS P-TRAP LOW LEVEL W.C. SINGLE MATERNITY PAD, UNVENTED, SHOWING THE LINEAR AND COMMON RELATIONSHIP BETWEEN VELOCITY AND  $\sqrt{L/G}$  IN ZONE 2 FOR ALL PIPE GRADIENTS. ARROWS INDICATE APPROXIMATE LIMIT OF EACH ZONE.  
STRAIGHT PLASTIC PIPE TESTS

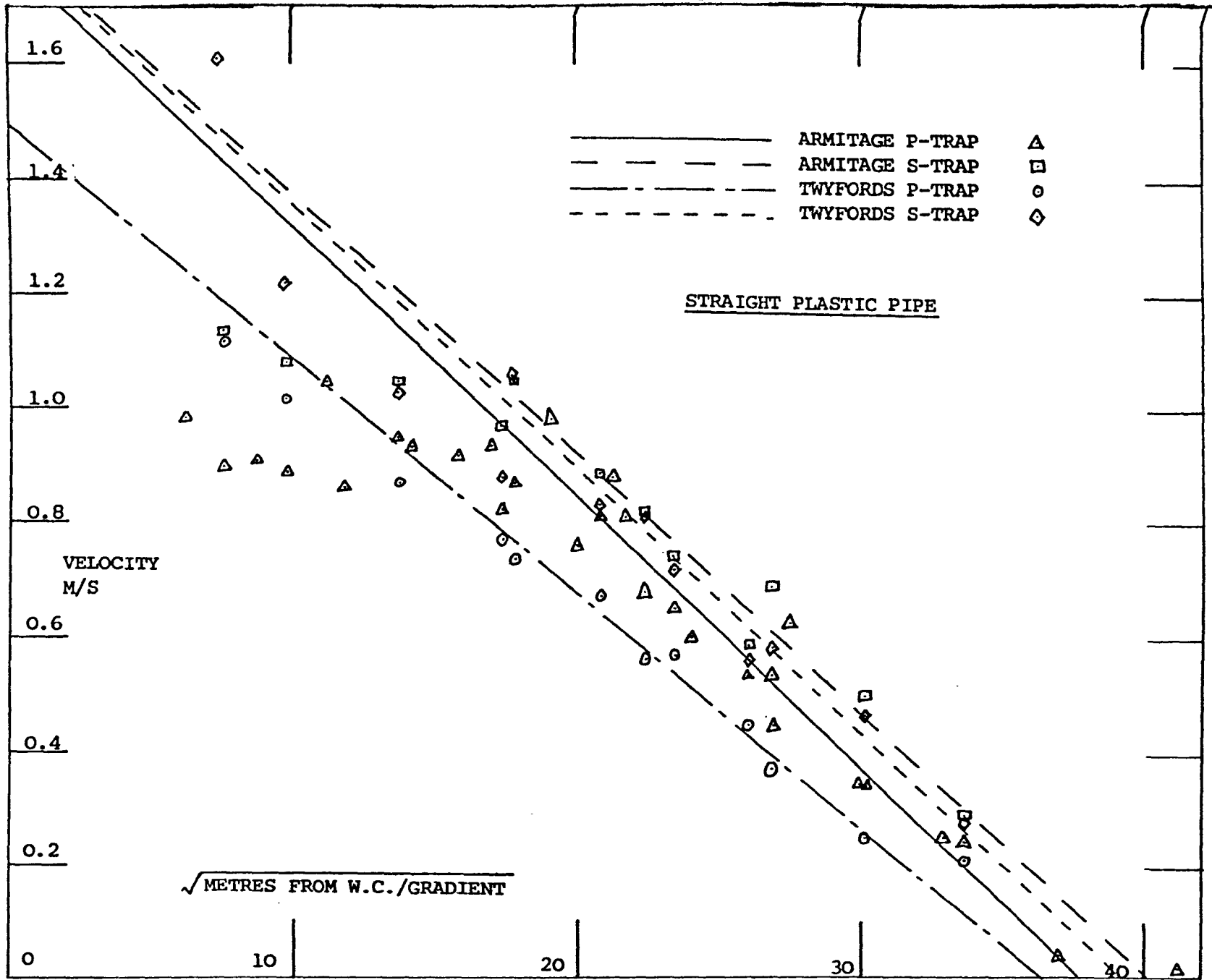


FIGURE 56. SINGLE MATERNITY PAD, UNVENTED. VELOCITY PROFILES PLOTTED AGAINST SQUARE ROOT OF (DISTANCE ALONG PIPE/GRADIENT), FOR ARMITAGE SHANKS AND TWYFORDS, P-TRAP AND S-TRAP W.C.'s. STRAIGHT PLASTIC PIPE TESTS

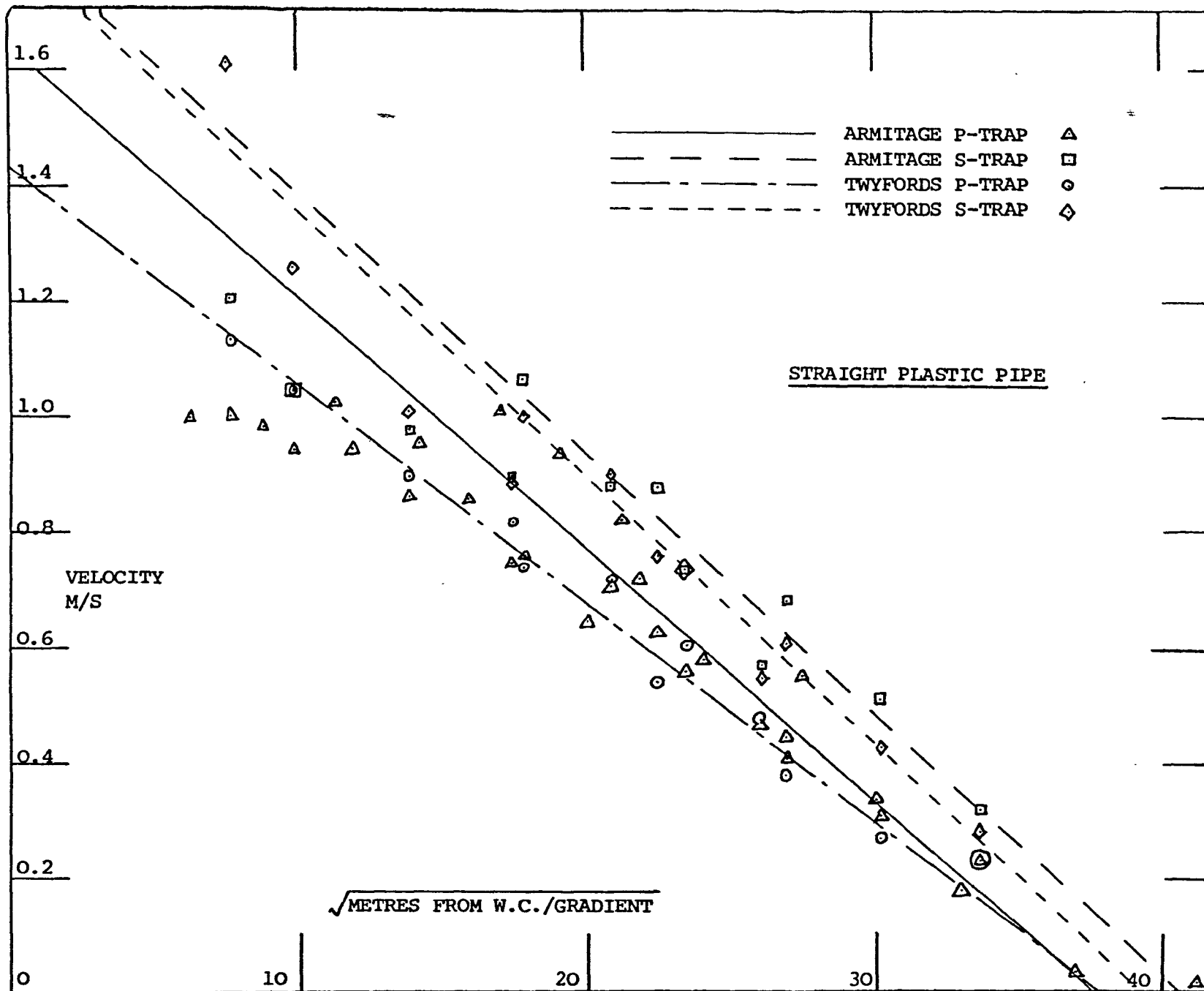


FIGURE 57. SINGLE MATERNITY PAD, VENTED. VELOCITY PROFILES PLOTTED AGAINST SQUARE ROOT OF (DISTANCE ALONG PIPE/GRADIENT) FOR ARMITAGE SHANKS AND TWYFORDS, P-TRAP AND S-TRAP W.C.'s. STRAIGHT PLASTIC PIPE TESTS

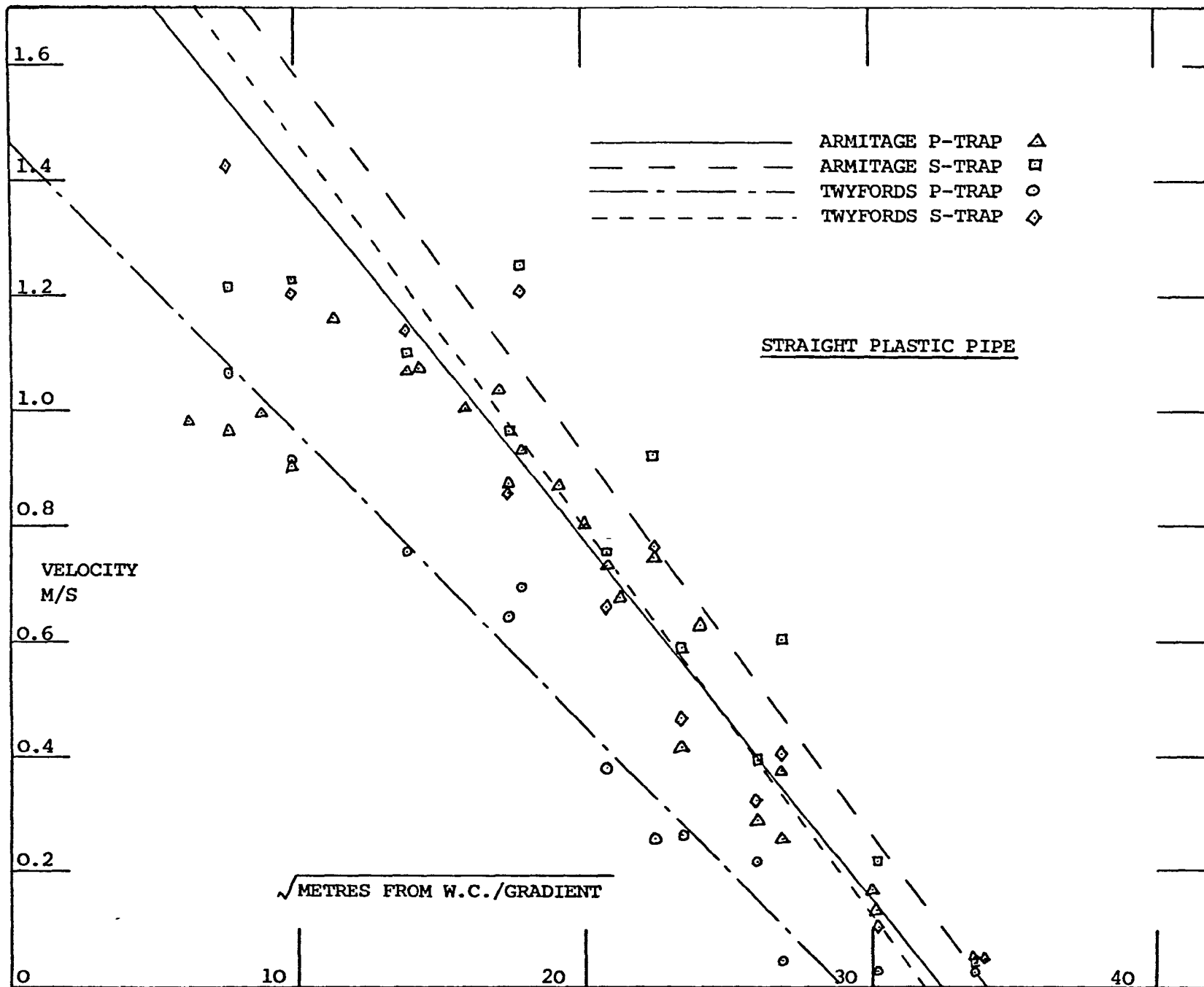


FIGURE 58. MATERNITY PAD + 3 KLEENEX TOWELS, UNVENTED, VELOCITY PROFILES PLOTTED AGAINST SQUARE ROOT OF (DISTANCE ALONG PIPE/GRADIENT) FOR ARMITAGE SHANKS AND TWYFORDS, P-TRAP AND S-TRAP W.C.'s. STRAIGHT PLASTIC PIPE TESTS

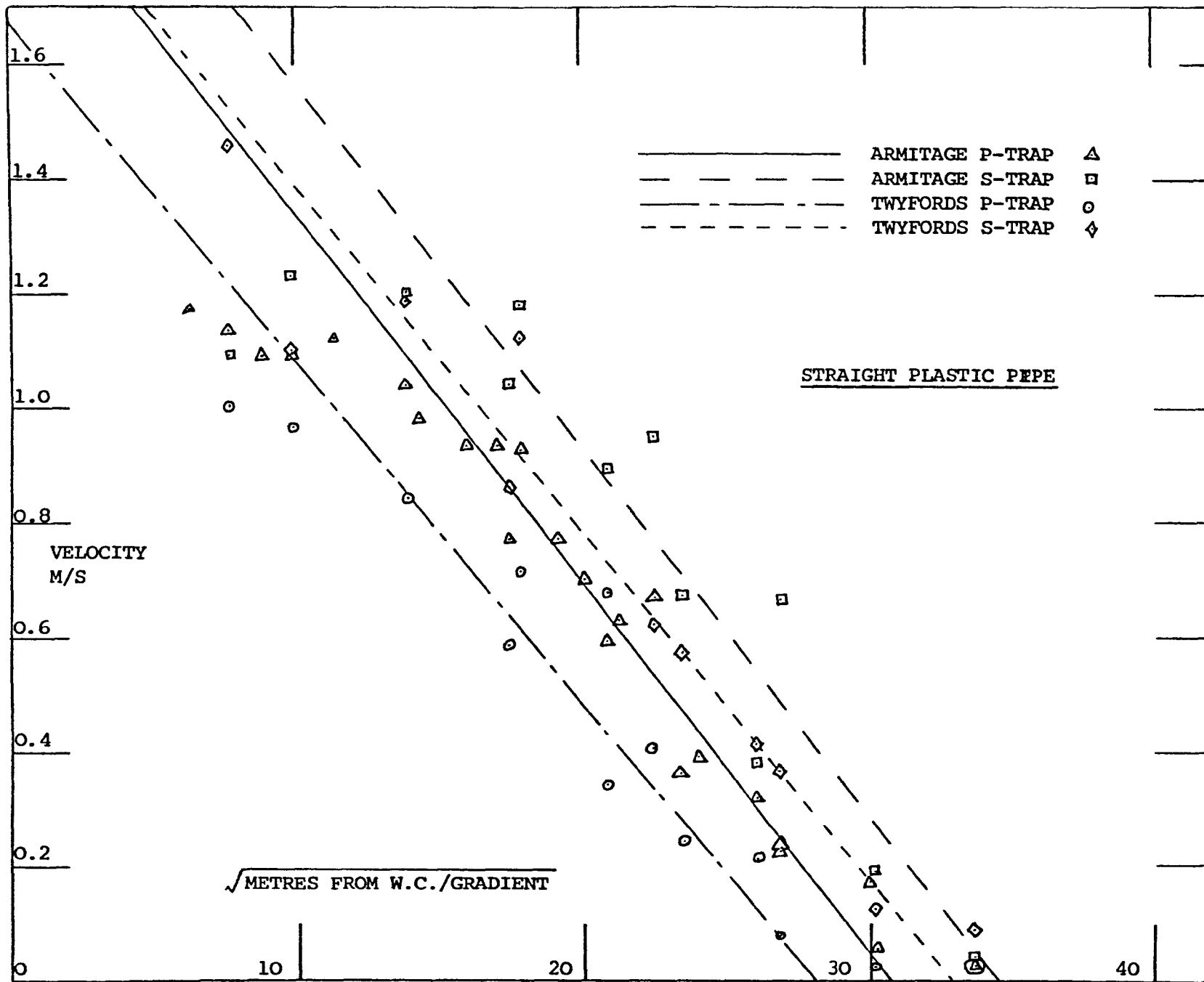


FIGURE 59. MATERNITY PAD + 3 KLEENEX TOWELS, VENTED. VELOCITY PROFILES PLOTTED AGAINST SQUARE ROOT OF (DISTANCE ALONG PIPE/GRADIENT) FOR ARMITAGE SHANKS AND TWYFORDS, P-TRAP AND S-TRAP W.C.'s. STRAIGHT PLASTIC PIPE TESTS.

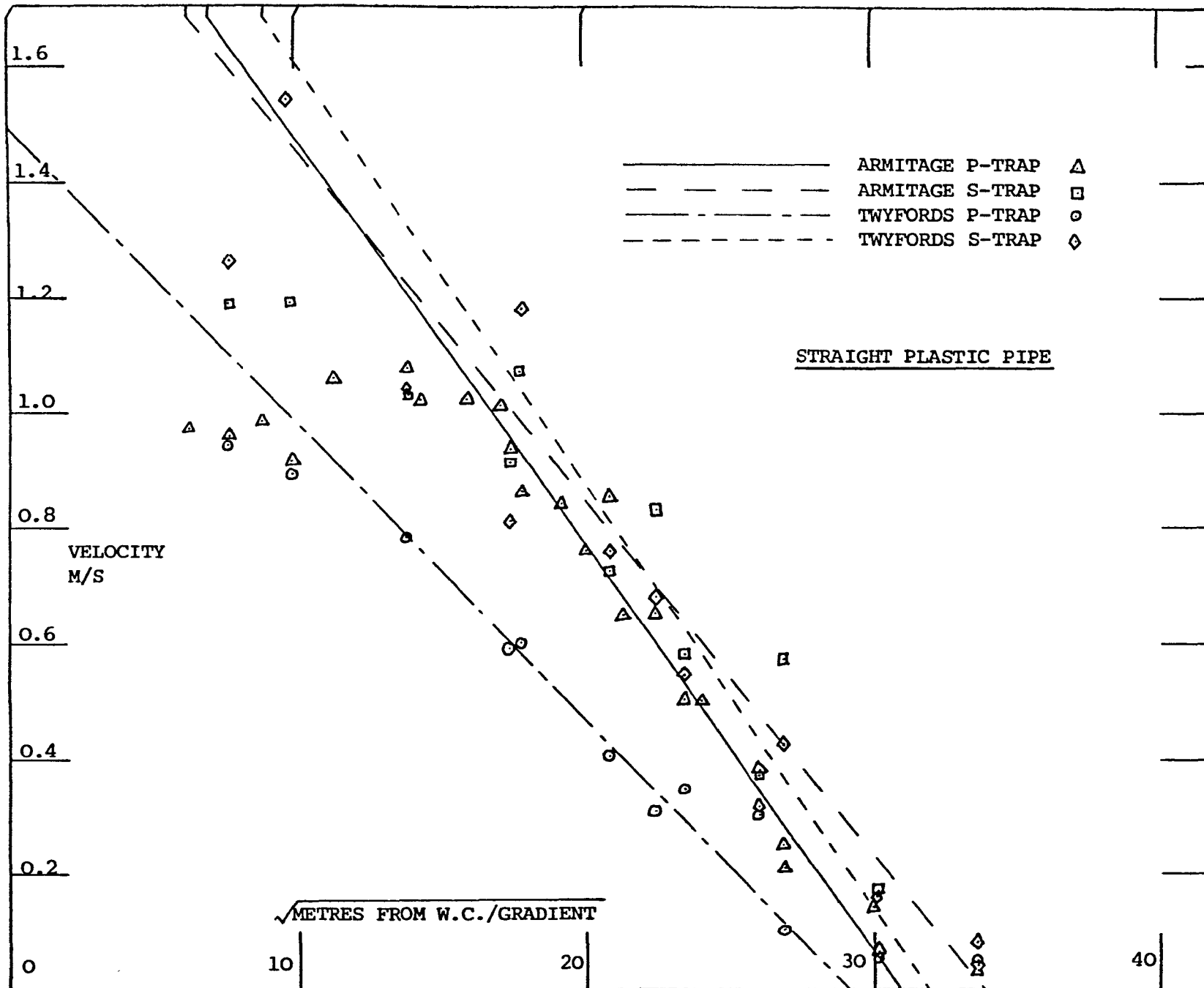


FIGURE 60. MATERNITY PAD + 3 BOWTOWELS, UNVENTED. VELOCITY PROFILES PLOTTED AGAINST SQUARE ROOT OF (DISTANCE ALONG PIPE/GRADIENT) FOR ARMITAGE SHANKS AND TWYFORDS, P-TRAP AND S-TRAP W.C.'s. STRAIGHT PLASTIC PIPE TESTS

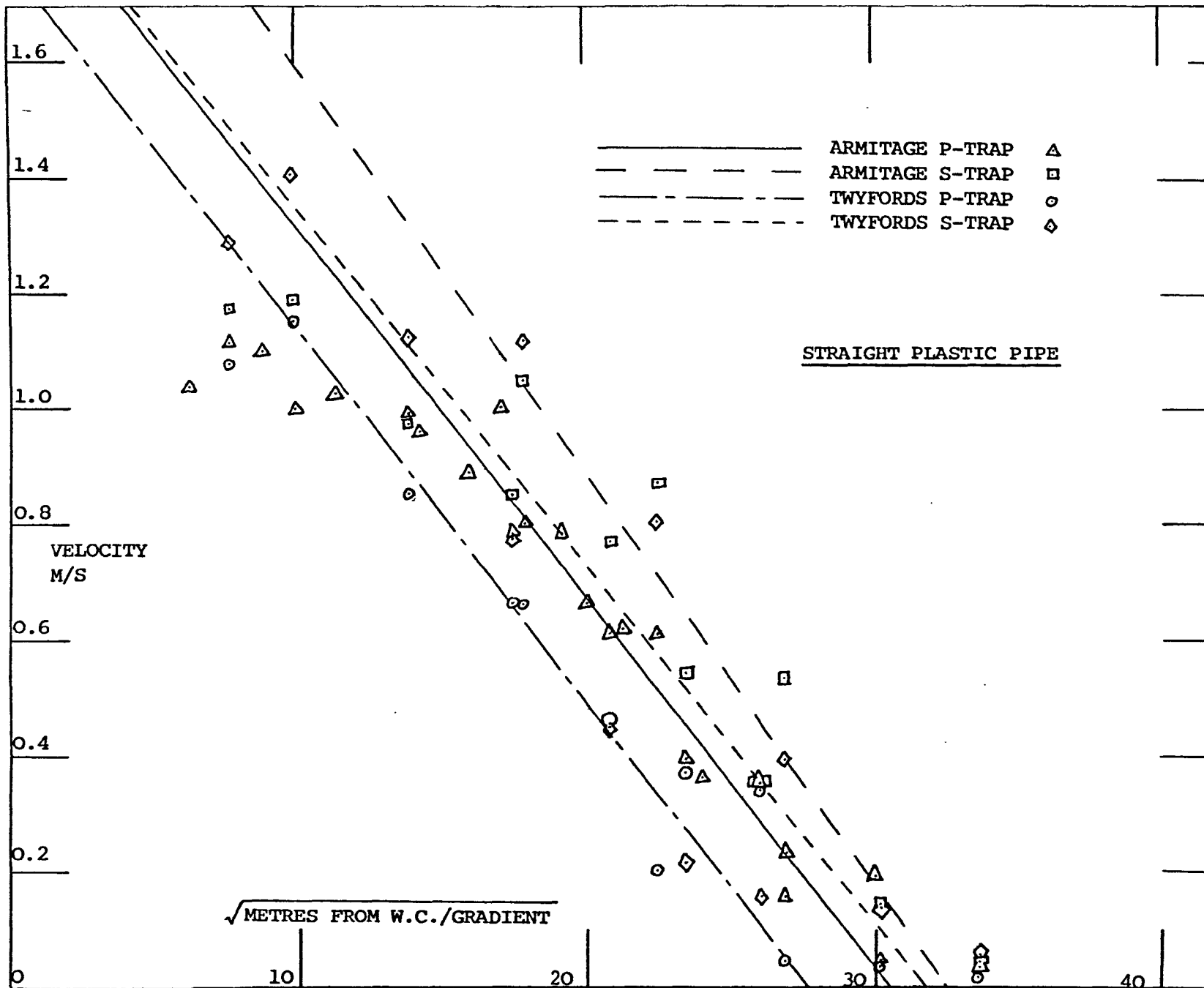


FIGURE 61. MATERNITY PAD + 3 BOWTOWELS, VENTED. VELOCITY PROFILES PLOTTED AGAINST SQUARE ROOT OF (DISTANCE ALONG PIPE/GRADIENT) FOR ARMITAGE SHANKS AND TWYFORDS, P-TRAP AND S-TRAP W.C.'s. STRAIGHT PLASTIC PIPE TESTS

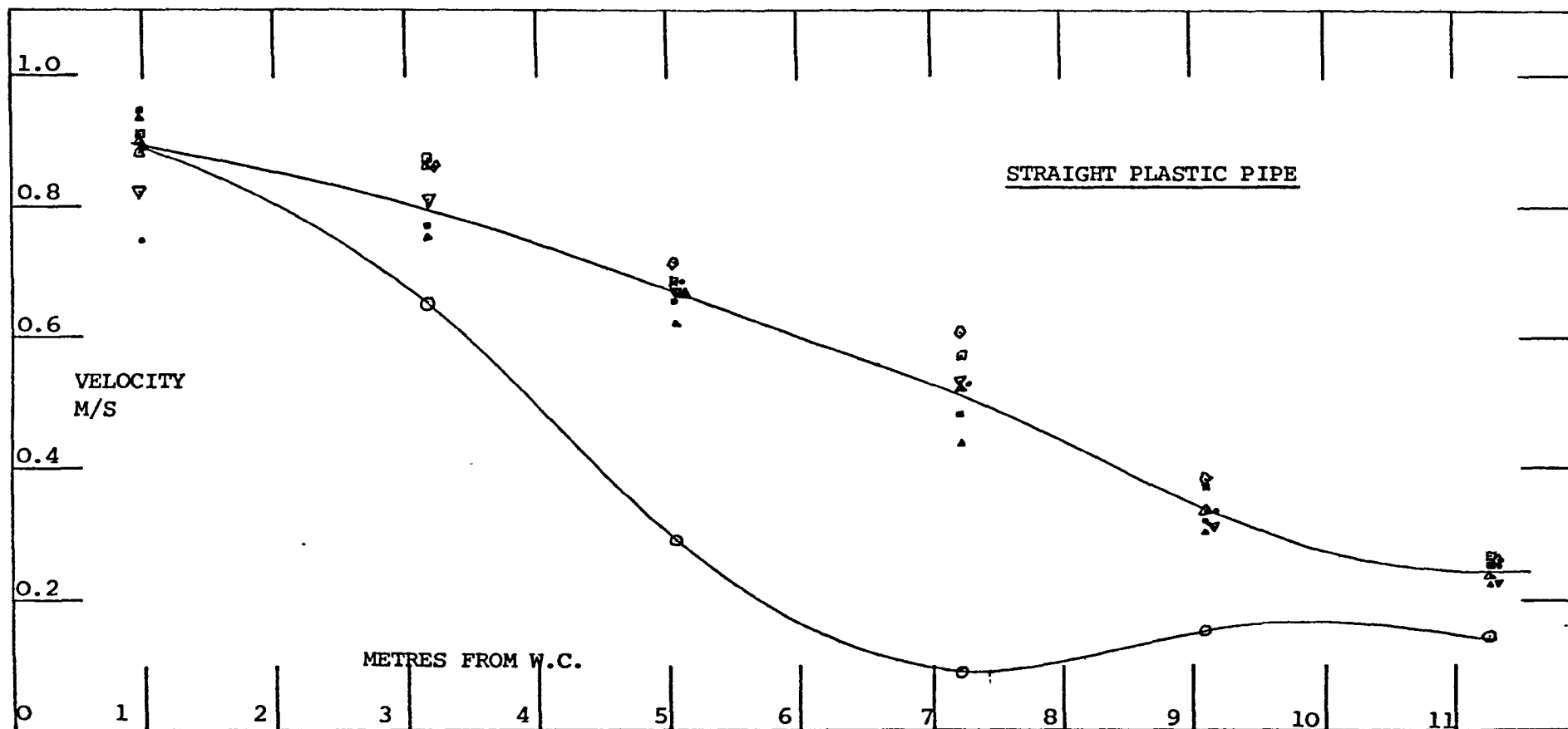


FIGURE 62. (APL1, 1/100) VELOCITY PROFILES FOR ARMITAGE SHANKS P-TRAP LOW LEVEL W.C., SINGLE MATERNITY PADS, SHOWING STACK VENTING EFFECT AT 1/100 PIPE GRADIENT. STRAIGHT PLASTIC PIPE

SYMBOL CODE

UPWARD STACK	DOWNWARD STACK	UNVENTED	VENTED
OPEN	OPEN	△	▲
CLOSED	OPEN	◻	■
CLOSED	CLOSED	○*	●**
OPEN	CLOSED	◇*	
OPEN	CLOSED	▽**	

\* = Downward Stack closed with 60mm water seal.  
 \*\* = Downward stack closed with 270mm water seal.

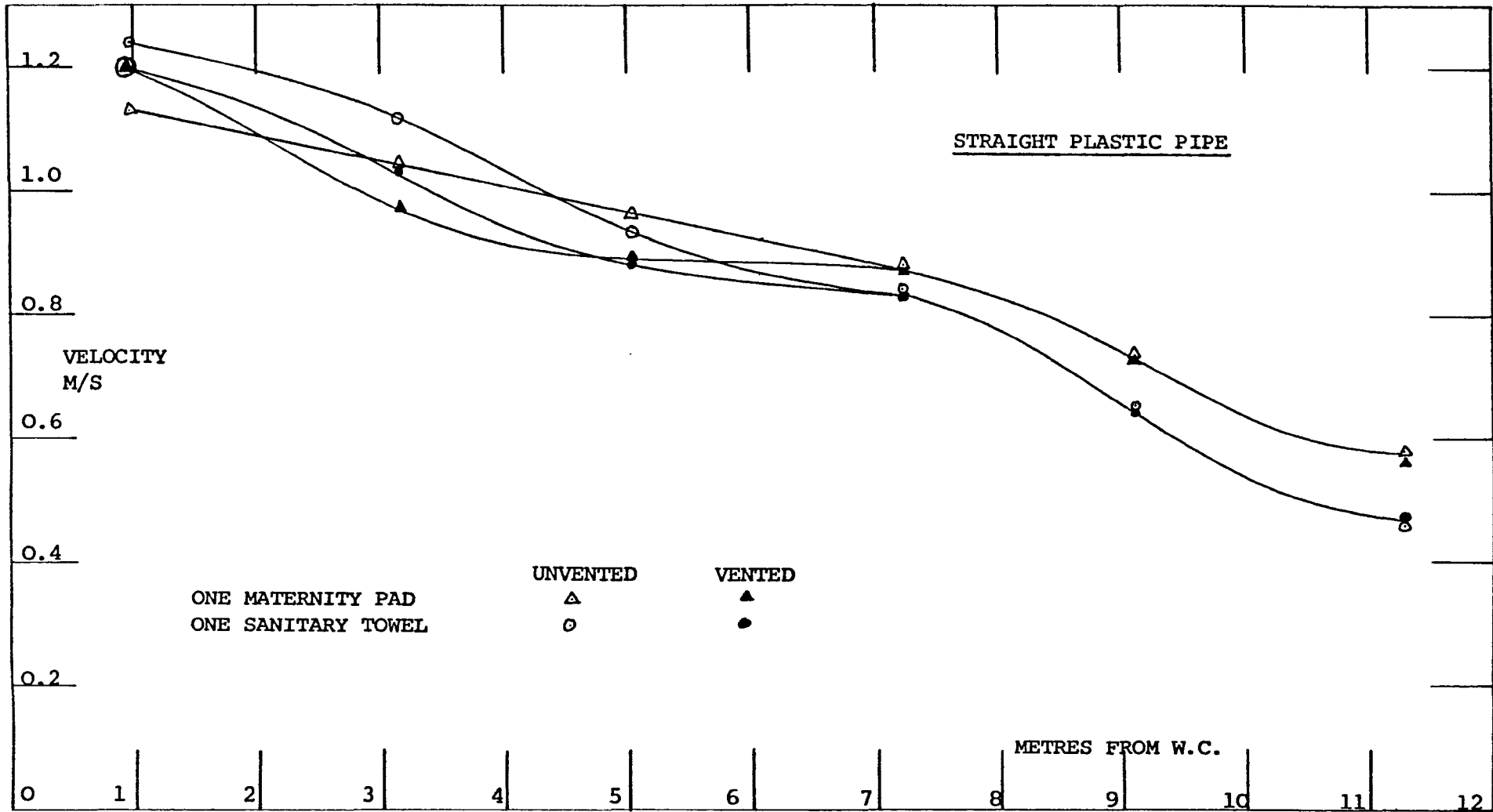
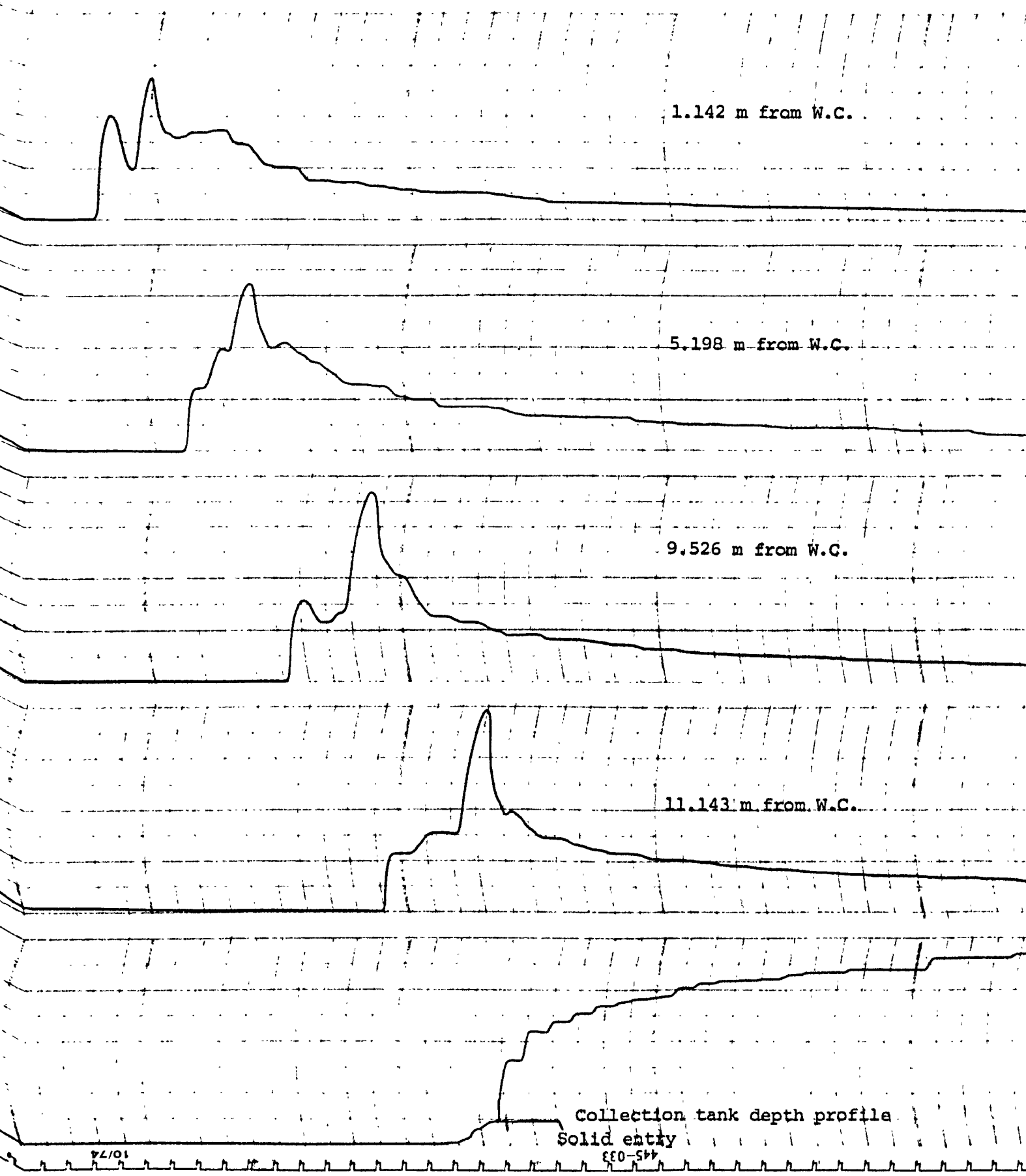


FIGURE 63. (ASL) VELOCITY PROFILES ALONG PIPE FOR ARMITAGE SHANKS S-TRAP LOW LEVEL W.C., PIPE GRADIENT 1/60, SHOWING VARIATION BETWEEN SINGLE MATERNITY PAD AND SINGLE SANITARY TOWEL FOR BOTH VENTED AND UNVENTED W.C. CONDITIONS. STRAIGHT PLASTIC PIPE



1 second timer

FIGURE 64. Pen recorder traces representing full scale depth of flow profiles along a straight plastic pipe for test (APLVI) at 1/40.

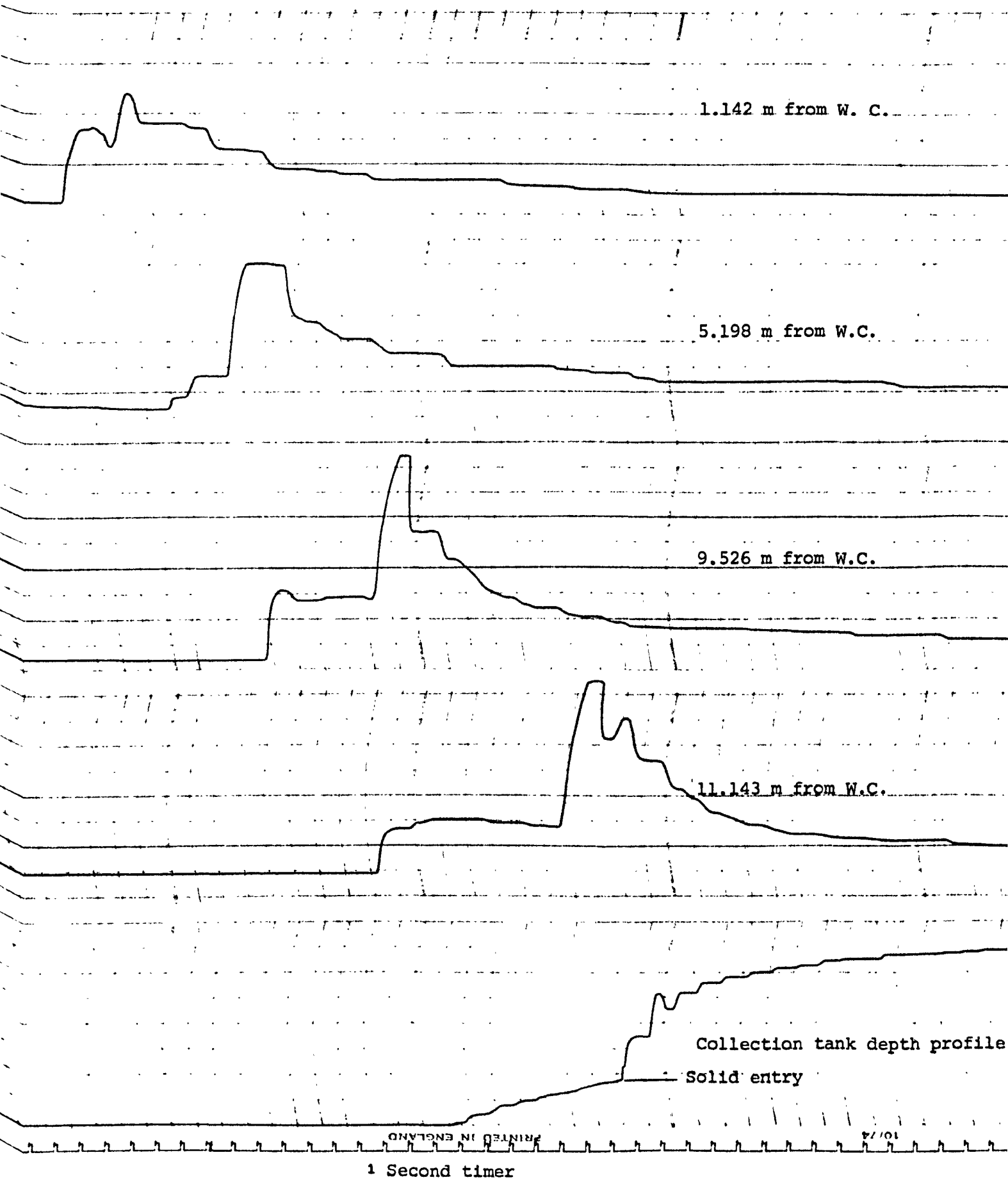


FIGURE 65. Pen recorder traces representing full scale depth of flow profiles along a straight plastic pipe for test (APLVI) at 1/60.

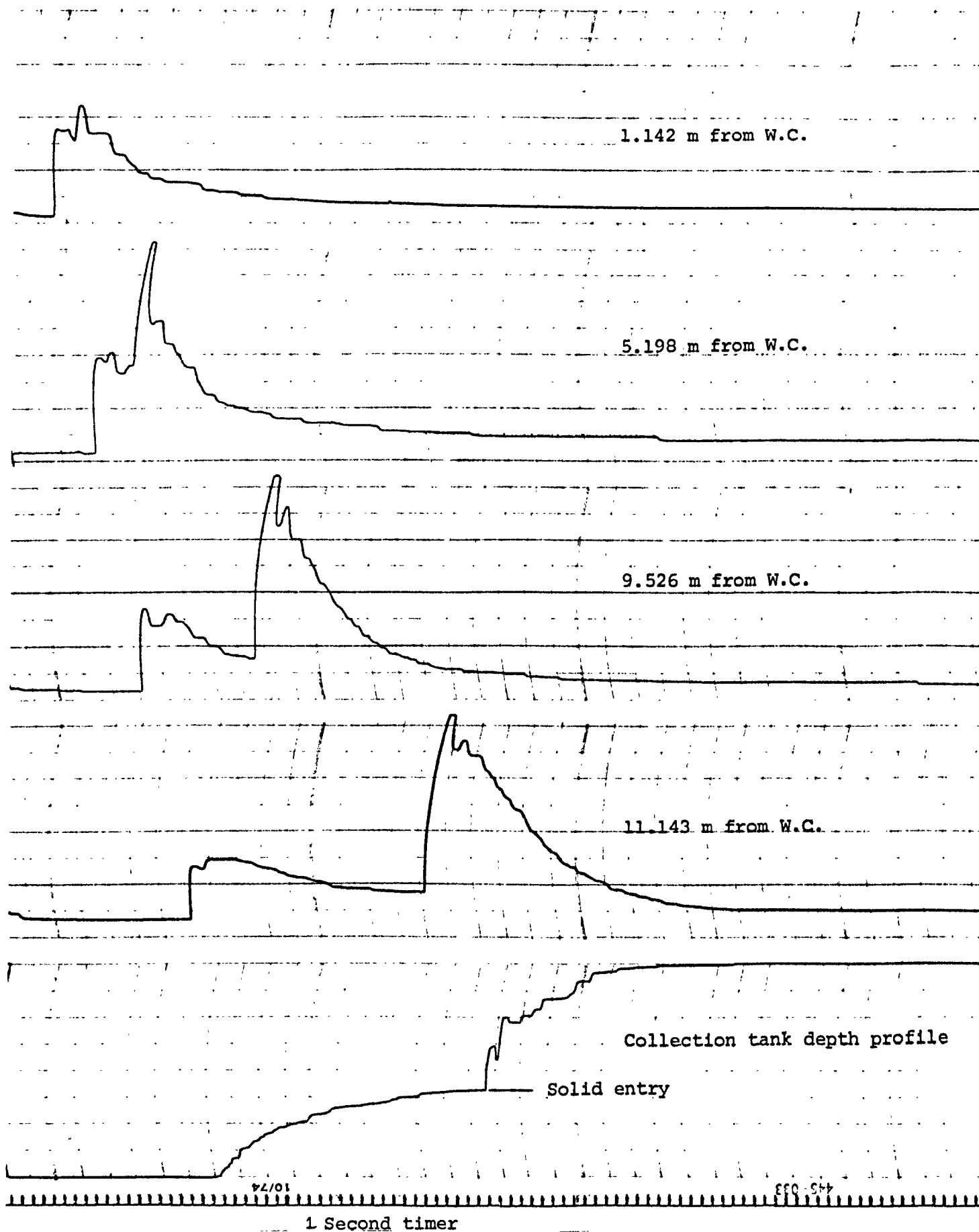


FIGURE 66. Pen recorder traces representing full scale depth of flow profiles along a straight plastic pipe for test (APLVI) at 1/80.

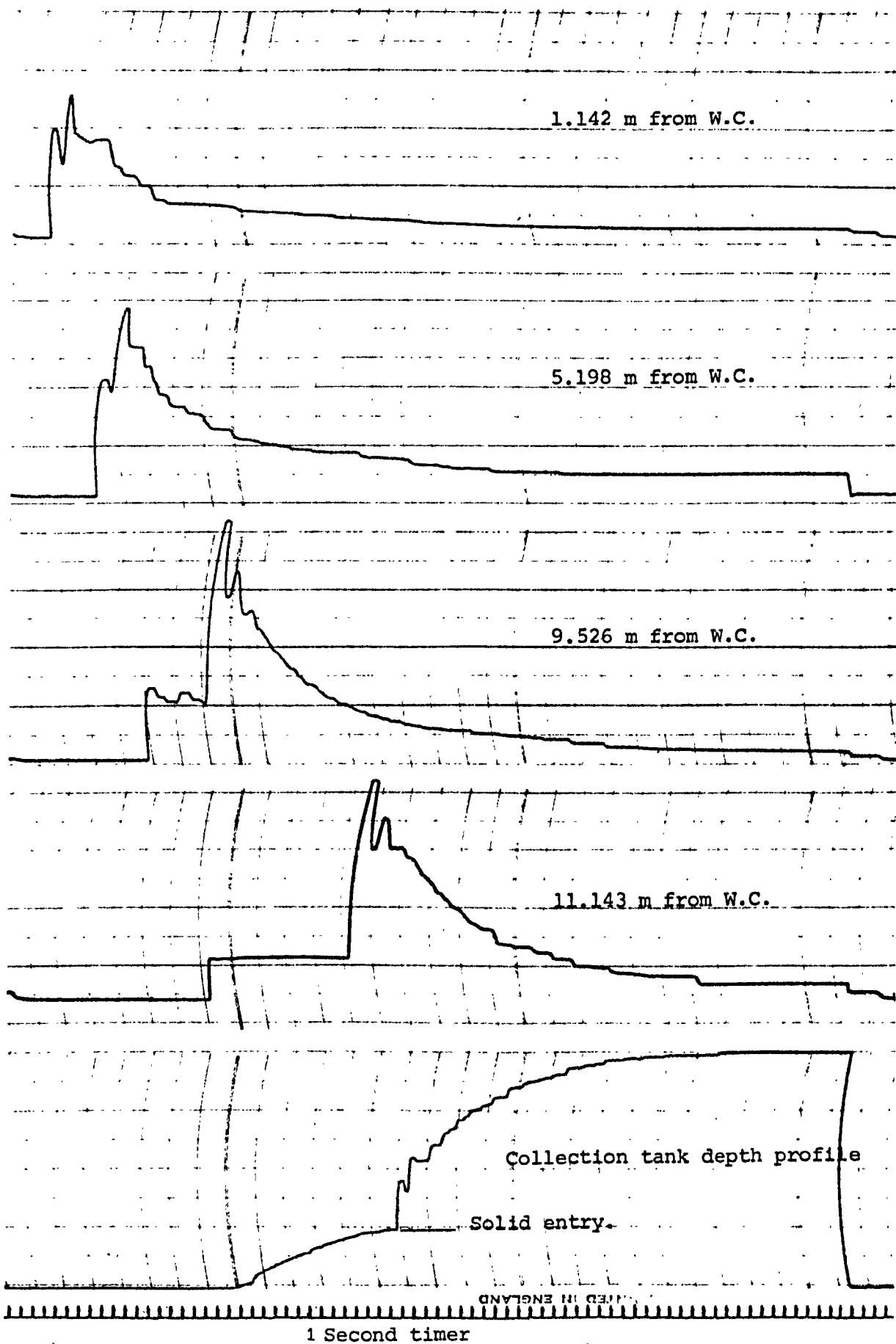


FIGURE 67. Pen recorder traces representing full scale depth of flow profiles along a straight plastic pipe for test (APLVI) at 1/100.

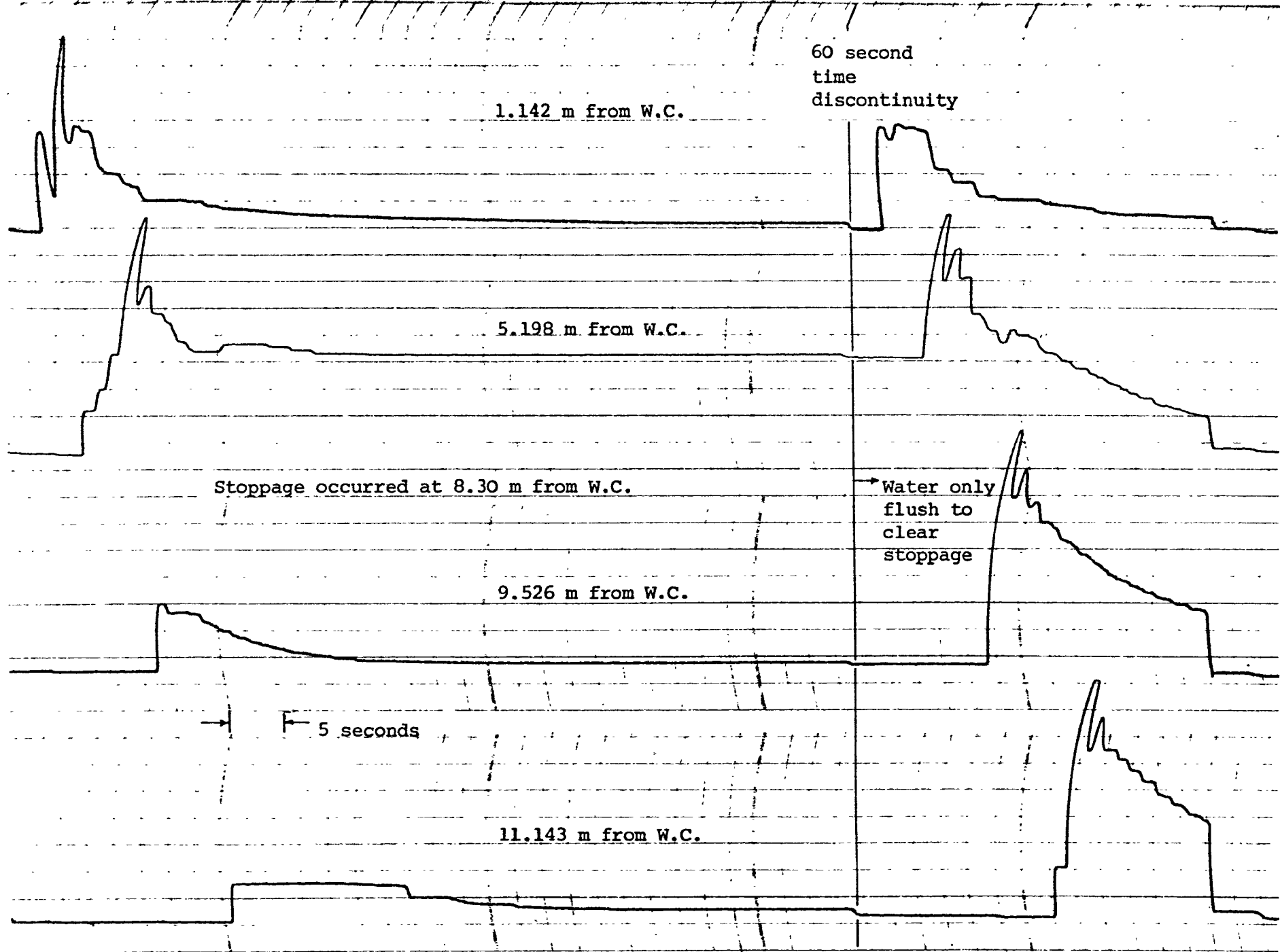


FIGURE 68. Pen recorder traces representing full scale depth of flow profiles along a straight plastic pipe for test (APLVI) at 1/150

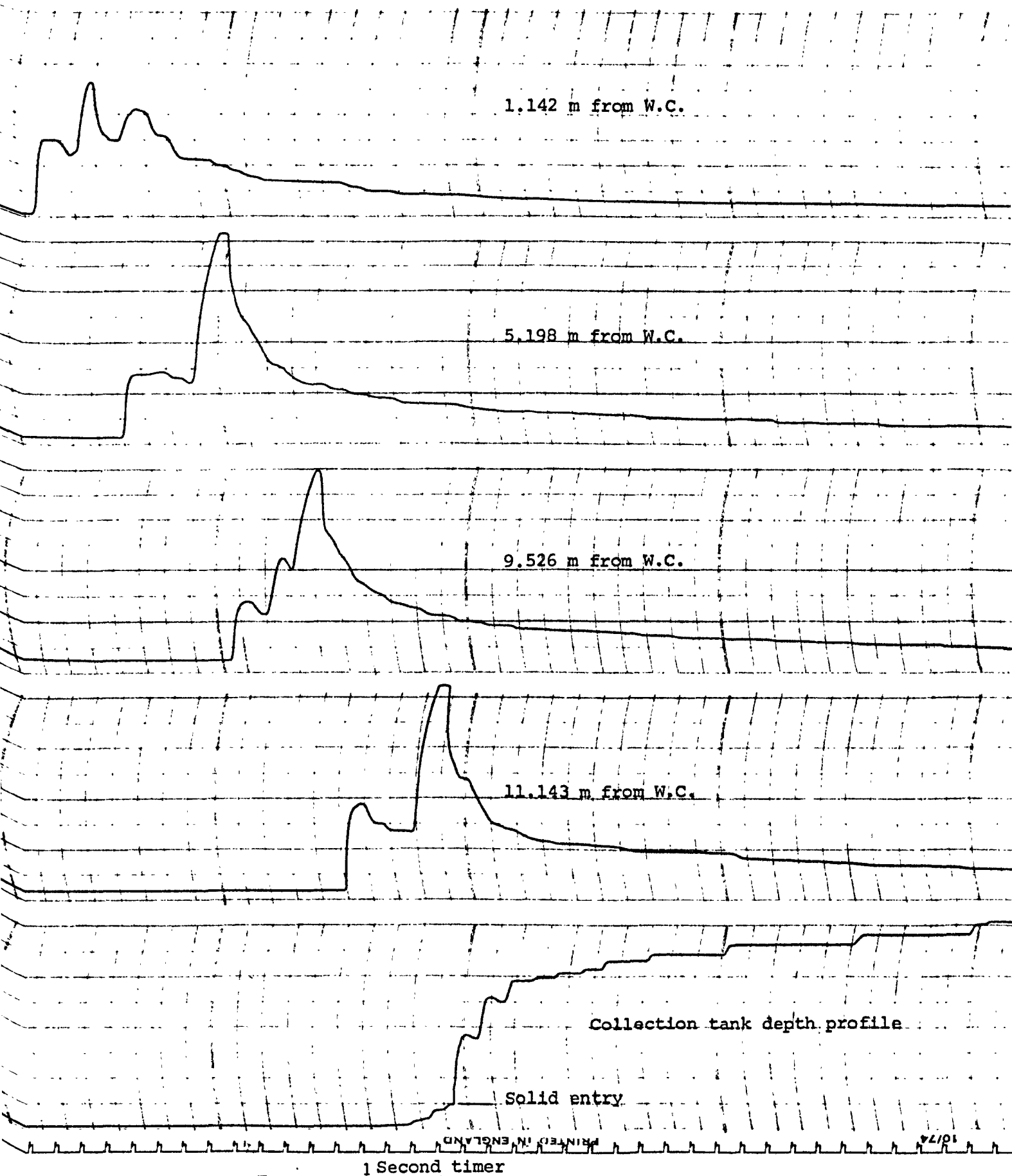


FIGURE 69. Pen recorder traces representing full scale depth of flow profiles along a straight plastic pipe for test (APLU3) at 1/40. Note: solids travelled together.

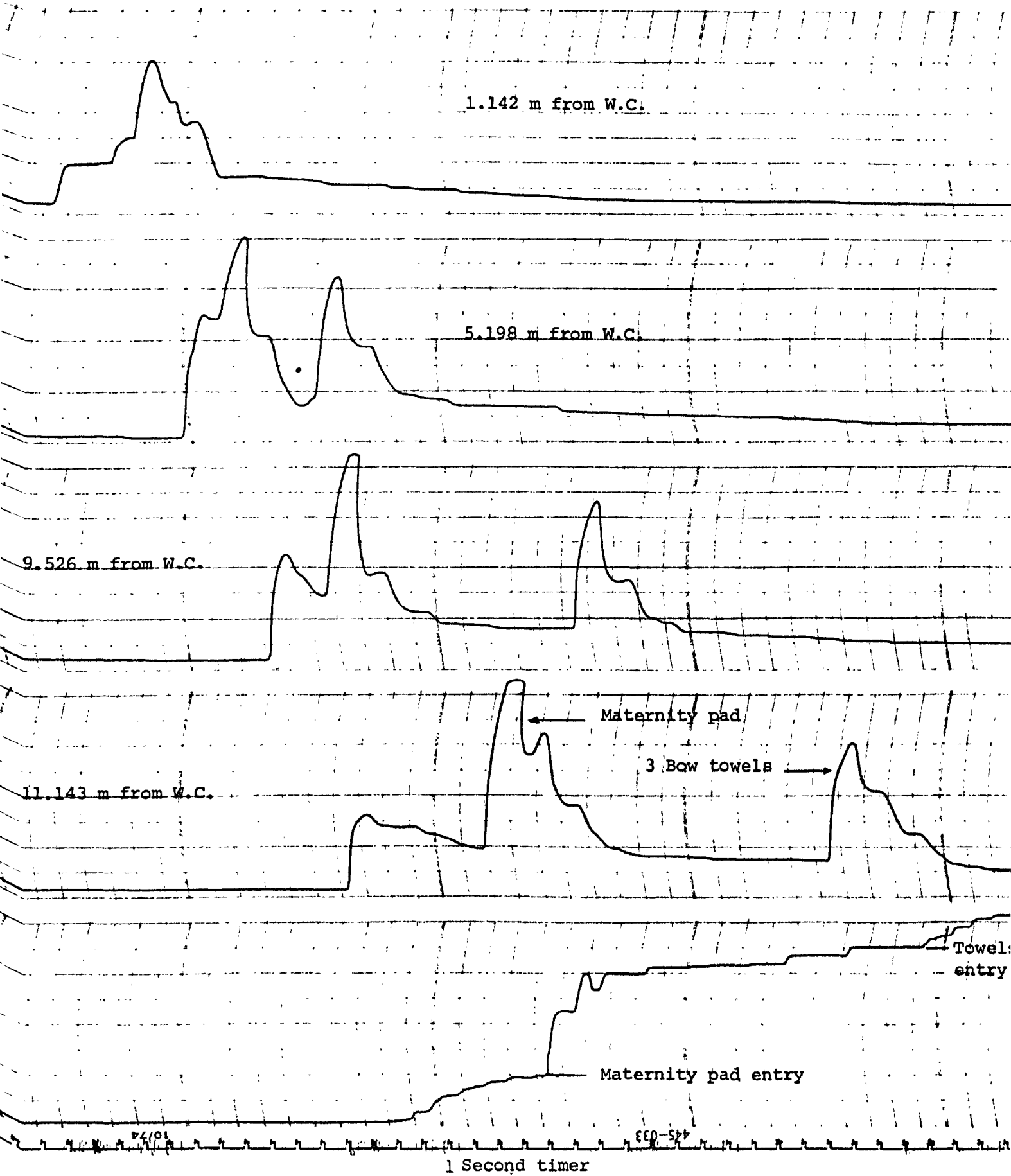


FIGURE 70. Pen recorder traces representing full scale depth of flow profiles along a straight plastic pipe for test (APLU3) at 1/40. Note: maternity pad travelled separately from the three Bowater Scott paper towels.

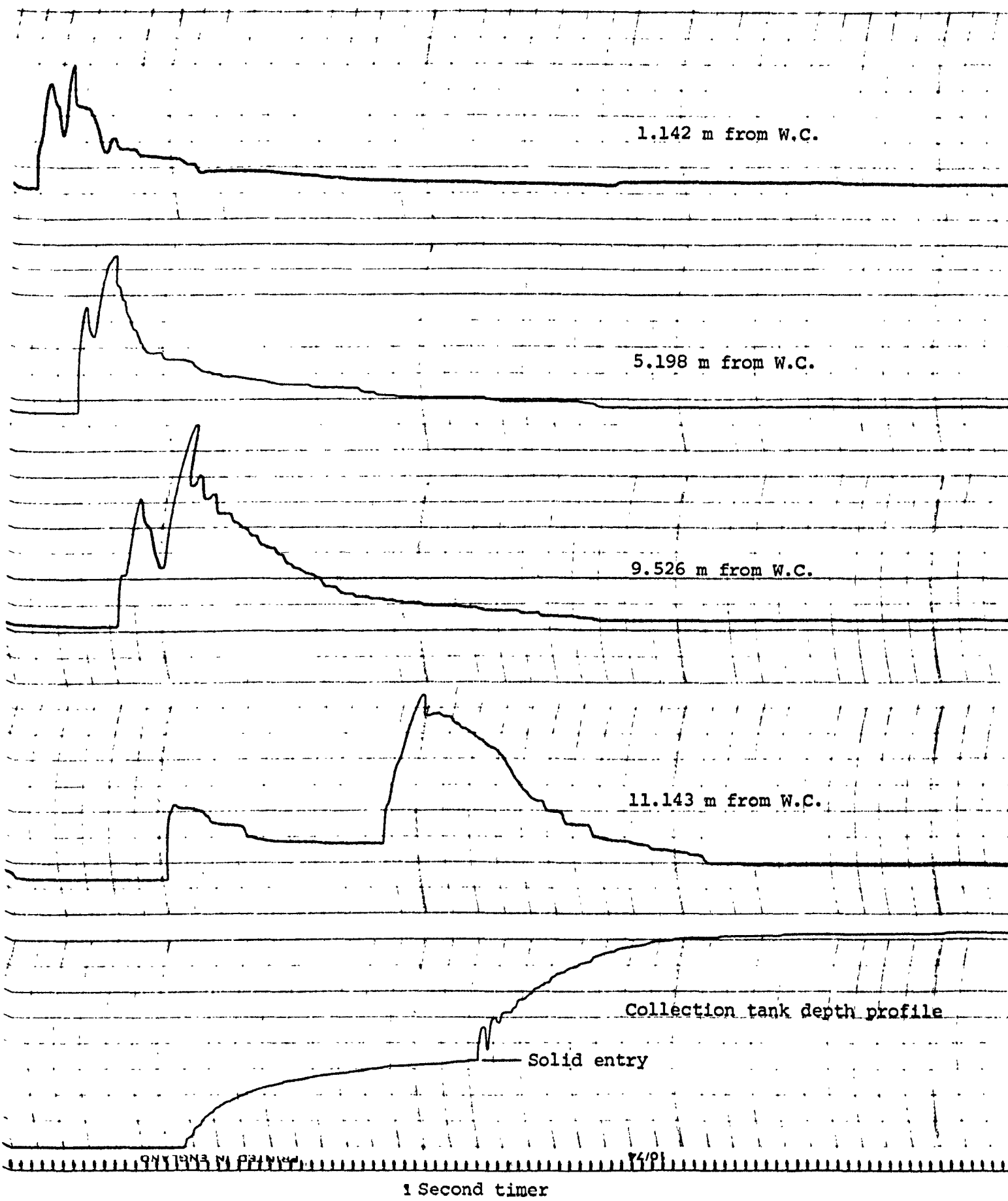


FIGURE 71. Pen recorder traces representing full scale depth of flow profiles along a straight plastic pipe for test (ASLVI) at 1/100

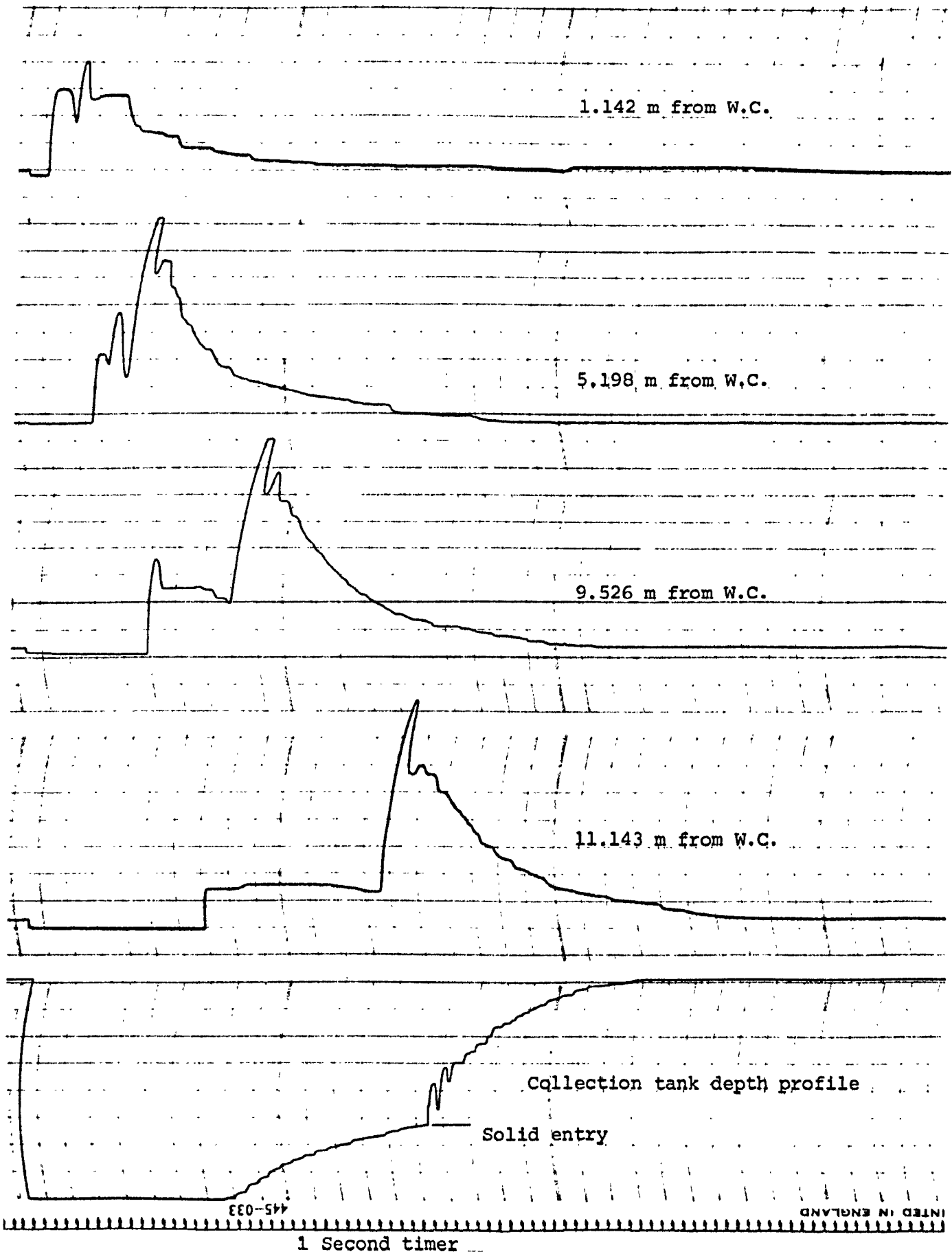


FIGURE 72. Pen recorder traces representing full scale depth of flow profiles along a straight plastic pipe for test (TPLVI) at 1/100.

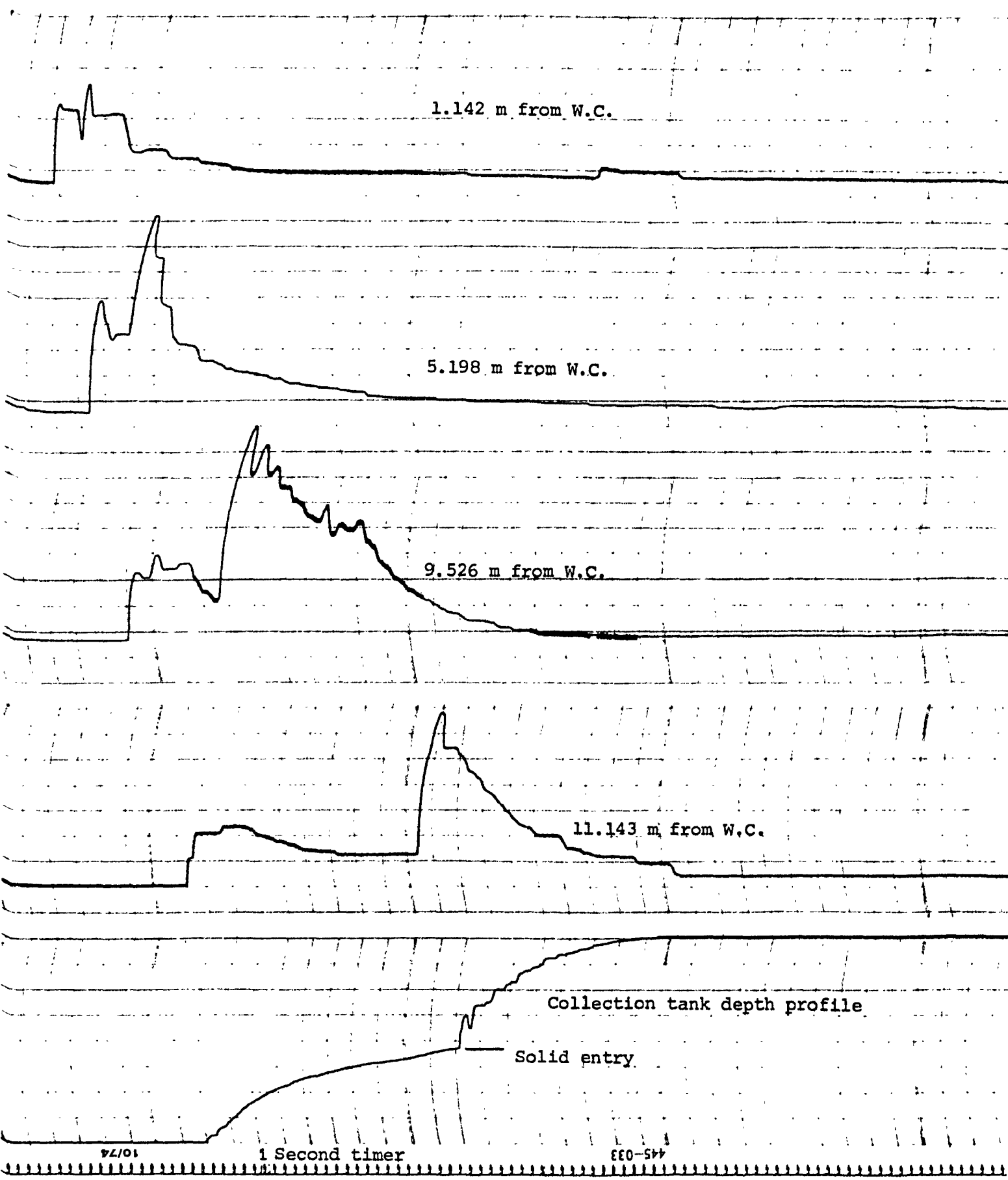


FIGURE 73. Pen recorder traces representing full scale depth of flow profiles along a straight plastic pipe for test (TSLVI) at 1/100.

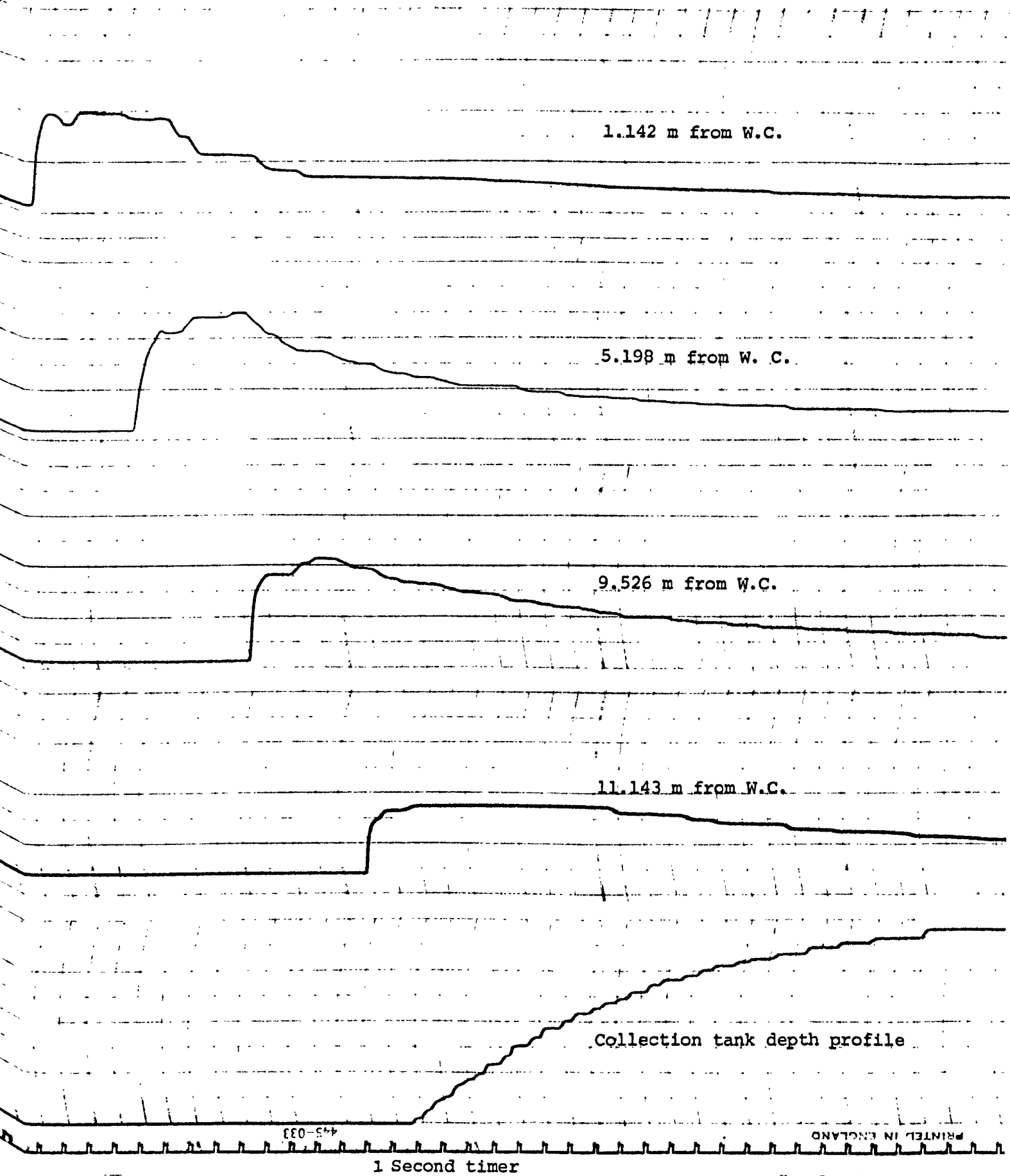


FIGURE 74. Pen recorder traces representing full scale depth of flow profiles along a straight plastic pipe for a water only flush from (APLV) at 1/100.

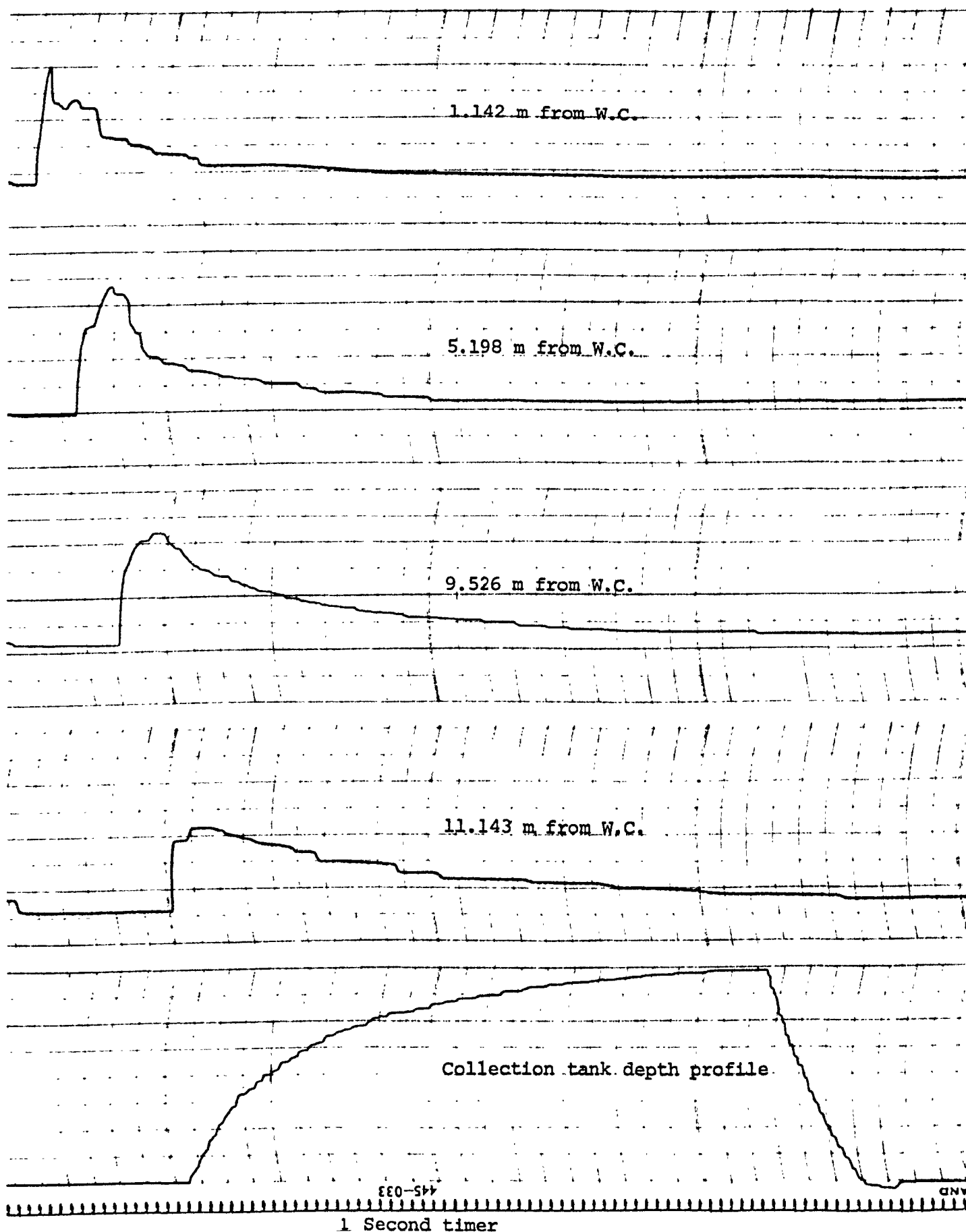


FIGURE 75. Pen recorder traces representing full scale depth of flow profiles along a straight plastic pipe for a water only flush (ASLV) at 1/100.

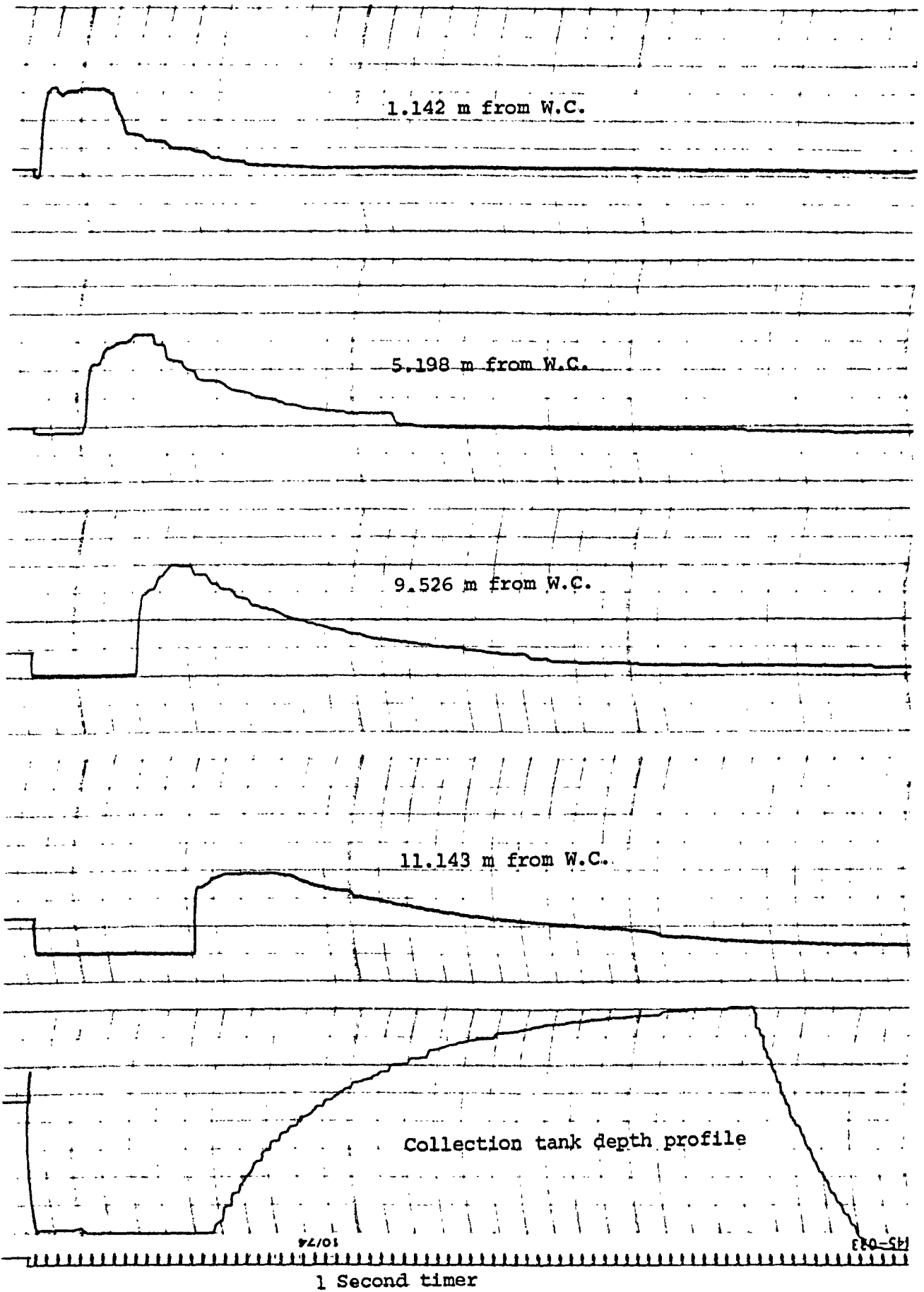


FIGURE 76. Pen recorder traces representing full scale depth of flow profiles along a straight plastic pipe for a water only flush from (TPLV) at 1/10

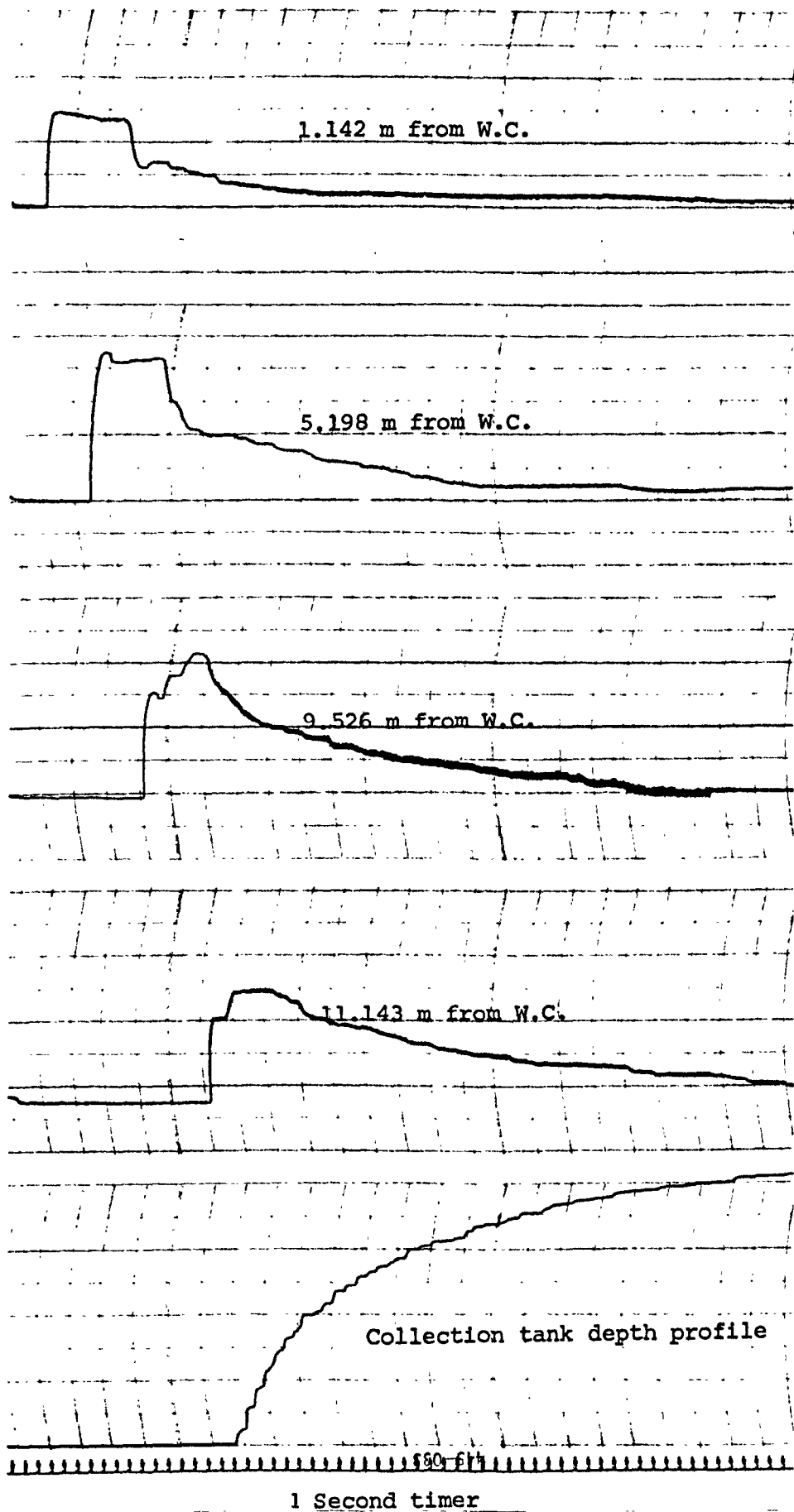


FIGURE 77. Pen recorder traces representing full scale depth of flow profiles along a straight plastic pipe for a water only flush from (TSLV) at 1/100.

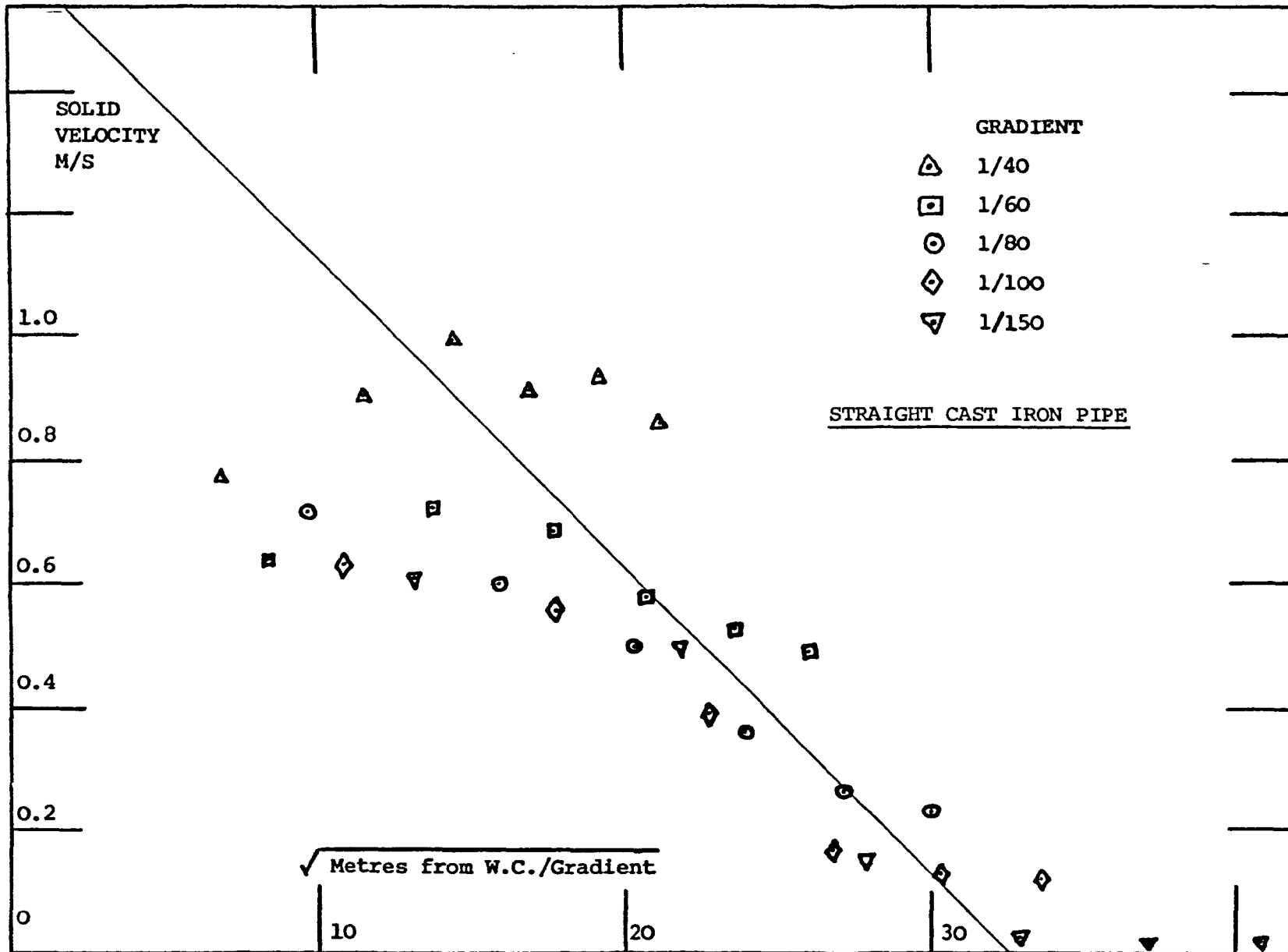


FIGURE 78.

SINGLE MATERNITY PAD, UNVENTED ARMITAGE SHANKS P-TRAP W.C. VELOCITY PROFILES PLOTTED AGAINST SQUARE ROOT OF (DISTANCE ALONG PIPE/GRADIENT). STRAIGHT CAST IRON PIPE.

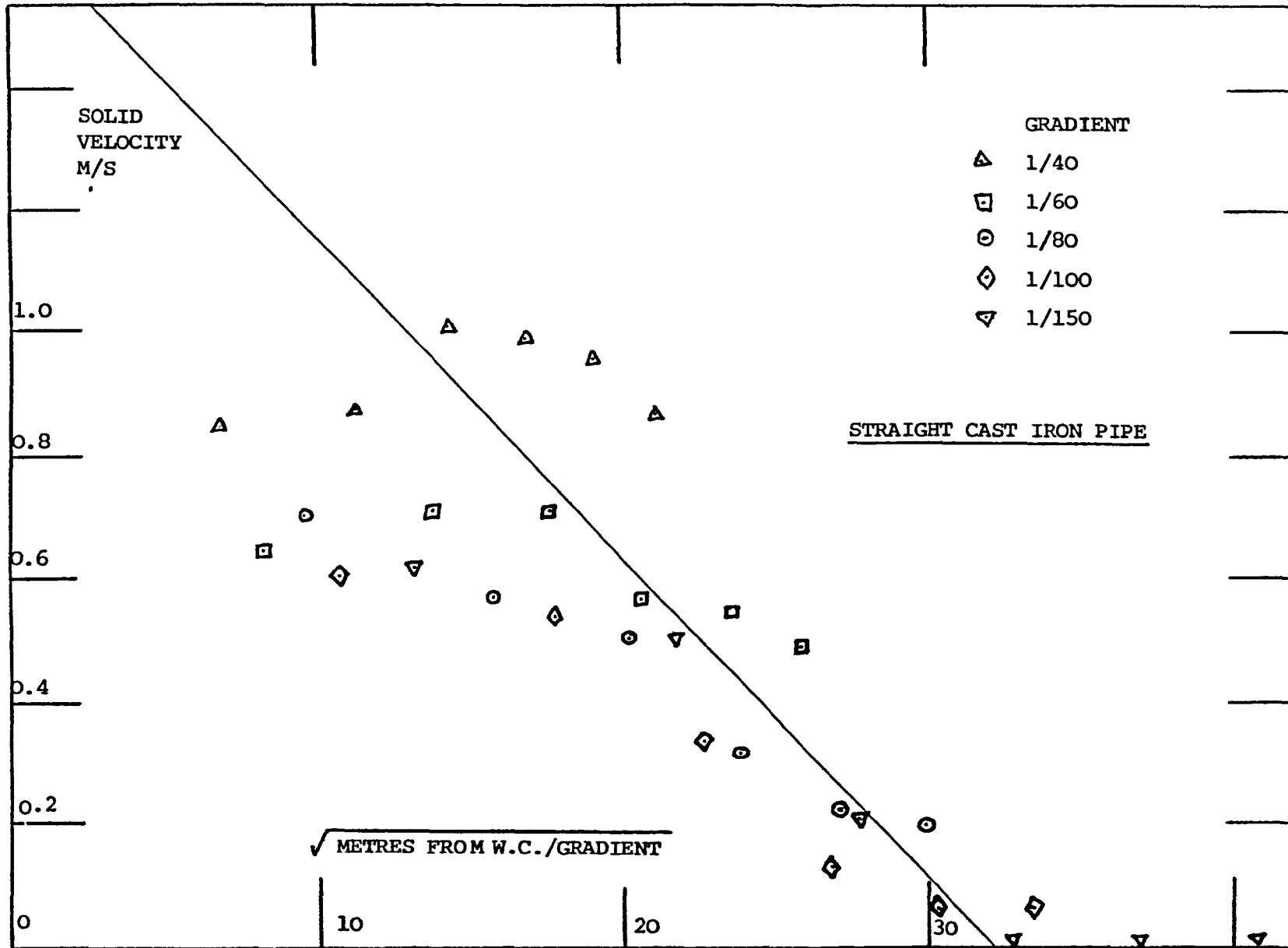


FIGURE 79. SINGLE MATERNITY PAD, VENTED ARMITAGE SHANKS P-TRAP W.C. VELOCITY PROFILES PLOTTED AGAINST SQUARE ROOT OF (DISTANCE ALONG PIPE/GRADIENT). STRAIGHT CAST IRON PIPE.

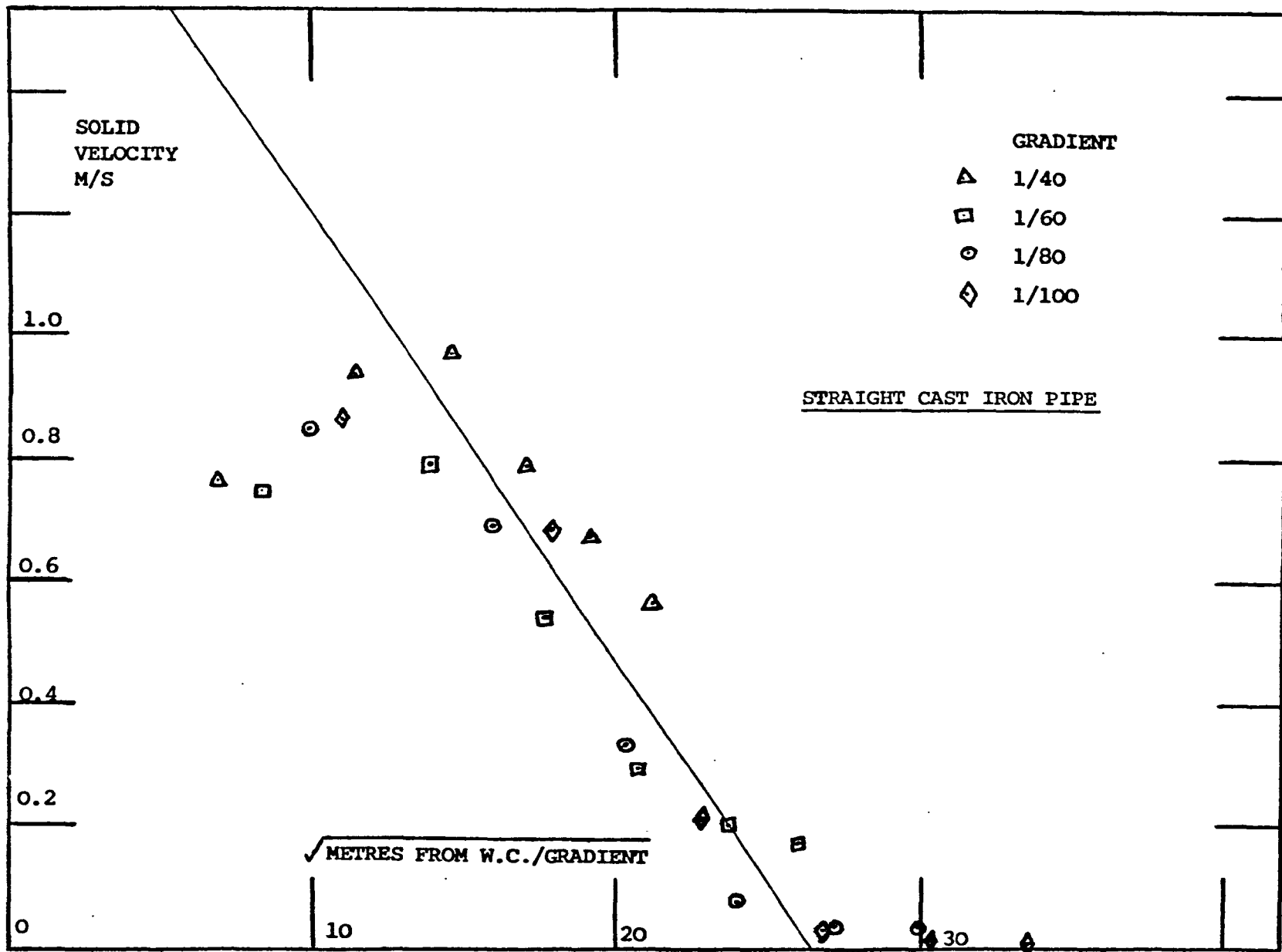


FIGURE 80. SINGLE MATERNITY PAD + 3 KLEENEX TOWELS, UNVENTED, ARMITAGE SHANKS P-TRAP W.C. VELOCITY PROFILES PLOTTED AGAINST SQUARE ROOT OF (DISTANCE ALONG PIPE/GRADIENT) STRAIGHT CAST IRON PIPE

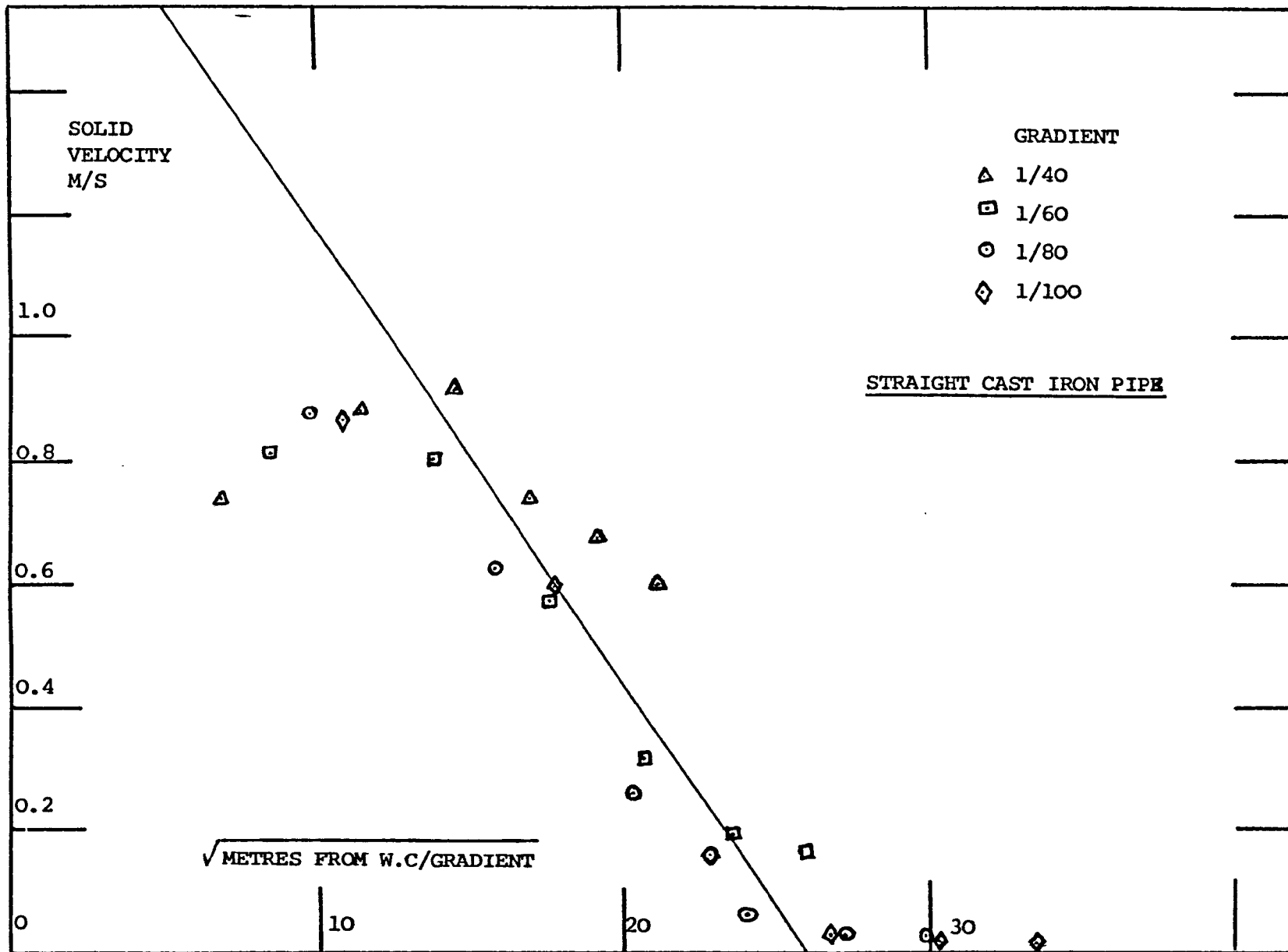


FIGURE 81. SINGLE MATERNITY PAD + 3 KLEENEX TOWELS, VENTED ARMITAGE SHANKS P-TRAP W.C. VELOCITY PROFILES PLOTTED AGAINST SQUARE ROOT OF (DISTANCE ALONG PIPE/GRADIENT) STRAIGHT CAST IRON PIPE.

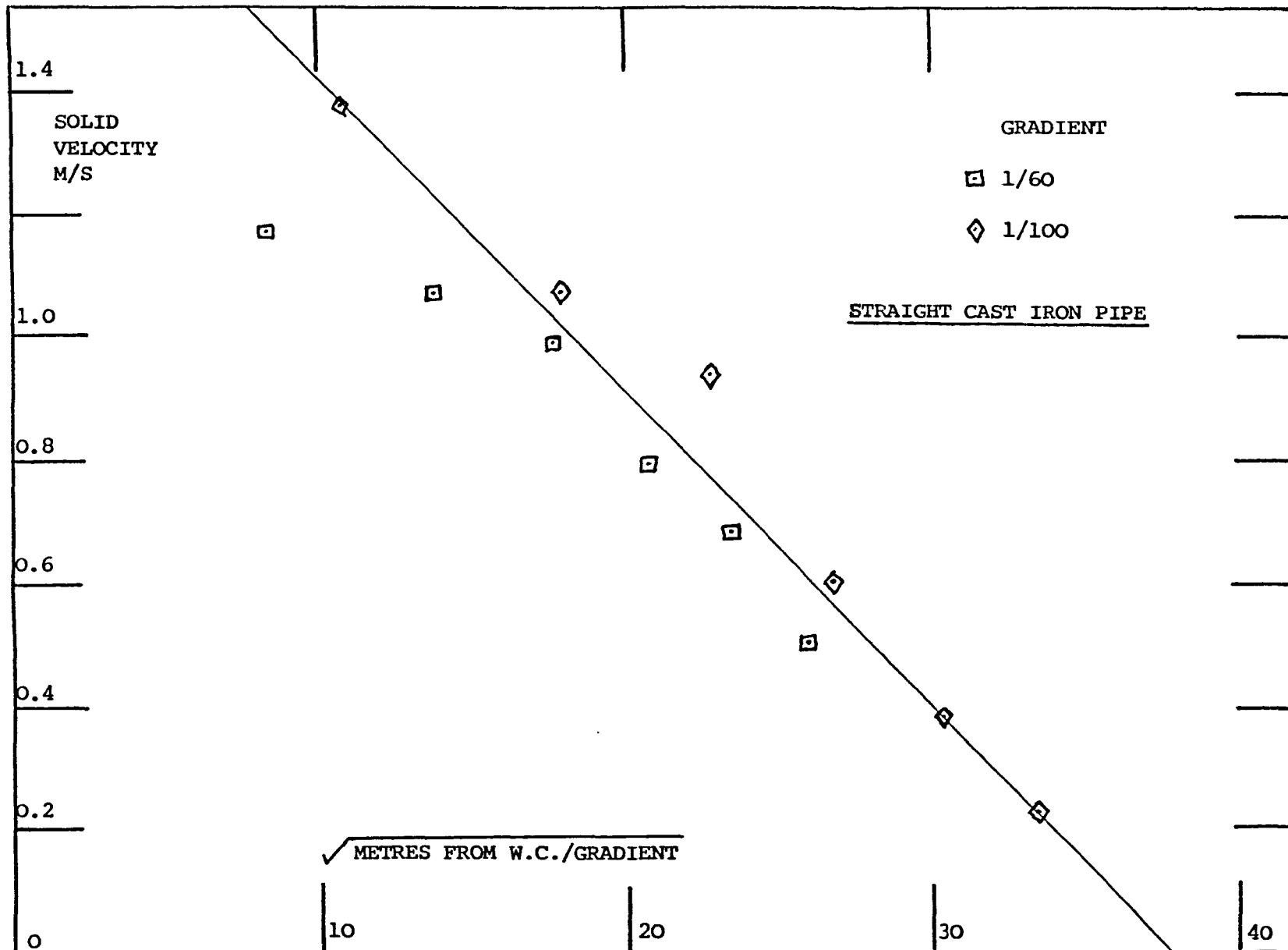


FIGURE 82. SINGLE MATERNITY PAD, UNVENTED, TWYFORDS S-TRAP W.C. VELOCITY PROFILES PLOTTED AGAINST SQUARE ROOT OF (DISTANCE ALONG PIPE/GRADIENT). STRAIGHT CAST IRON PIPE.

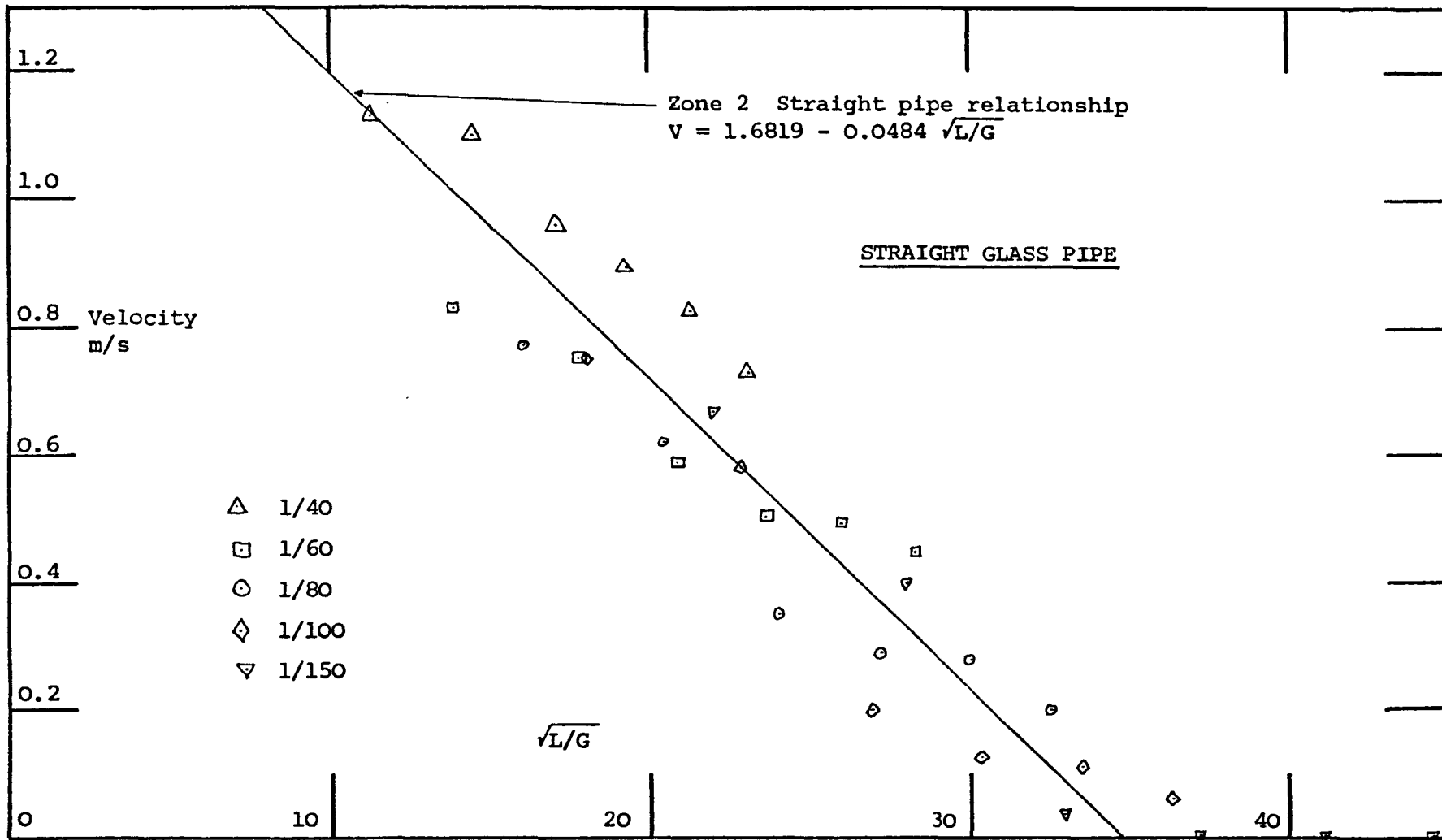


FIGURE 83. (APLVI) Armitage shanks P-trap low level W.C., single maternity pad, vented. Straight glass pipe.  
Velocity profiles plotted against square root of (Distance along pipe/gradient)

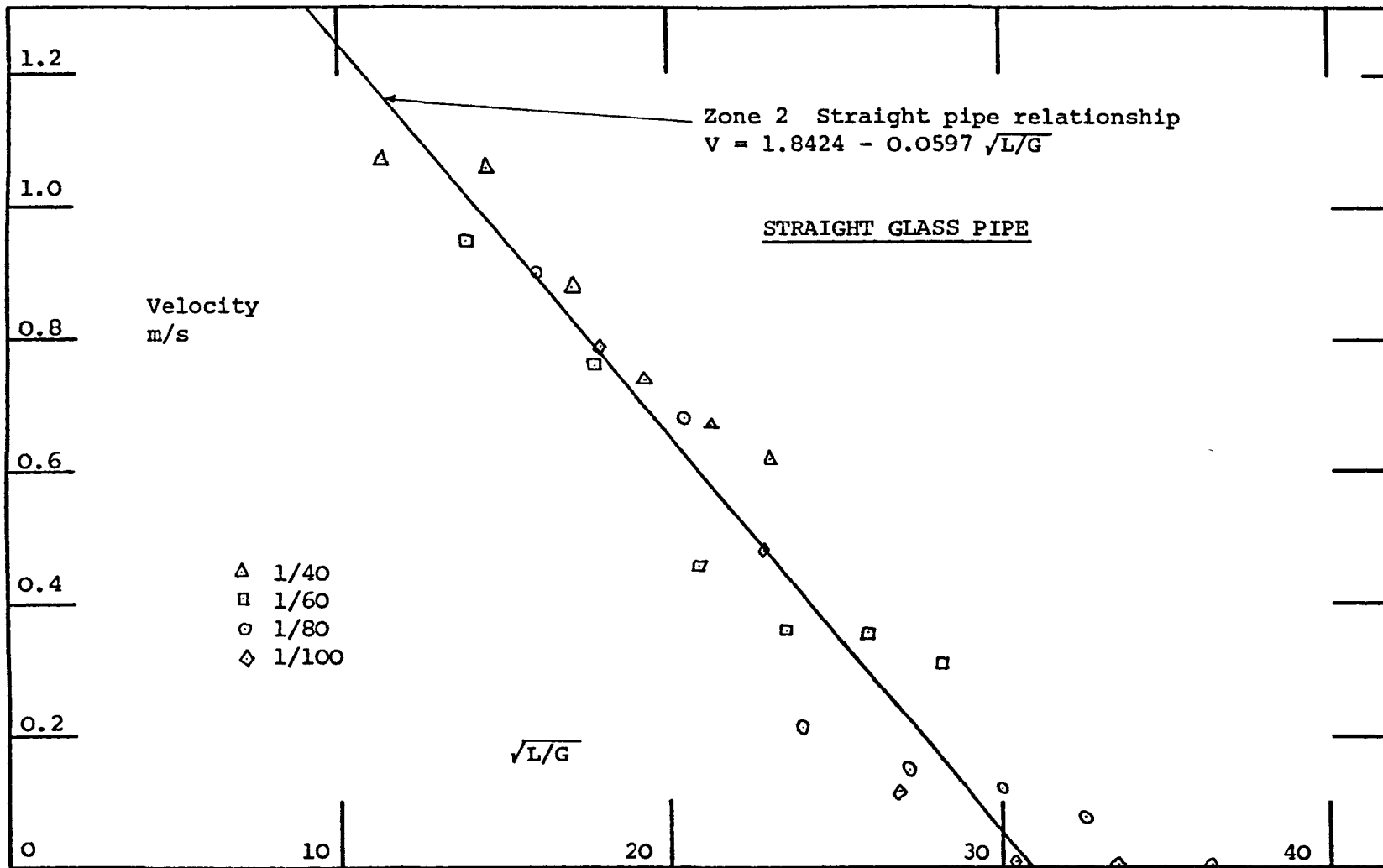


FIGURE 84. (APLV2) Armitage shanks P-trap low level W.C. single maternity pad plus three Kleenex paper towels, vented. Straight glass pipe. Velocity profiles plotted against square root of (Distance along pipe/Gradient).



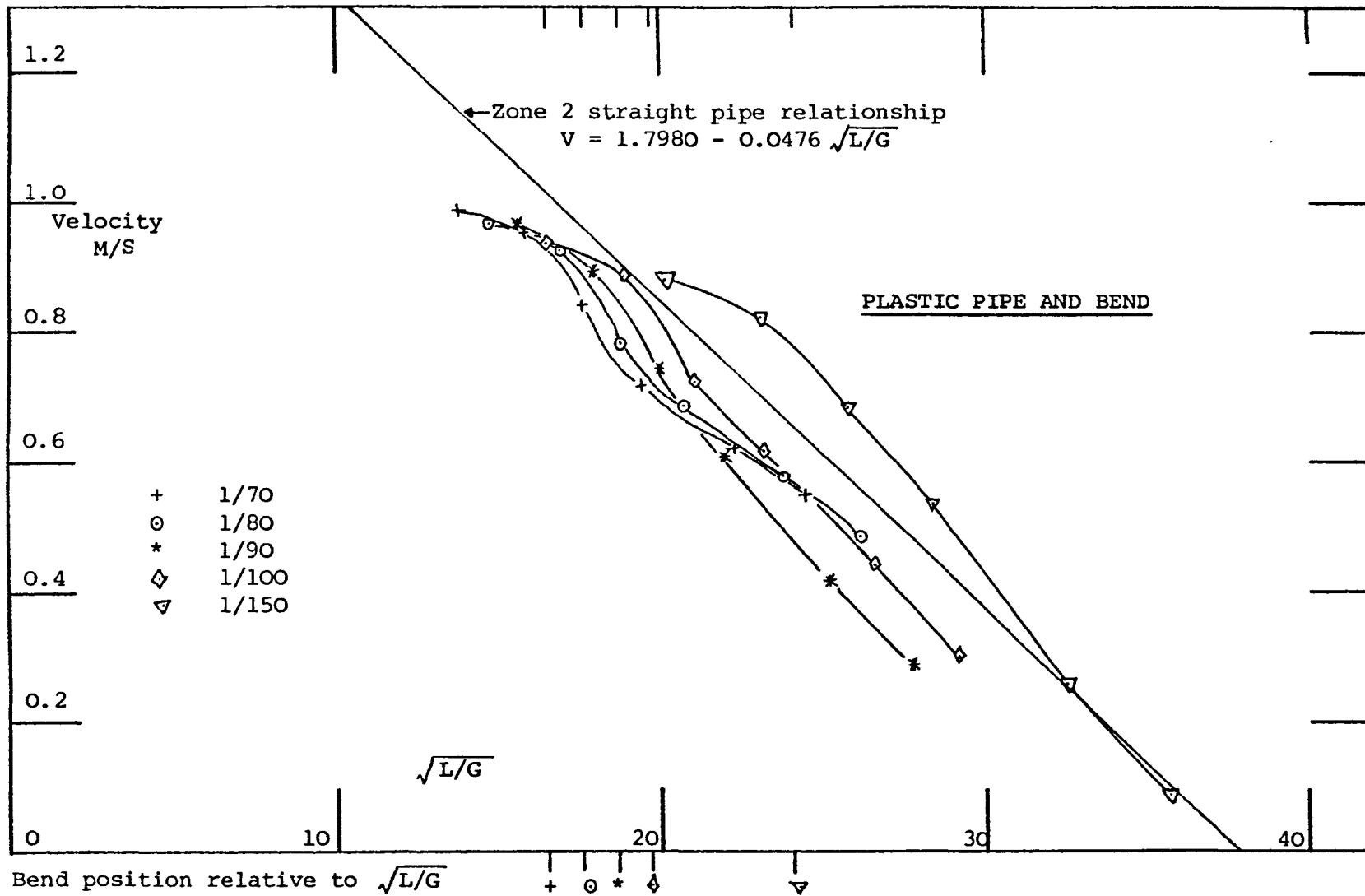


FIGURE 86. (APLU1) 135° Bend at 3.88 metres from w.c. Armitage Shanks P-trap low level w.c., single maternity pad, unvented. Velocity profiles plotted against square root of (Distance along pipe/Gradient) showing variation due to a bend compared to Zone 2 straight pipe relationship.

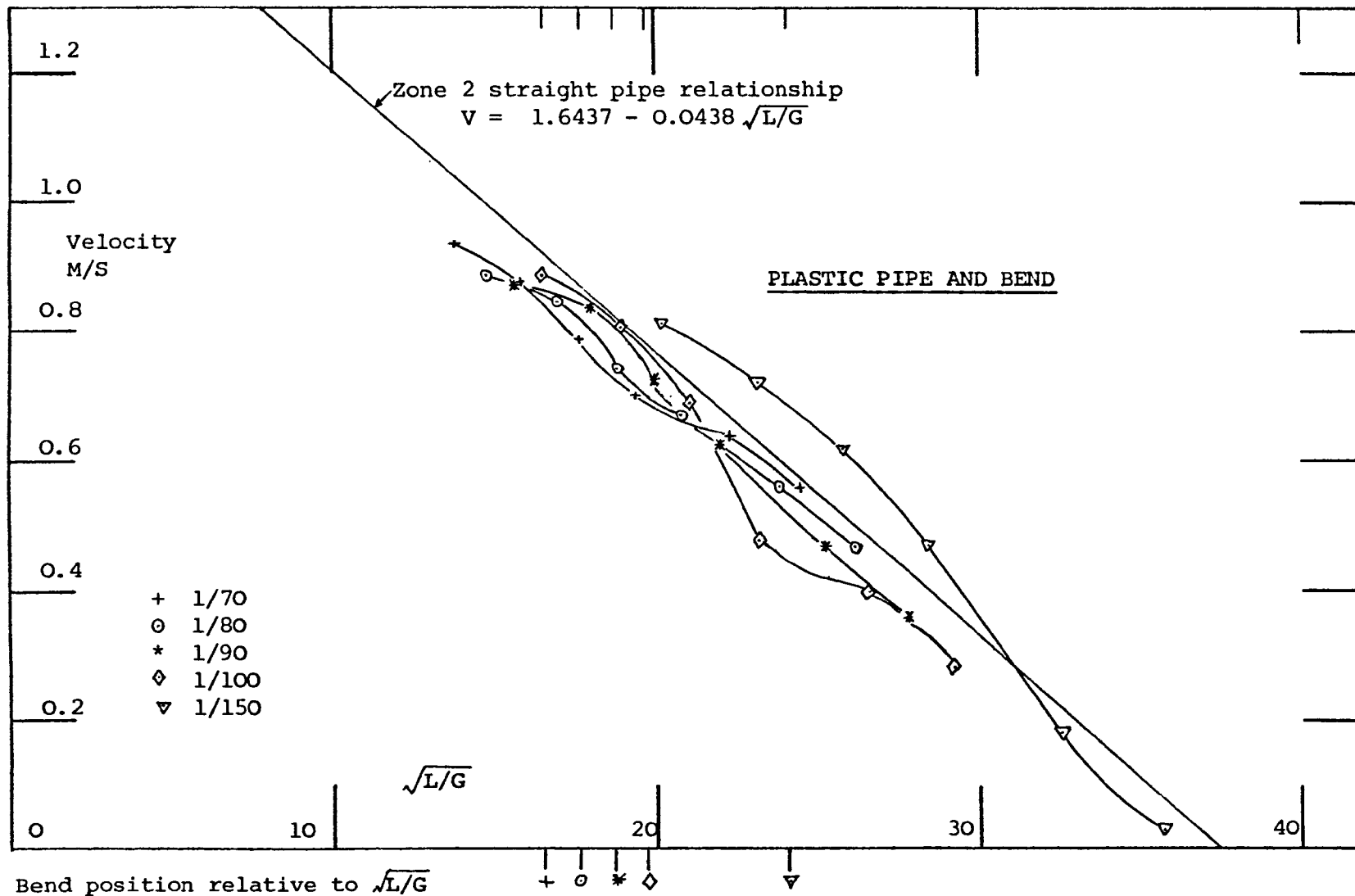


FIGURE 87. (APLV1) 135° Bend at 3.88 metres from w.c.  
 Armitage Shanks P-trap low level w.c., single maternity pad, vented.  
 Velocity profiles plotted against square root of (Distance along pipe/Gradient)  
 showing variation due to a bend compared to Zone 2 straight pipe relationship.

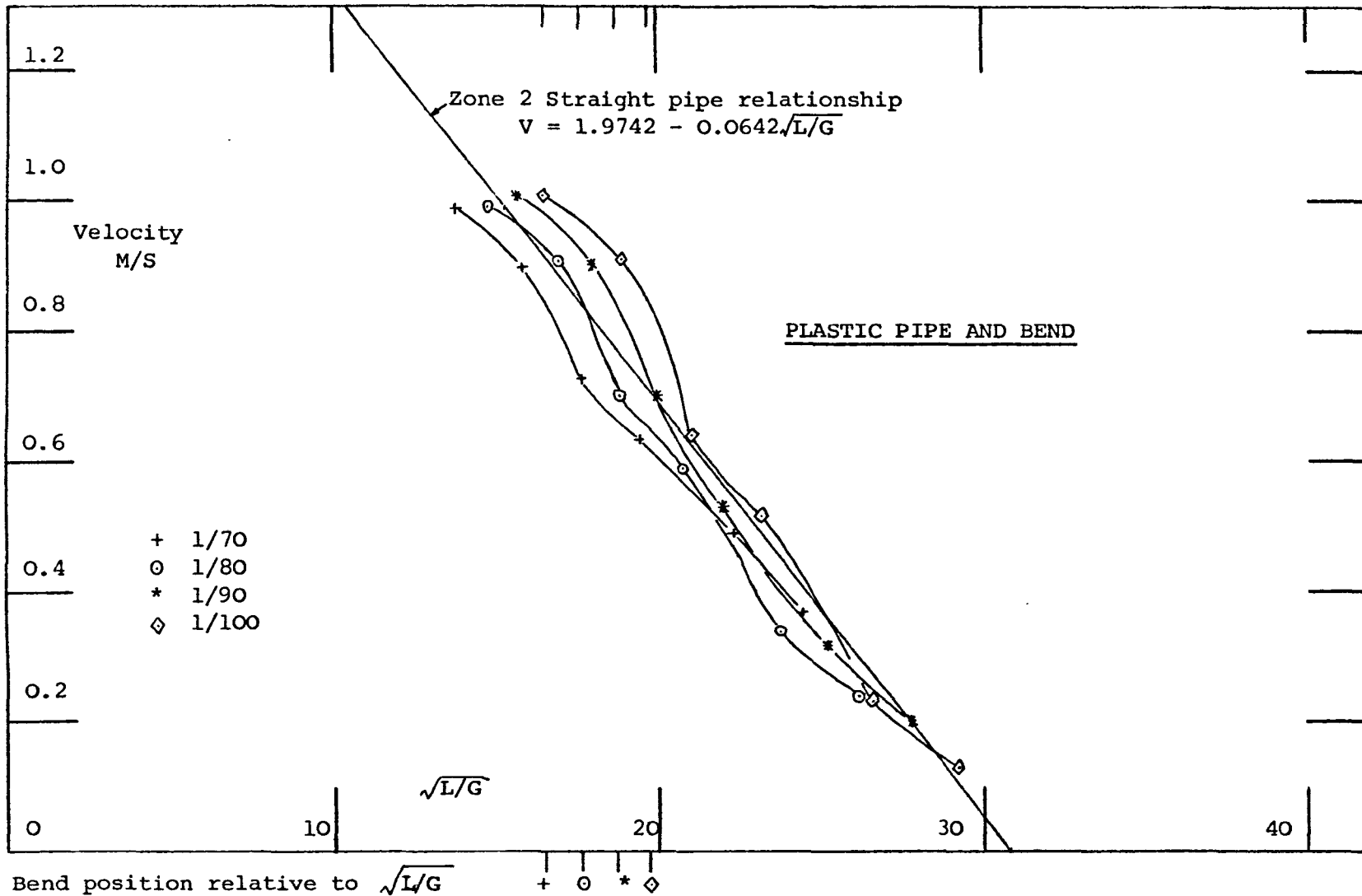


FIGURE 88. (APLV2) 135° Bend at 3.88 metres from w.c.  
 Armitage Shanks P-trap low level w.c., maternity pad plus three Kleenex paper towels, vented.  
 Velocity profiles plotted against square root of (Distance along pipe/Gradient)  
 showing variation due to a bend compared to Zone 2 straight pipe relationship

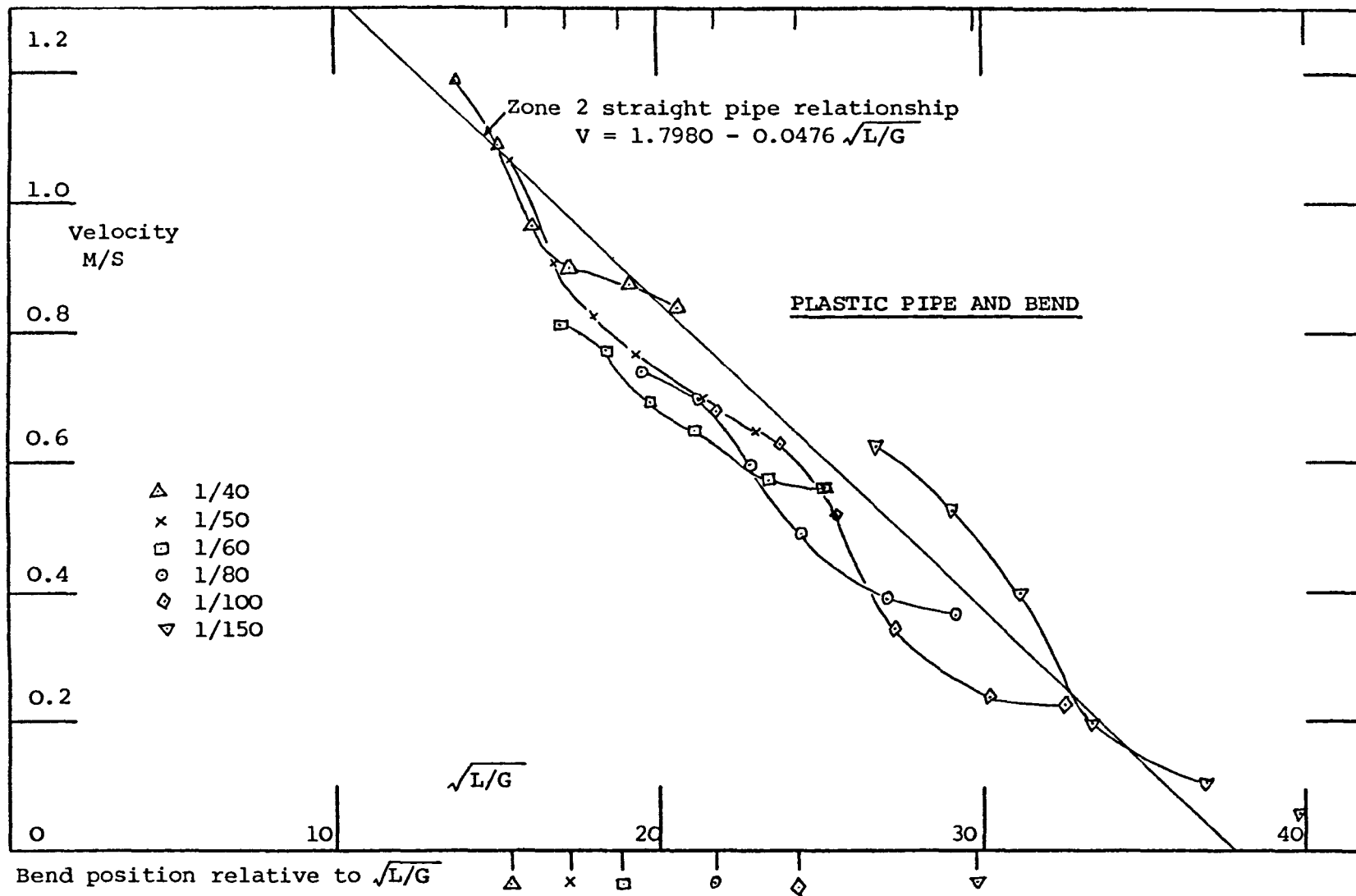


FIGURE 89. (APLU1) 135° Bend at 5.90 metres from w.c.  
 Armitage Shanks P-trap low level w.c., single maternity pad, unvented.  
 Velocity profiles plotted against square root of (Distance along pipe/Gradient)  
 showing variation due to a bend compared to Zone 2 straight pipe relationship.

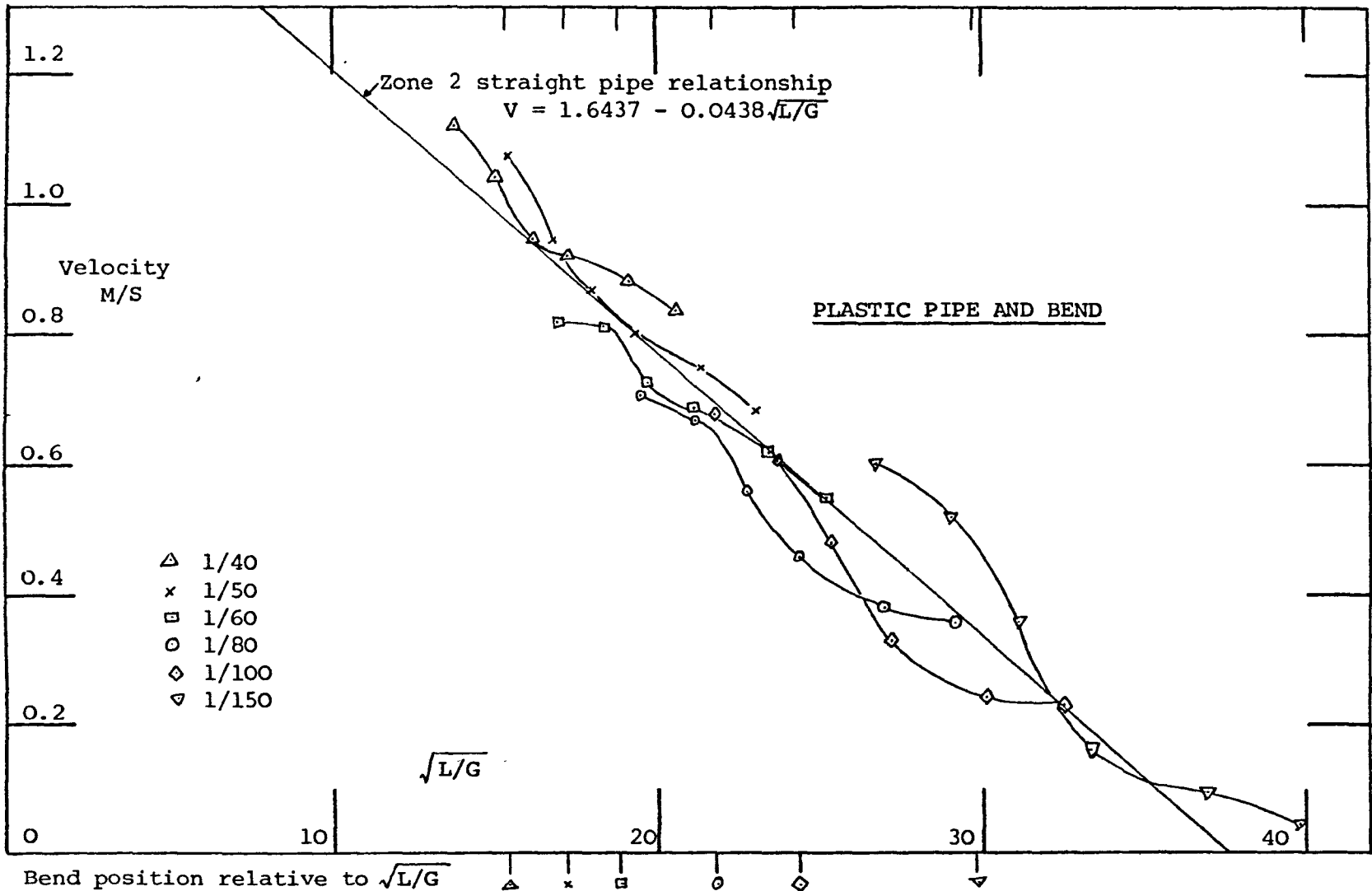


FIGURE 90. (APLV1) 135° Bend at 5.90 metres from w.c.  
 Armitage Shanks P-trap low level w.c., single maternity pad, vented.  
 Velocity profiles plotted against square root of (Distance along pipe/Gradient) showing variation due to a bend compared to Zone 2 straight pipe relationship.

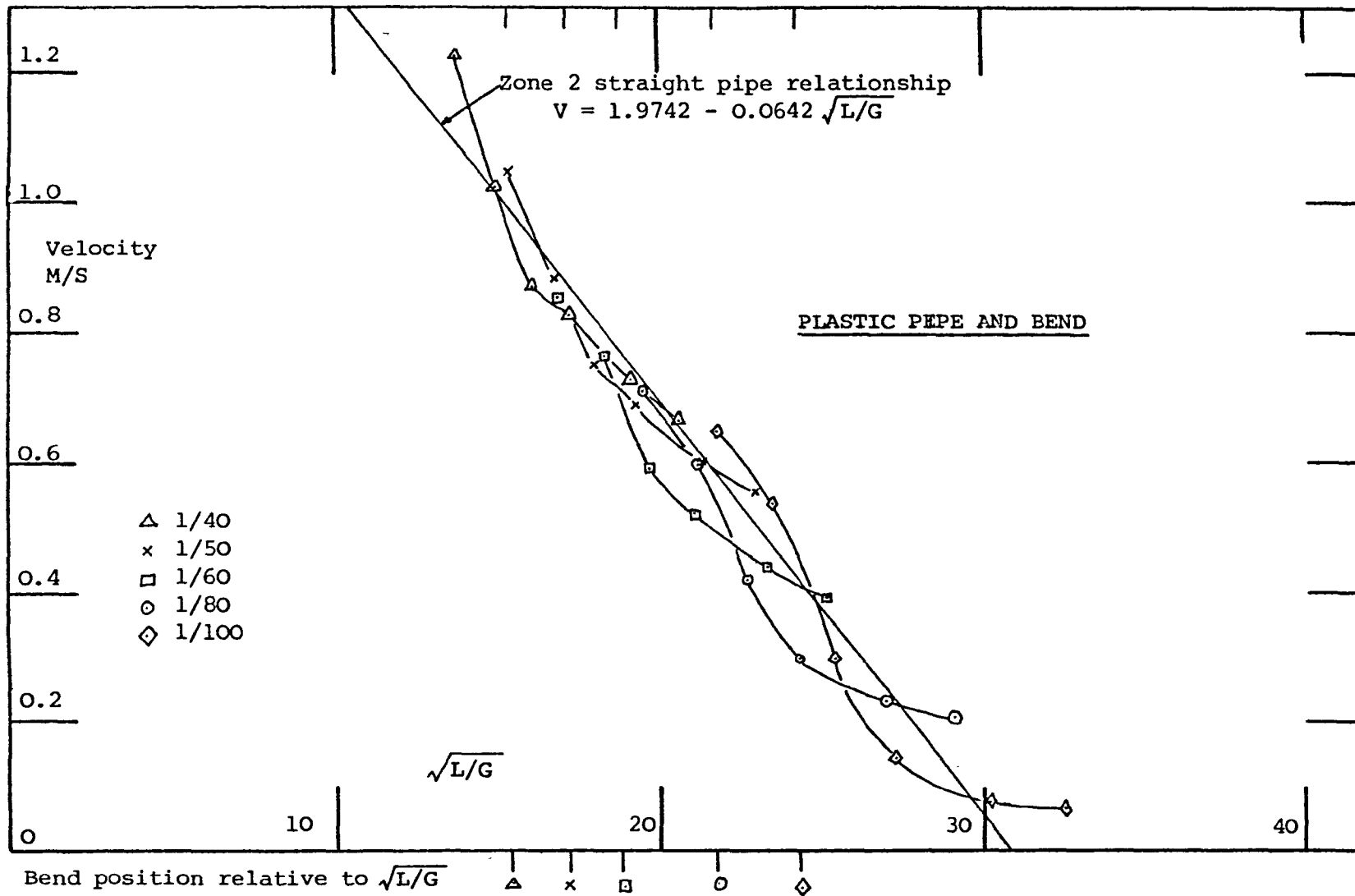


FIGURE 91. (APLV2) 135° Bend at 5.90 metres from w.c. Armitage Shanks P-trap low level w.c., maternity pad plus three Kleenex paper towels, vented. Velocity profiles plotted against square root of (Distance along pipe/Gradient) showing variation due to a bend compared to zone 2 straight pipe relationship.

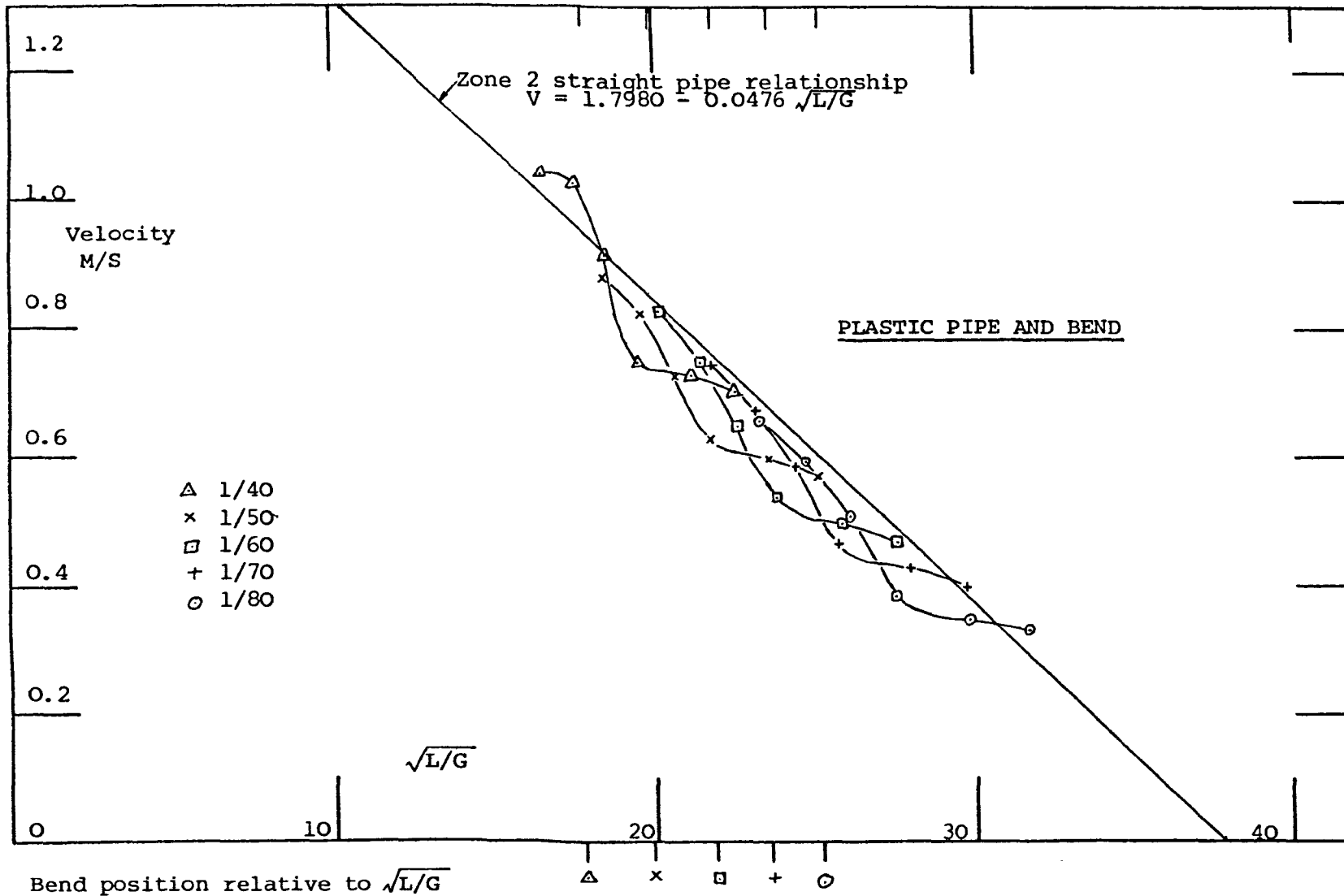


FIGURE 92.

(APLUI) 135° Bend at 7.937 metres from w.c.  
 Armitage Shanks P-trap low level w.c., single maternity pad, unvented.  
 Velocity profiles plotted against square root of (Distance along pipe/Gradient)  
 showing variation due to a bend compared to Zone 2 straight pipe relationship.

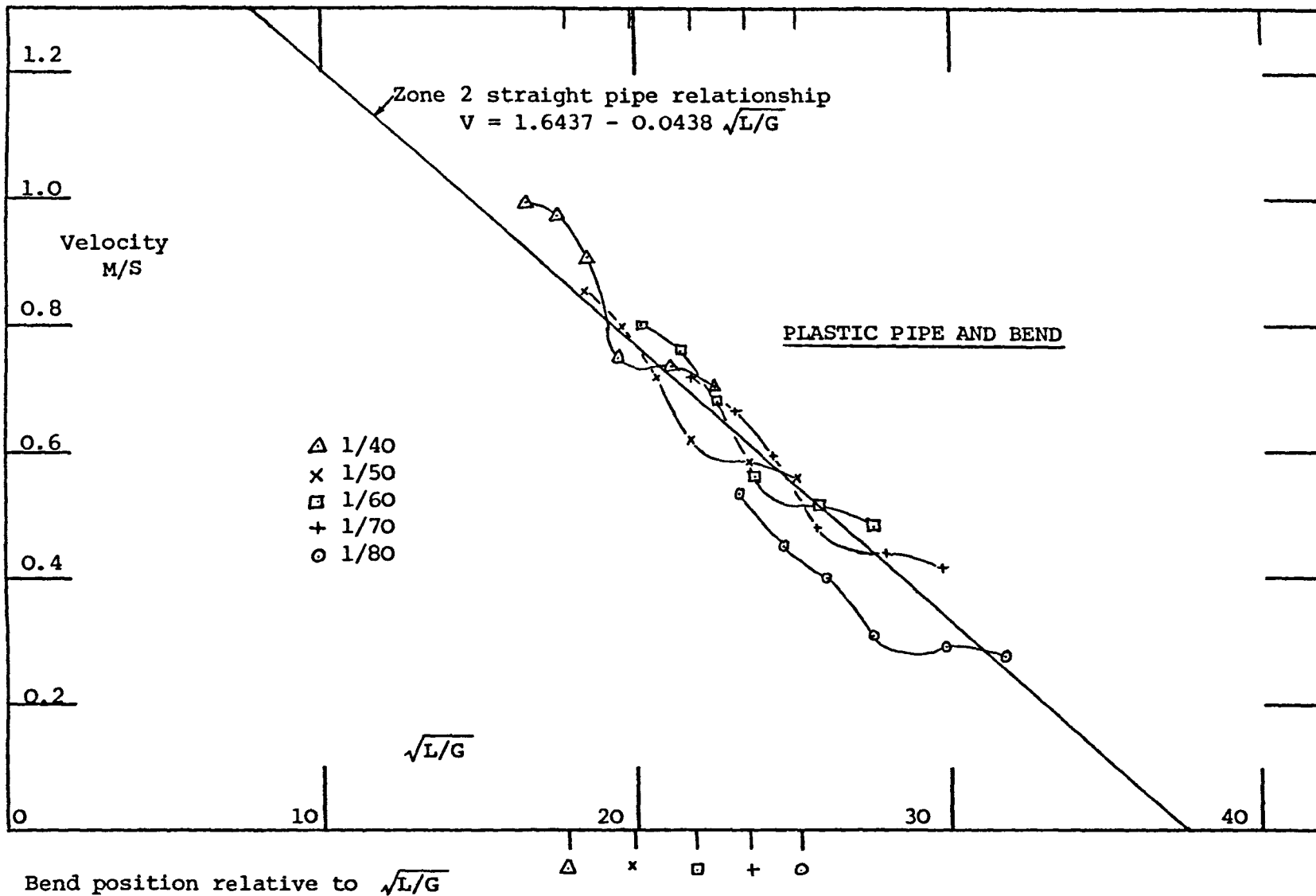


FIGURE 93. (APLV1) 135° Bend at 7.937 metres from w.c.  
 Armitage Shanks P-trap low level w.c., single maternity pad, vented.  
 Velocity profiles plotted against square root of (Distance along pipe/Gradient)  
 showing variation due to a bend compared to Zone 2 straight pipe relationship.

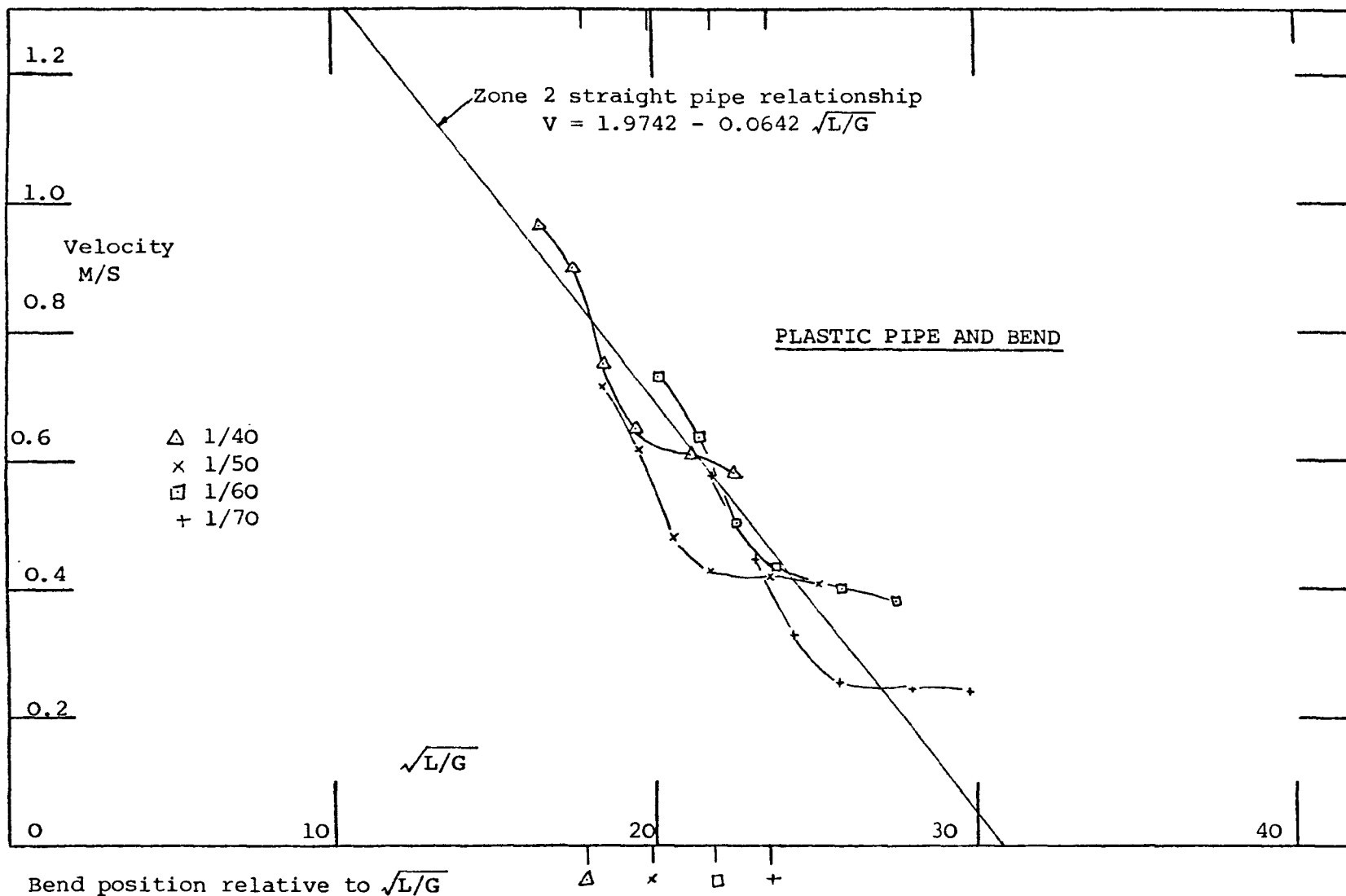


FIGURE 94. (APLV2) 135° Bend at 7.937 metres from w.c. Armitage Shanks P-trap low level w.c., maternity pad plus three Kleenex paper towels, vented. Velocity profiles plotted against square root of (Distance along pipe/Gradient) showing variation due to a bend compared to zone 2 straight pipe relationship.

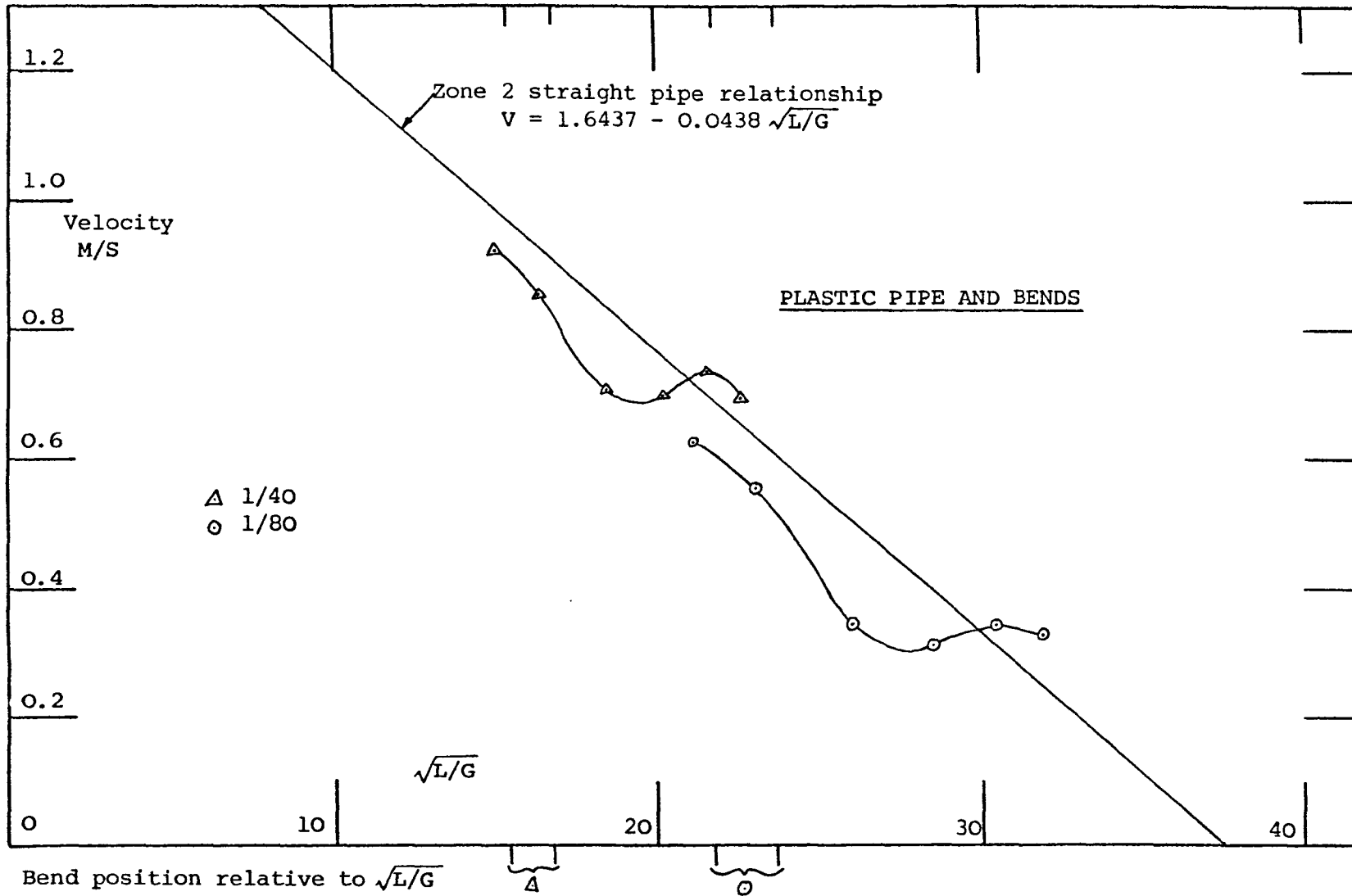


FIGURE 95. (APLV1) 2 x 135° Bends at 5.927 and 7.010 metres from w.c. Armitage Shanks P-trap low level w.c., single maternity pad, vented. Velocity profiles plotted against square root of (Distance along pipe/Gradient) showing variation due to two bends compared to zone 2 straight pipe relationship.

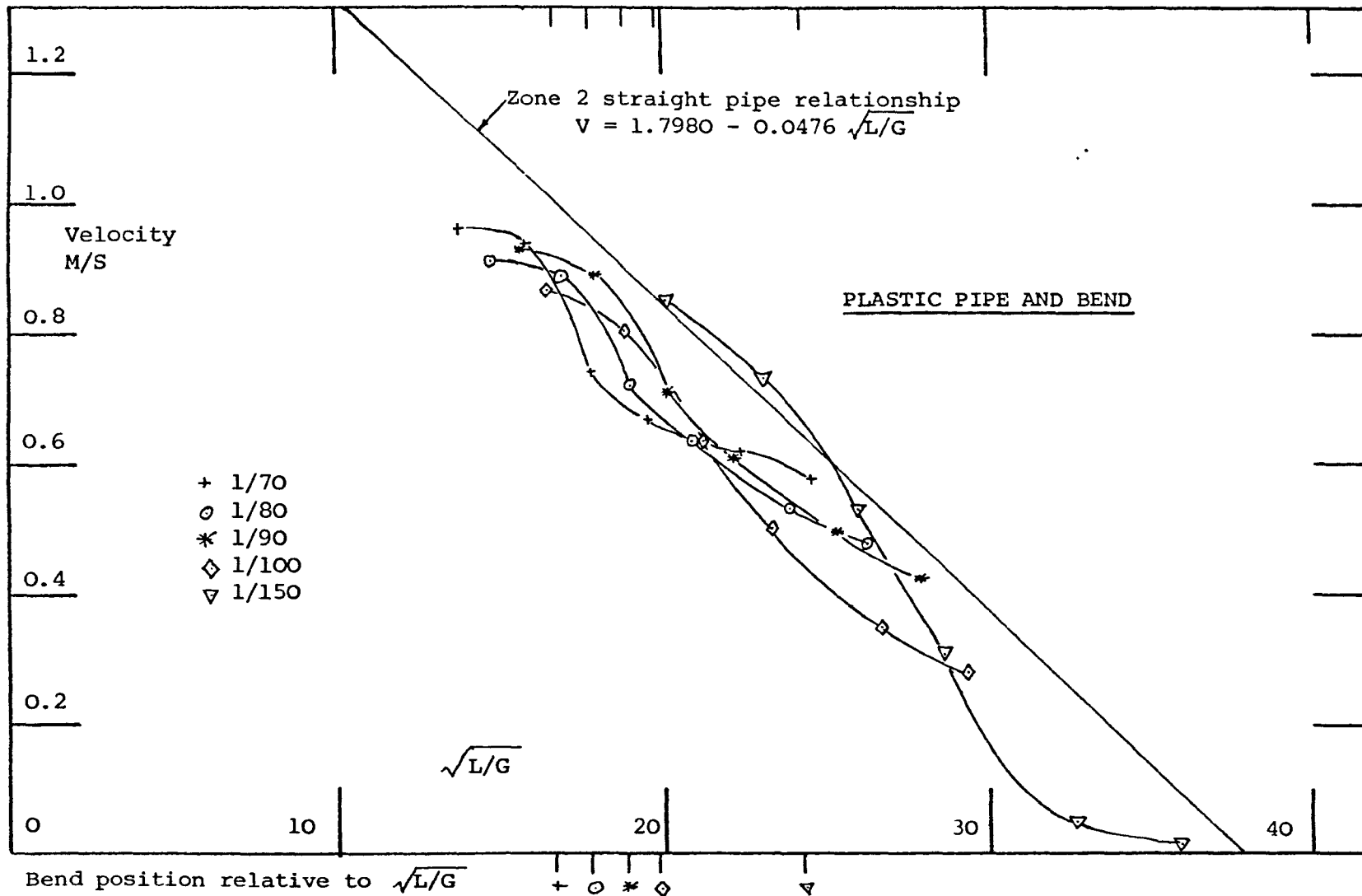


FIGURE 96. (APLU1) 92½° Bend at 3.93 metres from w.c.  
 Armitage Shanks P-trap low level w.c., single maternity pad, unvented.  
 Velocity profiles plotted against square root of (Distance along pipe/Gradient)  
 showing variation due to a bend compared to Zone 2 straight pipe relationship.

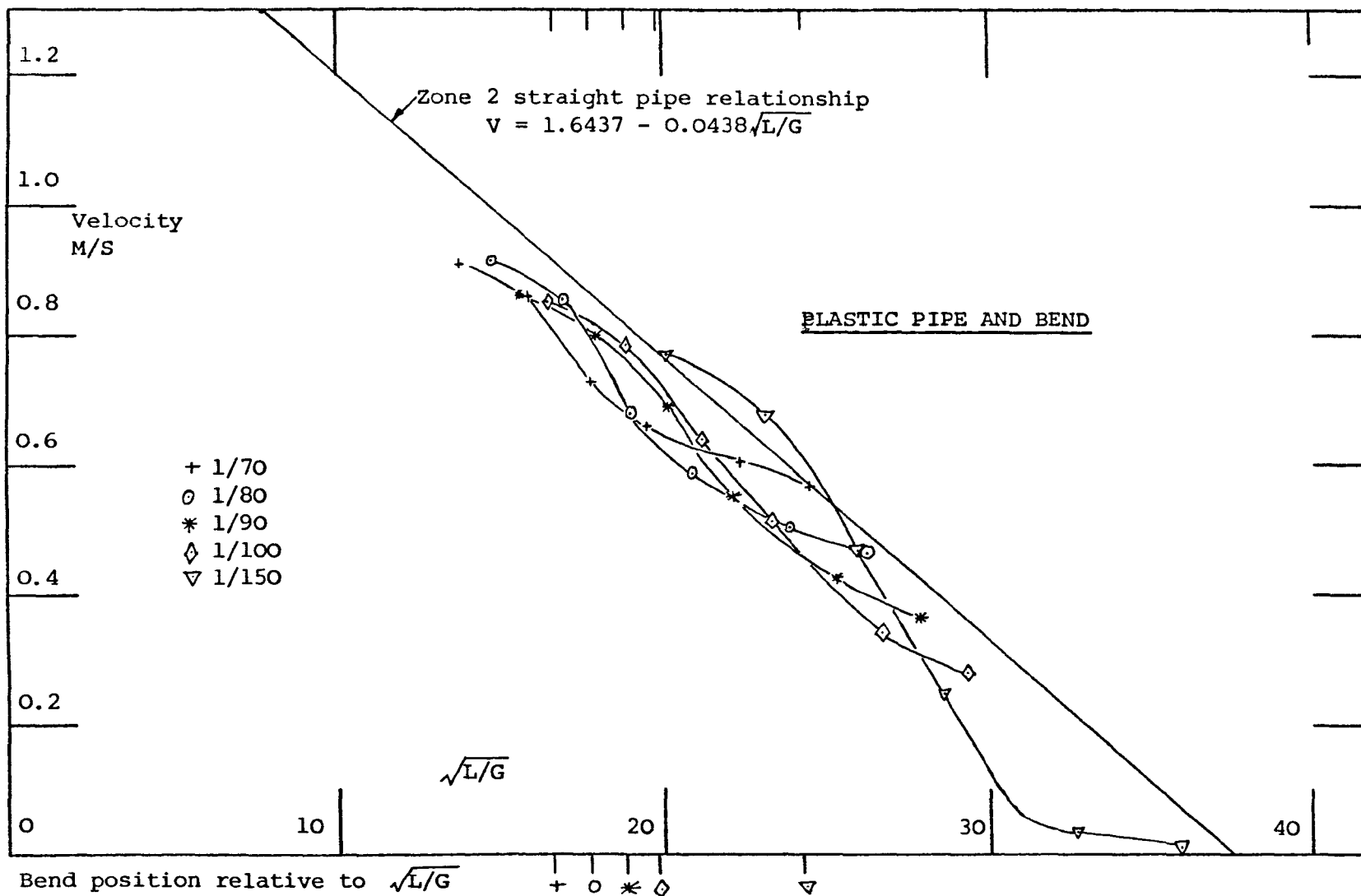


FIGURE 97. (APLV1) 92½° Bend at 3.93 metres from w.c.  
 Armitage Shanks P-trap low level w.c., single maternity pad, vented.  
 Velocity profiles plotted against square root of (Distance along pipe/Gradient)  
 showing variation due to a bend compared to Zone 2 straight pipe relationship.

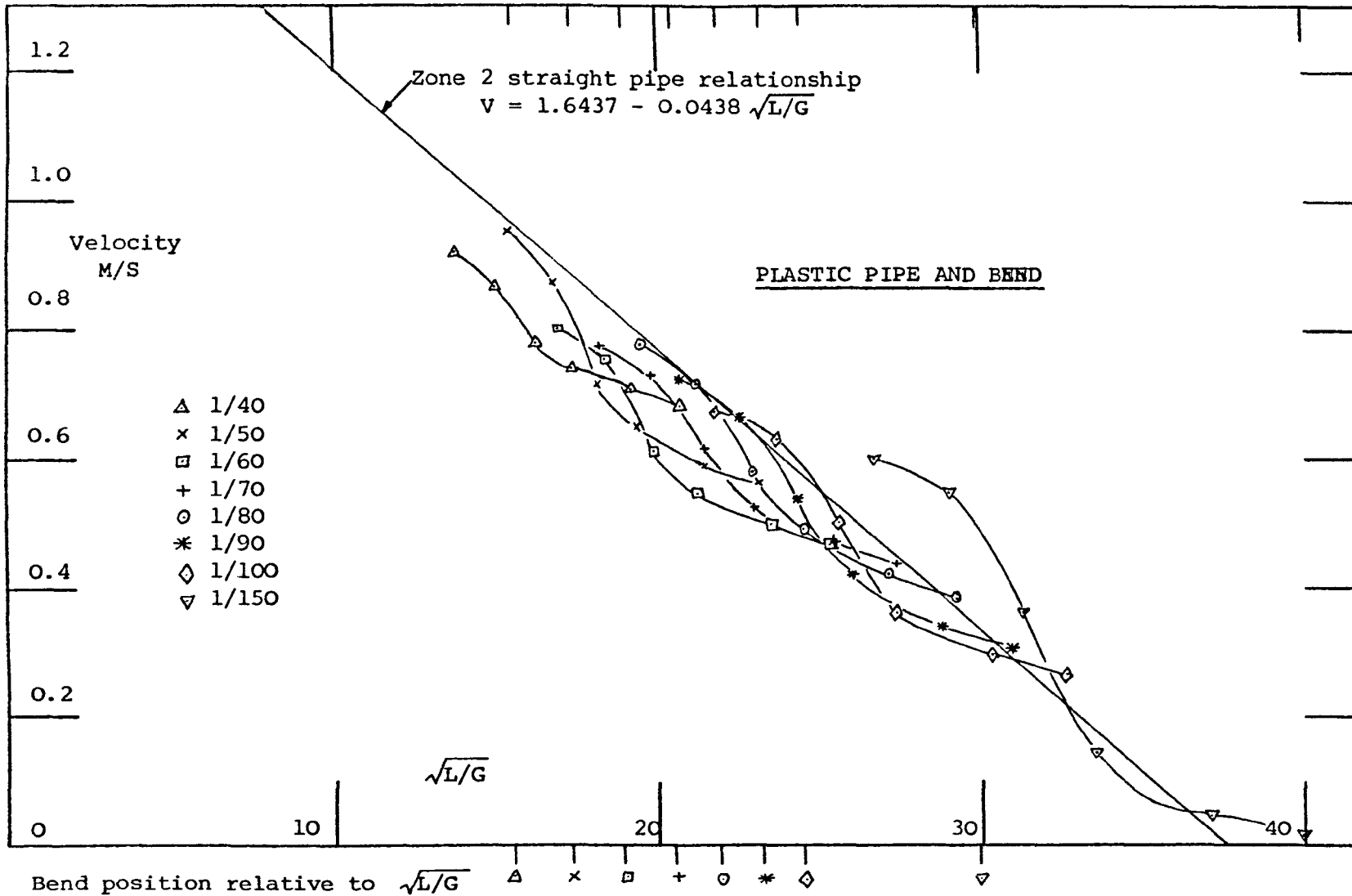


FIGURE 98. (APLV1)  $92\frac{1}{2}^\circ$  Bend at 5.975 metres from w.c.  
 Armitage Shanks P-trap low level w.c., single maternity pad, vented.  
 Velocity profiles plotted against square root of (Distance along pipe/Gradient)  
 showing variation due to a bend compared to Zone 2 straight pipe relationship.

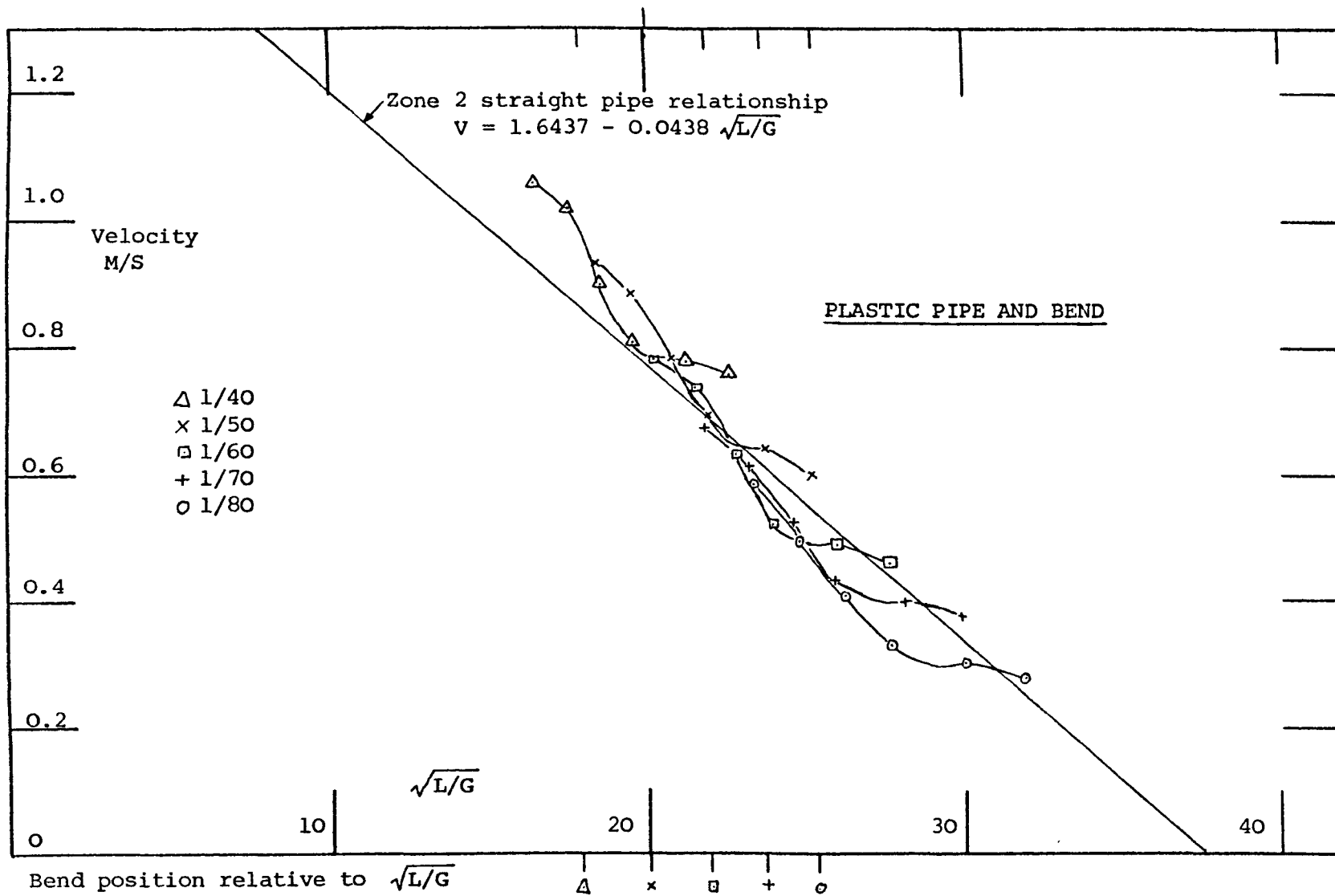


FIGURE 99. (APLV1) 92 $\frac{1}{2}$ <sup>o</sup> Bend at 8.017 metres from w.c.  
 Armitage Shanks P-trap low level w.c., single maternity pad, vented.  
 velocity profiles plotted against square root of (Distance along pipe/Gradient)  
 showing variation due to a bend compared to Zone 2 straight pipe relationship.

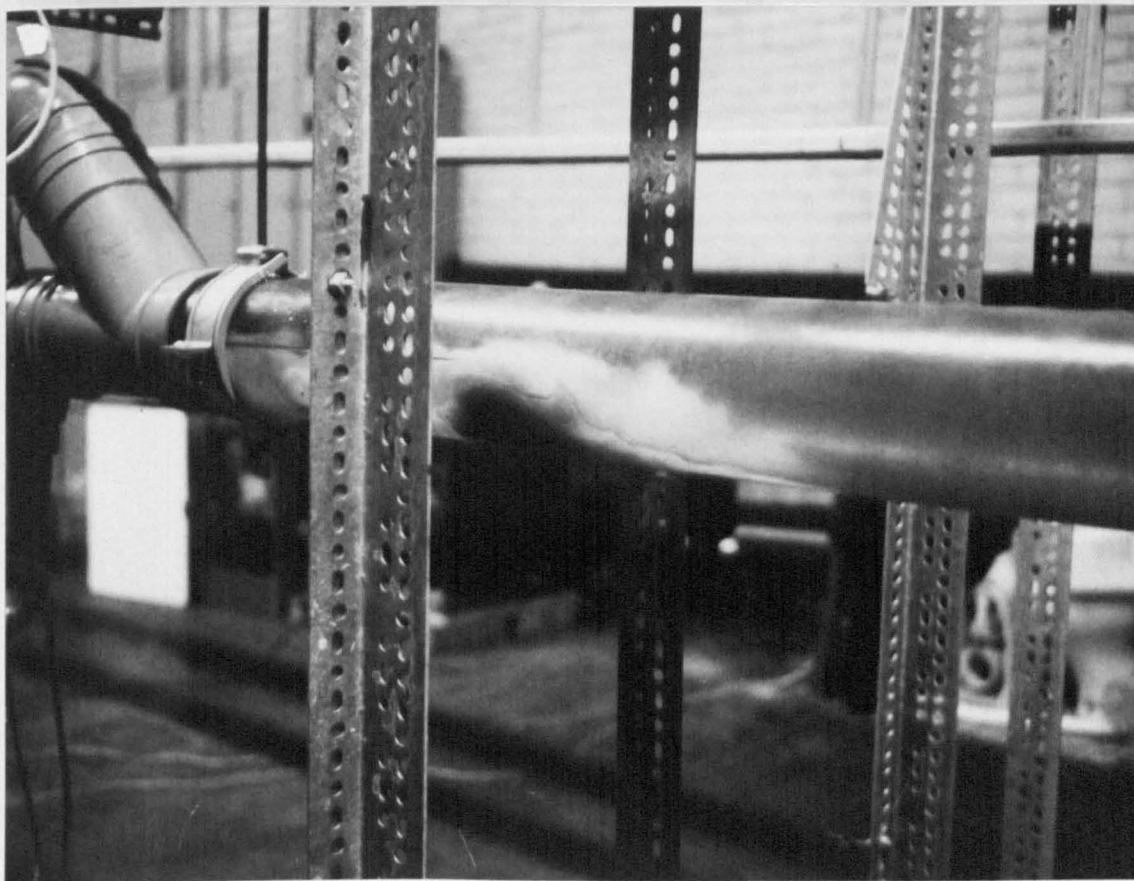


FIGURE 100. Reproduction of a polaroid photograph taken during the vertical junction entry tests. This photograph shows the start of the blockage build up after two w.c. flushes, each with a single maternity pad plus 3 Kleenex paper towels. At this stage the blockage consisted of three paper towels left in the junction after the first flush with the maternity pad and 3 paper towels from the second flush. The second maternity pad dropped on top of the stationary towels left from the first flush with the second batch of towels left in the junction. The main drain was now approximately half full of water behind the blockage.

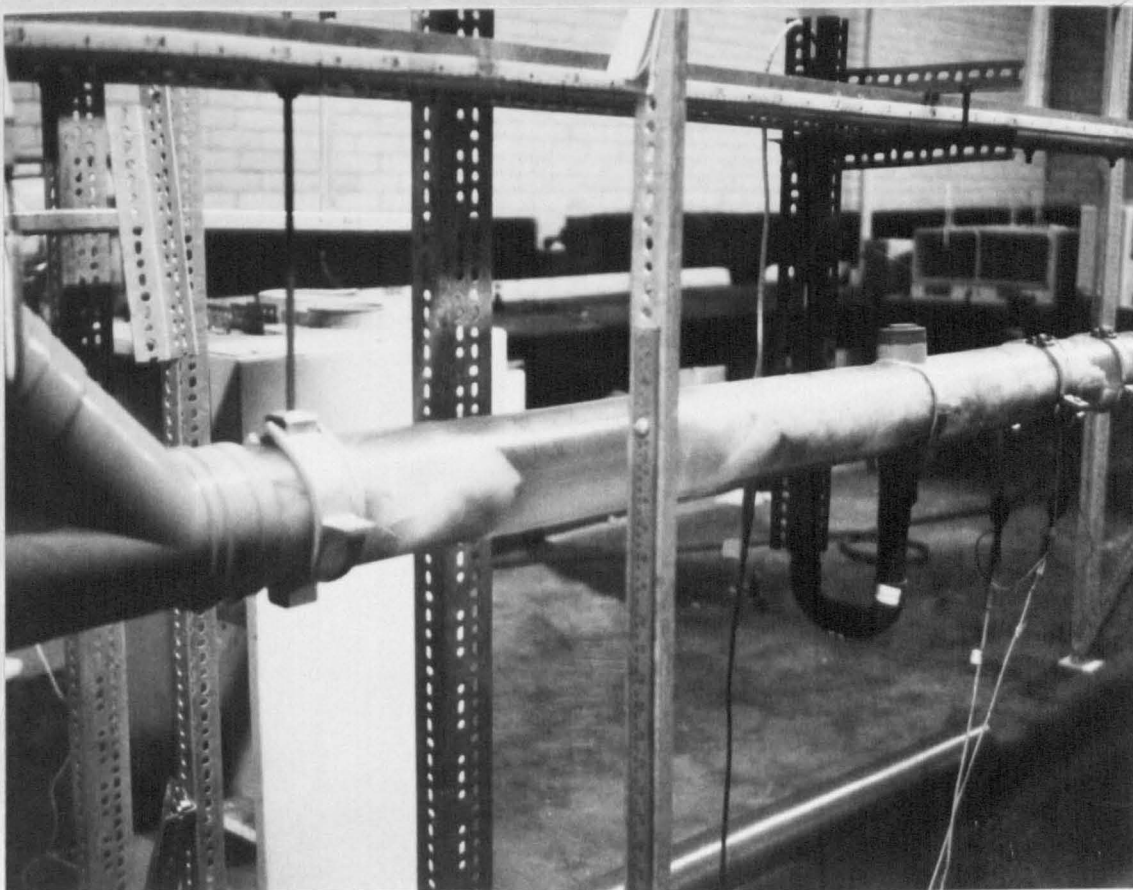


FIGURE 101. Photograph of the blockage after ten w.c. flushes, each with a single maternity pad and 3 Kleenex paper towels. The main drain was now totally blocked by the nine maternity pads and thirty paper towels, with only the maternity pad from the first w.c. flush having cleared the full 7.2 metre pipe length from the junction to the vertical stack. The main drain was now full of water and the blockage was totally immovable by further water only flushes.

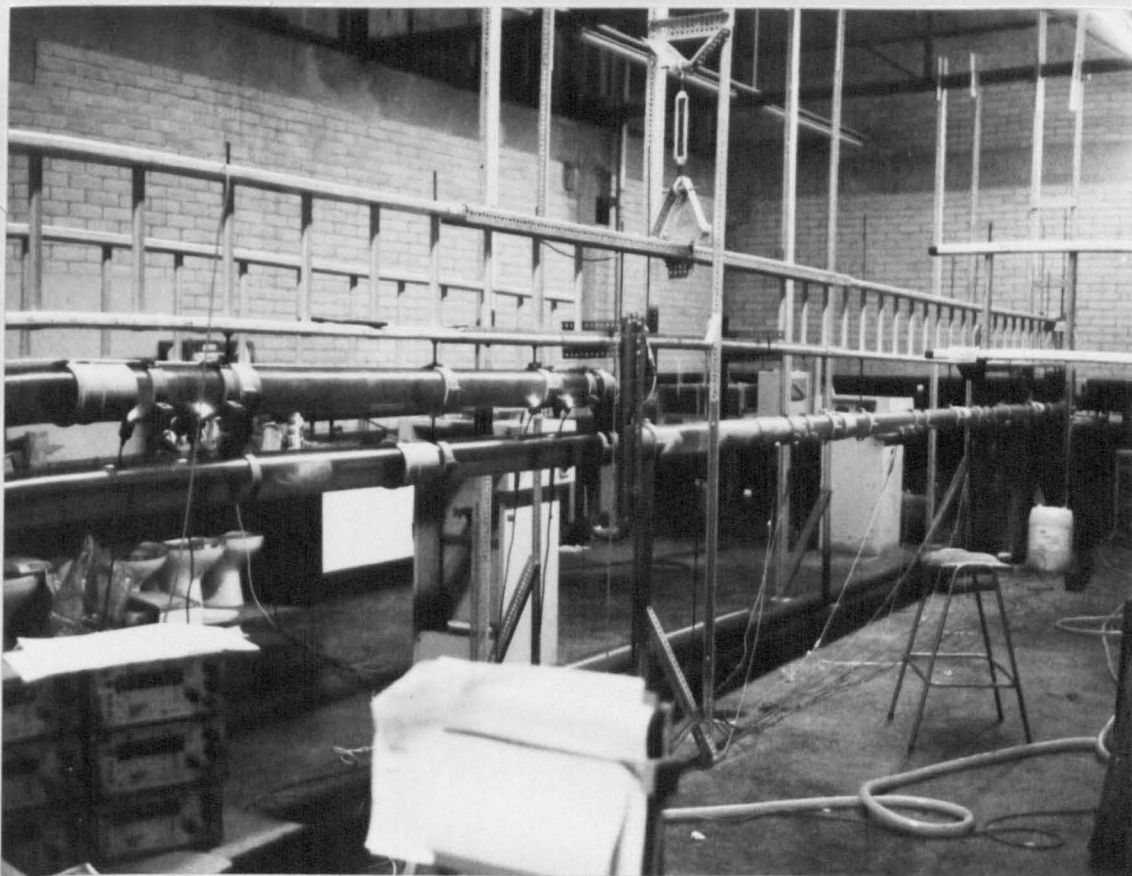


FIGURE 102. Photograph of the blockage after ten w.c. flushes, each with a single maternity pad and 3 Kleenex paper towels. The blockage is identical to that shown in Figure 101. The photograph shows the paper towel which had backflowed approximately 1.5 metres up the main drain which was full of water behind the blockage. The photograph also shows the ladder support system and slope adjusting bottle screws used throughout the research programme, as well as the pipe configuration used for the vertical junction entry tests.

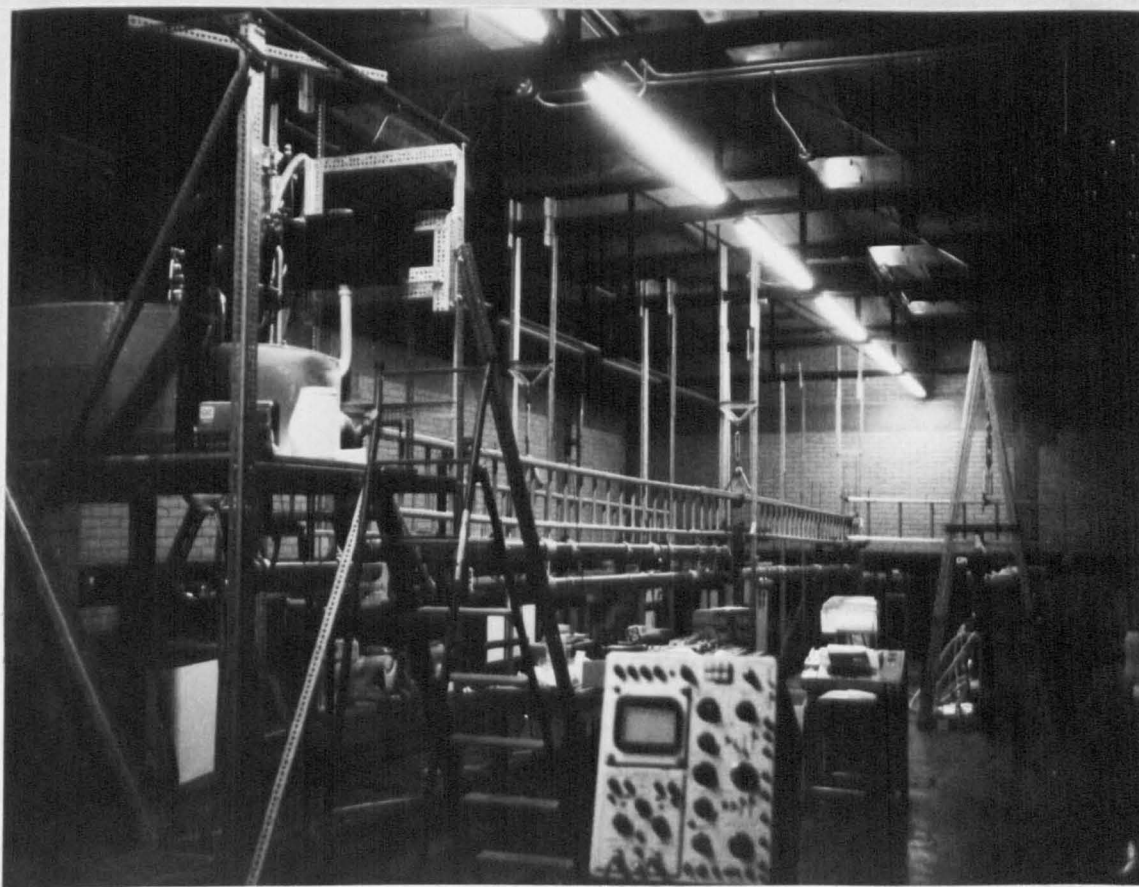


FIGURE 103. Photograph of the full test rig used during the vertical junction entry tests.

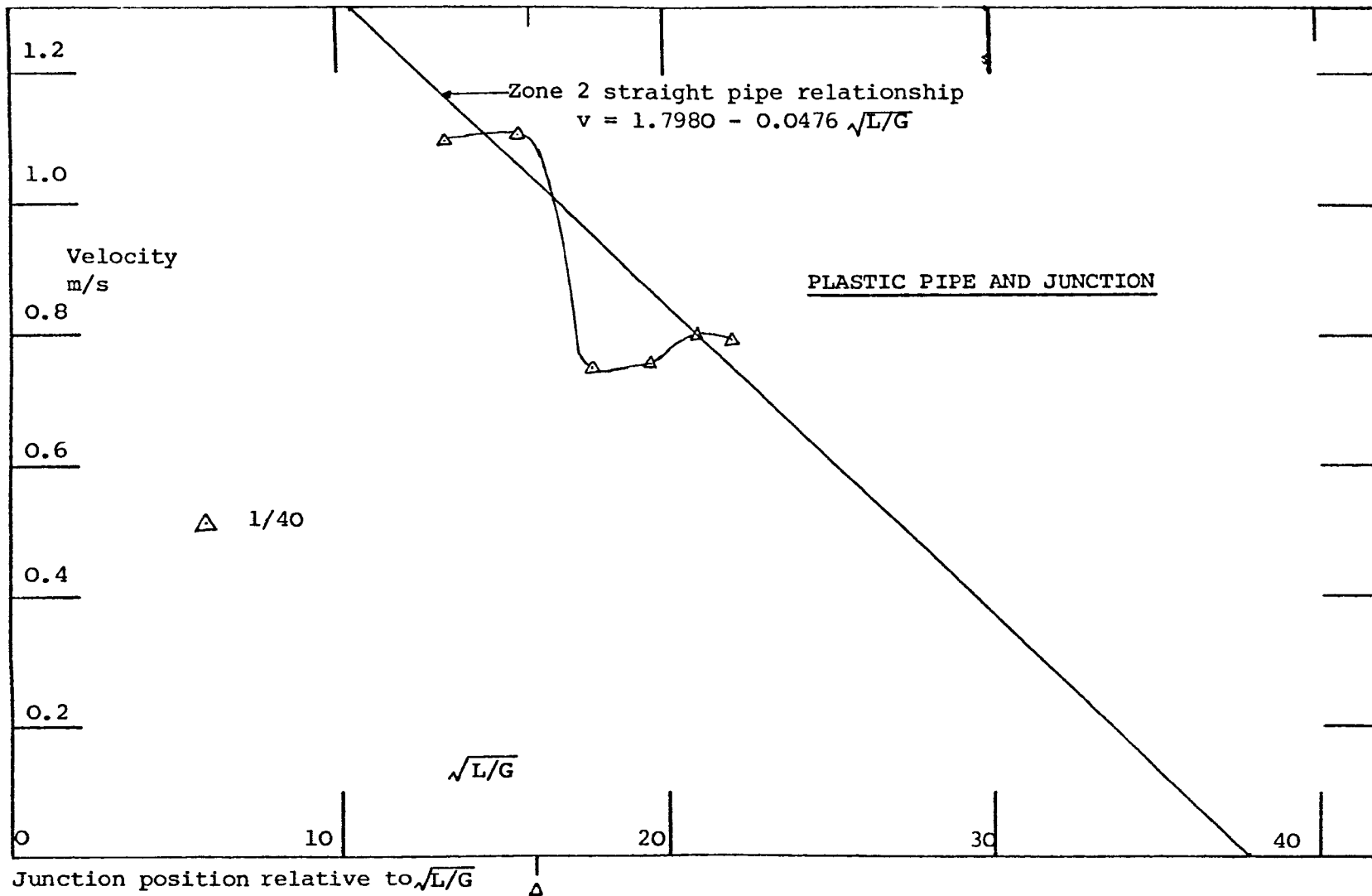
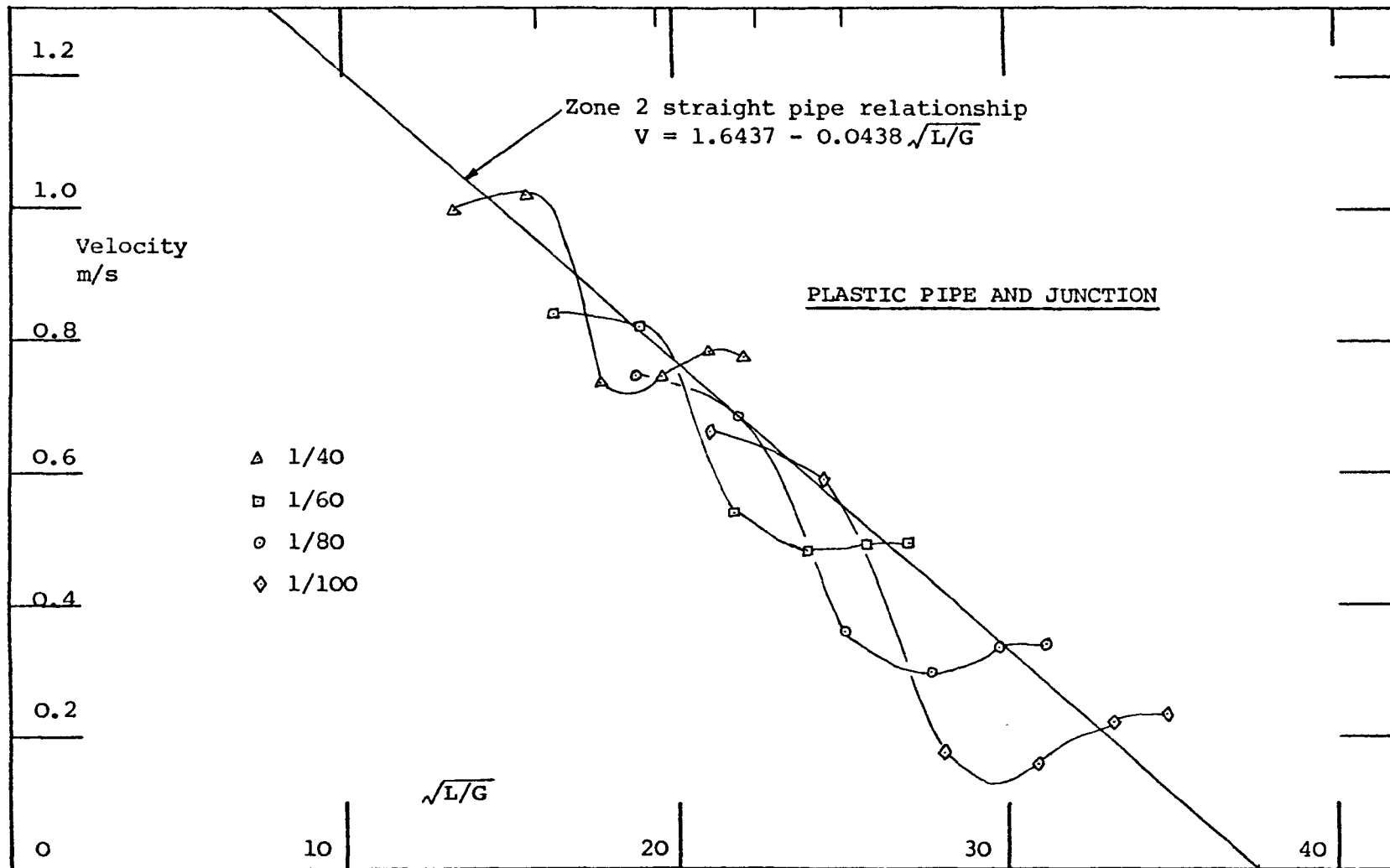


FIGURE 104. (APLU1) 135° Junction at 6.332 metres from w.c. Main line closed to atmosphere. Entry to main line flow via a 135° Junction with horizontal entry. Armitage Shanks P-trap low level w.c., single maternity pad, unvented. Velocity profile plotted against square root of (Distance along pipe/Gradient) showing variation due to a junction compared to zone 2 straight pipe relationship.



Junction position relative to  $\sqrt{L/G}$

FIGURE 105. (APLV1) 135° Junction at 6.332 metres from w.c., main line closed to atmosphere. Entry to main line via a 135° Junction with horizontal entry. Armitage Shanks P-trap low level w.c., single maternity pad, vented. Velocity profiles plotted against square root of (Distance along pipe/Gradient) showing variation due to a junction compared to Zone 2 straight pipe relationship.

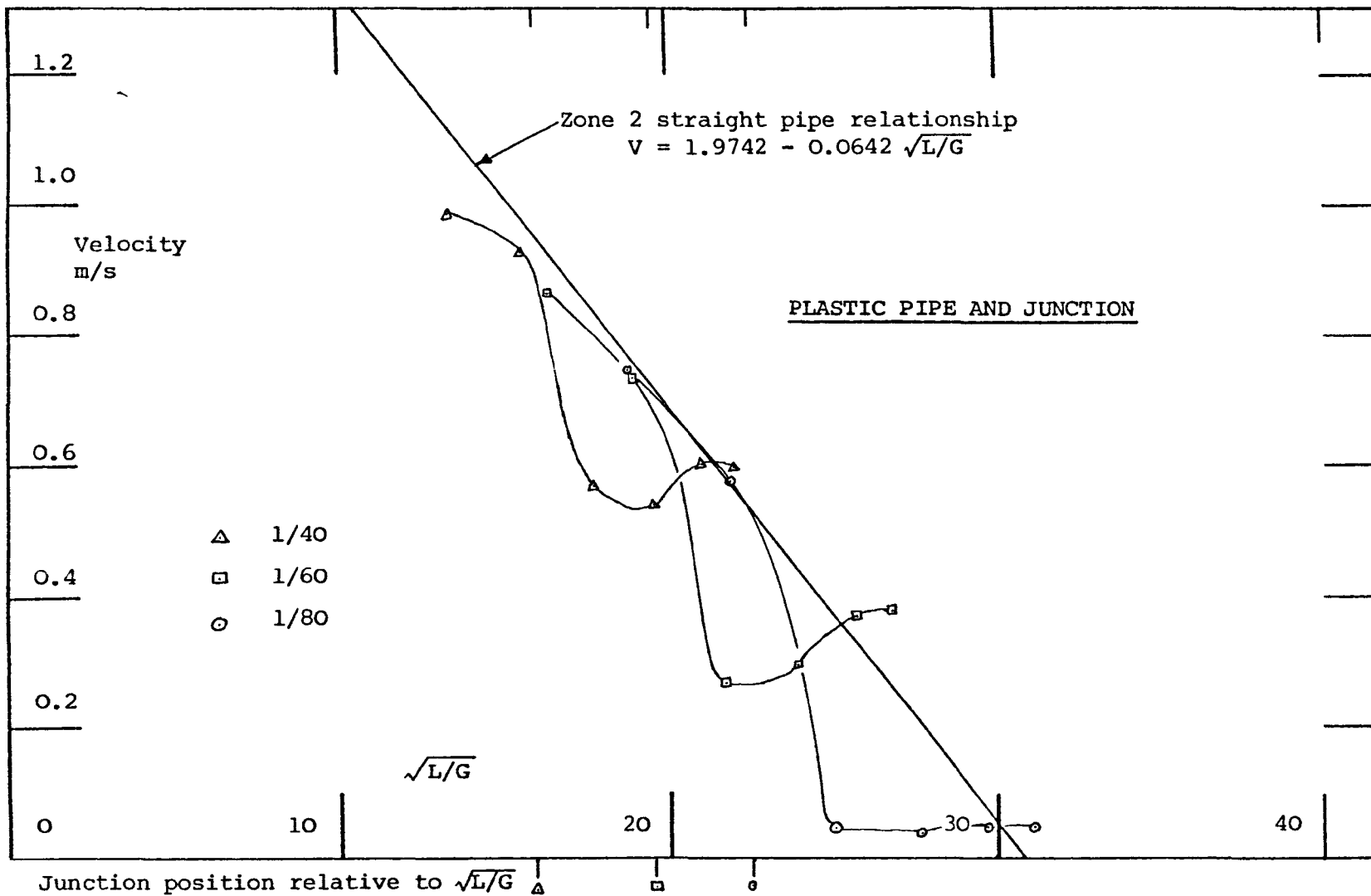


FIGURE 106. (APLV2) 135° Junction at 6.332 metres from w.c. Main line closed to atmosphere. Entry to main line flow via a 135° Junction with horizontal entry. Armitage Shanks P-trap low level w.c., maternity pad plus three Kleenex paper towels, vented. Velocity profiles plotted against square root of (Distance along pipe/Gradient) showing variation due to a junction compared to zone 2 straight pipe relationship.

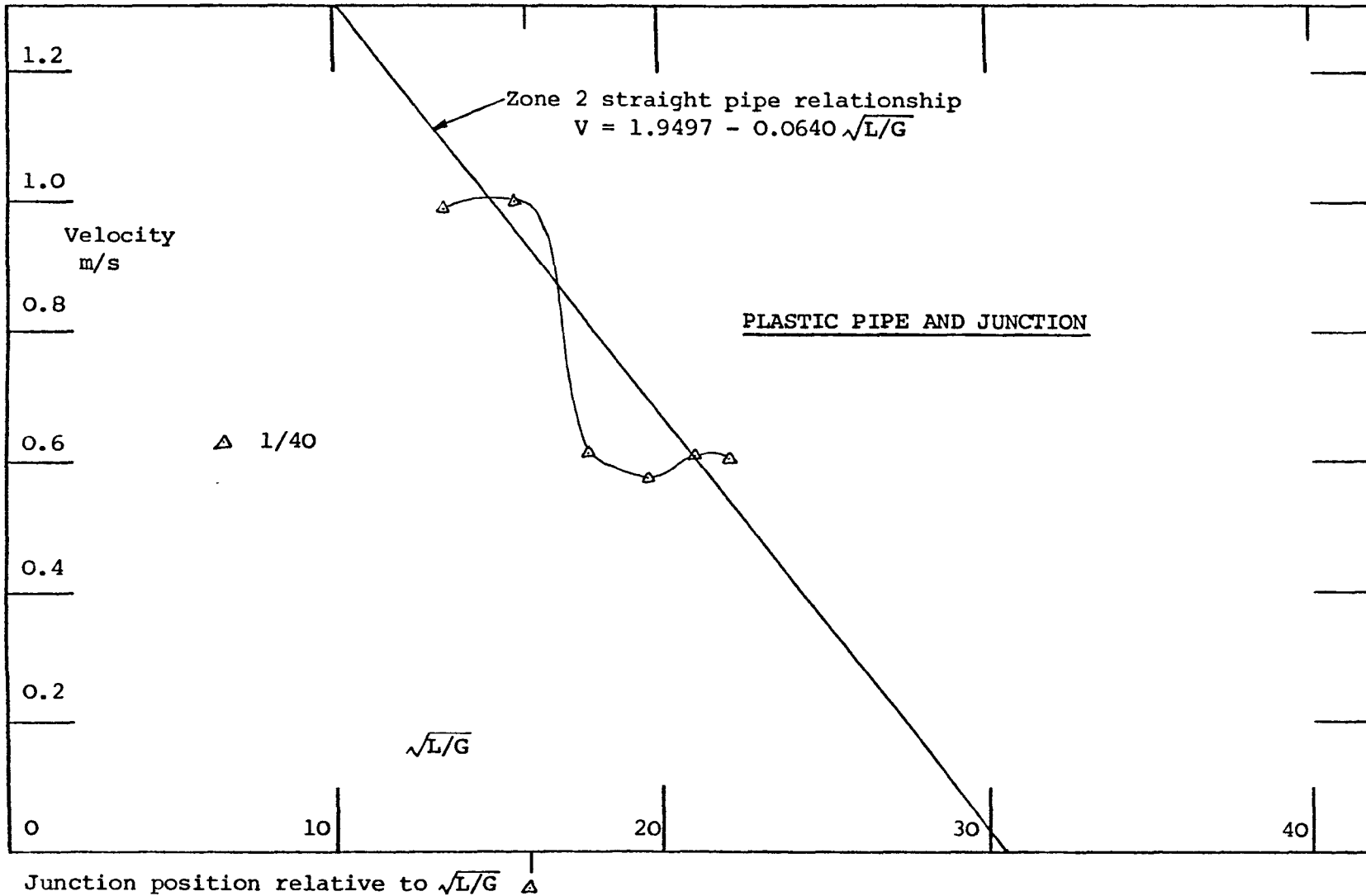


FIGURE 107. (APLV3) 135° Junction at 6.332 metres from w.c., main line closed to atmosphere. Entry to main line via a 135° Junction with horizontal entry. Armitage Shanks P-trap low level w.c., maternity pad plus three Bowtowels, vented. Velocity profile plotted against square of (Distance along pipe/Gradient) showing variation due to a junction compared to Zone 2 straight pipe relationship

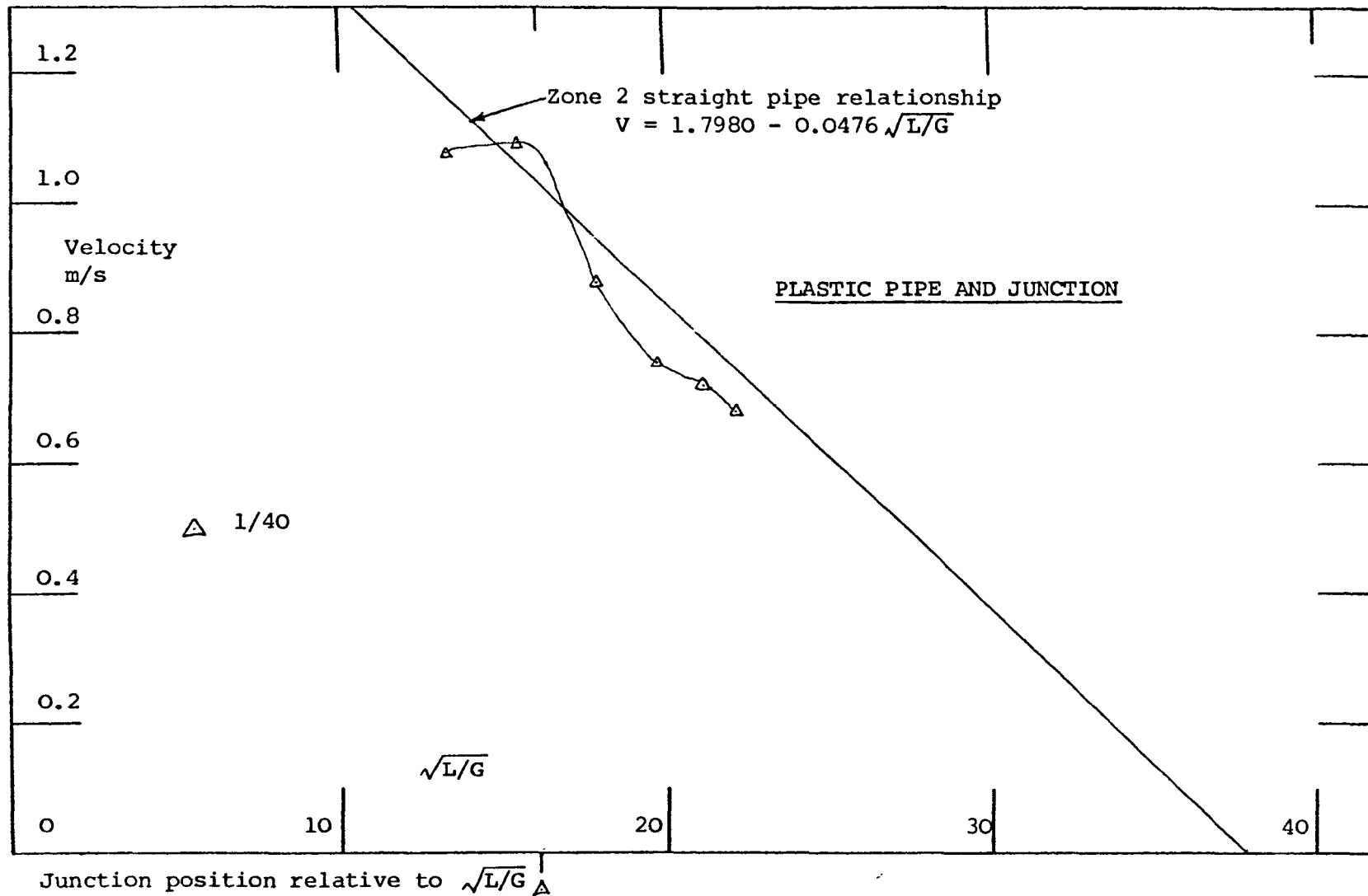


FIGURE 108. (APLU1) 135° Junction at 6.437 metres from w.c. Main line closed to atmosphere. Entry to main line via a 148° adjustable bend and 135° Junction with 45° entry. Armitage Shanks P-trap low-level w.c., single maternity pad, unvented. Velocity profile plotted against square root of (Distance along pipe/Gradient) showing variation due to a junction compared to zone 2 straight pipe relationship.

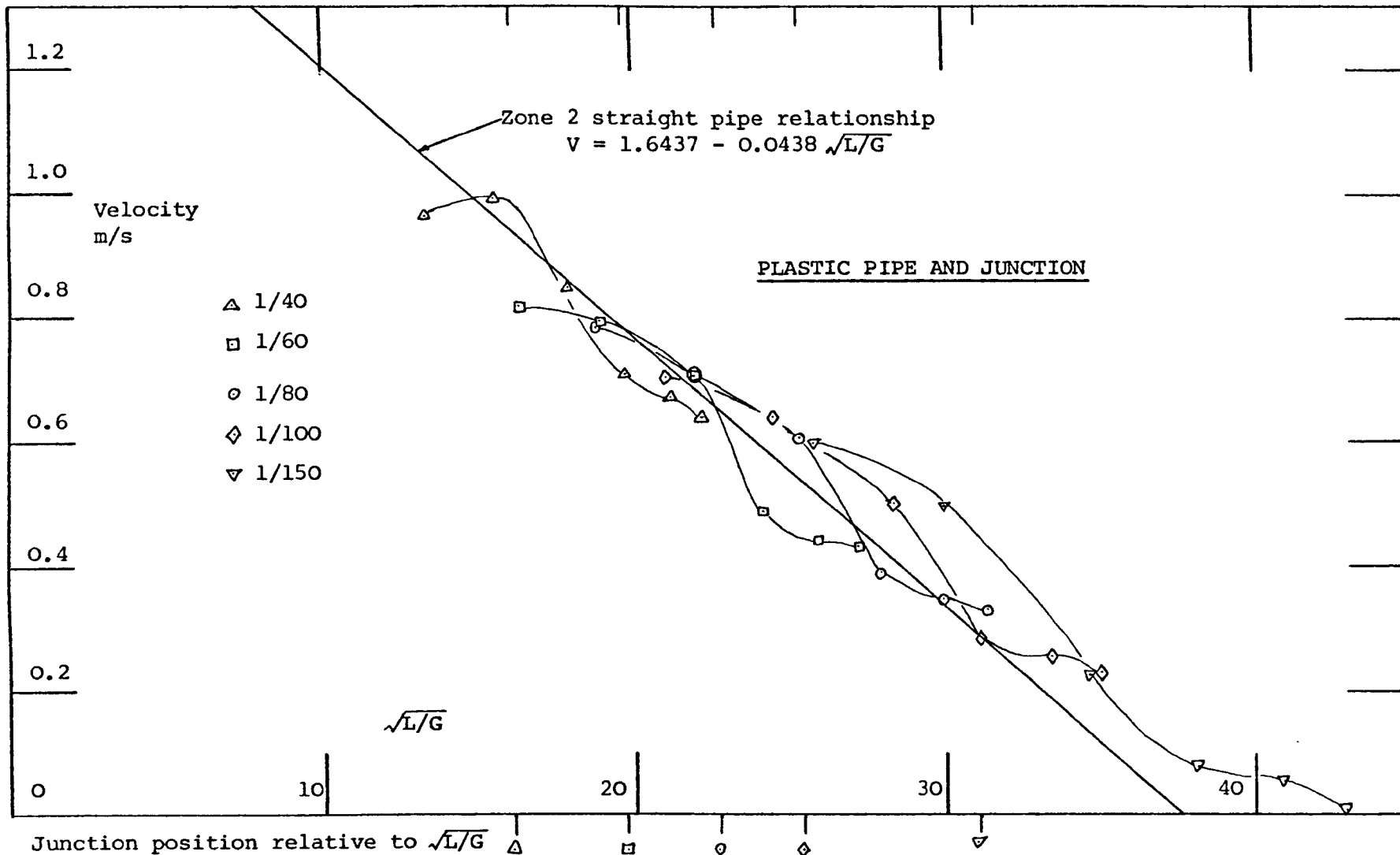


FIGURE 109. (APLV1) 135° Junction at 6.437 metres from w.c., main line closed to atmosphere. Entry to main line via a 148° adjustable bend and 135° Junction with 45° entry. Armitage Shanks P-trap low level w.c., single maternity pad, vented. Velocity profiles plotted against square root of (Distance along pipe/Gradient) showing variation due to a junction compared to Zone 2 straight pipe relationship.

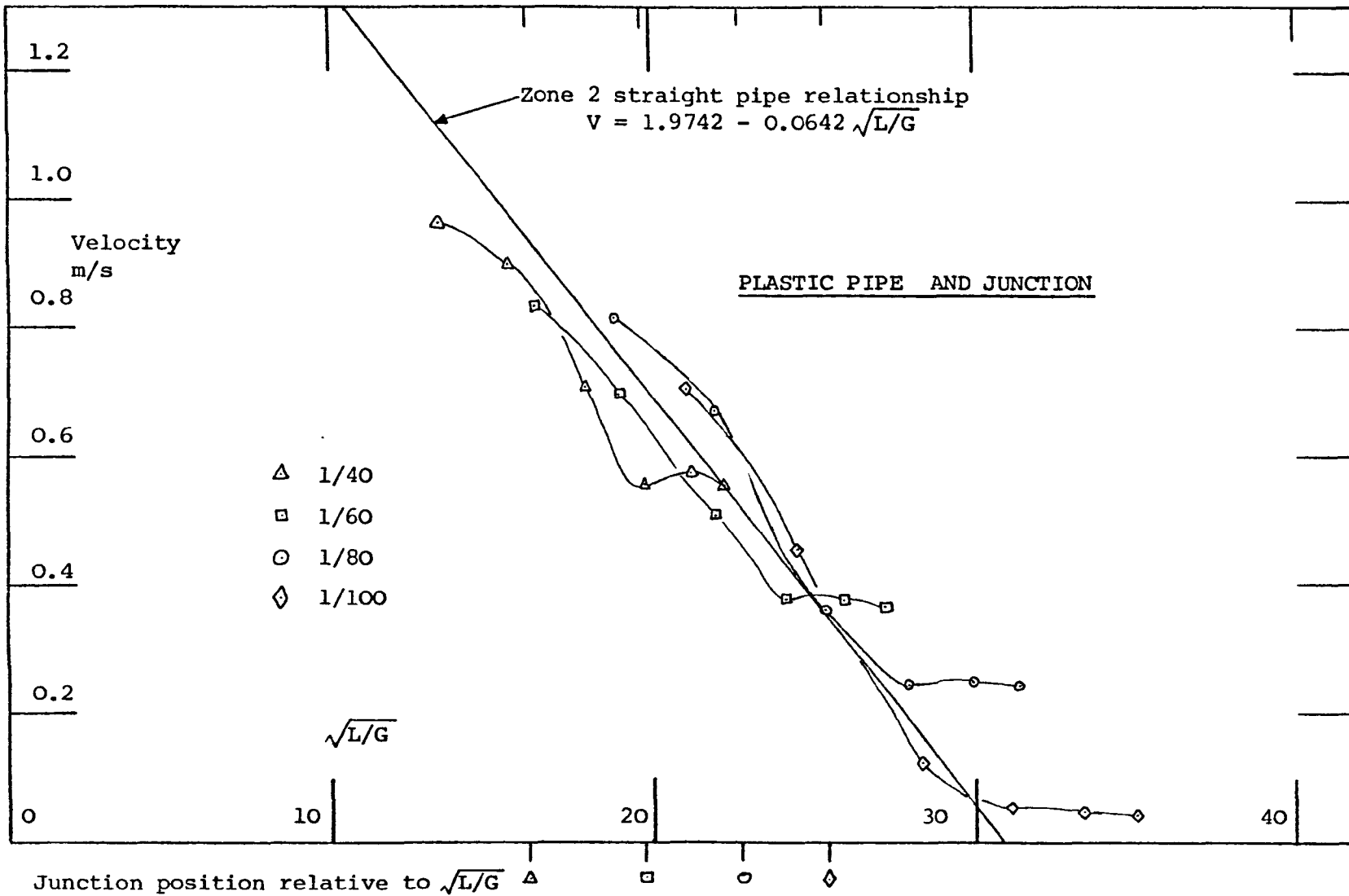


FIGURE 110. (APLV2) 135° Junction at 6.437 metres from w.c. Main Line closed to atmosphere. Entry to main line via a 148° adjustable bend and a 135° Junction with 45° entry. Armitage Shanks P-trap low level w.c., maternity pad plus three Kleenex paper towels, vented. Velocity profiles plotted against square root of (Distance along pipe/Gradient) showing variation due to a junction compared to zone 2 straight pipe relationship.

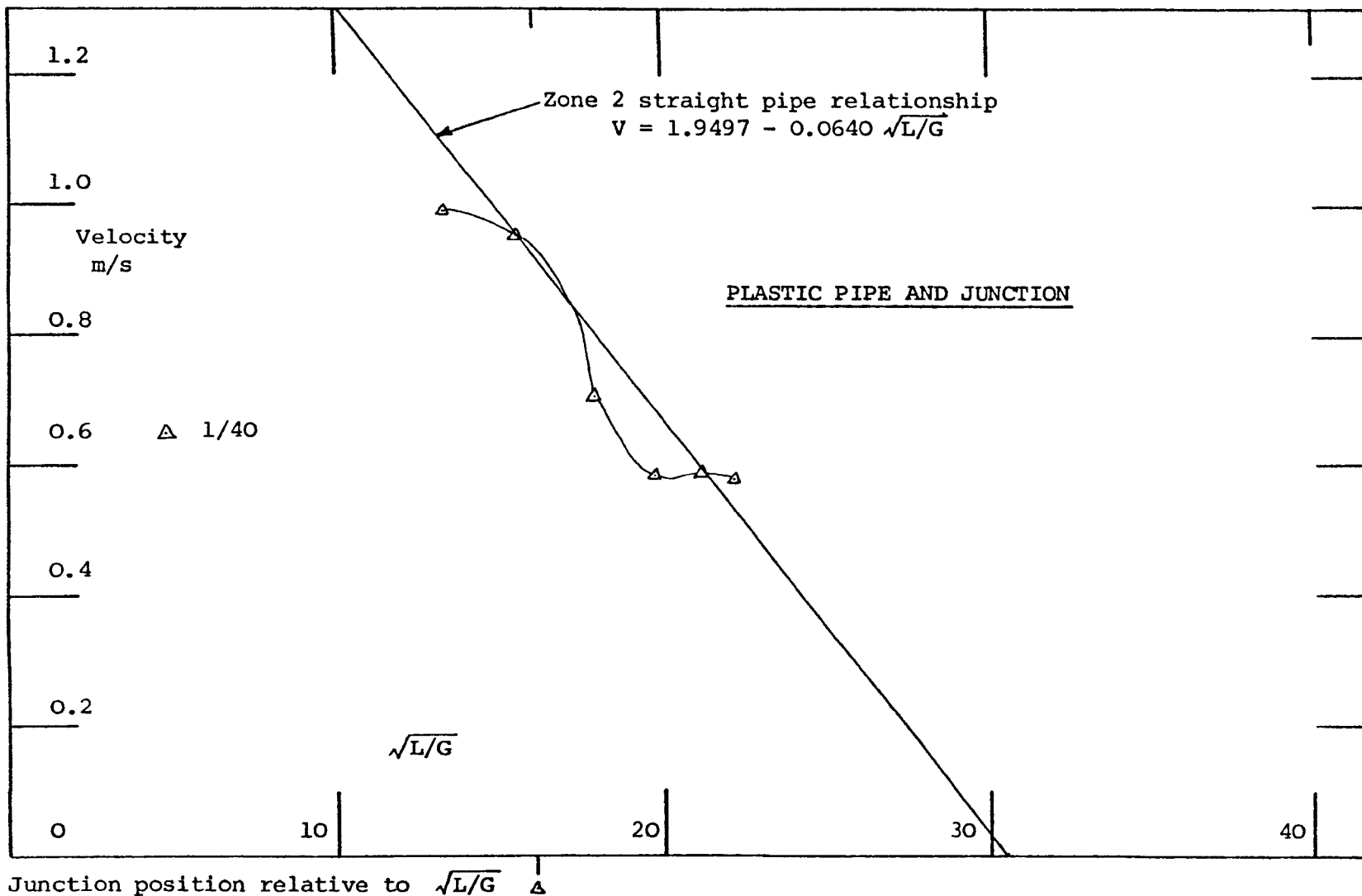
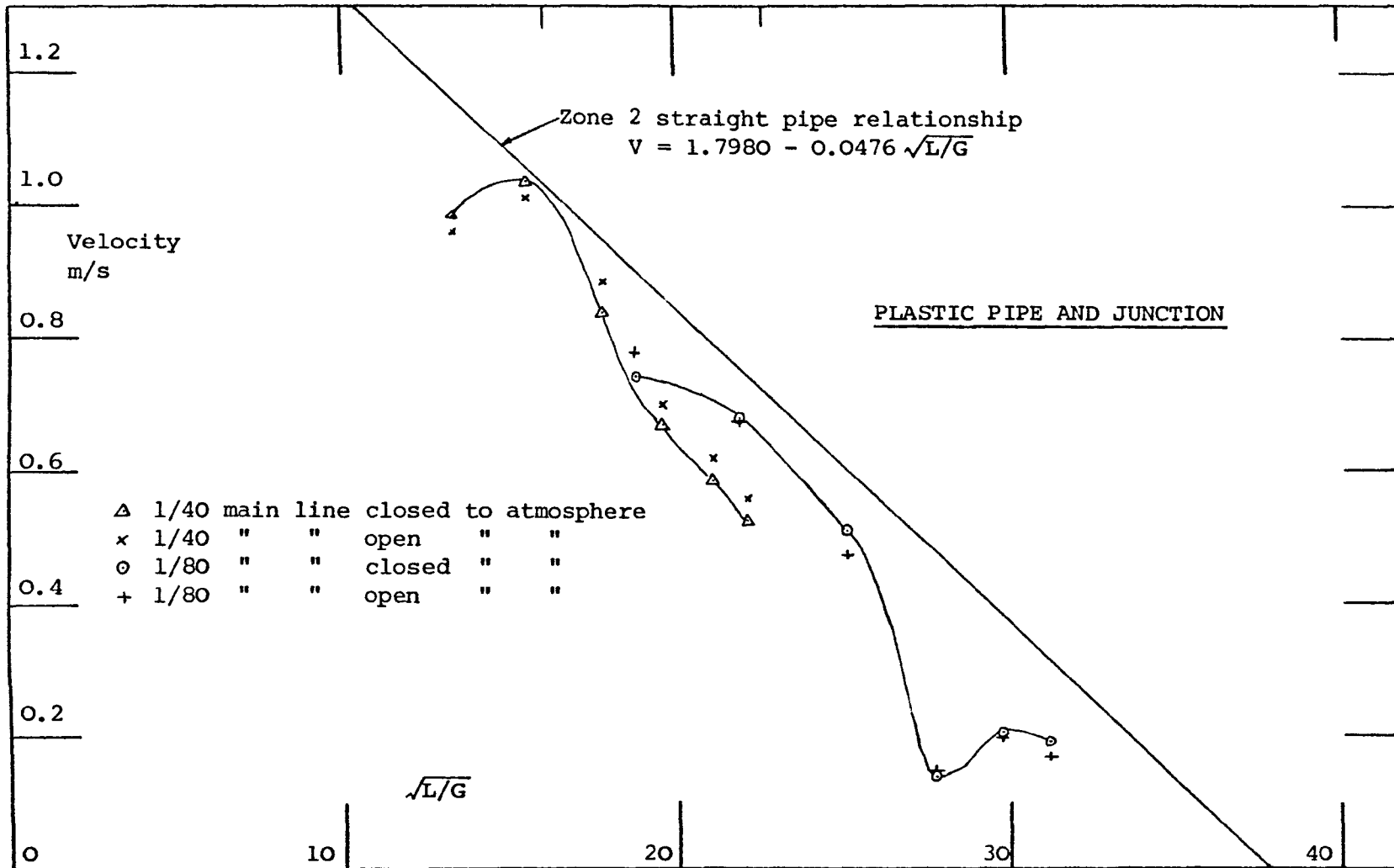


FIGURE 111. (APLV3) 135° Junction at 6.437 metres from w.c., main line closed to atmosphere. Entry to main line via a 148° adjustable bend and 135° Junction with 45° entry. Armitage Shanks P-trap low level w.c., maternity pad plus three Bowtowels, vented. Velocity profile plotted against square root of (Distance along pipe/Gradient) showing variation due to a junction compared to Zone 2 straight pipe relationship.



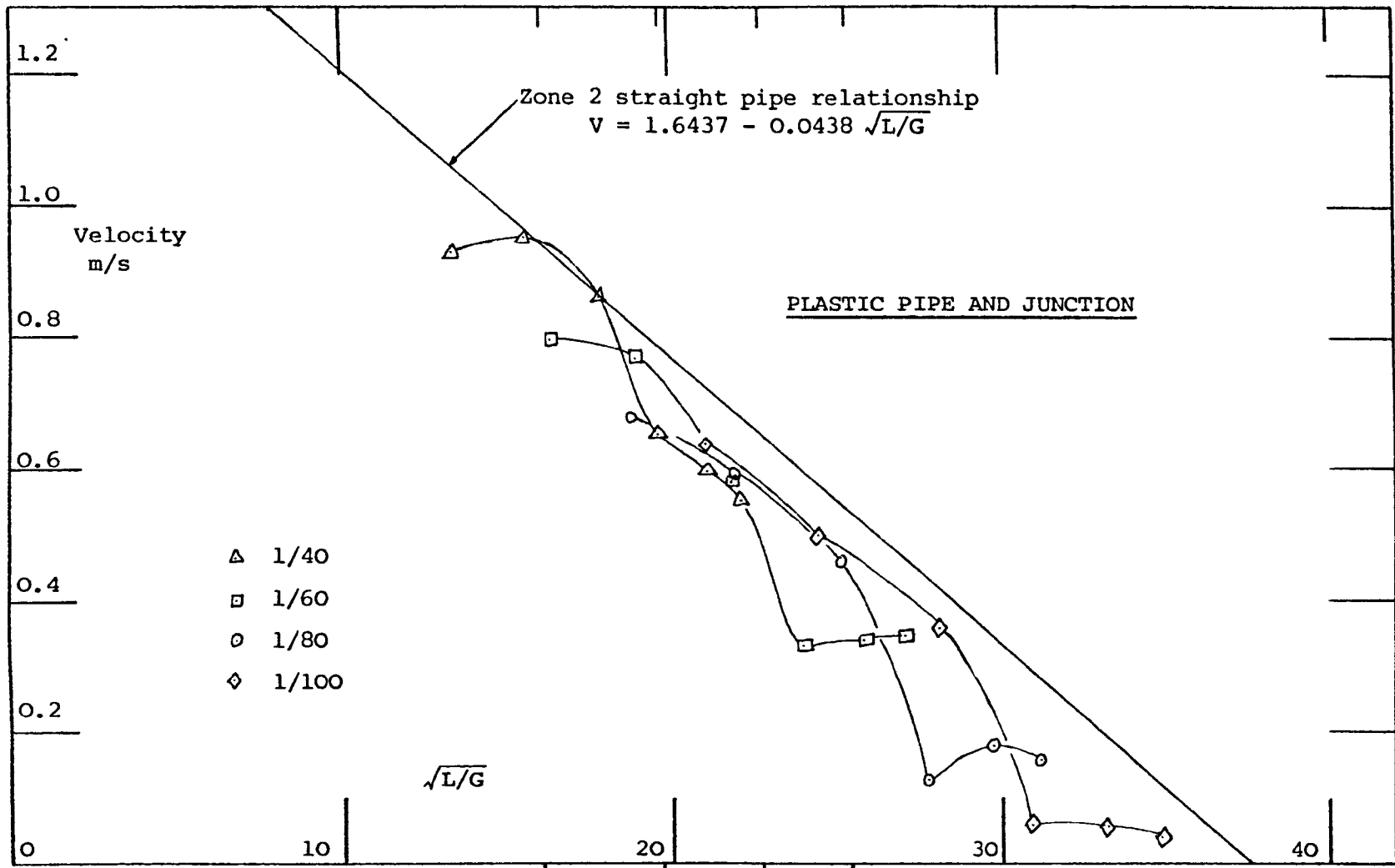
Junction position relative to  $\sqrt{L/G}$

FIGURE 112. (APLU1) 135° Junction at 6.430 metres from w.c.

Entry to main line via a 135° bend and a 135° junction with vertical entry.

Armitage Shanks P-trap low level w.c., single maternity pad, unvented.

Velocity profiles plotted against square root of (Distance along pipe/Gradient) showing variation due to venting or unventing main line pipe compared to Zone 2 straight pipe relationship.



Junction position relative to  $\sqrt{L/G}$   $\Delta$   $\square$   $\circ$   $\diamond$

FIGURE 113. (APLV1) 135° Junction at 6.430 metres from w.c., main line closed to atmosphere. Entry to main line via a 135° bend and 135° junction with vertical entry. Armitage Shanks P-trap low level w.c., single maternity pad, vented. Velocity profiles plotted against square root of (Distance along pipe/Gradient) showing variation due to a junction compared to Zone 2 straight pipe relationship.

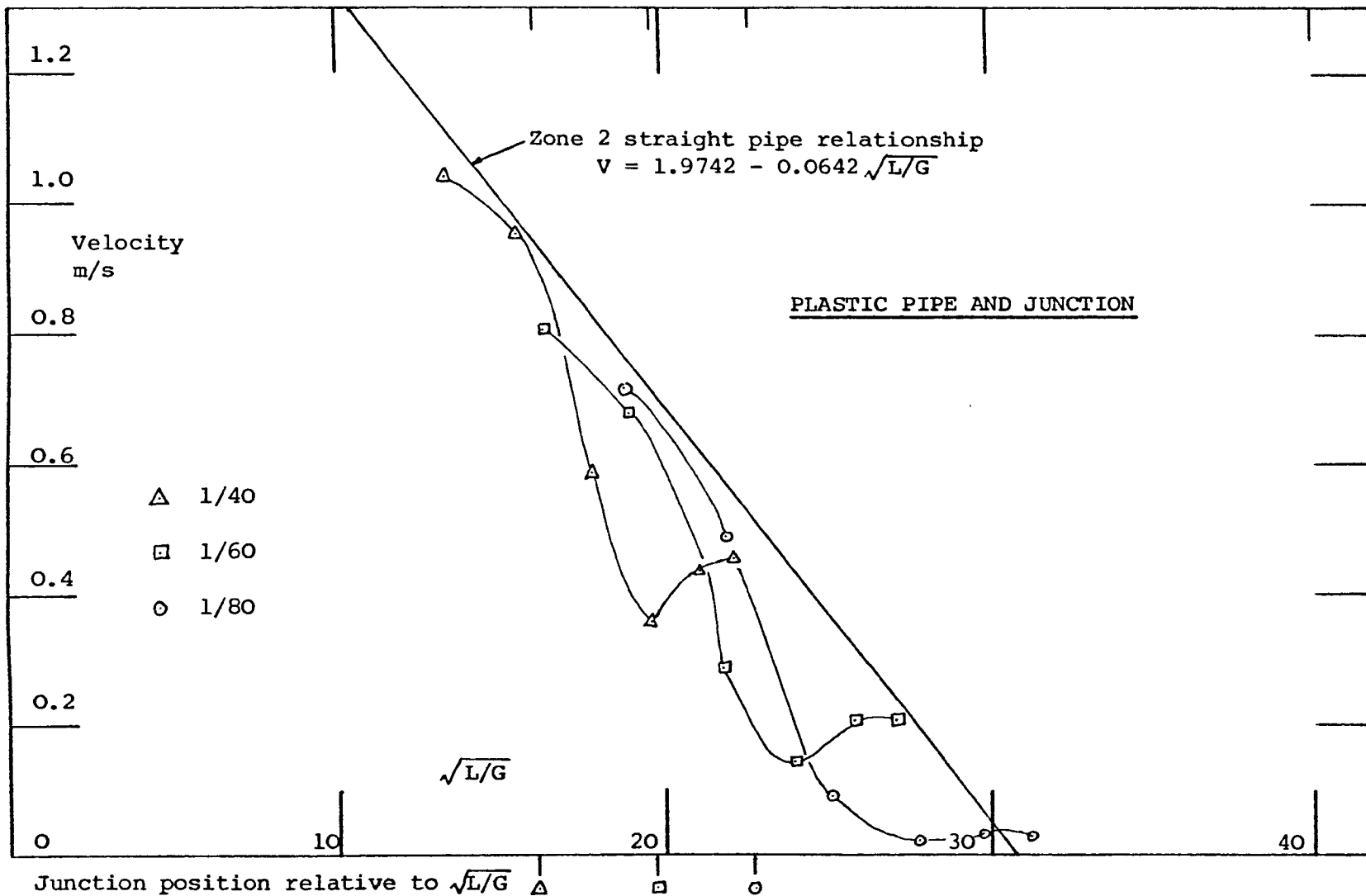


FIGURE 114. (APLV2) 135° junction at 6.430 metres from w.c. Main line closed to atmosphere. Entry to main line via a 135° bend and 135° junction with vertical entry. Armitage Shanks P-trap low level w.c., maternity pad plus three Kleenex paper towels, vented. Velocity profiles plotted against square root of (Distance along pipe/Gradient) showing variation due to a junction compared to zone 2 straight pipe relationship.

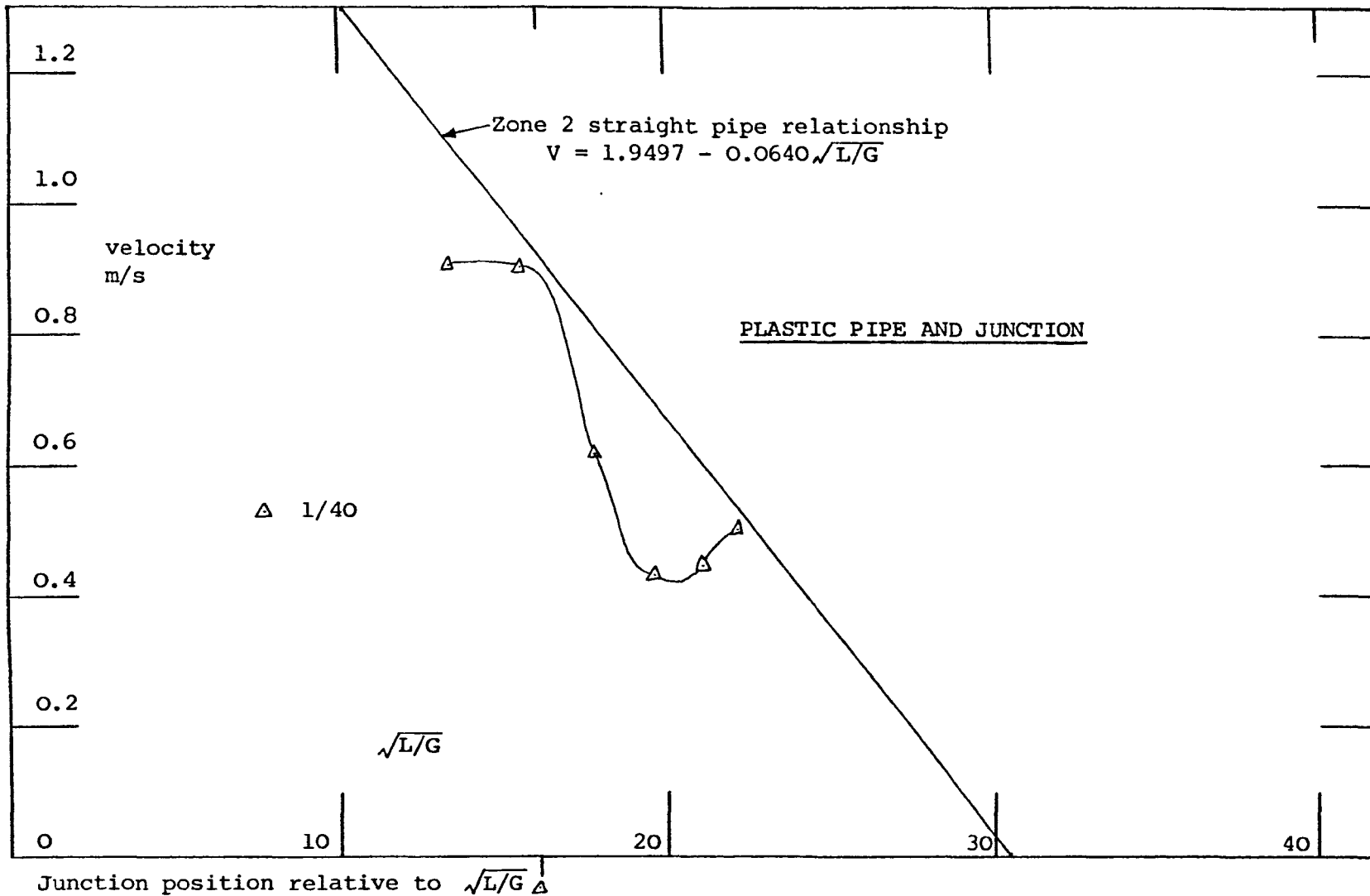


FIGURE 115. (APLV3) 135° Junction at 6.430 metres from w.c., main line closed to atmosphere  
 Entry to main line via a 135° bend and 135° junction with vertical entry.  
 Armitage Shanks P-trap low level w.c., maternity pad plus three Bowtowels, vented.  
 Velocity profile plotted against square root of (Distance along pipe/Gradient) showing  
 variation due to a junction compared to Zone 2 straight pipe relationship.

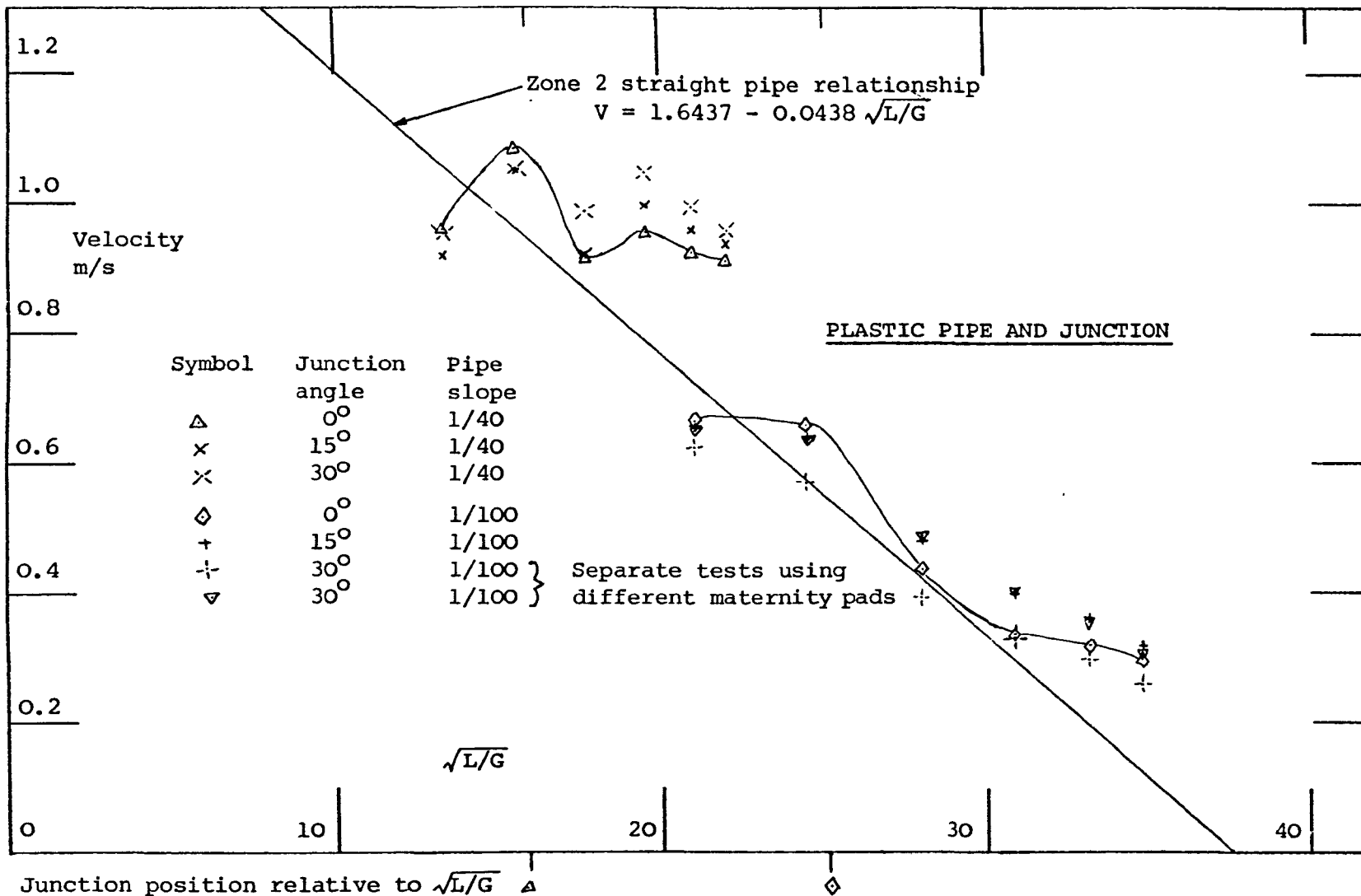


FIGURE 116. (APLV1) 135° junction at 6.332 metres from w.c. Branch closed to atmosphere. Straight pipe flow through junction with junction entry at varying angles. Armitage Shanks P-trap low level w.c., single maternity pad, vented. Velocity profiles plotted against square root of (Distance along pipe/Gradient) showing variation due to a junction compared to Zone 2 straight pipe relationship.

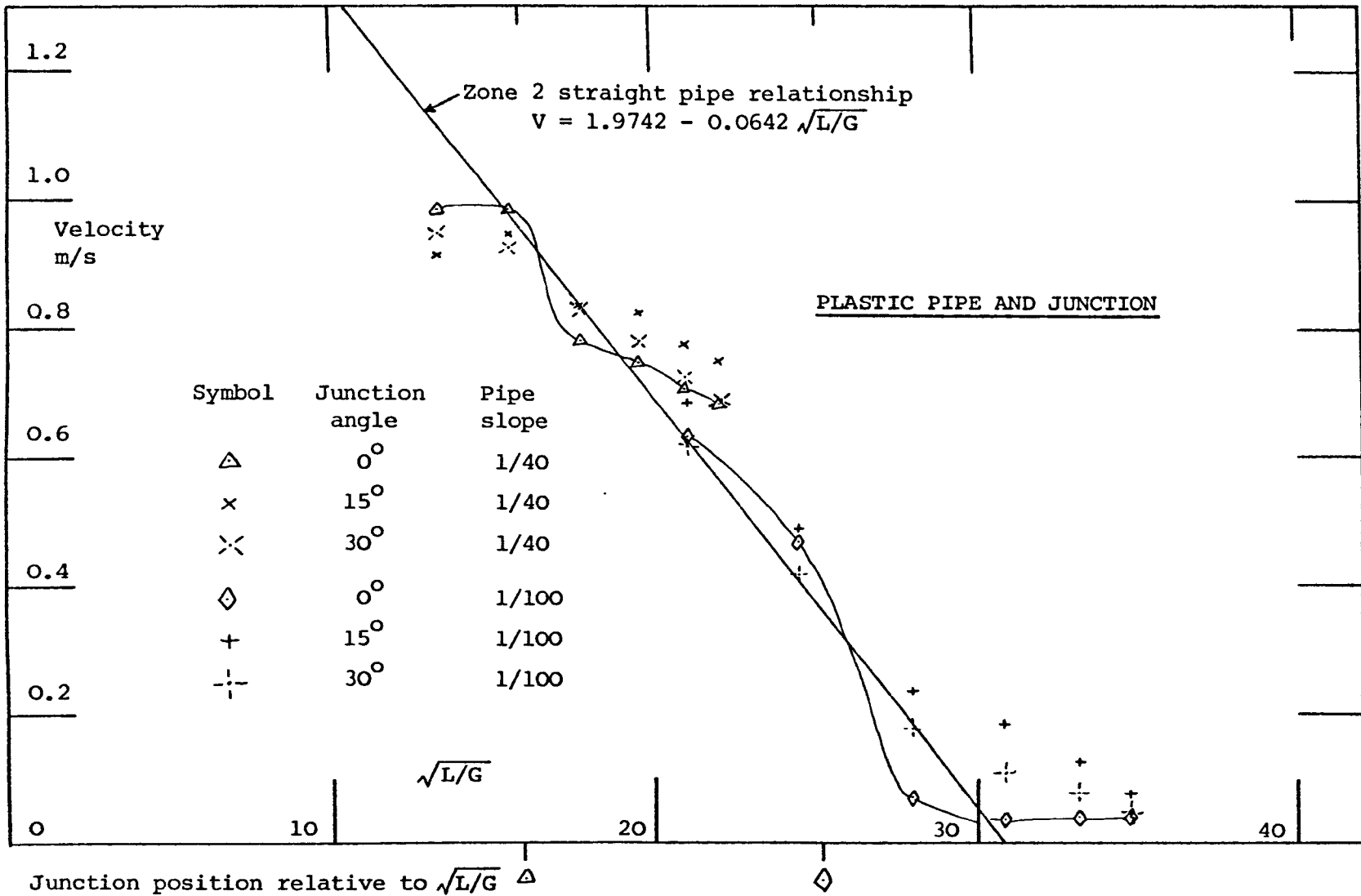


FIGURE 117. (APLV2) 135° Junction at 6.332 metres from w.c. Branch closed to atmosphere. Straight pipe flow through junction with junction entry at varying angles. Armitage Shanks P-trap low level w.c., maternity pad plus three Kleenex paper towels, vented. Velocity profiles plotted against square root of (Distance along pipe/Gradient) showing variation due to a junction compared to zone 2 straight pipe relationship.

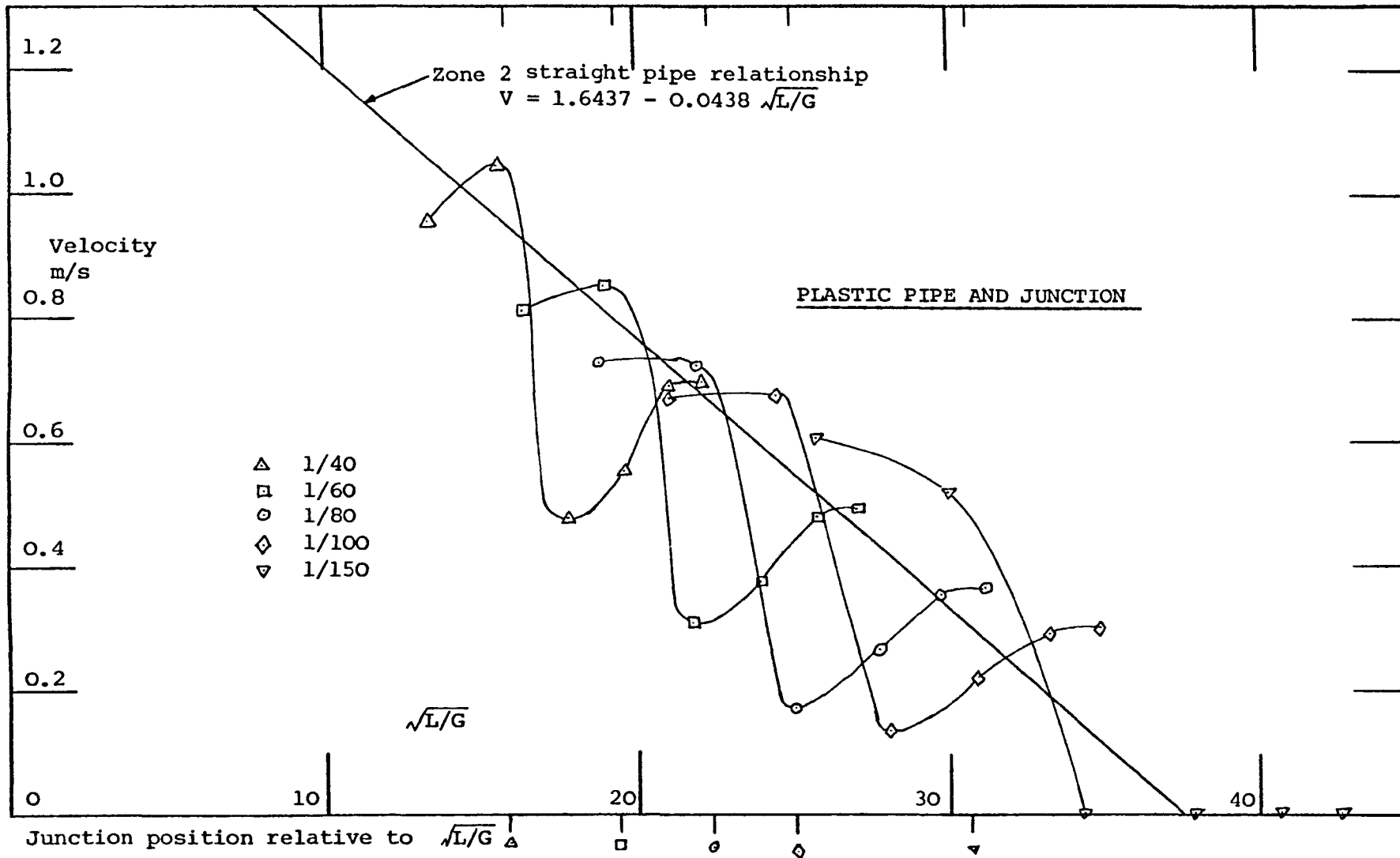


FIGURE 118. (APLV1)  $92\frac{1}{2}^\circ$  Junction at 6.288 metres from w.c., main line closed to atmosphere. Entry to main line via a  $92\frac{1}{2}^\circ$  junction with horizontal entry. Armitage Shanks P-trap low level w.c., single maternity pad, vented. Velocity profiles plotted against square root of (Distance along pipe/Gradient) showing variation due to a junction compared to Zone 2 straight pipe relationship.



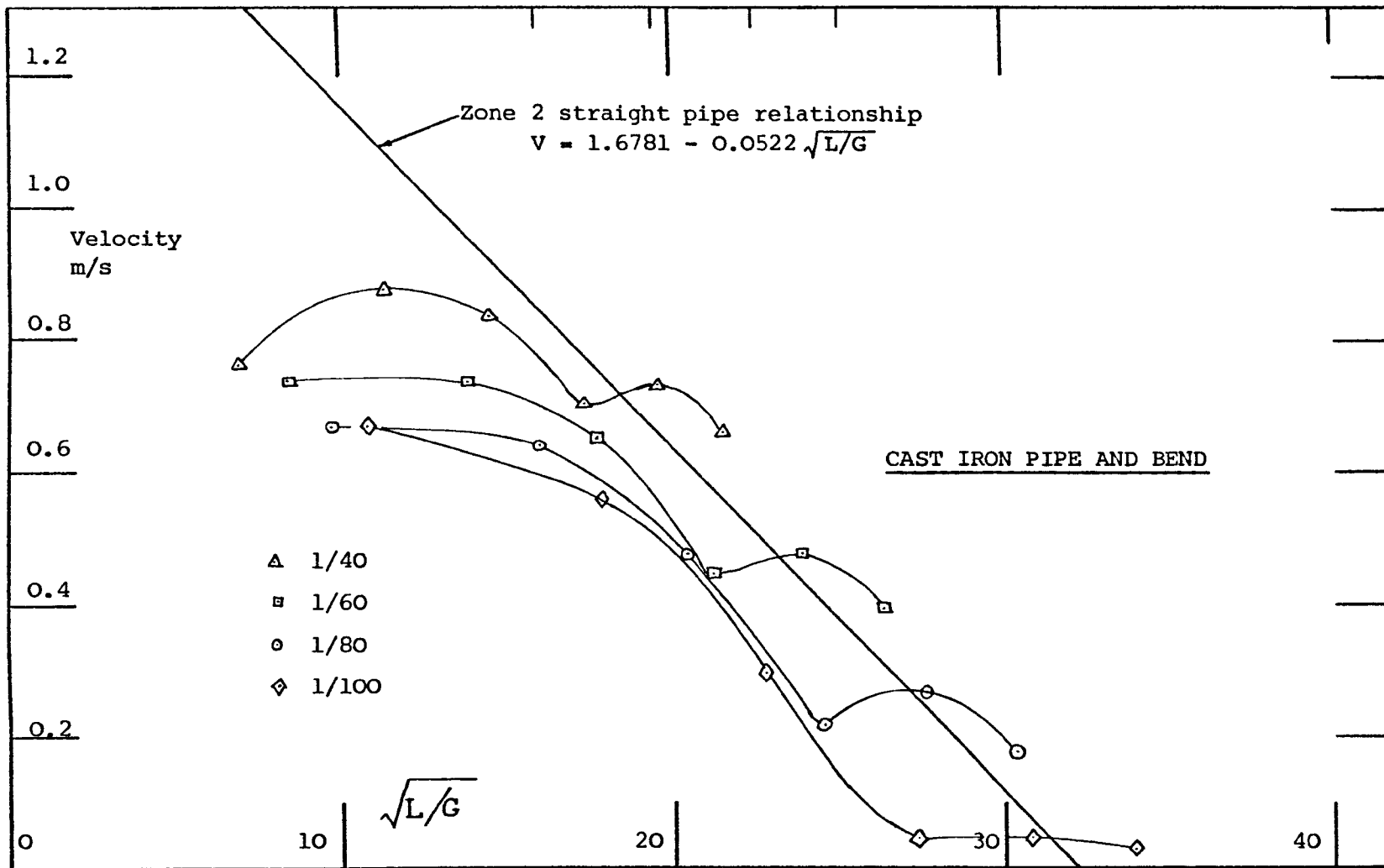
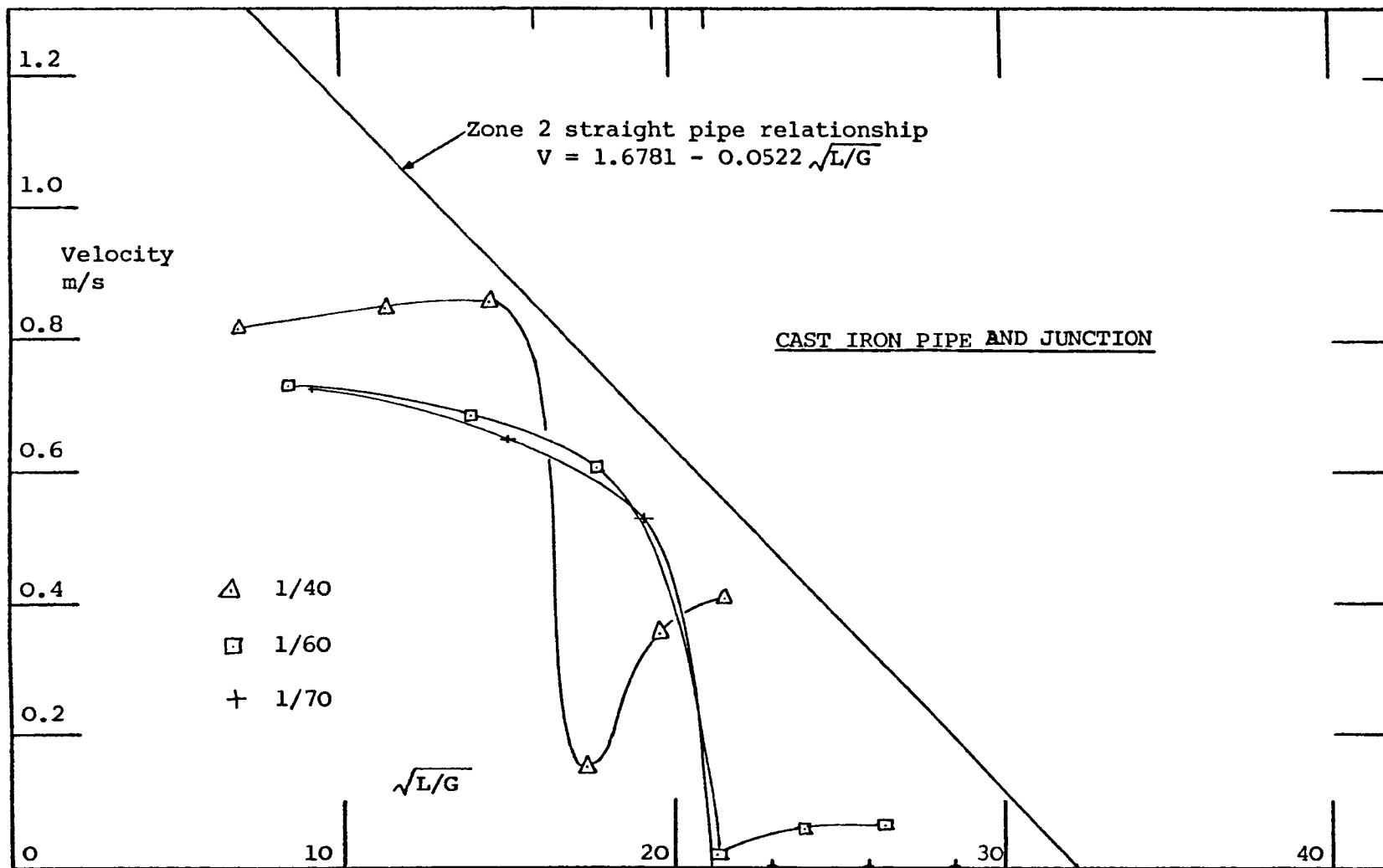
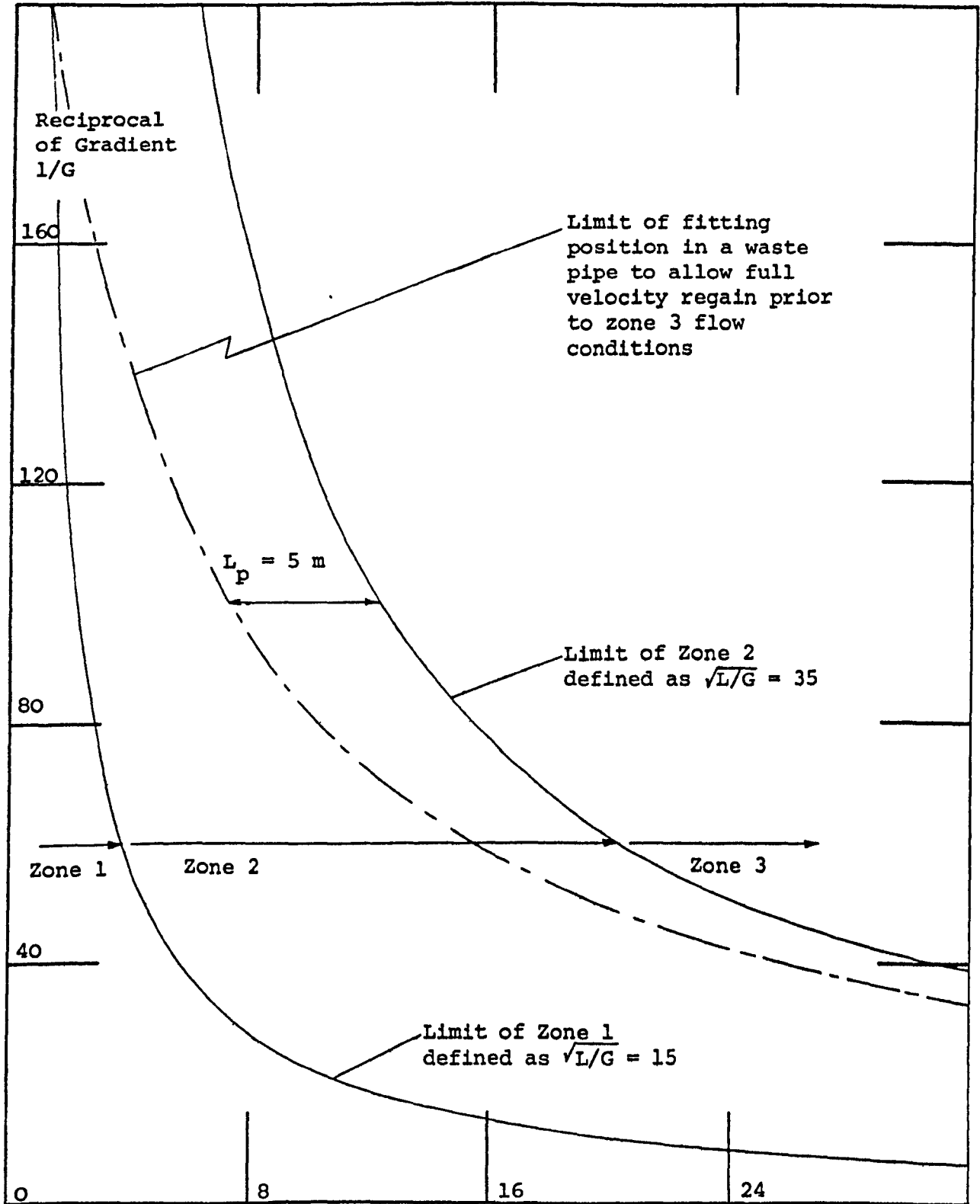


FIGURE 120. (APLV1) Cast iron 92½° bend at 6.323 metres from w.c.  
 Armitage Shanks P-trap low level w.c., single maternity pad, vented.  
 Velocity profiles plotted against square root of (Distance along pipe/Gradient)  
 showing variation due to a bend compared to Zone 2 straight pipe relationship.



Junction position relative to  $\sqrt{L/G}$

FIGURE 121. (APLV1) Cast iron 92½° junction at 6.323 metres from w.c. Main line closed to atmosphere Entry to main line via a 92½° junction with horizontal entry. Armitage Shanks P-trap low level w.c., single maternity pad, vented Velocity profiles plotted against square root of (Distance along pipe/Gradient) showing variation due to a junction compared to zone 2 straight pipe relationship.



Discharge pipe length from W.C. inlet. L m.

FIGURE 122. Schematic representation of the relationships governing zone boundaries and the effect of pipe fittings, such as bends or junctions, relative to Zone 3.  
 Zone limits taken as- Zone 1,  $\sqrt{L/G} < 15$   
 Zone 2,  $15 < \sqrt{L/G} < 35$ , Zone 3,  $\sqrt{L/G} < 35$ .  
 Applicable to plastic pipe and a single maternity pad.

TABLE 1. Summary of W.C. discharge characteristics test results including discharge velocities, %FAS,  $F_1$  and  $F_2$

W.c. / Test Code	No. Flushes	W.C. Failure Rate %	W.C. Partial Failure Rate %	Solid Velocity m/s			Mean % Flush Ahead of solid
				Min	Max	Mean	
APLU1	49	2	-	1.240	1.768	1.539	21.7
APLV1	50	0	-	1.372	1.880	1.592	19.9
APLU2	50	0	1.3	1.040	2.007	1.475	19.7
APLV2	52	0	3.2	0.963	2.139	1.546	18.9
APLU3	50	0	12.7	0.930	1.795	1.439	21.3
APLV3	50	0	18.0	1.056	2.431	1.674	25.4
ASLU1	50	2	-	0.980	3.319	1.679	23.6
ASLV1	50	4	-	1.235	2.302	1.709	25.3
ASLU3	50	19	10.7	0.947	3.422	1.709	23.9
ASLV3	50	29	8.0	0.982	2.937	1.829	22.9
ASLU2	50	24	1.3	0.962	2.701	1.796	20.9
ASLV2	50	28	3.3	1.062	2.757	1.781	24.0
TSHU5	30	0	-	1.709	2.655	2.113	24.2
TSHV5	30	0	-	1.708	2.347	2.043	24.3
TSHU6	40	0	0	1.509	2.411	2.026	25.5
TSHV6	30	0	0	1.680	2.294	2.009	26.6
TSHV4	30	0	-	1.774	2.246	1.998	26.0
TPLU1	30	0	-	1.463	1.843	1.683	21.2
TPLV1	30	0	-	1.583	2.195	1.849	20.0
TPLU2	40	0	9.2	1.017	1.970	1.558	26.5
TPLV2	50	2	8.0	1.005	2.467	1.581	27.3
TSLU1	30	0	-	1.563	2.372	1.875	25.5
TSLV1	30	0	-	1.672	2.249	1.934	27.4
TSLU2	40	0	3.3	1.386	2.199	1.854	29.1
TSLV2	40	0	0	1.587	2.405	1.997	30.8
TSHU1	30	12	-	1.095	2.252	1.803	38.5
TSHV1	30	14	-	1.527	2.221	1.865	38.9
TSHU2	30	3	8.9	1.494	2.542	1.900	33.5
TSHV2	30	12	2.2	1.162	2.317	1.811	30.6
TPHU1	30	0	-	1.131	1.941	1.609	30.5
TPHV1	30	0	-	1.160	2.127	1.636	31.3
TPHU2	40	0	0	0.993	2.097	1.471	30.0
TPHV2	40	5	4.2	1.148	2.277	1.660	29.5
APHU1	30	0	-	1.381	2.001	1.684	22.5
APHV1	30	3	-	1.353	2.258	1.779	24.0
APHU2	30	6	0	1.342	1.961	1.645	17.8
APHV2	30	0	0	1.495	2.432	1.883	17.2
APHV4	20	0	-	1.471	2.155	1.738	21.2
ASHU1	30	0	-	1.582	2.306	1.957	23.8
ASHV1	30	3	-	1.834	2.323	2.047	23.5
ASHU2	30	3	1.1	1.433	2.288	1.810	19.8
ASHV2	30	0	1.1	1.509	2.438	1.903	24.4
ASHV4	20	0	-	1.588	2.212	1.998	20.2

TABLE 2. Summary of the results obtained from testing a new Armitage Shanks S-trap low level cistern W.C. unit, compared to the previous results (in parenthesis). Tests carried out as part of W.C. discharge characteristic testing. Results from single maternity pads and maternity pads plus three Kleenex paper towel tests, with both vented and unvented W.C. discharge.

W.C. Test Code	Test No.	No. Flushes	W.C. Failure Rate %	W.C. Partial Failure Rate %	Solid Velocity m/s			%FAS
					Min.	Max.	Mean	
ASLUI	44 (7)	30 (50)	0 (2)	0 (0)	1.709 (0.980)	2.358 (3.319)	1.971 (1.679)	22.6 (23.6)
ASLVI	45 (8)	30 (50)	0 (4)	0 (0)	1.684 (1.235)	2.143 (2.302)	1.941 (1.709)	20.7 (25.3)
ASLU2	46 (11)	40 (50)	0 (24)	2.5 (1.3)	1.402 (0.962)	2.428 (2.701)	1.894 (1.796)	20.3 (20.9)
ASLV2	47 (12)	40 (50)	0 (28)	2.5 (3.3)	1.386 (1.062)	2.339 (2.757)	1.883 (1.781)	20.7 (24.0)

TABLE 3. Results of the straight plastic pipe tests.  
 Tabulation of the W.C. failure rate ( $F_1$ ), partial W.C. failure rate ( $F_2$ ) and various coefficients related as follows:

$$V = C_1 - C_2 \sqrt{L/G}$$

$$C_3 = C_1/C_2 \text{ which gives the value of } \sqrt{L/G} \text{ at } V = 0$$

TEST CODE	$C_1$ MS <sup>-1</sup>	$C_2$ M <sup>1/2</sup> S <sup>-1</sup>	$C_3$ M <sup>-1/2</sup>	$F_1$ %	$F_2$ %
APLU1	1.7980	0.0476	37.77	0.6	-
APLU2	2.0154	0.0623	32.35	0.8	0.3
APLU3	2.1857	0.0707	30.92	1.6	9.6
APLV1	1.6437	0.0438	37.53	1.3	-
APLV2	1.9742	0.0642	30.75	2.5	1.5
APLV3	1.9497	0.0640	30.46	4.1	14.2
ASLU1	1.8415	0.0459	40.12	0	-
ASLU2	2.2484	0.0663	33.91	5.0	1.0
ASLU3	2.0746	0.0614	33.79	8.3	11.7
ASLV1	1.8437	0.0455	40.52	0	-
ASLV2	2.2057	0.0639	34.52	8.3	2.7
ASLV3	2.3048	0.0710	32.51	3.3	15.5
TPLU1	1.4935	0.0411	36.34	1.6	-
TPLU2	1.4648	0.0506	28.95	1.6	11.3
TPLU3	1.4954	0.0514	29.09	1.6	28.3
TPLV1	1.4346	0.0380	37.75	1.6	-
TPLV2	1.6764	0.0598	28.03	0	5.0
TPLV3	1.7725	0.0641	27.65	0	36.0
TSLU1	1.8337	0.0468	39.18	0	-
TSLU2	2.1431	0.0673	31.84	0	0
TSLU3	2.3574	0.0739	31.90	0	13.3
TSLV1	1.8200	0.0464	39.22	0	-
TSLV2	1.9937	0.0607	32.85	0	3.3
TSLV3	1.9598	0.0617	31.76	0	4.9

STRAIGHT PLASTIC PIPE

## % FLUSH AHEAD OF SOLIDS

TEST CODE	W.C. DISCHARGE CHARACTERISTIC TESTS	SOLID DECELERATION CHARACTERISTIC TESTS				
		1/40	1/60	1/80	1/100	1/150
APLU1	21.7	20.6	22.7	25.0	23.3	25.3
APLU2	19.7	17.8	24.9	28.2	28.7	-
APLU3	21.3	24.4	27.8	33.0	28.1	-
APLV1	19.9	17.0	27.5	31.0	31.8	21.3
APLV2	18.9	17.8	25.3	30.1	27.5	-
APLV3	25.4	25.5	29.4	32.0	28.1	-
ASLU1	22.6		17.7		23.3	
ASLU2	20.3		21.8		28.9	
ASLU3	-		24.5		31.7	
ASLU4	-		36.5		-	
ASLV1	20.7		16.8		22.0	
ASLV2	20.7		25.1		28.6	
ASLV3	-		24.2		30.0	
ASLV4	-		33.6		-	
TPLU1	21.2		36.0		36.5	
TPLU2	26.5		42.6		41.1	
TPLU3	-		39.6		49.5	
TPLV1	20.0		36.6		40.4	
TPLV2	27.3		41.9		39.6	
TPLV3	-		37.0		51.25	
TSLU1	25.5		28.5		31.5	
TSLU2	29.1		32.4		31.1	
TSLU3	-		44.6		39.4	
TSLV1	27.4		32.1		36.0	
TSLV2	30.8		32.9		34.1	
TSLV3	-		57.8		37.9	

TABLE 4 % flush ahead of solid (%FAS) measured at collection tank during the straight plastic pipe testing and including the comparable results from the W.C. discharge characteristic tests.

TABLE 5. Results from straight cast iron pipe tests. Tabulation of % flush ahead of solid (%FAS) measured at collection tank.

TEST CODE	%FAS 1/40	%FAS 1/60	%FAS 1/80	%FAS 1/100	%FAS 1/150
APLU1	19.5	21.6	25.2	25.8	23.9
APLU2	23.1	27.8	33.0	34.4	
APLV1	15.5	24.2	28.0	26.7	21.5
APLV2	21.3	26.3	28.7	36.5	
TSLU1		30.1		28.2	

STRAIGHT CAST IRON PIPE

TABLE 6. Results from straight cast iron pipe tests. Tabulation of the W.C. failure rate ( $F_1$ ), partial W.C. failure rate ( $F_2$ ) and various coefficients related as follows:

$$V = C_1 - C_2 \sqrt{L/G}$$

$$C_3 = C_1/C_2 \text{ which gives the value of } \sqrt{L/G} \text{ at } V = 0$$

$$C_4 = \frac{C_3(\text{UPVC}) - C_3(\text{CI})}{C_3(\text{UPVC})} \times 100$$

TEST CODE	$C_1$ MS <sup>-1</sup>	$C_2$ M <sup>1/2</sup> S <sup>-1</sup>	$C_3$ M	$C_4$ %	$F_1$ %	$F_2$ %
APLU1	1.6339	0.0503	32.48	14.0	0	-
APLU2	1.9193	0.0727	26.40	18.4	5.0	1.67
APLV1	1.6781	0.0522	32.15	14.3	0	-
APLV2	1.9066	0.0735	25.94	15.6	5.83	1.11
TSLU1	1.9320	0.0511	37.81	4.0	0	-

STRAIGHT CAST IRON PIPE

TABLE 7. Results from straight glass pipe tests.  
Tabulation of % flush ahead of solid (%FAS)  
measured at collection tank.

TEST CODE	%FAS 1/40	%FAS 1/60	%FAS 1/80	%FAS 1/100	%FAS 1/150
APLV1	23.7	29.1	32.3	30.8	20.1
APLV2	24.8	34.4	29.4	24.8	-

## STRAIGHT GLASS PIPE

TABLE 8. Results from straight glass pipe tests.  
Tabulation of W.C. failure rate ( $F_1$ ), partial W.C. failure rate  
( $F_2$ ) and various coefficients related as follows:

$$V = C_1 - C_2 \sqrt{L/G}$$

$$C_3 = C_1/C_2 \text{ which gives the value of } \sqrt{L/G} \text{ at } V = 0$$

$$C_4 = \frac{C_3(\text{UPVC}) - C_3(\text{GLASS})}{C_3(\text{UPVC})} \times 100 \%$$

TEST CODE	$C_1$ MS <sup>-1</sup>	$C_2$ M <sup>1/2</sup> S <sup>-1</sup>	$C_3$ M <sup>-1/2</sup>	$C_4$ %	$F_1$ %	$F_2$ %
APLV1	1.6819	0.0484	34.75	7.4	0.9	-
APLV2	1.8424	0.0597	30.86	-0.4	11.3	3.7

## STRAIGHT GLASS PIPE

TABLE 9. Summary of results for the UPVC bend tests giving the values of  $\Delta V$ ,  $L_p$ , % FAS for all the tests in this series.

Test	Bend Angle	Test No	Bend posn	Pipe Gradient	$\Delta V$	$L_p$	%FAS
	degrees		metres	l/	m/s	m	%
APLU1	135	341	3.88	70	0.15	4.6	24.0
		344		80	0.13	3.6	23.0
		347		90	0.19	4.1	31.8
		350		100	0.11	3.2	30.1
		353		150	-0.14	-	31.8
APLU1	135	301	5.90	40	0.08	3.4	21.7
		316		50	0.12	5.2	27.2
		304		60	0.17	5.3	20.8
		307		80	0.15	5.3	24.3
		310		100	0.17	5.0	24.1
		313		150	0.02	1.8	27.9
APLU1	135	321	7.937	40	0.12	5.1	22.4
		324		50	0.14	5.0	25.5
		327		60	0.14	4.9	27.6
		330		70	0.12	4.4	26.3
		333		80	0.11	3.8	29.1
APLV1	135	342	3.88	70	0.10	4.0	21.0
		345		80	0.08	3.4	23.8
		348		90	0.07	3.3	27.3
		351		100	0.14	3.2	30.0
		354		150	-0.10	2.1	31.3
APLV1	135	302	5.90	40	0	-	24.3
		317		50	0	1.5	25.1
		305		60	0.06	2.9	18.4
		308		80	0.12	4.9	24.5
		311		100	0.11	4.7	25.3
		314		150	0.03	2.2	29.6
APLV1	135	322	7.937	40	0.04	2.9	23.6
		325		50	0.08	4.2	26.4
		328		60	0.04	3.2	24.4
		331		70	0.04	2.9	24.4
		334		80	0.14	4.1	37.9
APLV2	135	343	3.88	70	0.12	3.0	25.8
		346		80	0.12	-	31.3
		349		90	0.05	4.6	31.1
		352		100	0.03	4.2	34.8
APLV2	135	303	5.90	40	0.08	4.6	24.0
		318		50	0.07	3.5	24.1
		306		60	0.13	4.1	24.0
		309		80	0.12	2.8	22.8
		312		100	0.09	2.9	29.2
APLV2	135	323	7.937	40	0.07	3.3	23.0
		326		50	0.17	3.9	31.0
		329		60	0.04	1.8	26.4
		332		70	0.09	2.4	30.5

TABLE 9 (continued)

Test	Bend angle	Test No	Bend posn	Pipe Gradient	$\Delta V$	Lp	%FAS
	degrees		metres	1/	m/s	m	
APLV1	2 x 135	431	5.927 )	40	0.13	4.1	20.8
		432	7.010 )	80	0.15	4.2	24.6
APLU1	92½	401	3.93	70	0.21	4.7	22.3
		403		80	0.17	4.7	24.3
		405		90	0.15	4.7	28.1
		407		100	0.20	-	34.8
		409		150	0.20	-	31.0
APLV1	92½	402	3.93	70	0.13	4.7	23.8
		404		80	0.14	4.8	28.4
		406		90	0.13	5.0	31.9
		408		100	0.13	5.4	31.5
		410		150	0.18	5.1	31.6
APLV1	92½	411	5.975	40	0.15	5.4	33.2
		412		50	0.15	5.2	30.8
		413		60	0.18	5.4	32.0
		414		70	0.12	4.9	24.5
		415		80	0.09	4.2	24.8
		416		90	0.09	4.3	25.9
		417		100	0.09	3.7	26.9
		418		150	0.04	2.8	24.6
APLV1	92½	421	8.017	40	-0.01	-	24.7
		422		50	0	-	24.1
		423		60	0.08	3.8	26.1
		424		70	0.09	3.8	28.4
		425		80	0.12	4.0	27.8

TABLE 10. Summary of results for the UPVC junction tests giving the values of  $\Delta V$ ,  $L_p$ , %FAS for all the tests in this series.

Test	Junct type	Test No	Junct posn	Pipe Gradient	$\Delta V$	$L_p$	%FAS
	degrees		m	1/	m/s	m	
APLU1 Horiz.entry	135	501	6.332	40	0.21	4.7	20.8
APLV1 Horiz.entry	135	502	6.332	40	0.13	3.9	21.5
		505		60	0.16	5.0	22.7
		507		80	0.19	4.8	25.5
		509		100	0.25	4.4	26.8
APLV2 Horiz.entry	135	503	6.332	40	0.27	4.9	27.8
		506		60	0.32	4.3	25.6
		508		80	0.33	4.9	24.8
APLV3 Horiz.entry	135	504	6.332	40	0.21	4.6	28.2
APLU1 45° entry	135	510	6.437	40	0.11	4.8	19.8
APLV1 45° entry	135	511	6.437	40	0.08	4.8	24.5
		514		60	0.10	4.9	26.4
		516		80	0.04	4.5	25.5
		518		100	0	3.2	26.1
		520		150	0	2.5	29.8
APLV2 45° entry	135	512	6.437	40	0.15	4.4	23.8
		515		60	0.05	4.1	24.9
		517		80	0	—	25.3
		519		100	0.04	2.3	24.1
APLV3 45° entry	135	513	6.437	40	0.10	4.8	24.7
APLU1 vert.entry Branch closed	135	452	6.430	40	0.22	—	19.1
" open		451		40	0.19	—	18.1
" closed		459		80	0.35	—	22.2
" open		460		80	0.34	5.8	25.5
APLV1 vert.entry	135	453	6.430	40	0.13	—	18.3
		456		60	0.27	8.2	20.3
		458		80	0.31	—	23.7
		462		100	0.24	7.1	25.2

TABLE 10.(continued)

Test	Junct type	Test No	Junct posn	Pipe Gradient	$\Delta V$	Lp	%FAS
	degrees		m	1/	m/s	m	%
APLV2 vert. entry	135	454	6.430	40	0.35	7.7	22.7
		457		60	0.30	6.3	23.0
		461		80	0.29	5.1	23.8
APLV3 vert. entry	135	455	6.430	40	0.23	6.1	23.1
APLV1 Horiz. entry	92½	521	6.288	40	0.38	5.3	18.1
		523		60	0.38	5.2	17.9
		525		80	0.38	4.7	19.3
		526		100	0.29	3.8	20.0
		527		150	0.18	-	18.5
APLV2 Horiz. entry	92½	522	6.288	40	0.60	8.6	21.0
		524		60	0.51	8.5	21.4
APLV1 Straight pipe flow through junction	135	531	6.332	40	0		14.8
		533		100	0		19.4
		535		100	15		22.7
		537		40	15		17.8
		539		40	30		15.9
		541		100	30		23.6
		543		100	30		25.9
		544		100	30		26.3
545	100	30		23.0			
APLV2 Straight pipe flow through junction	135	532	6.332	40	0		17.9
		534		100	0		19.0
		536		100	15		24.1
		538		40	15		19.2
		540		40	30		19.3
		542		100	30		29.9

TABLE 11. Summary of results for the cast iron bend and junction tests giving the values of  $\Delta V$  and  $L_p$  for all the tests in this series, all tests being APLV1.

Test	Test No	Junction/ Bend position	Pipe Gradient	$\Delta V$	$L_p$	%FAS
		m	1/	m/s	m	%
92½° bend	601	6.323	40	0.07	2.1	24.2
	602		60	0.14	2.5	24.9
	603		80	0.19	2.9	29.4
	604		100	0.21	3.5	23.2
92½° junction horizontal entry	610	6.323	40	0.63	8.1	26.4
	611		60	0.56	-	24.0
	612		70	0.59	-	25.7

12. APPENDICES

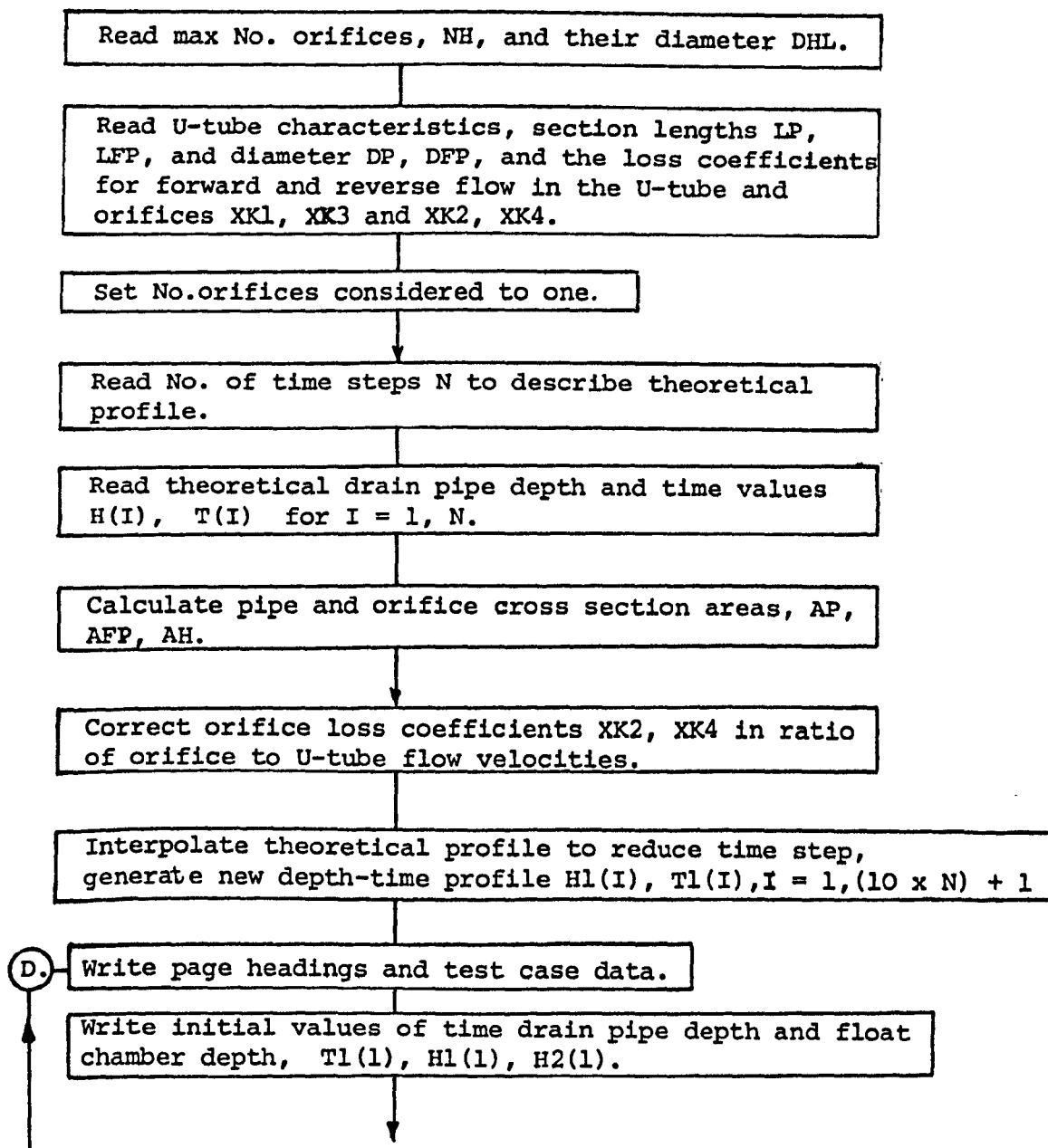
Appendices I to III contain flow diagrams, computer program print outs and examples of the computer output for each of the three main computer programs FLOT and SLOT, WCHAR, and LSQ1 respectively.

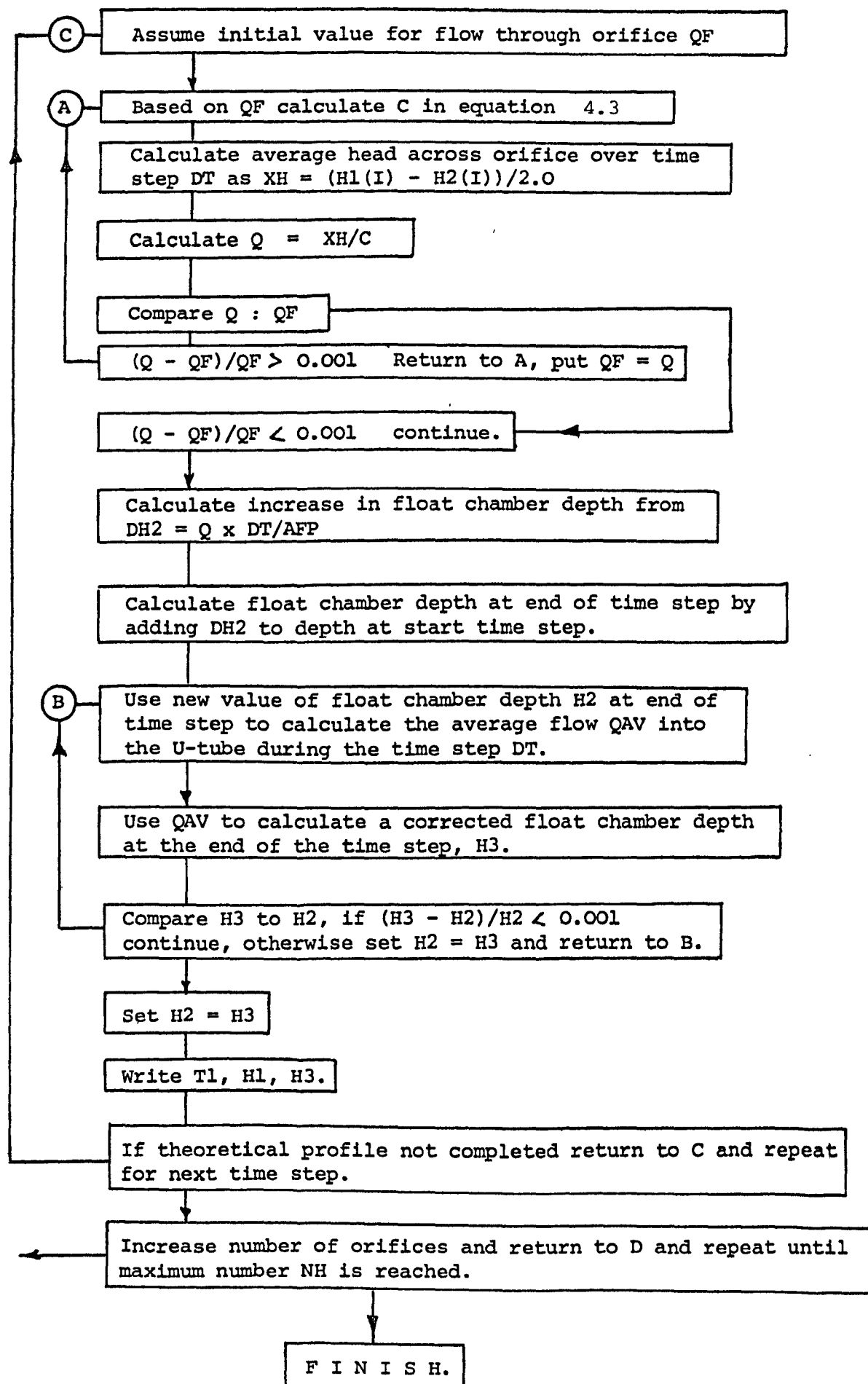
12.1 APPENDIX I. Prediction of Depth Measuring System  
Response. Computer Programs FLOT and SLOT

As described in section 5.2 the response of the float - LVDT depth recording system was predicted by a simple computer program utilising known fitting and orifice loss coefficients.

Two similar computer programs were used, namely FLOT, which dealt with circular orifices, and SLOT, which dealt with slot orifices. A flow diagram common to both FLOT and SLOT is presented together with a print out of both programs. An example of the output from the programs is included after the print out of each program.

## AI.1 Flow diagram FLOT/SLOT.





## AI.2 Print out and Output of Computer Program FLOT.

```

PROGRAM(FLOT)
INPUT 5 = CRO
OUTPUT 4 = LPO
END

```

```

MASTER KINGSIX
REAL LP, LFP
DIMENSION H1(100),H2(100),H(10),T(10),T1(100),H3(100)
20 READ(5,20) NH, DHL
FORMAT(I3, F10.6 )
NHF = NH
NH=4
1 READ(5,1)LP,DP,LFP,DFP,XK1,XK2,XK3,XK4
FORMAT (8F10.4)
XK=XK2
ZK = XK4
2 READ(5,2) N
FORMAT(I3)
3 DO 3 I = 1, N
4 READ(5,4) T(I), H(I)
50 CONTINUE
FORMAT(2F10.4)
AFP = (3.1412*DFP**2)/4.0
AP = (3.1412*DP**2)/4.0
AH = (3.1412*(DHL**2)/4.0)*FLOAT(NH)
XK2 = XK
XK4 = ZK
XK2 = XK2+(((DP/DHL)**2)/FLOAT(NH))**2
XK4 = XK4+(((DP/DHL)**2)/FLOAT(NH))**2
T1(1) = 0.0
H1(1) = 0.0

```

```

H2(1) = 0.0
H3(1) = 0.0
J1 = 1
DO 5 I = 1, N-1
DH = H(I+1) - H(I)
DT = T(I+1) - T(I)
T1(J1) = T(I)
H1(J1) = H(I)
J2 = J1 + 1
J3 = J1 + 10
DO 6 J = J2, J3
T1(J) = T1(J-1) + DT/10.0
H1(J) = H1(J-1) + DH/10.0
6 CONTINUE
J1 = J1 + 10
5 CONTINUE
XDHL = DHL * 1000.0
WRITE(6,11) NH, XDHL, AH, XK1, XK, XK2
WRITE(6,12) T1(1), H1(1), H2(1)
KI = (N-1)*10
DO 8 K = 1, KL
IF (K.EQ.40) GO TO 123
GO TO 821
123 WRITE (6,11) NH,XDHL,AH,XK1,XK,XK2
821 IF (K.EQ.1) GO TO 84
IF(T1(K).EQ.T(N)) GOTO 81
IF(H1(K+1).LT.H1(K)) GO TO 841
IF (H1(K+1).EQ.H1(K)) GO TO 831
GO TO 84
831 IF (ABS(H1(K)-H2(K)).LE.0.0010) GO TO 83
GO TO 84
83 H2(K+1)=H1(K+1)
H3(K+1)=H2(K+1)
GO TO 8
841 IF (ABS(H2(K)).LE.0.0003) K=KL
IF (K.EQ.KL) GO TO 8
84 QF=0.6*SQRT(2.0*9.81*ABS(H1(K+1)-H2(K))) /1000.0
251 CONTINUE
REF = 10.0**6*(DP+QF/AP)
REFP = (10.0**6)*DFP+QF/AFP
IF ( REFF. LE. 2300 ) GOTO 13
FF=0.079/REF**0.25
16 IF ( REFP. LE. 2300 ) GOTO 14
FFP = 0.079/REFP**0.25
GOTO 15
13 FF = 16.0/REF
GOTO 16
14 FFP = 16.0/REFP
15 CONTINUE
IF((H1(K+1)-H2(K)).LT.0.0) GO TO 271
A=XV1
B=XK2
QS=1.0
GO TO 28
271 A=XK3
B=XK4
QS=-1.0
28 CONTINUE
C = (4.0*(FF*LP/DP+FFP*(LFP+H2(K))/DFP)+A+B)/(2.0*9.81)
XH = (H1(K+1)-H2(K))/2.0
XH=ABS(XH)
C2 = ((3.1412*DP**2)/4.0)*SQRT(1.0/C)

```

```

      Q = C2*SQRT(XH)
      IF ( ABS((QF+Q)/Q) .LT. 0.001)      GOTO 60
      QF = Q
      GOTO 251
60    CONTINUE
      Q=QS*Q
      DH2 = Q*(T1(K+1)-T1(K))/AFP
      H2(K+1) = H2(K) + DH2
10    H3(K+1) = H2(K+1)
      Z1 = H1(K) - H2(K)
      IF(Z1.EQ.0.0) GOTO 24
      QZ1 = ABS(Z1)/Z1
      Q1 = C2*QZ1*SQRT(ABS(Z1))
      GOTO 25
24    Q1 = 0.0
      GOTO 25
25    CONTINUE
      Z2 = H1(K+1) - H2(K+1)
      IF(Z2.EQ.0.0) GOTO 27
      QZ2 = ABS(Z2)/Z2
      Q2 = C2*QZ2*SQRT(ABS(Z2))
      GOTO 26
27    Q2 = 0.0
26    CONTINUE
      QAV = (Q1+Q2)/2.0
      H2(K+1)=QAV*(T1(K+1)-T1(K))/AFP+H2(K)
      IF (ABS((H2(K+1)-H3(K+1))/H3(K+1)).LE.0.001) GOTO 9
      GOTO 10
9     CONTINUE
8     WRITE (6,12) T1(K+1), H1(K+1), H2(K+1)
81    CONTINUE
      IF(NH.GT.1) GOTO 51
      IF(NH.EQ.1) NH = 2
      GOTO 50
51    NH = NH + 4
      IF(NH.GT.NHF) GOTO 70
      GO TO 50
70    CONTINUE
11    FORMAT(1H1,///,15X,15HFLOAT RESPONSE.,///,
1     15X,18HNUMBER ORIFICES = ,13,/,
2     15X,19HDIAMETER ORIFICE = , F10.4,2X,3HMM.,/,
3     15X,21HTOTAL ORIFICE AREA = , F10.8,2X,5HSQ.M.,/,
4     15X,29HASSUMED U TUBE LOSS COEFF. = , F10.4,/,
5     15X,30HASSUMED ORIFICE LOSS COEFF. = ,F10.4,/,
4     15X,33HEQUIVALENT ORIFICE LOSS COEFF. = ,F10.4,///,
117X,4HTIME,6X,5HDRAIN,5X,10HFLOAT PIPE,/,27X,5HDEPTH,6X,5HDEPTH)
12    FORMAT(11X,3F11.4)
      STOP
      END

```

## FLOAT RESPONSE.

NUMBER ORIFICES = 2  
 DIAMETER ORIFICE = 3.6830 MM.  
 TOTAL ORIFICE AREA = 0.00002130 SQ.M.  
 ASSUMED U TUBE LOSS COEFF. = 2.9500  
 ASSUMED ORIFICE LOSS COEFF. = 3.0000  
 EQUIVALENT ORIFICE LOSS COEFF. = 542.4852

TIME	DRAIN DEPTH	FLOAT PIPE DEPTH
0.0000	0.0000	0.0000
0.1000	0.0025	0.0003
0.2000	0.0050	0.0008
0.3000	0.0075	0.0016
0.4000	0.0100	0.0025
0.5000	0.0125	0.0034
0.6000	0.0150	0.0045
0.7000	0.0175	0.0056
0.8000	0.0200	0.0068
0.9000	0.0225	0.0081
1.0000	0.0250	0.0094
1.1000	0.0250	0.0107
1.2000	0.0250	0.0119
1.3000	0.0250	0.0131
1.4000	0.0250	0.0143
1.5000	0.0250	0.0153
1.6000	0.0250	0.0163
1.7000	0.0250	0.0173
1.8000	0.0250	0.0182
1.9000	0.0250	0.0191
2.0000	0.0250	0.0199
2.1000	0.0250	0.0206
2.2000	0.0250	0.0213
2.3000	0.0250	0.0219
2.4000	0.0250	0.0224
2.5000	0.0250	0.0230
2.6000	0.0250	0.0234
2.7000	0.0250	0.0238
2.8000	0.0250	0.0241
2.9000	0.0250	0.0244
3.0000	0.0250	0.0246
3.1000	0.0250	0.0248
3.2000	0.0250	0.0249
3.3000	0.0250	0.0250
3.4000	0.0250	0.0250
3.5000	0.0250	0.0250
3.6000	0.0250	0.0250
3.7000	0.0250	0.0250
3.8000	0.0250	0.0250
3.9000	0.0250	0.0250

## FLOAT RESPONSE.

NUMBER ORIFICES = 2  
 DIAMETER ORIFICE = 3.6830 MM.  
 TOTAL ORIFICE AREA = 0.00002130 SQ.M.  
 ASSUMED U TUBE LOSS COEFF. = 2.9500  
 ASSUMED ORIFICE LOSS COEFF. = 3.0000  
 EQUIVALENT ORIFICE LOSS COEFF. = 542.4852

TIME	DRAIN DEPTH	FLOAT PIPE DEPTH
4.0000	0.0250	0.0250
4.1000	0.0250	0.0250
4.2000	0.0250	0.0250
4.3000	0.0250	0.0250
4.4000	0.0250	0.0250
4.5000	0.0250	0.0250
4.6000	0.0250	0.0250
4.7000	0.0250	0.0250
4.8000	0.0250	0.0250
4.9000	0.0250	0.0250
5.0000	0.0250	0.0250
5.1000	0.0225	0.0247
5.2000	0.0200	0.0242
5.3000	0.0175	0.0234
5.4000	0.0150	0.0225
5.5000	0.0125	0.0216
5.6000	0.0100	0.0205
5.7000	0.0075	0.0194
5.8000	0.0050	0.0182
5.9000	0.0025	0.0169
6.0000	0.0000	0.0156
6.1000	0.0000	0.0143
6.2000	0.0000	0.0131
6.3000	0.0000	0.0119
6.4000	0.0000	0.0108
6.5000	0.0000	0.0097
6.6000	0.0000	0.0087
6.7000	0.0000	0.0077
6.8000	0.0000	0.0068
6.9000	0.0000	0.0059
7.0000	0.0000	0.0051
7.1000	0.0000	0.0044
7.2000	0.0000	0.0037
7.3000	0.0000	0.0031
7.4000	0.0000	0.0026
7.5000	0.0000	0.0020
7.6000	0.0000	0.0016
7.7000	0.0000	0.0012
7.8000	0.0000	0.0009
7.9000	0.0000	0.0006
8.0000	0.0000	0.0004

## AI.3 Print out and Output of Computer Program SLOT.

```

PROGRAM(SLOT)
  INPUT 5 = CRO
  OUTPUT 6 = LPO
END

```

```

MASTER KINGSIX
REAL LP, LFP
DIMENSION H1(100), H2(100), H(10), T(10), T1(100), H3(100)
20 READ(5,20) NH, DHL
   FORMAT (I3, F16.12)
   NHF = NH
   NH = 4
1 READ(5,1) LP, DP, LFP, DFP, XK1, XK2, XK3, XK4
   FORMAT (8F10.4)
   XK = XK2
   ZK = XK4
2 READ(5,2) N
   FORMAT (I3)
3 DO 3 I = 1, N
4 READ(5,4) T(I), H(I)
50 FORMAT (2F10.4)
CONTINUE
AFP = (3.1412*DFP**2)/4.0
AP = (3.1412*DP**2)/4.0
AH = (3.1412*(DHL**2)/4.0)*FLOAT(NH)
XK2 = XK
XK4 = ZK
XK2 = XK2*(((DP/DHL)**2)/FLOAT(NH))**2
XK4 = XK4*(((DP/DHL)**2)/FLOAT(NH))**2
T1(1) = 0.0
H1(1) = 0.0

```

```

H2(1) = 0.0
H3(1) = 0.0
J1 = 1
DO 5 I = 1, N-1
DH = H(I+1) - H(I)
DT = T(I+1) - T(I)
T1(J1) = T(I)
H1(J1) = H(I)
J2 = J1 + 1
J3 = J1 + 10
DO 6 J = J2, J3
T1(J) = T1(J-1) + DT/10.0
H1(J) = H1(J-1) + DH/10.0
6 CONTINUE
J1 = J1 + 10
5 CONTINUE
XDHL = DHL * 1000.0
WRITE(6,11) NH, XDHL, AH, XK1, XK, XK2
WRITE(6,12) T1(1), H1(1), H2(1)
KL = (N-1)*10
DO 8 K = 1, KL
IF (K.EQ.40) GO TO 123
GO TO 821
123 WRITE (6,11) NH, XDHL, AH, XK1, XK, XK2
821 IF (K.EQ.1) GO TO 84
IF (T1(K).EQ.T(N)) GOTO 81
IF (H1(K+1).LT.H1(K)) GO TO 841
IF (H1(K+1).EQ.H1(K)) GO TO 831
GO TO 84
831 IF (ABS(H1(K)-H2(K)).LE.0.0040) GO TO 83
GO TO 84
83 H2(K+1)=H1(K+1)
H3(K+1)=H2(K+1)
GO TO 8
841 IF (ABS(H2(K)).LE.0.0003) K=KL
IF (K.EQ.KL) GO TO 8
84 QF=0.6*SQRT(2.0+9.81*ABS(H1(K+1)-H2(K))) /1000.0
251 CONTINUE
REF = 10.0**6*(DP*QF/AP)
REFP = (10.0**6)*DFP*QF/AFP
IF ( REF. LE. 2300 ) GOTO 13
FF=0.079/REF**0.25
16 IF ( REFP. LE. 2300 ) GOTO 14
FFP = 0.079/REFP**0.25
GOTO 15
13 FF = 16.0/REF
GOTO 16
14 FFP = 16.0/REFP
15 CONTINUE
IF ((H1(K+1)-H2(K)).LT.0.0) GO TO 271
A=XK1
B=XK2
QS=1.0
GO TO 28
271 A=XK3
B=XK4
QS=-1.0
28 CONTINUE
C = (4.0*(FF+LP/DP+FFP*(LEP+H2(K))/DFP)+A+B)/(2.0+9.81)
XH = (H1(K+1)-H2(K))/2.0
XH=ABS(XH)
C2 = ((3.1412+DP**2)/4.0)*SQRT(1.0/C)

```

```

      Q = C2*SQRT(XH)
      IF ( ABS((QF-Q)/Q). LT. 0.001)      GOTO 60
      QF = Q
      GOTO 251
60    CONTINUE
      Q=QS*Q
      DH2 = Q*(T1(K+1)-T1(K))/AFP
      H2(K+1) = H2(K) + DH2
10    H3(K+1) = H2(K+1)
      IF (K.LT.40.AND.H2(K+1).GT.H1(K+1)) GO TO 83
      IF (K.GT.40.AND.H1(K+1).GT.H2(K+1)) GO TO 83
      Z1 = H1(K) - H2(K)
      IF(Z1.EQ.0.0) GOTO 24
      QZ1 = ABS(Z1)/Z1
      Q1 = C2*QZ1*SQRT(ABS(Z1))
      GOTO 25
24    Q1 = 0.0
      GOTO 25
25    CONTINUE
      Z2 = H1(K+1) - H2(K+1)
      IF(Z2.EQ.0.0) GOTO 27
      QZ2 = ABS(Z2)/Z2
      Q2 = C2*QZ2*SQRT(ABS(Z2))
      GOTO 26
27    Q2 = 0.0
26    CONTINUE
      QAV = (Q1+Q2)/2.0
      H2(K+1)=QAV*(T1(K+1)-T1(K))/AFP+H2(K)
      IF (ABS((H2(K+1)-H3(K+1))/H3(K+1)).LE.0.001) GOTO 9
      GOTO 10
9     CONTINUE
8     WRITE (6,12) T1(K+1), H1(K+1), H2(K+1)
81    CONTINUE
      NH=NH+1
      IF(NH.GT.NHF) GOTO 70
      GO TO 50
70    CONTINUE
11    FORMAT(1H1,///,15X, 15HFLOAT RESPONSE., ///,
115X,15HNUMBER SLOTS = ,I3, /,
215X,29HFQUIVALENT ORIFICE DIAMETER = ,F10.4,3HMM., /,
3 15X, 21HTOTAL ORIFICE AREA = , F10.8, 2X, 5HSQ.M.,/,
4 15X, 29HASSUMED U TUBE LOSS COEFF. = , F10.4, /,
5 15X, 30HASSUMED ORIFICE LOSS COEFF. = ,F10.4,/,
4 15X, 33HFQUIVALENT ORIFICE LOSS COEFF. = ,F10.4,///,
117X,4HTIME,6X,5HDRAIN,5X,10HFLOAT PIPE,/,27X,5HDEPTH,6X,5HDEPTH
12    FORMAT(11X, 3F11.4 )
      STOP
      END

```

PILOT RESPONSE.

NUMBER SLOTS = 2  
 EQUIVALENT ORIFICE DIAMETER = 9.7129MM.  
 TOTAL ORIFICE AREA = 0.00014817 SQ.M.  
 ASSUMED U TUBE LOSS COEFF. = 2.9500  
 ASSUMED ORIFICE LOSS COEFF. = 3.0000  
 EQUIVALENT ORIFICE LOSS COEFF. = 11.2150

TIME	DRAIN DEPTH	PILOT PIPE DEPTH
0.0000	0.0000	0.0000
0.1000	0.0025	0.0011
0.2000	0.0050	0.0035
0.3000	0.0075	0.0059
0.4000	0.0100	0.0084
0.5000	0.0125	0.0109
0.6000	0.0150	0.0134
0.7000	0.0175	0.0159
0.8000	0.0200	0.0184
0.9000	0.0225	0.0209
1.0000	0.0250	0.0234
1.1000	0.0250	0.0250
1.2000	0.0250	0.0250
1.3000	0.0250	0.0250
1.4000	0.0250	0.0250
1.5000	0.0250	0.0250
1.6000	0.0250	0.0250
1.7000	0.0250	0.0250
1.8000	0.0250	0.0250
1.9000	0.0250	0.0250
2.0000	0.0250	0.0250
2.1000	0.0250	0.0250
2.2000	0.0250	0.0250
2.3000	0.0250	0.0250
2.4000	0.0250	0.0250
2.5000	0.0250	0.0250
2.6000	0.0250	0.0250
2.7000	0.0250	0.0250
2.8000	0.0250	0.0250
2.9000	0.0250	0.0250
3.0000	0.0250	0.0250
3.1000	0.0250	0.0250
3.2000	0.0250	0.0250
3.3000	0.0250	0.0250
3.4000	0.0250	0.0250
3.5000	0.0250	0.0250
3.6000	0.0250	0.0250
3.7000	0.0250	0.0250
3.8000	0.0250	0.0250
3.9000	0.0250	0.0250

## FLOAT RESPONSE.

NUMBER SLOTS = 2  
 EQUIVALENT ORIFICE DIAMETER = 9.7129MM.  
 TOTAL ORIFICE AREA = 0.00014817 SQ.M.  
 ASSUMED U TUBE LOSS COEFF. = 2.9500  
 ASSUMED ORIFICE LOSS COEFF. = 3.0000  
 EQUIVALENT ORIFICE LOSS COEFF. = 11.2150

TIME	DRAIN DEPTH	FLOAT PIPE DEPTH
4.0000	0.0250	0.0250
4.1000	0.0250	0.0250
4.2000	0.0250	0.0250
4.3000	0.0250	0.0250
4.4000	0.0250	0.0250
4.5000	0.0250	0.0250
4.6000	0.0250	0.0250
4.7000	0.0250	0.0250
4.8000	0.0250	0.0250
4.9000	0.0250	0.0250
5.0000	0.0250	0.0250
5.1000	0.0225	0.0239
5.2000	0.0200	0.0215
5.3000	0.0175	0.0191
5.4000	0.0150	0.0166
5.5000	0.0125	0.0141
5.6000	0.0100	0.0116
5.7000	0.0075	0.0091
5.8000	0.0050	0.0066
5.9000	0.0025	0.0041
6.0000	0.0000	0.0016
6.1000	0.0000	0.0000
6.2000	0.0000	0.0000
6.3000	0.0000	0.0000
6.4000	0.0000	0.0000
6.5000	0.0000	0.0000
6.6000	0.0000	0.0000
6.7000	0.0000	0.0000
6.8000	0.0000	0.0000
6.9000	0.0000	0.0000
7.0000	0.0000	0.0000
7.1000	0.0000	0.0000
7.2000	0.0000	0.0000
7.3000	0.0000	0.0000
7.4000	0.0000	0.0000
7.5000	0.0000	0.0000
7.6000	0.0000	0.0000
7.7000	0.0000	0.0000
7.8000	0.0000	0.0000
7.9000	0.0000	0.0000
8.0000	0.0000	0.0000

## 12.2 APPENDIX II      Data Presentation Program WCHAR

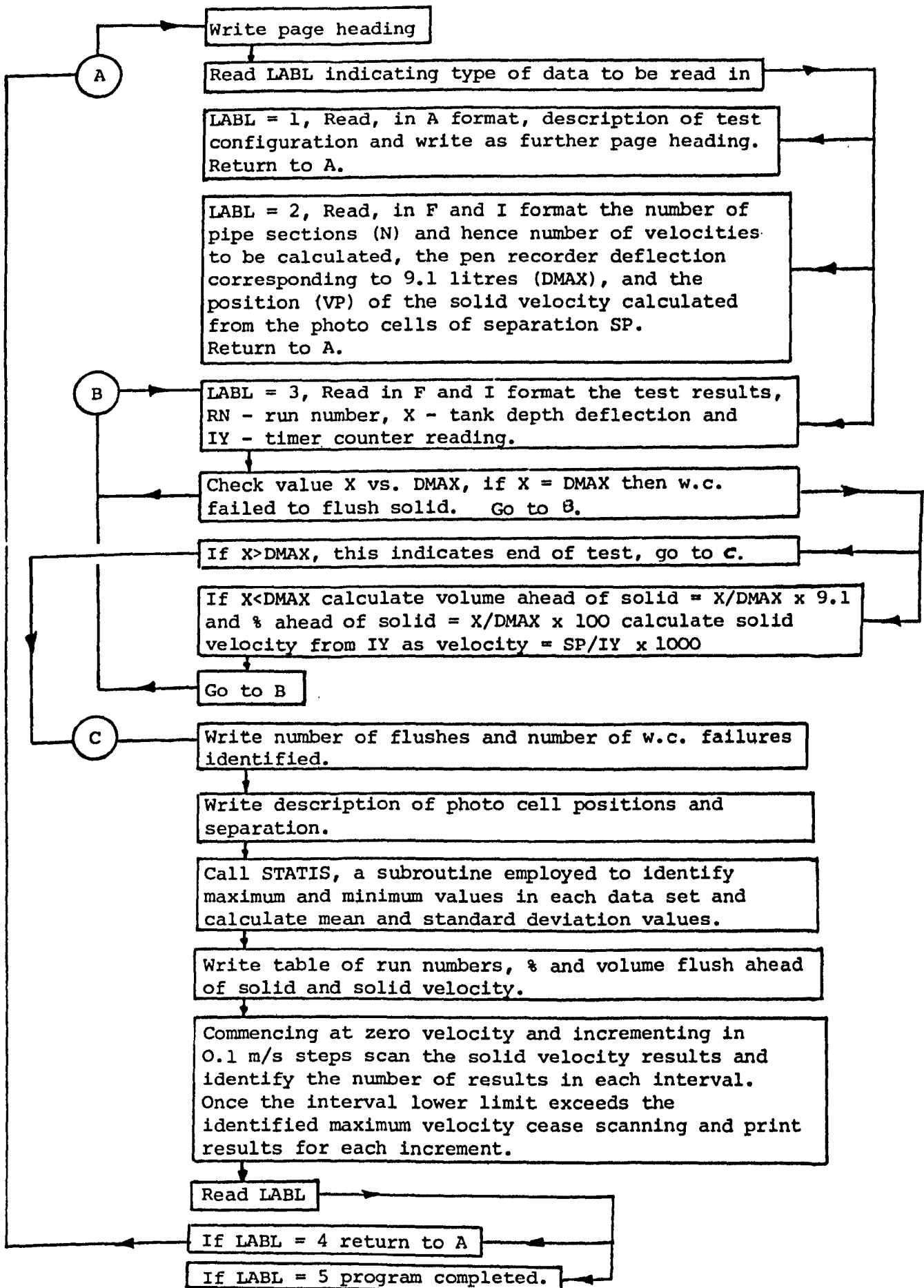
Program WCHAR is a simple data presentation program written in Fortran and run on the Brunel University 1903 computer. It accepts data describing the test configuration and layout of photocells, separation, etc., together with the run number, the values of travel time at each velocity monitoring position, the volume of flow entering the collection tank ahead of the solid and the position, if any, of the solid deposit along the pipe, all this data being punched onto paper tape.

From this data WCHAR prints out tabulated test results reproducing the test configuration, run number, % flush ahead of solid, water volume ahead of solid, stoppage position in metres, if any, and values of solid velocity at each velocity monitoring position.

WCHAR together with subroutine STATIS identifies the W.C. failure cases and the maximum and minimum test data values and calculates both the mean and standard deviation of each set of results. In order to aid in the plotting of histograms of the solid velocity distributions WCHAR also prints out the number of test results in each of a series of velocity intervals.

A flow diagram for WCHAR is presented followed by a print out of the program followed by an example of the output from the program.

## AII.1 Flow diagram WCHAR



AII.2 Print Out of WCHAR

Note. Due to the volume of computer analysis two identical computer programs were used WCHAR and COPY. The print out shown below is in fact COPY.

```
PROGRAM (COPY)
INPUT 5=CR0
OUTPUT 6=LP0
TRACE 2
END
```

```

MASTER DRAIN
DIMENSION E(9),Y(6),VOLP(300),VOL(300),VEL(6,300), VX(6),
1V(300),VN(6),VSD(6),VP(6),SP(6),AV(6), RUN(300)
2,IY(6),STP(300),NFREQ(6),STPOS(300)
DIMENSION FORM(13),COL(7)
DATA FORM(1),FORM(2),FORM(3),FORM(4),FORM(6),FORM(13)/7H(F19.3,.6)
1F11.3,.6HF14.3,.4H13X,.3H7X,.1H)/
DATA FCLR,FSTOP,FVEL,FBLNK/4H1A5,.5HF5.2,.5HF8.4,.3H8X,/
DATA CLEAR/4HFREE/
4 WRITE (6,200)
200 FORMAT (1H1,///,20X,
158HHOSPITAL DRAINAGE DESIGN - DECELERATION CHARACTERISTICS,/,
220X,58HDR.J.A.SWAFFIELD AND R.H.M.WAKELIN, DIV. OF BUILDING TECH.
3//)
NR=0
NS=0
NT=0
6 READ (5,99) LABL
GO TO (1,2,3),LABL
1 READ (5,100) (E(I),I=1,9)
100 FORMAT (9A8)
WRITE (6,201) (E(I),I=1,9)
```

```

201  FORMAT (20X,9A8)
99   FORMAT (I0)
      GO TO 6
2    READ (5,101) N,DMAX,(VP(I),I=1,N),(SP(I),I=1,N)
101  FORMAT (I0,15F0.0)
      GO TO 6
3    READ(5,102) RN,X,STPS,(IY(I),I=1,N)
102  FORMAT(3F0.0,6I0)
      IF (X.GT.DMAX) GO TO 5
      NP=NR+1
      IF (X.EQ.DMAX) GO TO 3
      IF (X.GT.0.0) NS=NS+1
      RUN(NS)=RN
C    DMAX=MAX. LDT DISPLACEMENT IN COLLECTION TANK.
C    X=DEFLECTION LDT DUE TO WATER AHEAD SOLID.
C    IF X=DMAX, W.C. FAILED TO FLUSH.
C    IF X GT. ZERO SOLID PASSED INTO TANK.
C    IF X GT. DMAX THE TEST RUN IS COMPLETE, NO MORE DATA TO BE READ.
C    NR=NUMBER RUNS, NS=NUMBER SUCCESSFUL W.C. OPERATIONS
      VOLP(NS)=(X/DMAX)*100.0
      VOL(NS)=(X/DMAX)*9.087
      STPOS(NS)=STPS
      IF (STPOS(NS).GE.0.0) NT=NT+1
      IF (STPOS(NS).GE.0.0) STP(NT)=STPOS(NS)
      DO 7 I=1,N
      IF (IY(I).EQ.0) GO TO 612
      Y(I) = FLOAT(IY(I))/10.0**4
      VEL(I,NS)=SP(I)/(Y(I))
      GO TO 611
612  VEL(I,NS) = 0.0
611  CONTINUE
7    CONTINUE
      GO TO 3
5    NF=NR-NS
      WRITE (6,206) NR,NF
206  FORMAT (20X,20HNUMBER OF FLUSHES = ,14,4X,
126HNUMBER OF W.C. FAILURES = ,14,/)
      IF (X.GT.12.0) GO TO 60
      WRITE (6,500) (I,I=1,N)
500  FORMAT (20X,15HPOINT VELOCITY.,35X,6(15,3X))
      WRITE (6,501) (VP(I),I=1,N)
501  FORMAT (20X,30HPOSITION VELOCITY M. FROM W.C.,19X,6F8.3)
      WRITE (6,502) (SP(I),I=1,N)
502  FORMAT (20X,19HSEP. SFNSORS METRES,30X,6F8.1)
      WRITE (6,202)
202  FORMAT(/12X,7HRUN NO.,1X,
1      13HPERCENT FLUSH,2X,14H VOLUME AHEAD ,4X,14HSTOPPAGE P
20SN.,21X,14HVELOCITY, M/S.)
      WRITE (6,203)
203  FORMAT (20X,12HAHEAD SOLID.,4X,14HSOLID, LITRES.,2X,16HMETRES FROM
1 W.C.)
      VMAX=0.0
      VPMAX=0.0
      VMTN=9.087
      VPMIN=100.0
      CALL STATIS (VOL,NS,AVOL,VMAX,VMIN,SDVOL)
      CALL STATIS (VOLP,NS,AVOLP,VPMAX,VPMIN,SDVOIP)
      STPMX = 0.0
      STPMN = 20.0
      CALL STATIS (STP,NT,STPM,STPMX,STPMN,STPSD)
      DO 9 K=1,N
      DO 10 J=1,NS

```

```

47  CONTINUE
    WRITE(6,300) V1,V2,(NFREQ(K3),K3=1,N)
300  FORMAT(/,12X,11HINTERVAL = ,F7.4,3H = ,F7.4,8H  M/SEC.,20X,6(16,2X
    1))
    GOTO 46
60  CONTINUE
    READ (5,99) LABL
    IF (LABL.EQ.4) GO TO 4
208  FORMAT (/,12X,5HMEAN.,6X,F7.3,8X,F6.3,12X,F6.2,7X,6F8.4)
209  FORMAT (12X,4HMAX.,7X,F7.3,8X,F6.3,12X,F6.2,7X,,F8.4)
210  FORMAT (12X,4HMIN.,7X,F7.3,8X,F6.3,12X,F6.2,7X,,F8.4)
211  FORMAT (12X,8HST. DEV.,3X,F7.3,8X,F6.3,12X,F6.2,7X,6F8.4)
    STOP
    END

```

MENT, LENGTH 1050, NAME DRAIN

```

SUBROUTINE STATIS (X,N,XM,XXM,XMN,XSD)
DIMENSION X(300)
SUM1=0.0
SUM2=0.0
NZ=N
IF ( N.EQ.0 ) GOTO 10
DO 1 J=1,N
IF (X(J).LT.0.0) GO TO 6
SUM1=SUM1+X(J)
IF (X(J).GT.XMX) XXM=X(J)
IF (X(J).LT.XMN) XMN=X(J)
GO TO 1
6  NZ=NZ-1
1  CONTINUE
   XM=SUM1/FLOAT(NZ)
   DO 2 J=1,N
   IF (X(J).LT.0.0) GO TO 7
   SUM2=SUM2+(X(J)-XM)**2
7  CONTINUE
2  CONTINUE
   XSD=SQRT(SUM2/FLOAT(NZ))
   GOTO 9
10  XM = 0.0
    XXM = 0.0
    XMN = 0.0
    XSD = 0.0
9  CONTINUE
   RETURN
   END

```

```

V(J)=VEL(K,J)
IF (STPOS(J).GT.0.0.AND.STPOS(J).LT.VP(K)) V(J)=0.0
10 CONTINUE
VELX=0.0
VELN=5000.0
CALL STATIS (V,NS,AVEL,VELX,VFLN,SDVEL)
VX(K)=VELX
VN(K)=VFLN
VSD(K)=SDVEL
AV(K)=AVEL
9 CONTINUE
DO 11 J=1,NS
IF (STPOS(J).LT.0.0) GO TO 805
FORM(5)=FSTOP
COL(1)=STPOS(J)
GO TO 806
805 FORM(5)=FCLR
COL(1) = CLEAR
806 K=1
DO 810 I=1,N
IF (VEI(I,J).LT.0.0) GO TO 812
K=K+1
COL(K)=VEL(I,J)
FORM(I+6)=FVEL
GO TO 810
812 FORM(I+6)=FRLNK
810 CONTINUE
WRITE (6,FORM) RUN(J),VOLP(I),VOL(J),(COL(I),I=1,K)
11 CONTINUE
WRITE (6,678) RUN(1),RUN(NS)
678 FORMAT (////,1H1,////,20X,15HTEST NUMBERS = ,F8.3,4H TO ,F8.3)
WRITE (6,702)
702 FORMAT (////,20X,13HPERCENT FLUSH,2X,14H VOLUME AHEAD ,4X,14HS
1TOPPAGE POSH.,21X,14HVELOCITY, M/S.)
WRITE (6,703)
703 FORMAT (20X,12HAHEAD SOLID.,4X,14HSOLID, LITRES.,2X,16HMETRES FROM
1 W.C.)
WRITE (6,208) AVOLP,AVOL,STPM,(AV(K),K=1,N)
WRITE (6,209) VPMAX,VMAX,STPMX,(VX(K),K=1,N)
WRITE (6,210) VPMIN,VMIN,STPMN,(VN(K),K=1,N)
WRITE (6,211) SDVOLP,SDVOL,STPSD,(VSD(K),K=1,N)
V1=0.0
V2=0.0001
GO TO 619
46 VINT=0.1
V1=V2
V2=V1+VINT
IF (V1.EQ.0.0001) V2=0.1
619 CONTINUE
DO 48 K1=1,N
IF(V2.GT.VN(K1)) GOTO 700
48 CONTINUE
700 CONTINUE
DO 49 K1=1,N
IF (V1.LT.VX(K1)) GOTO 50
49 CONTINUE
GOTO 60
50 CONTINUE
DO 47 K1=1,N
NFRFQ(K1)=0
DO 47 K2=1,NS
IF(VEL(K1,K2).LT.V2.AND.VEI(K1,K2).GE.V1) NFRFQ(K1)=NFRFQ(K1)+1

```

ARMITAGE SHANKS P-TRAP BACK ENTRY LOW LEVEL W.C. UNVENTED DISCHARGE.  
 TEST NUMBER 123, SOLID DECELERATION SERIES.  
 14 METRE PLASTIC WASTE PIPE, SLOPE 1/100.  
 STRAIGHT PIPE.  
 DECEMBER 3 RD. 1975.  
 MATERNITY PAD + 3 BOWTOWELS.  
 NUMBER OF FLUSHES = 32      NUMBER OF W.C. FAILURES = 2

POINT VELOCITY,	1	2	3	4	5	6
POSITION VELOCITY M. FROM W.C.	0.963	3.151	5.023	7.210	9.081	11.268
SEP. SENSORS METRES	0.2	0.2	0.2	0.2	0.2	0.2

RUN NO.	PERCENT FLUSH AHEAD SOLID.	VOLUME AHEAD SOLID, LITRES.	STOPPAGE POSN. METRES FROM W.C.	VELOCITY, M/S.					
123.010	35,000	3.180	6.21	1.1056	1.0065	0.6498	0.5076	0.3320	0.2623
123.020	25,000	2.272	9.45	1.1261	0.8857	0.6821	0.3577	0.0098	0.4785
123.030	18,750	1.704	6.97	0.8123	1.0157	0.6013	1.0101	0.7233	0.6373
123.040	43,750	3.976	7.29	0.7619	1.0309	0.7176		0.6281	0.5602
123.050	33,750	3.067	FREE	0.5687	0.9341	0.8261	0.5915	0.2946	0.2076
123.070	20,000	1.817	10.27	0.9217	0.7599	0.7605	0.4308	0.2061	0.5244
123.080	25,000	2.272	12.20	1.0565	0.7722	0.6030	0.5342	0.1617	0.1102
123.090	25,000	2.272	12.22	0.9551	0.8471	0.6394	0.4361	0.2157	0.1207
123.100	25,000	2.272	12.30	0.7952	0.9766	0.7890	0.5731	0.2431	0.0263
123.110	25,000	2.272	6.69	0.8478	0.6462	0.3729	0.8929	0.7743	0.5947
123.120	28,750	2.613	12.31	0.7593	1.0460	0.7143	0.4789	0.2609	0.1965
123.130	32,500	2.953	8.89	1.3624	0.9079	0.6691	0.5035		0.4394
123.140	32,500	2.953	9.75	0.6720	1.1086	0.7698	0.6736	0.1712	0.6502
123.150	22,500	2.045	8.23	0.9074	0.6388	0.6868	0.1597	0.5525	0.5476
123.160	26,250	2.385	13.06	1.3793	0.7502	0.7391	0.5499	0.2409	0.1883
123.170	41,250	3.748	5.84	0.9814	0.7418	0.5713	0.7386	0.6209	0.5502
123.190	28,750	2.613	7.61	0.8937	0.7905	0.6680	0.0838	0.5432	0.3949
123.200	37,500	3.408	12.32	0.7648	0.8045	0.6682	0.4260	0.2418	0.1694
123.210	25,000	2.272	7.37	1.1841	0.8780	0.6649	0.1233	0.6402	0.5972
123.220	25,000	2.272	6.85	0.7539	0.7223	0.4678	0.9046	0.6481	0.5807
123.230	32,500	2.953	6.76	1.0917	1.0526	0.6433	0.7115	0.5152	0.4211
123.240	43,750	3.976	8.23	1.0537	1.0081	0.6404	0.2026	0.5609	0.5019
123.250	22,500	2.045	8.23	0.7896	1.0015	0.7651		0.7477	0.6094
123.260	25,000	2.272	9.25	0.8288	0.8643	0.7042	0.4368	0.0078	0.6252
123.270	22,500	2.045	6.19	0.8610	0.4216	0.3307	0.8170	0.7452	0.4467
123.280	27,500	2.499	7.09	0.8133	1.0081	0.5350	0.6205	0.7573	0.5855
123.290	17,500	1.590	7.59	0.5671	0.9970	0.6768	0.1746	0.5502	0.4021
123.300	32,500	2.953	6.92	0.8460	0.7728	0.7613	0.8969	0.6127	0.5058
123.310	25,000	2.272	7.95	1.1641	0.9799	0.5531	0.1333	0.6629	0.4041
123.320	18,750	1.704	7.22	0.9747	0.6462	0.7463		0.7654	0.6527

TEST NUMBERS = 123,010 TO 123,320

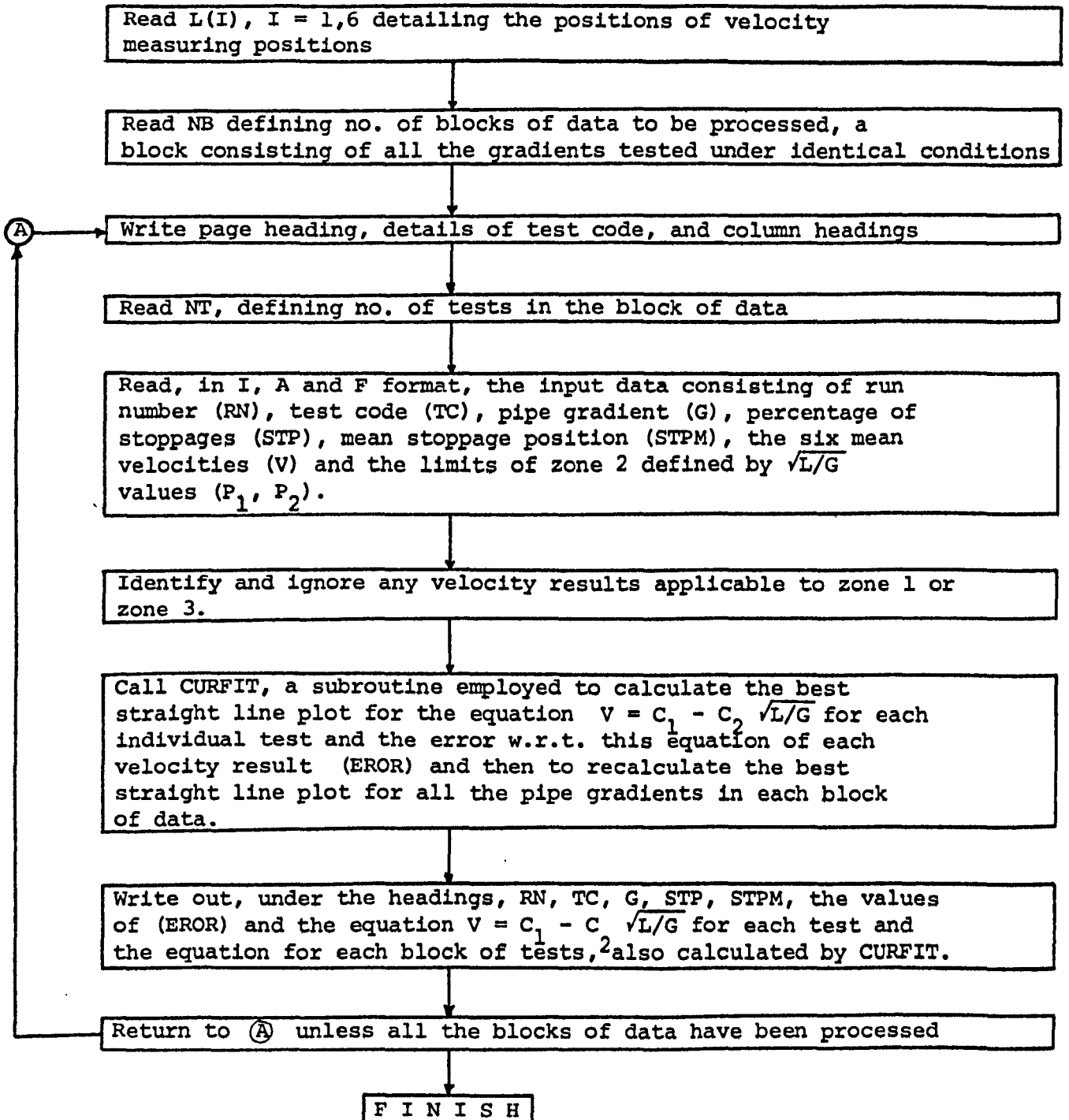
	PERCENT FLUSH AHEAD SOLID.	VOLUME AHEAD SOLID, LITRES.	STOPPAGE POSN. METRES FROM W.C.	VELOCITY, M/S.					
MEAN.	28.125	2.556	8.66	0.9200	0.8672	0.6539	0.2544	0.0684	0.0340
MAX.	43.750	3.976	13.06	1.3793	1.1086	0.8261	0.6736	0.2946	0.2076
MIN.	17.500	1.590	5.84	0.5671	0.4216	0.3307	0.0000	0.0000	0.0000
ST. DEV.	6.943	0.631	2.18	0.1981	0.1568	0.1127	0.2332	0.1056	0.0680
INTERVAL =	0.0000 -	0.0001	M/SEC.	0	0	0	0	0	0
INTERVAL =	0.0001 -	0.1000	M/SEC.	0	0	0	1	2	1
INTERVAL =	0.1000 -	0.2000	M/SEC.	0	0	0	4	2	5
INTERVAL =	0.2000 -	0.3000	M/SEC.	0	0	0	1	7	2
INTERVAL =	0.3000 -	0.4000	M/SEC.	0	0	2	1	1	1
INTERVAL =	0.4000 -	0.5000	M/SEC.	0	1	1	5	0	6
INTERVAL =	0.5000 -	0.6000	M/SEC.	2	0	3	6	5	10
INTERVAL =	0.6000 -	0.7000	M/SEC.	1	3	13	2	6	5
INTERVAL =	0.7000 -	0.8000	M/SEC.	6	7	10	2	6	0
INTERVAL =	0.8000 -	0.9000	M/SEC.	7	5	1	3	0	0
INTERVAL =	0.9000 -	1.0000	M/SEC.	5	5	0	1	0	0
INTERVAL =	1.0000 -	1.1000	M/SEC.	3	8	0	1	0	0
INTERVAL =	1.1000 -	1.2000	M/SEC.	4	1	0	0	0	0
INTERVAL =	1.2000 -	1.3000	M/SEC.	0	0	0	0	0	0
INTERVAL =	1.3000 -	1.4000	M/SEC.	2	0	0	0	0	0

### 12.3 APPENDIX III Least Squares Analysis Program LSQ1

Program LSQ1, together with a suitable available subroutine CURFIT is a least squares analysis program written in Fortran and run on the Brunel University 1903 computer. It accepts the mean velocity data output by program WCHAR together with the run number, test code, pipe gradient, percentage of stoppages, mean stoppage position and position of photocells.

From this data subroutine CURFIT carries out a least squares analysis of the mean velocities with respect to  $\sqrt{L/G}$  in zone 2, initially for each test carried out and then for each block of tests containing the data for each W.C., material and venting condition, and taking all gradients into account. LSQ1 then prints out tabulated results defining the test, slope, stoppage information, the correction in m/s applied to each relevant mean velocity read in, in order to give the best straight line plot with respect to  $\sqrt{L/G}$  and finally the equation of this straight line plot. LSQ1 then carries out another least squares analysis of all the readings relevant to zone 2 and including all the pipe gradients for a particular W.C., venting and material combination and prints out the equation of the best straight line plot with respect to  $\sqrt{L/G}$  for all these readings.

A flow diagram for LSQ1 is presented, followed by a print out of the program followed by an example of the output from the program.

A III.1 Flow diagram LSQ1

AIII.2 Print out of LSQ1

```

PROGRAM (LSQ1)
INPUT 1=CRO
OUTPUT 2=LPO
TRACE 2
END.

```

```

MASTER LEAST SQUARES ANALYSIS
DIMENSION X(100),Y(100),XX(100),YY(100),C(11),V(100),EROR(100),
1Y2(100),X3(100),Y3(100),C1(11),Y4(100),EROR1(100)
INTEGER RN
REAL L(6)
READ (1,101) (L(I),I=1,6)
101  FORMAT (6F0.0)
READ (1,102) NB
102  FORMAT (I0)
DO 100 K4=1,NB
WRITE (2,301)
301  FORMAT (1H1,////////,17X,
182HHOSPITAL DRAINAGE DESIGN - LEAST SQUARES ANALYSIS OF DECELERATI
20N CHARACTERISTICS.,/,17X,
383HDR.J.A.SWAFFIELD AND R.H.M.WAKELIN, DIV. OF BUILDING TECHNOLOGY
4, BRUNEL UNIVERSITY.,////////)
WRITE (2,302)
302  FORMAT (17X,68HTHE TEST CODE USED IS : A = ARMITAGE SHANKS.
1      T = TWYFORDS.,/,41X,
242HS = S-TRAP,                P = P-TRAP.,/,41X,
322HL = LOW LEVEL CISTERN.,/,41X,
452HU = UNVENTED DISCHARGE.    V = VENTED DISCHARGE.,/,41X,

```

```

564H1 = SINGLE MATERNITY PAD.      2 = 1MP + 3K.      3 = 1MP + 3BS
6.,/////
WRITE (2,303)
303  FORMAT (108H  RUN TEST  SLOPE  STOPS  MEAN  ERROR1  ERROR2  ER
1ROR3  ERROR4  ERROR5  ERROR6  EQUATION OF LINE)
WRITE (2,304)
304  FORMAT (80H  NO. CODE  1/  PERCENT  STOP  M/S  M/S  M/
1S  M/S  M/S  M/S)
WRITE (2,305)
305  FORMAT (28X,5HPOSN.)
WRITE (2,306)
306  FORMAT (27X,6HMETRES,/)
103  READ (1,103) NT
103  FORMAT (I0)
J1=0
DO 50 J3=1,NT
J1=J1
104  READ (1,104) RN,TC,G,STP,STPM,(V(I),I=1,6),P1,P2
104  FORMAT (I3,A6,11F0.0)
DO 1 I=1,6
X(I)=SQRT(L(I)*G)
Y(I)=V(I)
1  CONTINUE
K=0
J5=1
DO 2 J=1,6
IF (X(J).LT.P1) GO TO 3
IF (X(J).GT.P2) GO TO 2
GO TO 4
3  J5=J5+1
GO TO 2
4  K=K+1
XX(K)=X(J)
YY(K)=Y(J)
2  CONTINUE
DO 7 I=1,K
J1=J1+1
X3(J1)=XX(I)
Y3(J1)=YY(I)
7  CONTINUE
CALL CURFIT (XX,YY,K,1,C,Y2,EROR)
J6=8-J5-K
GO TO (601,602,603,604),J6
601  GO TO (501,502,503,504,505),J5
501  WRITE (2,201) RN,TC,G,STP,STPM,(EROR(I),I=1,K),(C(J),J=1,2)
201  FORMAT (I5,A6,F7.1,F7.2,F8.2,1X,6F8.4,6H V =,F8.4,1X,F8.4,
110H*SQRT(L/G))
GO TO 50
502  WRITE (2,202) RN,TC,G,STP,STPM,(EROR(I),I=1,K),(C(J),J=1,2)
202  FORMAT (I5,A6,F7.1,F7.2,F8.2,9X,5F8.4,6H V =,F8.4,1X,F8.4,
110H*SQRT(L/G))
GO TO 50
503  WRITE (2,203) RN,TC,G,STP,STPM,(EROR(I),I=1,K),(C(J),J=1,2)
203  FORMAT (I5,A6,F7.1,F7.2,F8.2,17X,4F8.4,6H V =,F8.4,1X,F8.4,
110H*SQRT(L/G))
GO TO 50
504  WRITE (2,204) RN,TC,G,STP,STPM,(EROR(I),I=1,K),(C(J),J=1,2)
204  FORMAT (I5,A6,F7.1,F7.2,F8.2,25X,3F8.4,6H V =,F8.4,1X,F8.4,
110H*SQRT(L/G))
GO TO 50
505  WRITE (2,205) RN,TC,G,STP,STPM,(EROR(I),I=1,K),(C(J),J=1,2)
205  FORMAT (I5,A6,F7.1,F7.2,F8.2,33X,2F8.4,6H V =,F8.4,1X,F8.4,
110H*SQRT(L/G))

```

```

        GO TO 50
602    GO TO (511,512,513,514,515),J5
511    WRITE (2,211) RN,TC,G,STP,STPM,(EROR(I),I=1,K),(C(J),J=1,2)
211    FORMAT (I5,A6,F7.1,F7.2,F8.2, 1X,5F8.4,8X,
16H    V =,F8.4,1X,F8.4,10H*SQRT(L/G))
        GO TO 50
512    WRITE (2,212) RN,TC,G,STP,STPM,(EROR(I),I=1,K),(C(J),J=1,2)
212    FORMAT (I5,A6,F7.1,F7.2,F8.2, 9X,4F8.4,8X,
16H    V =,F8.4,1X,F8.4,10H*SQRT(L/G))
        GO TO 50
513    WRITE (2,213) RN,TC,G,STP,STPM,(EROR(I),I=1,K),(C(J),J=1,2)
213    FORMAT (I5,A6,F7.1,F7.2,F8.2,17X,3F8.4,8X,
16H    V =,F8.4,1X,F8.4,10H*SQRT(L/G))
        GO TO 50
514    WRITE (2,214) RN,TC,G,STP,STPM,(EROR(I),I=1,K),(C(J),J=1,2)
214    FORMAT (I5,A6,F7.1,F7.2,F8.2,25X,2F8.4,8X,
16H    V =,F8.4,1X,F8.4,10H*SQRT(L/G))
        GO TO 50
515    WRITE (2,215) RN,TC,G,STP,STPM,(EROR(I),I=1,K),(C(J),J=1,2)
215    FORHAT (I5,A6,F7.1,F7.2,F8.2,33X, F8.4,8X,
16H    V =,F8.4,1X,F8.4,10H*SQRT(L/G))
        GO TO 50
603    GO TO (521,522,523,524),J5
521    WRITE (2,221) RN,TC,G,STP,STPM,(EROR(I),I=1,K),(C(J),J=1,2)
221    FORMAT (I5,A6,F7.1,F7.2,F8.2, 1X,4F8.4,16X,
16H    V =,F8.4,1X,F8.4,10H*SQRT(L/G))
        GO TO 50
522    WRITE (2,222) RN,TC,G,STP,STPM,(EROR(I),I=1,K),(C(J),J=1,2)
222    FORMAT (I5,A6,F7.1,F7.2,F8.2, 9X,3F8.4,16X,
16H    V =,F8.4,1X,F8.4,10H*SQRT(L/G))
        GO TO 50
523    WRITE (2,223) RN,TC,G,STP,STPM,(EROR(I),I=1,K),(C(J),J=1,2)
223    FORMAT (I5,A6,F7.1,F7.2,F8.2,17X,2F8.4,16X,
16H    V =,F8.4,1X,F8.4,10H*SQRT(L/G))
        GO TO 50
524    WRITE (2,224) RN,TC,G,STP,STPM,(EROR(I),I=1,K),(C(J),J=1,2)
224    FORMAT (I5,A6,F7.1,F7.2,F8.2,25X, F8.4,16X,
16H    V =,F8.4,1X,F8.4,10H*SQRT(L/G))
        GO TO 50
604    GO TO (531,532),J5
531    WRITE (2,231) RN,TC,G,STP,STPM,(EROR(I),I=1,K),(C(J),J=1,2)
231    FORMAT (I5,A6,F7.1,F7.2,F8.2, 1X,3F8.4,24X,
16H    V =,F8.4,1X,F8.4,10H*SQRT(L/G))
        GO TO 50
532    WRITE (2,232) RN,TC,G,STP,STPM,(EROR(I),I=1,K),(C(J),J=1,2)
232    FORMAT (I5,A6,F7.1,F7.2,F8.2, 9X,2F8.4,24X,
16H    V =,F8.4,1X,F8.4,10H*SQRT(L/G))
50     CONTINUE
        CALL CURFIT (X3,Y3,J1,1,C1,Y4,EROR1)
        WRITE (2,701) (C1(J),J=1,2)
701    FORMAT(////,6X,72HTHE EQUATION OF THE LINE TAKING ALL THE ABOVE RE
1ADINGS INTO ACCOUNT IS :,4X,6H    V =,F8.4,1X,F8.4,10H*SQRT(L/G))
100    CONTINUE
        STOP
        END

```

SEGMENT, LENGTH 1065, NAME LEASTSQUARESANALYSIS

SUBROUTINE CURFIT (X,Y,N,M,C,YY,EROR)  
 DIMENSION X(100),Y(100),YY(100),EROR(100),P(20),C(11),B(11),

```

1A(11,11)
C THIS SUBROUTINE FITS EXPERIMENTAL DATA TO A POLYNOMIAL
C FUNCTION. IT ALSO CALCULATES THE ERROR BETWEEN EXPERIMENTAL
C VALUES AND CALCULATED VALUES.
29 MX2=M+2
DO 1 I=1,MX2
P(I)=0.0
DO 1 J=1,N
1 P(I)=P(I)+X(J)**I
NXY=N
NI=M+1
DO 2 I=1,NI
DO 2 J=1,NI
K=I+J-2
4 IF(K=0) 3,3,4
A(I,J)=P(K)
GOTO 2
3 A(1,1)=NXY
2 CONTINUE
B(1)=0.0
DO 5 J=1,NXY
5 B(1)=B(1)+Y(J)
DO 6 I=2,NI
B(I)=0.0
DO 6 J=1,NXY
6 B(I)=B(I)+Y(J)*X(J)**(I-1)
C PIVOTAL CONDENSATION
NM1=NI-1
DO 7 K=1,NM1
KPI=K+1
L=K
DO 8 I=KPI,NI
IF(ABS(A(I,K))-ABS(A(L,K))) 8,8,9
9 L=I
8 CONTINUE
IF(L=K) 10, 10, 11
11 DO 12 J=K,NI
TEMP=A(K,J)
A(K,J)=A(L,J)
12 A(L,J)=TEMP
TEMP=B(K)
B(K)=B(L)
B(L)=TEMP
C ELIMINATION, BACK SOLUTION, RESULTS.
10 DO 7 I=KPI,NI
FACTOR = A(I,K)/A(K,K)
A(I,K) = 0.0
DO 13 J=KPI,NI
13 A(I,J)=A(I,J)-FACTOR*A(K,J)
7 B(I)=B(I)-FACTOR*B(K)
C(NI)=B(NI)/A(NI,NI)
I=NM1
14 IP1=I+1
SUM=0.0
DO 15 J=IP1,NI
15 SUM=SUM+A(I,J)*C(J)
C(I) = (B(I)-SUM)/A(I,I)
I = I-1
IF(I=0) 21,21,14
21 DO 22 J=1,NXY
YY(J)=C(1)
DO 22 K=2,M+1
YY(J)=YY(J)+C(K)*X(J)**(K-1)

```

```
22  CONTINUE
    DO 51 J=1,NXY
51  QR=QR+(Y(J)-YY(J))**2
    KDEGR = ( NXY - 1 )
    DEGR=KDEGR
    VARIN = QR / DEGR
    DO 25 I=1,NXY
    IF ( Y(I)) 251, 252, 251
252 EROR(I) = 0.0
    GOTO 25
251 EROR(I)=(Y(I)-YY(I))
25  CONTINUE
    RETURN
    END
```

---

HOSPITAL DRAINAGE DESIGN - LEAST SQUARES ANALYSIS OF DECELERATION CHARACTERISTICS.  
 DR. J. A. SWAFFIELD AND R. H. M. WAKELIN, DIV. OF BUILDING TECHNOLOGY, BRUNEL UNIVERSITY.

THE TEST CODE USED IS :

A = ARMITAGE SHANKS.	T = TWYFORDS.
S = S-TRAP.	P = P-TRAP.
L = LOW LEVEL CISTERN.	V = VENTED DISCHARGE.
U = UNVENTED DISCHARGE.	2 = 1MP + 3K.
1 = SINGLE MATERNITY PAD.	3 = 1MP + 3BS.

RUN NO.	TEST CODE	SLOPE 1/	STOPS PERCENT	MEAN STOP POSN. METRES	ERROR1 M/S	ERROR2 M/S	ERROR3 M/S	ERROR4 M/S	ERROR5 M/S	ERROR6 M/S	EQUATION OF LINE
01	APLU1	40.0	0.00	0.00					0.0000	-0.0000	V = 1.8816 -0.0473*SQRT(L/G)
07	APLU1	60.0	0.00	0.00				0.0095	-0.0186	0.0091	V = 1.9166 -0.0537*SQRT(L/G)
13	APLU1	80.0	3.33	6.24			-0.0004	0.0099	-0.0180	0.0085	V = 1.6134 -0.0428*SQRT(L/G)
19	APLU1	100.0	10.00	11.03			-0.0063	0.0271	-0.0324	0.0116	V = 1.5914 -0.0407*SQRT(L/G)
25	APLU1	150.0	100.00	9.23		-0.0400	0.0711	-0.0164	-0.0147		V = 1.9827 -0.0522*SQRT(L/G)

THE EQUATION OF THE LINE TAKING ALL THE ABOVE READINGS INTO ACCOUNT IS : V = 1.7980 -0.0476\*SQRT(L/G)